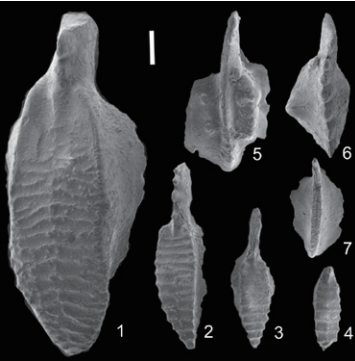
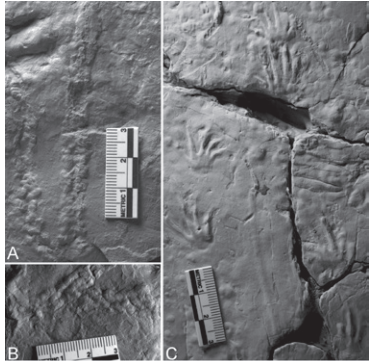
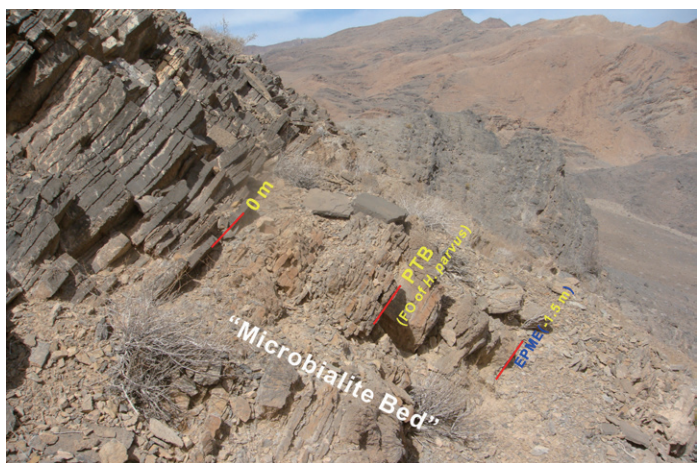




Permophiles

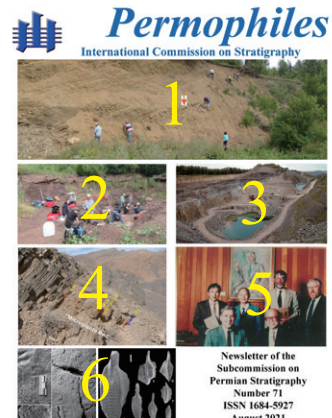
International Commission on Stratigraphy



Newsletter of the
Subcommission on
Permian Stratigraphy
Number 71
ISSN 1684-5927
August 2021

Table of Contents

Notes from SPS Secretary	3
Yichun Zhang	
Notes from SPS Chair	4
Lucia Angiolini	
Henderson's Harangue #8	6
Charles M. Henderson	
Report on the activities of the Carboniferous – Permian –Triassic Nonmarine-Marine Correlation Working Group for 2020 and 2021	7
Joerg W. Schneider, Spencer G. Lucas, Lorenzo Marchetti, Ausonio Ronchi, Michael O. Day, Shu-zhong Shen, Stanislav Opluštil, Hendrik Klein, Hafid Saber, Tariq Zouheir, Ralf Werneburg, Sebastian Voigt, Jörg Fröbisch, Ronny Rößler, Vladimir V. Silantiev, Veronika Zharinova	
Q&A on the Guadalupian	16
New age data for Permian strata on the Mogollon Rim, central Arizona, USA	18
Spencer G. Lucas, Charles M. Henderson	
Upper Pennsylvanian, Permian, and Lower? Triassic continental successions in SW Sardinia (Italy): a petro-sedimentological update of the molassoid Sulcis basin	21
Luca G. Costamagna	
Digital geological modelling of the Tambach Formation around the Bromacker fossil-lagerstätte (Early Permian, Germany)	27
Frank Scholze	
Recent progress and prospect of high-precision U-Pb age constraints on the Permian marine-terrestrial system of the North China block	32
Qiong Wu, Jahandar, Ramezani, Hua Zhang, Jun Wang, Fan-gui Zeng, Yi-chun Zhang, Feng Liu, Jun Chen, Yao-feng Cai, Zhang-shuai Hou, Chao Liu, Wang Yang, Charles M. Henderson, Shu-zhong Shen	
Upper Permian brachiopods from the Abadeh section, Central Iran	36
Marco Viaretti, Gaia Crippa, Shuzhong Shen, Lucia Angiolini	
Reply to the Comment of Horacek et al. (2021) on the Permian-Triassic boundary at the Abadeh section, central Iran	39
Jun Chen, Dong-xun Yuan, Shu-zhong Shen	
Short note to the editors and about ethical publishing - and about the temperature change around the Permian-Triassic Boundary (PTB)	43
Michal Horacek, Leopold Krystyn, Aymon Baud	
Proposal for the Global Stratotype Section and Point (GSSP) for the base-Artinskian Stage (Lower Permian)	45
Valery V. Chernykh, Charles M. Henderson, Ruslan V. Kutygin, Tatiana V. Filimonova, Guzal M. Sungatullina, Marina S. Afanasieva, Tatiana N. Isakova, Rafael Kh. Sungatullin, Michael H. Stephenson, Lucia Angiolini, Boris I. Chuvashov	
OBITUARY	72
He Xilin	
Shu-zhong Shen	
SUBMISSION GUIDELINES FOR ISSUE 72	76
Fig. 1. The Dal'ny Tulkas, the proposed base-Artinskian GSSP, Chernykh et al., this issue.	
Fig. 2. Tetrapod lagerstätte Bromacker in the Thuringian Forest basin, Schneider et al., this issue.	
Fig. 3. Remigiusberg Quarry, southwest Germany, Schneider et al., this issue.	
Fig. 4. Permian-Triassic boundary interval at the Abadeh section, Chen et al., this issue.	
Fig. 5. Prof. He Xilin visited Deakin University in 1994. Shen, this issue.	
Fig. 6. Trace fossils and conodonts from the Supai Group in Arizona, Lucas and Henderson, this issue.	



Notes from the SPS secretary

Yichun Zhang

Introduction and thanks

Covid-19 epidemic virus is still a threat across the whole world that hampers the participation in meetings, joint international fieldtrips and international collaborations. But, hopefully, webinars and online lectures are a good opportunity. On 1 April, Prof. Mark Schmitz gave us a webinar about Radioisotopic Dating. The record of the webinar is now available on SPS website. Thanks to Mark for this interesting presentation.

During the past months, as suggested by SPS Chair Lucia Angiolini, I have compiled a full content of *Permophiles* for the convenience of readers. That is available on the SPS website (<https://permian.stratigraphy.org/publications>), and will be renewed as new issue is released.

I am happy to have worked with Lucia Angiolini and Michael H. Stephenson to edit this *Permophiles* issue by frequent email contacts, especially during July and this month. Thanks for their great efforts for editing this issue.

Many thanks to the contributors of this issue: Charles M. Henderson, Shuzhong Shen, Joerg W. Schneider and co-authors, Spencer G. Lucas, Luca G. Costamagna, Frank Scholze, Qiong Wu and co-authors, Marco Viaretti and co-authors, Jun Chen and co-authors, Micha Horacek and co-authors, Valery V. Chernykh and co-authors.

Finally, I would like to keep drawing your attention to the new SPS website <https://permian.stratigraphy.org/>, where you can find all issues of *Permophiles*, updated Permian Timescales and news about the Permian subcommission.

Permophiles 71

This issue of *Permophiles* contains fruitful contributions covering diverse aspects such as GSSP proposal, high-resolution dating, new Permian fossil groups, application of GIS system, comments, and replies. Especially for those comments and replies, *Permophiles* is always an open platform for free discussions on Permian topics which is significant for improving Permian studies.

This issue starts with the eighth harangue by Charles M. Henderson. He highlighted the seriousness of choosing a GSSP that should integrate biostratigraphy, sedimentary sequences, isotopic stratigraphy, and other evidence, which deserves our serious consideration.

Joerg W. Schneider and co-authors reported activities of the Carboniferous-Permian-Triassic nonmarine-marine correlation working group during 2020 and 2021. Their excellent work has promoted the understanding of marine-nonmarine correlations.

Qiong Wu and Shuzhong Shen replied the questions raised by a SPS corresponding member about the Roadian-Wordian boundary and the position of Illawara Reversal. Such open questions and replies are significant to make clear some critical questions.

Spencer G. Lucas and Charles M. Henderson reported new tetrapod footprints and conodonts from the Supai Group in the Mogollon Rim, central Arizona, USA. These fossils provide age

constraints to the formation.

Luca G. Costamagna introduced his work in the Sulcis basin in southwestern Sardinia, Italy. The new and revised stratigraphic and sedimentological data have revealed a more complex sedimentary evolution in the Sulcis continental basin during Late Carboniferous to Early Triassic.

Frank Scholze reported the recent work about the digital geological modelling work on the Tambach Formation in the Tambach-Dietharz Basin in central Germany. The digital geological modelling by software QGIS has the potential to reveal the distribution pattern of the Tambach Formation in the basin.

Qiong Wu and her colleagues reported latest high-precision CA-ID-TIMS dating on the ash beds from the Permian strata in North China. The updated Permian ages allowed to recognize a considerable unconformity with a gap of about 20 Ma at the top of the Upper Shihhotse Formation, which is compatible with the closure of the Paleo-Asian ocean and invasion of Angaran flora into North China.

Marco Viaretti and his colleagues reported the Upper Permian brachiopods from the Abadeh section, Central Iran. The preliminary work established three brachiopod zones, which have a good potential in regional correlations.

Jun Chen and his colleagues replied to the comments by Micha Horacek and this colleagues in last issue of *Permophiles*. They explain in detail about the conodont definitions, correlations and discrepancies about the position of PTB. They slightly modified the conodont biostratigraphy at the Abadeh Section and placed the PTB in the middle of the "Microbialite Bed".

Micha Horacek and co-authors provided a short note that supplement their comment in *Permophiles* 70. They highlight the rapid warming occurred from latest Permian to Early Triassic.

In this issue, we are circulating the base-Artinskian GSSP proposal. The proposal has been updated compared with the version published in 2013 (*Permophiles* 58). I would call all SPS voting members to read the proposal carefully. I appreciate comments or discussions that will promote our better understanding of the Sakmarian-Artinskian Boundary and the proposal prior to voting this Fall by SPS Voting Members.

Finally, very sadly, one obituary commemorates eminent educator and expert on Carboniferous and Permian brachiopods and plant fossils, Prof. He, Xilin, who away on January, 2021.

Future issues of *Permophiles*

The next issue of *Permophiles* will be the 72nd issue.

We welcome contributions related to Permian studies around the world. So, I kindly invite our colleagues to contribute harangues, papers, reports, comments and communications.

The deadline for submission to Issue 72 is 31 Dec 2021. Manuscripts and figures can be submitted via email address (yczhang@nigpas.ac.cn) as attachment.

To format the manuscript, please follow the TEMPLATE on SPS website.

Notes from the SPS Chair

Lucia Angiolini

We are still not free from the Covid-19 pandemic. Going back to the field, especially abroad, remains a difficult task to achieve and participation in congresses and events is still online, from a distance. Whether this arrangement favours collaboration and circulation of ideas is a matter of debate, but personally I am not very positive about this.

We wanted to organize a field excursion on the last Permian GSSPs that remain to be established; we have money for it, but for the moment it remains a remote aim.

However, notwithstanding the difficult times, this *Permophiles* issue demonstrates that, in the last months, Permian studies have been stimulated and promoted, and correlation and the resolution of the Permian Timescale have been improved, and issues and controversies have been solved.

The Permian community is widening in diversity, international coverage and young researchers: in the last months we have ten new corresponding members including three students and five women from several European countries and China.

To increase the Permian audience and promote Permian research, in February 2021, a new video was released <https://www.youtube.com/watch?v=s2f1647pCpI> and on the 1 April 2021, a webinar “Bringing Deep Time into Focus: Opportunities and Challenges for Radioisotopic Dating and Time Scale Calibration” by Mark Schmitz went live online through zoom. The record of the webinar is on the SPS website maintained by Yichun Zhang at <https://permian.stratigraphy.org/Interests/Mark>

A new webinar is scheduled for October 2021: “Uses and abuses of palaeogeographic reconstructions for Permian workers” by Giovanni Muttoni, Università di Milano.

One of the main goals set by SPS officers is to turbocharge the Artinskian-base and Kungurian-base GSSPs. As you can see from the report at the end of the issue, Valery Chernykh and Charles Henderson with colleagues have worked hard to prepare the Artinskian-base GSSP proposal at Dal’ny Tulkas. The section and point, already presented in *Permophiles* 58 (Chuvashov et al., 2013) and *Permophiles* 69 (Chernykh, 2020), is a good one being characterized by continuous sedimentation, being richly fossiliferous (conodonts, ammonoids, fusulines, small foraminifers, radiolarians), and having good geochronologic ages, and C and Sr isotope data. As shown by Chernykh & Henderson (2021) in *Permophiles* 70, the problems concerning conodont taxonomy have been solved. The proposal published in this issue has been contextually sent to the voting members with a request for comments before voting in 20 September 2021, immediately followed by call for a vote of voting members.

If promoting the completion of the Permian System is the most urgent task, also the improvement of the resolution of the Permian Timescale is of paramount importance. Shen Shuzhong and his working group have proposed an update of the Permian Time Scale on 26 June 2021, as follows:

- base of the Guadalupian (base of the Roadian): 273.01 ± 0.14 Ma (Shen et al., 2020, *Earth-Science Reviews* 211, 103412);
- base of the Wordian: 266.9 ± 0.4 Ma (Wu et al., 2020, *Palaeogeography, Palaeoclimatology, Palaeoecology* 548

109668);

- Illawarra geomagnetic polarity reversal: 267.4 ± 0.4 Ma to 266.5 ± 0.3 Ma (Wu et al., 2020, *Palaeogeography, Palaeoclimatology, Palaeoecology* 548 109668);
- base of the Capitanian: is 264.28 ± 0.16 Ma (Wu et al., 2020, *Palaeogeography, Palaeoclimatology, Palaeoecology* 548 109668);
- base of the Lopingian (base of the Wuchiapingian): 259.51 ± 0.21 Ma (Yang et al., 2018, *Earth and Planetary Science Letters* 492, 102-111).

Finally, as anticipated by Shuzhong Shen in his SPS Past Chair Notes in *Permophiles* 69, among the challenges still open is the revision of the Guadalupian Series in the Glass and Guadalupe Mountains. This is because, although the three GSSPs were ratified by IUGS in 1999, proper publications on the section and point have never been published; moreover, the base-Wordian GSSP needs further studies due to scant conodont occurrence.

According to a communication I received from Shuzhong Shen in July 2021, he and his research group have completed the base-Capitanian GSSP paper and will then focus on the base-Roadian and finally base-Wordian GSSPs. Also, they will complete the proposal for the replacement section for the previously-defined base-Lopingian GSSP at the Penglaitan section in Guangxi, South China that has been permanently flooded due to a dam.

I conclude my notes asking all of you to contribute to the discussion on Permian topics and to *Permophiles* and urging your comments and opinions which are very important to move Permian studies forward.

Finally, we are going to organize a call to fund small projects of young researchers on Permian correlation: please stay tuned!

APPENDIX [Names and Addresses of Current Officers and Voting Members]

Prof. Lucia Angiolini (SPS Chair)

Dipartimento di Scienze della Terra “A. DESIO”
Via Mangiagalli 34, 20133, Milano, Italy
E-mail: lucia.angiolini@unimi.it

Dr. Alexander Biakov

Northeast Interdisciplinary Scientific Research Institute
Far East Branch, Russian Academy of Sciences,
Portovaya ul. 16, Magadan, 685000 Russia
E-mail: abiakov@mail.ru

Dr. Valery Chernykh

Institute of Geology and Geochemistry
Urals Branch of Russian Academy of Science
Pochtovy per 7, Ekaterinburg 620154 Russia
E-mail: vtschernich@mail.ru

Dr. Nestor R. Cuneo

Museo Paleontologico Egidio Feruglio
(U9100GYO) Av. Fontana 140,
Trelew, Chubut, Patagonia Argentina
E-mail: rcuneo@mef.org.ar

Prof. Charles M. Henderson

Dept. of Geoscience, University of Calgary
Calgary, Alberta, Canada T2N1N4
E-mail: cmhender@ucalgary.ca

Dr. Valeriy K. Golubev

Borissiak Paleontological Institute, Russian Academy of Sciences
Profsoyuznaya str. 123, Moscow, 117997 Russia
E-mail: vg@paleo.ru

Prof. Spencer G. Lucas

New Mexico Museum of Natural History and Science
1801 Mountain Road N. W., Albuquerque, New Mexico 87104-1375 USA
E-mail: spencer.lucas@state.nm.us

Prof. Ausonio Ronchi

Dipartimento di Scienze della Terra e dell'Ambiente
Università di Pavia - Via Ferrata 1, 27100 PV, ITALY
voice +39-0382-985856
E-mail: ausonio.ronchi@unipv.it

Dr. Tamra A. Schiappa

Department of Geography, Geology and the Environment
Slippery Rock University, Slippery Rock, PA 16057 USA
E-mail: tamra.schiappa@sru.edu

Prof. Mark D. Schmitz

Isotope Geology Laboratory
Department of Geosciences
Boise State University, 1910 University Drive
Boise, ID 83725-1535, USA
E-mail: markschmitz@boisestate.edu

Prof. Joerg W. Schneider

Freiberg University of Mining and Technology
Institute of Geology, Dept. of Palaeontology,
Bernhard-von-Cotta-Str.2, Freiberg, D-09596, Germany
E-mail: Joerg.Schneider@geo.tu-freiberg.de

Prof. Shuzhong Shen

School of Earth Sciences and Engineering
Nanjing University, 163 Xianlin Avenue,
Nanjing, Jiangsu 210023, P.R. China
E-mail: szshen@nju.edu.cn

Prof. Guang R. Shi

School of Life and Environmental Sciences,
Deakin University, Melbourne Campus (Burwood),
221 Burwood Highway, Burwood, Victoria 3125, Australia
E-mail: guang@uow.edu.au

Prof. Michael H. Stephenson (SPS Vice-Chair)

British Geological Survey, Kingsley Dunham Centre
Keyworth, Nottingham NG12 5GG
United Kingdom
E-mail: mhste@bgs.ac.uk

Prof. Katsumi Ueno

Department of Earth System Science
Fukuoka University, Fukuoka 814-0180 JAPAN
E-mail: katsumi@fukuoka-u.ac.jp

Prof. Yue Wang

Nanjing Institute of Geology and Paleontology,
39 East Beijing Rd. Nanjing, Jiangsu 210008, China
E-mail: yuewang@nigpas.ac.cn

Prof. Yichun Zhang (SPS Secretary)

Nanjing Institute of Geology and Palaeontology
39 East Beijing Road, Nanjing, Jiangsu 210008, China
E-mail: yczhang@nigpas.ac.cn

Working group leaders

- 1) Artinskian-base and Kungurian-base GSSP Working Group;
Chair-Valery Chernykh.
 - 2) Correlation between marine and continental Guadalupian
Working Group; Chair-Charles Henderson.
 - 3) Carboniferous-Permian-Triassic Nonmarine-Marine
Correlation Working Group ; Chair-Joerg Schneider.
-

Honorary Members

Prof. Giuseppe Cassinis

Dipartimento di Scienze della Terra e dell'Ambiente
Università di Pavia
Via Ferrata 1, 27100 PV, Italy
E-mail: cassinis@unipv.it

Dr. Boris I. Chuvashov

Institute of Geology and Geochemistry Urals Baranch of
Russian Academy of Science
Pochtovy per 7
Ekaterinburg 620154 Russia
E-mail: chuvashov@igg.uran.ru

Prof. Ernst Ya. Leven

Geological Institute
Russian Academy of Sciences
Pyjevskyi 7
Moscow 109017 Russia
E-mail: erleven@yandex.ru

Dr. Galina Kotylar

All-Russian Geological Research Institute
Sredny pr. 74
St. Petersburg 199206 Russia
E-mail: Galina_Kotlyar@vsegei.ru

Prof. Claude Spinosa

Department of Geosciences
Boise State University
1901 University Drive
Boise ID 83725 USA
E-mail: cspinosa@boisestate.edu

Henderson's Harangue #8

Charles M. Henderson

Department of Geoscience, University of Calgary, Calgary, Alberta, Canada T2N 1N4

To be or not to be a GSSP?

Introduction

As an attempt to stimulate debate or perhaps simply because something smells fishy, I deliver my eighth harangue. In Italian, it would be “L’ arringa di Henderson” (the double “r” is important).

In *Permophiles* 69, I wrote a Shakespearean (apologies to William) harangue “To be or not to be *Sweetognathus whitei*”. In the same issue I described the tale of this conodont that purports to define the base-Artinskian stage. In short, there are two ‘whitei’ species that represent imperfect homeomorphs, one is an imposter. The late Heinz Kozur was the first to suggest to me that there was a difference and told me to collect some topotype material of the species from Wyoming. I always listened to Heinz – we rarely agreed it seems, as judged by discussions in past *Permophiles*, but I always listened. In this case, he was right. The fact that these homeomorphs went unrecognized for many years testifies to how difficult this business of geology can be. How can you really tell when standing on an outcrop of a marine flooding surface in a largely red-bed succession in Wyoming that the conodonts you will find are 4.4 million years older than those you might find in bed 4b at the Dal’ny Tulkas section in the Ural Mountains of Russia? The answer is you keep an open mind and do the science by collaborating with many other specialists who tell time differently. It turns out that some people actually don’t use conodont evolution to tell time – this seems unbelievable, I know, but it is true. Some actually use other fossils, and others sacrifice conodonts to retrieve strontium and oxygen isotopes, some dissolve zircons looking for uranium and lead, while others consider isotopic excursions of carbon or the binary signal of magnetism. Working with all of these different people has been one of the joys of my professional life. I am not sure that we can ever truly prove something in geology, but we can determine beyond a reasonable doubt by the preponderance of evidence. And in some cases you can do detailed morphometric analysis using R-Studio on high resolution 3D scans of different species of *Sweetognathus*, as my student Wyatt Petryshen did for his MSc – he elegantly “proved” that there were two lineages that evolved according to parallel evolution (Petryshen et al., 2020; see references in the GSSP proposal). This type of work seems like the future of paleontology and it also helped convince my colleague Valery Chernykh.

In *Permophiles* 70, Valery Chernykh and I wrote a short article called “To be or not to be *Sweetognathus asymmetricus*” in which we agreed that the Artinskian species is indeed different. I have long respected Valery’s work and so I was very pleased to write this short article with him. I saw the passion of his life work in his eyes during a camping field trip in the south Urals in 2007. *Sweetognathus asymmetricus* was defined at the Tieqiao section in South China by Sun et al. (2017). Higher in that

same section this species gradually evolved into *Sweetognathus subsymmetricus* by becoming, among other things, longer and narrower. Wang Chengyuan was the first to recognize the difference of the earliest forms at Tieqiao, which he called *Sweetognathus whitei* (Wang et al., 1987). In my review of Sun et al., I pointed out that their specimens from the transgressive deposits of the lower Chihsia Formation were not *Sweetognathus whitei* and suggested they could name them a new species or refer to them as *Sweetognathus aff. whitei*.

In this issue of *Permophiles* 71, Chernykh et al. provide a Global Stratotype Section and Point proposal for consideration by the corresponding and voting members of SPS. It shouldn’t have taken so long, but we are finally there. I am convinced of the veracity of this GSSP, particularly because of the strong sequence biostratigraphic signature (see my first Harangue for the importance of considering the rock sequences). The forms that we now call *Sweetognathus asymmetricus* appear within the transgressive systems tract (at or close to the maximum flooding surface) of a major 3rd order sequence. It is not associated with cyclothem, nor with the genus *Streptognathodus*. Not everyone believes this, but I hope that the other stratigraphic correlation tools will convince most workers that this is a very good GSSP.

I normally don’t use the word “believe” when discussing science. ‘To believe’ seems more like a religious statement. Each of us believes or finds spiritual inspiration in a different way and that is one of the beautiful things that characterizes our species. It does seem that one GSSP in particular has many fervent disciples – this is the GSSP that defines the base-Induan Stage or Permian-Triassic (PTB) or Paleozoic-Mesozoic boundary. There have been some recent ‘comments and replies’ on this topic in *Permophiles* and elsewhere. Horacek et al. in *Permophiles* 70 commented on a paper by Jun Chen and others. They were impressed by the sea surface water temperature curve across the PTB, but were concerned by the biostratigraphy. Sometimes these comments can become a little personal and this does not inspire the best reactions. It is important, I believe, that we constructively criticize only the science, and not each other. In this issue of *Permophiles* 71 Jun Chen and others reply. The main result of this ‘comment and reply’ is that the authors have moved their biostratigraphic boundary a little lower to be within the microbialite unit at the Abadeh section in Iran. This is a good result. There is a preponderance of evidence that the PTB is defined within a transgressive system tract after the main event of the end-Permian Mass Extinction (EPME). There is also a preponderance of evidence that the interval between the extinction and the PTB is very short and measured as a few 10’s of thousands of years +/- a few 10’s of thousands of years. In other words we are currently at the limits of our radiometric age dating resolution and therefore most certainly at the limits of our biostratigraphic resolution. For now, let’s say it is 40 Kyr. It is estimated that 95% of species become extinct at the EPME, but how quickly this occurred is uncertain. Some species that are counted in the 95% estimate are actually from an extinction somewhere in the vicinity of the Guadalupian-Lopingian boundary. Both the GLB and PTB are defined in transgressive systems tracts following major lowstands of sea-level. Many of the species counted in the 95% estimate became extinct at or

close to the EPME and many undoubtedly continued to become extinct in the harsh conditions of the 40 Kyr interval leading to the PTB. The PTB is actually defined by a speciation event – that of *Hindeodus parvus*. How quickly did this species arise? Did it develop rapidly from a small peripheral isolate with a high anterior denticle (not cusp) or did this morphotype gradually become more prevalent in populations of *Hindeodus praeparvus*? My point is that there are many serious questions that challenge our ability to correlate at this level of resolution. But that doesn't mean we should not attempt to correlate; we should always try to integrate biostratigraphy with isotopic stratigraphy as well as all other tools. We should build on previous work, rather than ignore it.

In many Tethyan sections (but not Boreal sections) there is a significant microbialite unit in the vicinity of the PTB. These microbialites have been referred to as anachronistic facies, harkening back to a time in the Proterozoic when multicellular life was absent or very rare, allowing bacteria to build immense stromatolite deposits in the absence of grazing pressure. This was briefly true again near the PTB. Given that the extinction occurs before the PTB it is most likely that *Hindeodus parvus* will first occur (FO) within the microbialite unit as opposed to below or above the unit. But the FO of *Hindeodus parvus* and also the microbialite will likely be diachronous (at the ~10 Kyr level?) since the appearance of each demands certain conditions like time to migrate or water depths within the photic zone. Can we live with this level of diachroneity? Is there a better way to discuss this as a level of probability? Is there a way to improve further the resolution of our stratigraphic tools? Time will tell.

Report on the activities of the Carboniferous – Permian –Triassic Nonmarine-Marine Correlation Working Group for 2020 and 2021

Joerg W. Schneider

Technical University Bergakademie Freiberg,
Institute of Geology, Dept. Paleontology and Stratigraphy
Bernhard-von-Cotta-Str. 2, D-09599 Freiberg, Germany
Institute of Geology and Petroleum Technologies, Kazan (Volga Region) Federal University,
Kremlyovskaya str. 18, 420008 Kazan, Russia
Email: Joerg.Schneider@geo.tu-freiberg.de

Spencer G. Lucas

New Mexico Museum of Natural History and Science,
1801 Mountain Road N.W., Albuquerque, New Mexico, 87104,
USA
Email: Spencer.lucas@state.nm.us

Lorenzo Marchetti

Museum für Naturkunde Berlin, Leibniz-Institut für Evolutions- und Biodiversitätsforschung, Invalidenstr. 43, 100115 Berlin, Germany
Email: lorenzo.marchetti@mfn.berlin

Ausonio Ronchi

Department of Earth and Environmental Sciences,
University of Pavia,
Via Ferrata 1, I-27100 Pavia, Italy
Email: ausonio.ronchi@unipv.it

Michael O. Day

Department of Earth Sciences,
The Natural History Museum (NHMUK),
Cromwell Road, London SW7 5BD, United Kingdom
Email: michael.day@nhm.ac.uk

Shu-zhong Shen

School of Earth Sciences and Engineering, Nanjing University,
163 Xianlin Avenue, Nanjing, Jiangsu 210023, P.R. China
Email: szshen@nju.edu.cn

Stanislav Opluštil

Institute of Geology and Paleontology, Charles University in Prague, Faculty of Science Albertov 6, 128 43 Praha 2, Czech Republic
Email: oplustil@natur.cuni.cz

Hendrik Klein

Saurierwelt Paläontologisches Museum,
Alte Richt 7, D-92318 Neumarkt, Germany
Email: Hendrik.Klein@combyphone.eu

Hafid Saber

Laboratory of Geodynamic and Geomatic, Dept. of Geology, Faculty of Sciences, Chouaïb Doukkali University, B.P. 20, El Jadida 24000, Morocco
Email: hafidsaber@yahoo.fr

Tariq Zouheir

Laboratory of Geodynamic and Geomatic, Dept. of Geology, Faculty of Sciences, Chouaïb Doukkali University, B.P. 20, El Jadida 24000, Morocco
Email: zouheirtariq@gmail.com

Ralf Werneburg

Naturhistorisches Museum Schloss Bertholdsburg, Burgstr. 6, D-98553 Schleusingen, Germany
Email: werneburg@museum-schleusingen.de

Sebastian Voigt

Urweltmuseum GEOSKOP, Burg Lichtenberg (Pfalz), Burgstraße D-66871 Thallichtenberg, Germany
Email: s.voigt@pfalzmuseum.bv-pfalz.de

Jörg Fröbisch

Museum für Naturkunde Berlin, Leibniz-Institut für Evolutions- und Biodiversitätsforschung, Invalidenstr. 43, 100115 Berlin, Germany
Email: joerg.froebisch@mfn-berlin.de

Ronny Rößler

Museum für Naturkunde Chemnitz, Moritzstr. 20, 09111 Chemnitz, Germany
 Technical University Bergakademie Freiberg,
 Institute of Geology, Dept. Paleontology and Stratigraphy
 Bernhard-von-Cotta-Str. 2, D-09599 Freiberg, Germany
 Email: roessler@naturkunde-chemnitz.de

Vladimir V. Silantiev

Institute of Geology and Petroleum Technologies, Kazan (Volga Region) Federal University,
 Kremlyovskaya str. 18, 420008, Kazan, Russia
 Email: vsilant@gmail.com

Veronika Zharinova

Institute of Geology and Petroleum Technologies, Kazan (Volga Region) Federal University
 Kremlyovskaya str. 18, 420008, Kazan, Russia
 Email: nika_zharinova@mail.ru

The years 2020 and 2021 were marked worldwide by the corona pandemic with restrictions on fieldwork at home and abroad, with limited personal communication and restricted access to fossil and rock collections. Still, remarkable progress has been made by the international team of our working group as shown below by a number of publications, the participation in several online meetings and by the organization of future cooperative research work. Moving up through the geological timescale, we report the following.

Carboniferous

The Geological Society, London, is in the process of publishing a comprehensive volume on the Carboniferous timescale as part of its Special Publications Series, co-edited by Spencer G. Lucas, Joerg W. Schneider, Xiangdong Wang and Svetlana Nikolaeva. Many of the articles are already published online, and the volume will likely be finished in September. The papers already published online on nonmarine biostratigraphy are those of Opluštil et al. (2021) on macrofossil plant biostratigraphy, Lucas (2021a) on tetrapod biostratigraphy (Fig. 1) and Lucas et al. (2021b) on tetrapod footprint biostratigraphy. Papers by Chen et al. (2021) on Carboniferous isotope stratigraphy and by Hounslow (2021) on Carboniferous magnetostratigraphy are also relevant to Carboniferous nonmarine-marine correlations. Additional papers in this volume not yet published concern nonmarine bivalve biostratigraphy (Amler and Silantiev, in review), combined insect-conchostracean biostratigraphy (Schneider et al., in review), palynostratigraphy (Eble) as well as cyclostratigraphy (Montañez, in review) and the Carboniferous numerical timescale (Ramezani).

In early 2021, years of research were culminated by publication of New Mexico Museum of Natural History and Science Bulletin 84, “The Kinney Brick Quarry Lagerstätte, Late Pennsylvanian of New Mexico,” a 466-page volume of 20 articles edited by Spencer G. Lucas, William A. DiMichele and Bruce D. Allen (free download here: The Kinney Brick Quarry Lagerstätte,

Late Pennsylvanian of New Mexico - Google Books). Kinney has been known as an important Lagerstätte since the 1960s, where a mixture of nonmarine fossils (especially plants, insects and amphibians) are found together with marine fossils (notably brachiopods, bivalves and conodonts) and with an extensive fish assemblage of mixed nonmarine and marine origin (also see Stack et al., 2020). A 2014 controlled excavation at Kinney (the first such excavation) overseen by Spencer G. Lucas and Joerg W. Schneider provided much of the impetus (and new data) for the volume (Schneider et al., 2021a,b) (Fig.2). The conodonts at Kinney and fusulinids found stratigraphically just below the quarry indicate it is of early Missourian (Kasimovian) age, so Kinney provides an important tie point between nonmarine and marine biostratigraphy (see discussion by Schneider et al., 2020).

On May 23-27, 2021, an online meeting on a zoom platform provided by the Smithsonian Institution titled “The Kasimovian Workshop” was sponsored by the Carboniferous Subcommission, and it was co-organized by William A. DiMichele, Spencer G. Lucas, Stanislav Opluštil and Xiangdong Wang. The meeting brought together about 40 scientists from across the globe to present research on diverse aspects of the Late Pennsylvanian world. Many presentations focused on nonmarine depositional systems, paleontology, biostratigraphy and correlation. Smithsonian technical staff are now working to put almost all of the presentations (they were recorded) up on a YouTube channel. Stay tuned!

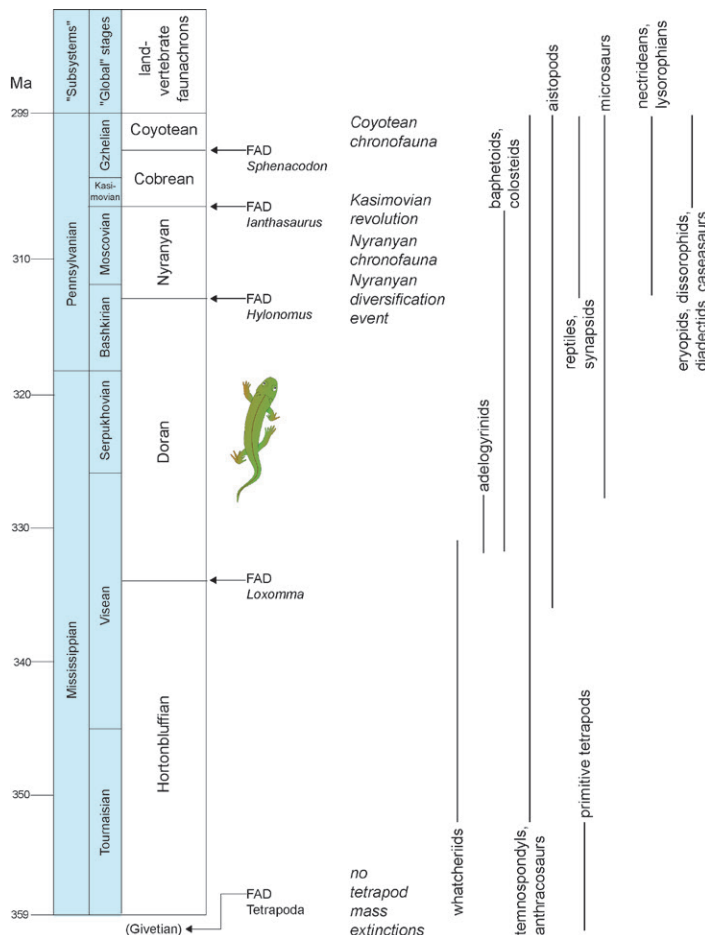


Fig.1. Carboniferous tetrapod biochronology (from Lucas, 2021).

A related article by DiMichele et al. (2020) discussed taphonomic biases in the late Paleozoic plant record, particularly with regard to the problems of so-called “upland” floras. It provides another cautionary note in the use of macrofossil plants in late Paleozoic correlations. In a related paper, Bashforth et al. (2021) have just published an extensive discussion of “mixed” upper Paleozoic floras, those with both wet and dry elements. They argue that the idea that the dryland floral elements grew in uplands and were transported into the mixed floral settings has little support, another example of the problems of facies control of macrofloral assemblages. Nelson and Lucas (2021) published a critique of the ill-defined Cantabrian substage (stage), a chronostratigraphic unit based on macroplant biostratigraphy. Lucas and Tanner (2021) documented calcareous paleosols (“calcretes”) from Kasimovian strata in far western Pangea (New Mexico, USA), one of the few well-studied paleosol records of this age. Lucas et al. (2021a) published a monographic study of the Pennsylvanian strata in the Sacramento Mountains of New Mexico that include important Missourian paleofloras and a nonmarine animal fossil record (conchostracans, ostracods, bivalves, insects, fish bits) that merits further development and study.

Lüthardt et al. (2020) report on sedimentation and magmatism in one of the most extensive Carboniferous/Permian vulcanite areas, the Flechtingen Volcanic Complex (FVC), at the southern border of the younger Southern Permian basin. Supported by radioisotopic ages, this study contributes to the clarification of stratigraphic constraints on upper Carboniferous to Lower Permian continental deposits and sheds new light on the stratigraphy of significant upper Palaeozoic volcanic deposits. The Mammendorf quarry, situated in the FVC, exposes the above mentioned vulcanites as well as upper middle to lowermost upper Permian sediments, and is gaining growing importance as one of the youngest (Capitanian) locations of Permian tetrapod tracks in Europe (Buchwitz et al., 2019).

Trümper et al. (2020a) described fluvial red beds containing anatomically preserved large woody debris in the Kyffhäuser area of the Saale basin (Central Germany), which shed new light on seasonally dry biomes of the Pennsylvanian–Permian transition. The radioisotopic U-Pb age of $299 + 3.2$ Ma of this bed improves the calibration of Upper Pennsylvanian (Gzhelian) insect and conchostracean zones.

The age of the world-famous upper Palaeozoic insect locality Xiaheyan in Northwest China has been corrected from an assumed late Namurian age by conodont and ammonoid biostratigraphy as well as by radioisotope ages to latest Bashkirian (latest Duckmantian) to middle Moscovian (Bolsovian) by a Chinese/French/German team (Trümper et al., 2020b). The insect fauna of this locality is of importance for the palaeobiogeographic and biostratigraphic relations of the Cathaysian to the Angaran and Euramerican biotic provinces.

Permian

Spencer G. Lucas, in collaboration with Charles Henderson (University of Calgary, Canada), have been sampling Permian limestones intercalated with nonmarine red beds in Texas, New Mexico and Arizona. The sampling has yielded extensive

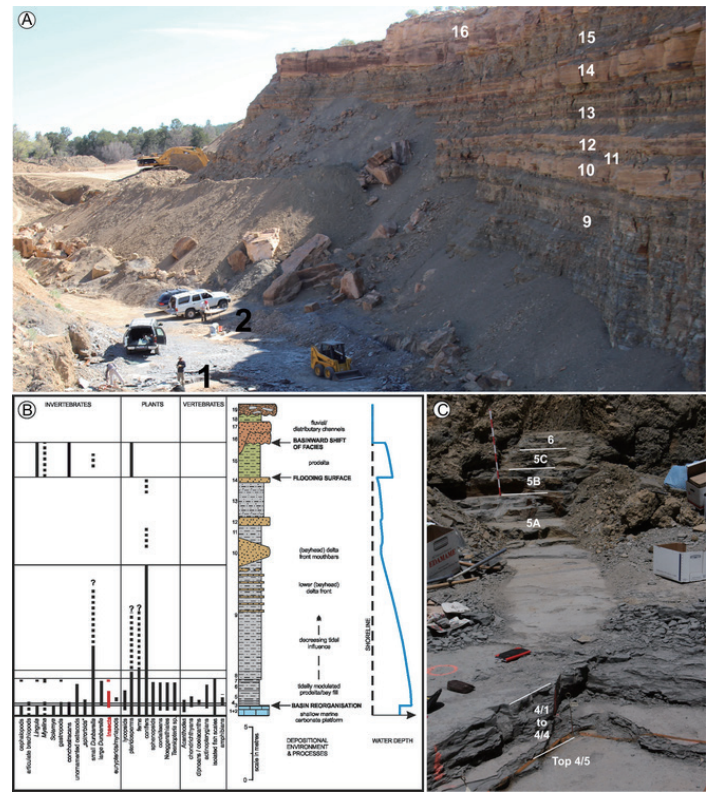


Fig. 2. Kinney Brick Quarry. A, Locations of controlled excavation of beds 2 to 5 (1) and the unit 3 fish bed (2); 9 to 16 are bed numbers in the quarry wall. B, Lithology and fossil content of beds 1 to 19 (modified after Williams and Lucas, 2013) and inferred depositional environments/processes. C, Trench from bed 4/5 into bed 6, which connects the excavation site with the quarry wall section; bed 4 and 5 bear the highest content of fossil insects. Scale near beds 5-6 is 1 m. From Schneider et al. (2021b).

Kungurian conodont assemblages from the Blaine Formation (Texas), Yeso Group (New Mexico) and Fort Apache Limestone (Arizona). In this issue of *Permophiles*, Lucas and Henderson present an initial report on the Arizona conodonts. The Texas (Blaine) conodonts confirm that Olson’s gap is longer than previously expected, as earlier concluded by Lucas and Golubev (2019). This work will be published in the near future, as it provides important tiepoints between nonmarine Permian tetrapod and tetrapod footprint assemblages and the marine Permian timescale.

A German-French team has completed the study of a new huge caseid synapsid of estimated 3.6 m length from the Guadalupian La Lieude Formation of the Lodève basin in Southern France, which will appear in press at the end of 2021 (Werneburg et al., 2021, in review). In Germany has started this year after a break of about 10 years a new research project on the world-famous early Permian tetrapod track and skeleton locality Bromacker near Tambach-Dietharz town in the Thuringian Forest basin (Fig. 3). “Opening science: new ways of knowledge transfer using the example of the research project Bromacker” is the title of an interdisciplinary cooperative research project, which started in August 2020 and is funded by the Federal Ministry of Research and Education. Participating institutions are the



Fig. 3. Start of the new 5-years excavation period at the world-famous Lower Permian tetrapod lagerstätte Bromacker in the Thuringian Forest basin, July 2021. J.W. Schneider.

Museum für Naturkunde Berlin – Leibniz-Institute for Evolution and Biodiversity Research, the Stiftung Schloss Friedenstein Gotha, the Friedrich-Schiller-Universität Jena and the recently declared UNESCO Global GeoPark Thüringen Inselsberg-Drei Gleichen, as well as other national and international partners. The focus is not only on investigating the world-famous tetrapod locality Bromacker near Tambach-Dietharz, but essentially the entire Lower Permian Tambach Formation in the Thuringian Forest. The combined record of tracks and body fossils from the Bromacker site, their excellent preservation and extraordinary species richness provide a unique window into the paleobiology and ecology of early tetrapods and their ecosystems. Special focus is being placed on geology, climate, biodiversity, ecology, biomechanics, and physiology. One of the main goals of this project, in addition to the scientific progress, is to enable the participation of the general public in this integrative research project by applying novel science transfer approaches. The first results have been published by Marchetti et al. (2021a) and Buchwitz et al. (2021).

The excavations of the museum Geoskop in southwest Germany in the active Remigiusberg quarry (Fig. 4) will make this site one of the most complex fossil Lagerstätten in Europe with a diverse tetrapod fauna (Voigt et al., 2019). The so far known tetrapod fauna includes fully aquatic (dvinosaurian temnospondyl), semiaquatic (eryopid) and terrestrial (sphenacodontid and edaphosaurid synapsid) animals. First high-precision U-Pb CA-ID-TIMS age from near the base of the overlying Altenglan Formation supports the biostratigraphic data that indicate the Remigiusberg Formation is of latest Gzhelian to earliest Asselian age (Voigt et al., 2021; in review).

Rößler (2021) published a comprehensive report on “the most entirely known Permian terrestrial ecosystem on Earth...,” the Chemnitz Fossil Forest in Germany, preserved by explosive volcanism during the late Sakmarian/early Artinskian (291+ 2 Ma). Two excavations at Chemnitz, ongoing since 2008, have opened a unique window into a low-latitude “wet spot” ecosystem, characterized by a dense hygrophilous arborescent vegetation and a diverse fauna of vertebrates and invertebrates.

The team from Kazan University, Tatarstan, other Russian institutions, and Boise State University, Idaho, USA, have delivered very interesting new results of a multidisciplinary study of the Permian-Triassic transition in the continental deposits of the Kuznetsk Basin, Russia (Davydov et al., 2021). These data are important in two aspects. First, the region is proximal to the Siberian Large Igneous Province, and the effects of the flood basalt volcanism in the Kuznetsk Basin may have been of similar scale to the main area of the Siberian Traps distribution, e.g. the Tunguska and Taymyr regions. Second, it provides new insights in the latitudinal effects of the Permian/Triassic crisis, which seems to have been much stronger in low latitudes than in the higher latitudes of Siberia. A climate shift poleward during the Permian-Triassic transition caused the replacement (turnover) of the humid-related biotas by the dry climate-related communities, which continued to expand throughout the Triassic in terrestrial habitats. Additionally, high precision CA-IDTIMS U-Pb zircon ages combined with conchostracean biostratigraphy of the PT-transition are a valuable contribution to nonmarine-marine correlations of the Angaran to the Euramerican biotic region.

Cathaysia correlations

Shuzhong Shen reports that great progress has been made on the Carboniferous and Permian in the North China Block. A series of high-precision CA-ID-TIMS dates from the upper Carboniferous Taiyuan Formation and Permian strata have been published (Wu et al., 2021). The new dates indicate that the lower part of the Taiyuan Formation is of Late Carboniferous age, and the upper part of the Taiyuan, the Shansi and the Lower and Upper Shihhotse formations, all belong to the Cisuralian. A considerable unconformity of ca. 20 m.y. is present that encompasses the late Cisuralian to Guadalupian at the top of the Upper Shihhotse Formation in the northern North China block. The overlying Sunjiagou Formation is of Lopingian age. An analogous unconformity was reported from correlative Permian successions in eastern Xinjiang (Yang et al., 2010). The



Fig. 4. Remigiusberg Quarry, near Kusel, southwest Germany. Exposed are the quarried subvolcanite and above fluvio-lacustrine sediments of the Remigiusberg Formation of latest Gzhelian to earliest Asselian age. Excavations of the Museum Geoskop, Burg Lichtenberg (Pfalz) deliver the so far most diverse tetrapod fauna in this time frame of Europe.

unconformity has been suggested to be related to subduction of the Paleo-Asian Ocean generating arc-continent and retro-arc fold-thrust deformation or to its final closure leading to continental collision during the late Cisuralian to Guadalupian. Another review paper on the Permian stratigraphy in the North China Block has been completed and will be submitted to a journal shortly. In addition, a 10 km-thick Carboniferous-Permian section in the northeastern part of Xinjiang Province has been measured by our group. The succession consists of the Batamayineishan, Shiqiantan, Jingou, Jiangjunmiao, Pingdiquan and Wutonggou formations, in ascending order. More than 100 ash beds were collected, and numerous brachiopods and plant fossils were collected. These samples are the priority for our group to analyze in the near future. They are critical to determining the ages of those formations in the Carboniferous and Permian.

Scholze et al. (2020) have added new information on conchostracean biostratigraphy of the Permian/Triassic transition in Southwest China compared with P/T sections in Russia and Europe.

North-South correlations

Despite the disruption of fieldwork presented by the Coronavirus pandemic, the last year has seen a particularly large number of papers concerning the biostratigraphy of the main Karoo Basin. Most of these form part of broad review of the tetrapod assemblage zones of the Beaufort Group, published in a special issue of the *South African Journal of Geology* (Botha and Smith, 2020; Day and Rubidge, 2020; Day and Smith, 2020; Hancox et al., 2020; Rubidge and Day, 2020; Smith, 2020; Smith et al., 2020; Viglietti, 2020; Viglietti et al., 2020a, 2020b). Though based mainly on the previous assemblage zones (AZ), these papers considerably revised the ranges of known taxa in light of collecting efforts over the past 25 years. Notable changes included: the partitioning of the former *Pristerognathus* AZ between the *Tapinocephalus* AZ and a resurrected *Endothiodon* AZ, the reduction of the *Tropidostoma* AZ to subzone status, the qualification of the *Lystrosaurus* AZ to *Lystrosaurus* declivis AZ, and the replacement of the defunct and informal name *Euskelosaurus* AZ with the new *Scalenodontoides* AZ. They also provided formal recognition of subzones within the *Tapinocephalus*, *Endothiodon*, *Daptocephalus*, and *Cynognathus* assemblage zones.

There has also been continued attention to the mass extinctions of vertebrates recorded in the main Karoo Basin, and especially their chronology. Day and Rubidge (2021) provided a review of the Capitanian mass extinction in South Africa and included a large primary dataset that allowed them to identify a phased extinction, similar to that described for the End-Permian mass extinction (Fig. 5). This latter was the subject of two papers that presented CA-ID-TIMS ages from a site at Nooitgedacht, although they did not agree; Botha et al. (2020) argued for the synchronicity of vertebrate extinction horizon in the Palingkloof Member with the marine Permian-Triassic extinctions based on geochemical and a detrital zircon age, whereas Gastaldo et al. (2020) used an in situ zircon U-Pb age combined with palaeomagnetism and palynology and found that the extinction

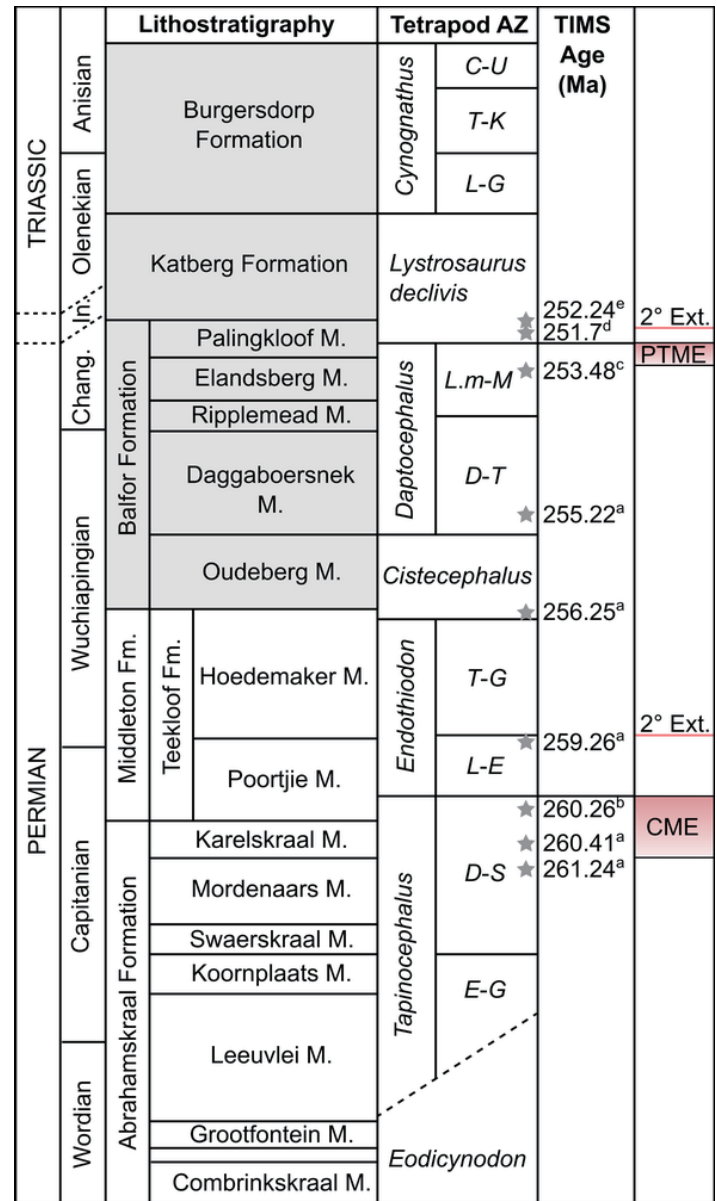


Fig. 5. Stratigraphy of the Beaufort Group showing position of mass extinction intervals. Subzone abbreviations: C-U, *Cricodon-Ufudocyclops*; D-S, *Diictodon-Styracocephalus*; D-T, *Dicynodon-Theriognathus*; E-G, *Eosimops-Glanosuchus*; L-E, *Lycosuchus-Eunotosaurus*; L-G, *Langbergia-Garjainia*; L.m-M, *Lystrosaurus maccaigi-Moschorhinus*; T-G, *Tropidostoma-Gorgonops*; T-K, *Trirachodon-Kannemeyeria*. Other abbreviations: CME, Capitanian mass extinction; Chang, Changhsingian; Fm., Formation; In, Induan; M, member; EPME, end-Permian mass extinction. Lithostratigraphic units in grey found only in the Eastern Cape. Stratigraphy and biozonation modified after Smith et al. (2020) and position of end-Permian mass extinction after Botha et al. (2020). U-Pb ages after: a, Rubidge et al., 2013; b, Day et al., 2015a; c, Gastaldo et al., 2015; d, Botha et al., 2020; e, Gastaldo et al., 2020. Actual position of the Permian-Triassic boundary is disputed. M. Day.

horizon occurs several hundred thousand years prior to the marine extinction. In the Triassic, the first comprehensive

geochronological constraints on the Elliot Formation were presented by Bordy et al. (2020), suggesting that the lower part of this formation is mid-Norian to Rhaetian in age and indicates that sauropodomorph dinosaurs were well-established in the Karoo by 220 Ma.

Carboniferous to Triassic tetrapod footprint and tetrapod biostratigraphy

During 2020 and 2021, a significant number of new papers further investigated the ichnotaxonomy and the tetrapod footprint biostratigraphy in the framework of the activities of the working group on upper Palaeozoic-lower Mesozoic continental chronostratigraphy. The earliest reptile ichnotaxon, *Notalacerta missouriensis*, was comprehensively revised in Marchetti et al. (2020a), significantly extending its biostratigraphic range (middle Bashkirian-Artinskian). A review of the Italian Carboniferous tetrapod footprint ichnotaxonomy and biostratigraphy was provided by Marchetti et al. (2020b), and a review of the Italian Cisuralian tetrapod footprint ichnotaxonomy and biostratigraphy was provided by Santi et al. (2020). In the same volume, devoted to the state of the art of Italian tetrapod ichnology and edited by M. Romano and P. Citton, an updated list of references on Italian tetrapod ichnology was also provided (Antonelli et al., 2020).

A synthesis of Carboniferous tetrapod footprint biostratigraphy was provided by Lucas et al. (2021b). In this work, the base of the *Dromopus* tetrapod footprint biochron has been lowered to the Kasimovian base. A further paper investigated the ichnotaxonomy, biostratigraphy and producers of the Carboniferous material assigned to *Hylopus hardingi*, *Notalacerta missouriensis*, *Varanopus microdactylus* and *Dromopus lacertoides* (Marchetti et al., 2021a). With regard to the Permian, a new study analyzed the Cisuralian-Guadalupian ichnotaxon *Pachypes ollieri* (Marchetti et al., 2020c). Mujal and Marchetti (2020) documented the occurrence of *Ichniotherium cottae* from the lower Cisuralian units of the Lodeve Basin. Another study revised the tetrapod footprint ichnotaxonomy and biostratigraphy of the Carboniferous-Permian units from the Grand Canyon of Arizona (Marchetti et al., 2020d).

Reviews of the Cisuralian and Lopingian Italian tetrapod footprint ichnotaxonomy and biostratigraphy were provided by Santi et al. (2020) and Marchetti et al. (2020e), respectively. A new upper Cisuralian-Guadalupian tetrapod ichnoassociation has been described from the continental basins of Morocco (Zouicha et al., 2021). The tetrapod ichnoassociation from the Capitanian Hornburg Formation of Germany has been revised by Buchwitz et al. (2020), with the addition of new material assigned to *Capitosauroides* isp. This corroborates the Capitanian age of the unit. Voigt and Fischer (2020) described *Pachypes* from the Zechstein of W Germany. Klein and Lucas (2021) provided an extensive revision of the ichnotaxonomy and biostratigraphy of Triassic tetrapod footprints, which did not change the Triassic tetrapod footprint biochron boundaries given by Schneider et al. (2020). Marchetti et al. (2020f) described some new *Synaptichnium* material from the Muschelkalk of Germany. Marchetti et al. (2021b) revised the tetrapod footprint ichnofauna from the Monti Pisani of Italy, and assigned to it a Ladinian age. They also proposed to move the base of the *Ateipus*-

Grallator footprint biochron to the base of the Ladinian. Citton et al. (2020) report on the first tetrapod tracks from the Triassic of the Nurra region (north-western Sardinia, Italy). Lithologic and petrographic features allowed an assignment of the track-bearing blocks to the middle-upper portion of the Anisian (Middle Triassic) Arenarie di Cala Viola (“Buntsandstein”). Footprints are attributed to the ichnotaxa *Rhynchosauroides* and *Rotodactylus*, two common ichnotaxa of late Early Triassic and Middle Triassic of Europe and the United States, commonly referred in the literature to neodiapsid and archosaur producers, respectively.

During 2020, a Spanish-Italian team (Lloret et al., 2020) focused on the Olenekian-Anisian continental record of the Central-Eastern Pyrenean basin (NE Spain). This multidisciplinary study, embracing sedimentology, mineralogy, palaeontology, palaeopedology and palaeogeography, of 10 complete and well dated Lower-Middle Triassic field sections has allowed: (1) the location and characterization of the oldest Mesozoic sedimentary record in the basin, which is of late Smithian age and overlies the upper-middle Permian continental rocks and of (2) the Smithian-Spathian transition (SST), (3) the timing of biotic recovery during the late Spathian-Anisian, (4) the characterization of the first incursion of the Tethys sea into the basin, and (5) the comparison of the evolution of this basin with other basins of the same age in SW Europe. The same group (Lloret et al., 2021) used paleosols as stratigraphic tools in the study of Permian and Triassic continental basins in the Central-eastern Pyrenees and offers information on the complex interplay between the factors that control the filling of basins, such as accommodation, deposition, erosion, and climate, which exerts a great influence on the supply rate of sediment and water from the sources to the basin. Grouped into palaeocatenas, the lateral variation of pedotypes across the landscape is used to interpret topography and water table variations, which was explained by variations in climate, available accommodation space, and sedimentary supply. The study of hydrological and climatic conditions was complemented by the identification of the mineralogical composition of the parent material and $\delta^{13}\text{C}$ and $\delta^{18}\text{O}$ isotopic signatures from the inorganic pedogenic carbonate of paleosols and lacustrine limestones.

A Moroccan-German team is preparing a publication on Middle to Upper Triassic invertebrate ichnia of the continental Argana basin in continuation of the report of tetrapod tracks from there (Zouheir et al., 2020). A section of approximately 760 m thickness, covering the Anisian to Carnian, was measured sedimentologically and palaeontologically with high resolution. It exhibits remarkable changes of the sedimentary and palaeobiological environments, which may be related to the Carnian pluvial episode (Zouheir et al., in prep.).

As noted above, in early 2021, Hendrik Klein and Spencer G. Lucas published a comprehensive, 194-page-long review of the global Triassic tetrapod footprint record: “The Triassic tetrapod footprint record:” New Mexico Museum of Natural History and Science Bulletin 83 (free download at: THE TRIASSIC TETRAPOD FOOTPRINT RECORD - HENDRIK KLEIN, SPENCER G. LUCAS - Google Books)

Other published work on Triassic biostratigraphy included a review of Upper Triassic metoposaurid biostratigraphy (Lucas,

2020), which demonstrates that the Carnian pluvial episode created a cosmopolitan distribution of metoposaurids followed by their provincialization, largely by the drier climates of the Norian (Fig. 6). Also, Rigo et al. (2020) identified Pangea-wide carbon isotope excursions (chaotic carbon) across the Norian-Rhaetian boundary that correspond to the largest of the stepwise extinctions across the Triassic-Jurassic boundary. The cause of this carbon isotope behavior, however, remains enigmatic, perhaps a little known large igneous province in what is now Alaska and vicinity.

Concluding remarks

On 13 November, 2020, the SPS Chair Lucia Angiolini and ViceChair Mike Stephenson, with the help of Jeanine Newham (BGS), organized a zoom webinar for the corresponding members. Point three of the summary given by our nonmarine-marine working group was: *The most challenging future task for nonmarine-marine correlations in the Late Carboniferous–Middle Triassic are global north-south correlations. Biostratigraphic correlations among the biotic provinces of Euramerica, Angara, Cathaysia, and Gondwana are still in a very unsatisfactory state. Sections of the East European Platform and Siberia in Russia, those of the Karoo basin in South Africa, sections in North China,*

in Jordan and North Africa as well as in the Paraná basin of South America should be in the focus of further research of the SPS.

As summarized above, the working group has completed extensive work. And, the above indicates, we could change the name and field of research of our group to encompass the entire Carboniferous and the entire Triassic.

References

- Antonelli, M., Avanzini, M., Belvedere, M., Bernardi, M., Ceoloni, P., Citton, P., Conti, M. A., Dalla Vecchia, F. M., D’Orazi Porchetti, S., Gianolla, P., Leonardi, G., Manni, R., Marchetti, L., Mariotti, N., Massari, F., Mietto, P., Muscio, G., Palombo, M. R., Panarello, A., Petruzzelli, M., Petti, F. M., Pignatti, J., Pillola, G. L., Piubelli, D., Raia, P., Romano, M., Ronchi, A., Sacchi, E., Sacco, E., Salvador, I., Santi, G., Schirolli, P., Valentini, M., Wagensommer, A., & Zoboli, D., 2020. Reference list. Journal of Mediterranean Earth Sciences, v. 12, <https://doi.org/10.3304/jmes.2020.17069>
 Bashforth, A. R., DiMichele, W. A., Eble, C. F., Falcon-Lang, H. J., Looy, C. V., and Lucas, S. G., 2021. The environmental implications of upper Paleozoic plant-fossil assemblages with mixtures of wetland and drought-tolerant

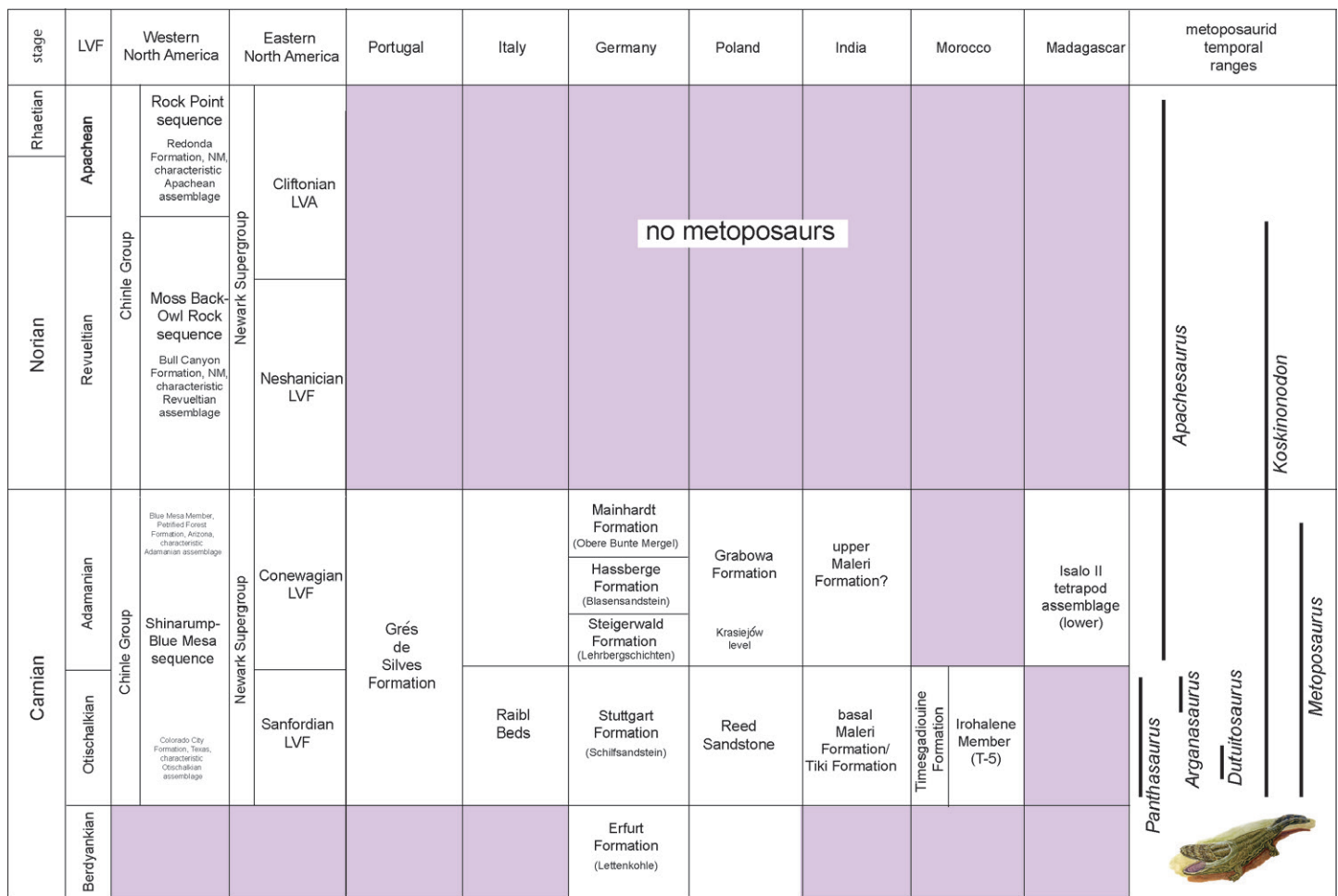


Fig. 6. Upper Triassic metoposaurid amphibian biostratigraphy (from Lucas, 2020).

- taxa in tropical Pangea. *Geobios*, <https://doi.org/10.1016/j.geobios.2021.04.002>
- Bordy, E. M., Abrahams, M., Sharman, G. R., Viglietti, P. A., Benson, R. B., McPhee, B. W., and Choiniere, J. N., 2020. A chronostratigraphic framework for the upper Stormberg Group: Implications for the Triassic-Jurassic boundary in southern Africa. *Earth-Science Reviews*, v. 203, 103120.
- Botha, J., and Smith, R. M. H., 2020. Biostratigraphy of the Lystrosaurus declivis Assemblage Zone (Beaufort Group, Karoo Supergroup), South Africa. *South African Journal of Geology* 2020, v. 123, p. 207–216.
- Botha, J., Huttenlocker, A. K., Smith, R. M., Prevec, R., Viglietti, P., and Modesto, S. P., 2020. New geochemical and palaeontological data from the Permian-Triassic boundary in the South African Karoo Basin test the synchronicity of terrestrial and marine extinctions. *Palaeogeography, Palaeoclimatology, Palaeoecology*, v. 540, 109467.
- Buchwitz, M., Klein, H., Falk, D., and Wings, O., 2019. Overview of the Permian and Triassic trackway localities in Saxony-Anhalt, Germany. In Buchwitz, M., Falk, D., Klein, H., Mertmann, D., Perl, A., and Wings, O. (eds.), 3rd International Conference of continental Ichnology, Halle 2019 – Abstract Volume and Field Trip Guide. Hallesches Jahrbuch für Geowissenschaften, B, v. 46, p. 4–5.
- Buchwitz, M., Marchetti, L., Jansen, M., Falk, D., Trostheide, F., and Schneider, J. W., 2020. Ichnotaxonomy and trackmaker assignment of tetrapod tracks and swimming traces from the Middle Permian Hornburg Formation of Saxony-Anhalt (Germany). *Annales Societatis Geologorum Poloniae*, v. 90, p. 291–320.
- Buchwitz, M., Jansen, M., Renaudie, J., Marchetti, L., and Voigt, S., 2021. Evolutionary change in locomotion close to the origin of amniotes inferred from trackway data in an ancestral state reconstruction approach. *Frontiers in Ecology and Evolution*, v. 9:674779. doi: 10.3389/fevo.2021.674779
- Chen, J., Chen, B., and Montañez, I. P., 2021. Carboniferous isotope stratigraphy. In Lucas, S. G., Schneider, J. W., Wang, X. and Nikolaeva, S. (eds.) The Carboniferous Timescale. Geological Society, London, Special Publications, 512, <https://doi.org/10.1144/SP512-2020-72>
- Citton, P., Ronchi, A., Nicosia, U., Sacchi, E., Maganuco, S., Cipriani, A., and Romano, M., 2020. Tetrapod tracks from the Middle Triassic of NW Sardinia (Nurra region, Italy). *Italian Journal of Geosciences*, v. 139, p. 309–320.
- Day, M. O., and Rubidge, B. S., 2020. Biostratigraphy of the Tapinocephalus Assemblage Zone (Beaufort group, Karoo Supergroup), South Africa. *South African Journal of Geology* 2020, v. 123, p. 149–164.
- Day, M. O., and Smith, R. M. H., 2020. Biostratigraphy of the Endothiodon Assemblage Zone (Beaufort Group, Karoo Supergroup), South Africa. *South African Journal of Geology* 2020, v. 123, p. 165–180.
- Day, M. O., and Rubidge, B. S., 2021. The late Capitanian mass extinction of terrestrial vertebrates in the Karoo Basin of South Africa. *Frontiers in Earth Science*, v. 9, 15.
- DiMichele, W. A., Bashforth, A. R., H. J. Falcon-Lang, H. J. and Lucas, S. G., 2020. Uplands, lowlands, and climate: Taphonomic megabiases and the apparent rise of a xeromorphic, drought-tolerant flora during the Pennsylvanian-Permian transition: Paleogeography, Palaeoclimatology, Paleoecology, v. 559, 109965.
- Gastaldo, R. A., Kamo, S. L., Neveling, J., Geissman, J. W., Looy, C. V., and Martini, A. M., 2020. The base of the Lystrosaurus Assemblage Zone, Karoo Basin, predates the end-Permian marine extinction. *Nature Communications*, v. 11(1), 1–8.
- Hancox, P. J., Neveling, J., and Rubidge, B. S., 2020. Biostratigraphy of the Cynognathus Assemblage Zone (Beaufort Group, Karoo Supergroup), South Africa. *South African Journal of Geology* 2020, v. 123, p. 217–238.
- Hounslow, M. W., 2021. A geomagnetic polarity timescale for the Carboniferous. In Lucas, S. G., Schneider, J. W., Wang, X. and Nikolaeva, S. (eds,) The Carboniferous Timescale. Geological Society, London, Special Publications, 512, <https://doi.org/10.1144/SP512-2020-102>
- Klein, H., and Lucas, S. G., 2021. The Triassic tetrapod footprint record. *New Mexico Museum of Natural History and Science, Bulletin* 83.
- Lloret, J., De la Horra, R., Gretter, N., Borruel-Abadía, V., Barrenechea, J. F., Ronchi, A. Diez J.B., Arche A., and López-Gómez, J., 2020. Gradual changes in the Olenekian-Anisian continental record and biotic implications in the central-eastern Pyrenean basin, NE Spain. *Global and Planetary Change*, v. 192, 103252.
- Lloret J., De la Horra R., López-Gómez J., Barrenechea J. F., Gretter N. and Ronchi A., 2021. Permian and Triassic paleosols in the fluvial lacustrine record of the central Pyrenees Basin, Spain: A stratigraphic tool for interpreting syntectonic sedimentary evolution and paleoclimate. *Newsletters on Stratigraphy*, v. 54, p. 377–404
- Lucas, S. G., 2020. Biochronology of Late Triassic Metoposauridae (Amphibia, Temnospondyli) and the Carnian pluvial episode: *Annales Societatis Geologorum Poloniae*, v. 90, p. 409–418.
- Lucas, S. G., 2021. Carboniferous tetrapod biostratigraphy, biochronology and evolutionary events. In Lucas, S. G., Schneider, J. W., Wang, X. and Nikolaeva, S. (eds.) The Carboniferous Timescale. Geological Society, London, Special Publications, 512, <https://doi.org/10.1144/SP512-2021-5>
- Lucas, S. G. and Golubev, V. K., 2019. Age and duration of Olson's Gap, a global hiatus in the Permian tetrapod fossil record: *Permophiles*, no. 67, p. 20-23.
- Lucas, S. G. and Tanner, L. H., 2021. Late Pennsylvanian calcareous paleosols from central New Mexico: implications for paleoclimate: *New Mexico Geology*, v. 43, p. 3-9.
- Lucas, S. G., DiMichele, W. A., Krainer, K., Barrick, J. E., Vachard, D., Donovan, M. P., Looy, C., Kerp, H. and Chaney, D. S., 2021a. The Pennsylvanian System in the Sacramento Mountains, New Mexico, USA: Stratigraphy, petrography, depositional systems, paleontology, biostratigraphy and geologic history: *Smithsonian Contributions to Paleobiology*, no. 104, 215 p.
- Lucas, S. G., Stimson, M. R., King, O. A., Calder, J. H. , Mansky,

- C. F., Hebert, B. L. and Hunt, A. P., 2021b. Carboniferous tetrapod footprint biostratigraphy, biochronology and evolutionary events. In Lucas, S. G., Schneider, J. W., Wang, X. and Nikolaeva, S. (eds.) *The Carboniferous Timescale*. Geological Society, London, Special Publications, 512, <https://doi.org/10.1144/SP512-2020-235>
- Lüthardt, L., Breitkreuz, C., Schneider, J.W., Gaitzsch, B., Brink, J., Stanek, K.P., Linnemann, U., Hofmann, M., Ehling, B.-C., 2020. An andesitic sill complex in the Southern Permian Basin: volcanogenetic model and stratigraphic implications. *International Journal of Earth Sciences*, v. 109, p. 2447–2466.
- Marchetti, L., Voigt, S., Lucas, S. G., Stimson, M. R., King, O. A., and Calder, J. H., 2020a. Footprints of the earliest reptiles: *Notalacerta missouriensis*—Ichnotaxonomy, potential trackmakers, biostratigraphy, palaeobiogeography and palaeoecology. *Annales Societatis Geologorum Poloniae*, v. 90, p. 271–290.
- Marchetti, L., Muscio, G., Petti, F. M., Pillola, G. L., and Zoboli, D., 2020. The Carboniferous tetrapod ichnoassociation from Italy. *Journal of Mediterranean Earth Sciences*, v. 12.
- Marchetti, L., Voigt, S., Mujal, E., Lucas, S. G., Francischini, H., Fortuny, J., and Santucci, V. L., 2020c. Extending the footprint record of *Parciasauromorpha* to the Cisuralian: earlier appearance and wider palaeobiogeography of the group. *Papers in Palaeontology*.
- Marchetti L., Francischini H., Lucas S.G., Voigt S., Hunt A.P., and Santucci V.L., 2020d. Paleozoic vertebrate ichnology of Grand Canyon National Park. In Santucci, V.L. and Tweet, J. S. (eds.), *Grand Canyon National Park: Centennial paleontological resource inventory (non-sensitive version)*. Natural Resource Report NPS/GRCA/NRR—2020/2103. National Park Service, Fort Collins, Colorado, p. 333–379.
- Marchetti, L., Ceoloni, P., Leonardi, G., Massari, F., Mietto, P., Sacchi, E., and Valentini, M., 2020e. The Lopingian tetrapod ichnoassociation from Italy, a key for the understanding of low-latitude faunas before the end-Permian crisis. *Tetrapod ichnology in Italy: the state of the art*. *Journal of Mediterranean Earth Sciences*, v. 12, p. 61–81.
- Marchetti, L., Klein, H., Falk, D., and Wings, O., 2020f. Synaptichnium tracks from the middle Muschelkalk (Middle Triassic, Anisian) Bernburg site (Saxony-Anhalt, Germany). *Annales Societatis Geologorum Poloniae*, v. 90, p. 321–330.
- Marchetti, L., Voigt, S., Buchwitz, M., MacDougall, M. J., Lucas, S. G., Fillmore, D. L., and Fröbisch, J., 2021a. Tracking the origin and early evolution of reptiles. *Frontiers in Ecology and Evolution*, v. 9, 385.
- Marchetti, L., Collareta, A., Belvedere, M., and Leonardi, G., 2021b. Ichnotaxonomy, biostratigraphy and palaeoecology of the Monti Pisani tetrapod ichnoassociation (Tuscany, Italy) and new insights on Middle Triassic Dinosauromorpha. *Palaeogeography, Palaeoclimatology, Palaeoecology*, 110235.
- Mujal, E. and Marchetti, L., 2020. Ichniotherium tracks from the Permian of France, and their implications for understanding the locomotion and palaeobiogeography of large diadectomorphs. *Palaeogeography, Palaeoclimatology, Palaeoecology*, v. 547, 109698.
- Nelson, W. J. and Lucas, S. G., 2021. The Cantabrian and Barruelian substages (Stephanian stage, Carboniferous) were never properly defined and should be dropped from formal usage: New Mexico Museum of Natural History and Science, Bulletin 82, p. 285–296.
- Opluštil, S., Cleal, C. J., Wang, J., and Wan, M., 2021. Carboniferous macrofloral biostratigraphy: an overview. In Lucas, S. G., Schneider, J. W., Wang, X. and Nikolaeva, S. (eds.) *The Carboniferous Timescale*. Geological Society, London, Special Publications, 512, <https://doi.org/10.1144/SP512-2020-97>
- Rigo, M., Onoue, T., Tanner, L. H., Lucas, S. G., Godfrey, L., Katz, M. E., Zaffani, M., Grice, K., Cesar, J., Yamashita, D., Marona, M., Tackett, L.S., Campbell, H., Tateo, F., Concheri, G., Agnini, C., Chiari, M., and Bertinelli, A., 2020. The Late Triassic extinction at the Norian/Rhaetian boundary: Biotic evidence and geochemical signature. *Earth-Science Reviews*, v. 204, 103180.
- Rößler, R., 2021. The most entirely known Permian terrestrial ecosystem on Earth – kept by explosive volcanism. *Palaeontographica, Abt. B, Palaeobotany – Palaeophytology* (in press)
- Rubidge, B. S., and Day, M. O., 2020. Biostratigraphy of the Eodicynodon Assemblage Zone (Beaufort Group, Karoo Supergroup), South Africa. *South African Journal of Geology* 2020, v. 123, p. 141–148.
- Santi, G., Marchetti, L., Schirolli, P., and Ronchi, A., 2020. The Cisuralian tetrapod ichnoassociation from Italy: from historical findings to a standard reference status. *Tetrapod ichnology in Italy: the state of the art*. *Journal of Mediterranean Earth Sciences*, v. 12, p. 39–59.
- Schneider, J.W., Lucas, S.G., Scholze, F., Voigt, S., Marchetti, L., Klein, H., Opluštil, S., Werneburg, R., Golubev, V.K., Barrick, J.E., Nemyrovska, T., Ronchi, A., Day, M.O., Silantiev, V.V., Rößler, R., Saber, H., Linnemann, U., Zharinova, V., and Shen, S.-Z., 2020. Late Paleozoic–early Mesozoic continental biostratigraphy — Links to the Standard Global Chronostratigraphic Scale. *Palaeoworld*, v. 29, p. 186–238.
- Schneider, J. W., Lucas, S. G., Scholze, F., Voigt, S., Marchetti, L., Klein, H., ... and Shen, S. Z., 2020. Late Paleozoic–early Mesozoic continental biostratigraphy—links to the standard global chronostratigraphic scale. *Palaeoworld*, v. 29, p. 186–238.
- Schneider, J.W., Legler, B., Brosig, A., Krainer, K., and Lucas, S.G., 2021a. Sedimentology and depositional environment of the Kinney Brick Quarry Fossil Lagerstätte (Missourian, Late Pennsylvanian), central New Mexico. *New Mexico Museum of Natural History and Science, Bulletin* 84, p. 93–123.
- Schneider, J.W., Scholze, F., Germann, S. and Lucas S.G., 2021b. The Late Pennsylvanian nearshore insect fauna of the Kinney Brick Quarry Fossil Lagerstätte, New Mexico. *New Mexico Museum of Natural History and Science, Bulletin*, 82, p. 255–286.
- Scholze, F., Shen, S.-Z., Backer, M., Wei, H.-B., Hübner, M., Cui, Y.-Y., Feng, Z., and Schneider, J.W., 2020. Reinvestigation of conchostracans (Crustacea: Branchiopoda) from the Permian–Triassic transition in Southwest China. *Palaeoworld*, v. 29, p. 368–390.

- Smith, R. M. H., 2020. Biostratigraphy of the Cistecephalus Assemblage Zone (Beaufort Group, Karoo Supergroup), South Africa. *South African Journal of Geology* 2020, v. 123, p. 181–190.
- Smith, R. M. H., Rubidge, B. S., Day, M. O., and Botha, J., 2020. Introduction to the tetrapod biozonation of the Karoo Supergroup. *South African Journal of Geology* 2020, v. 123, p. 131–140.
- Stack, J., Hodnett, J.-P., Lucas, S. G. and Sallan, L., 2020. Tanyrhinichthys mcallisteri, a long-rostrumed Pennsylvanian ray-finned fish (Actinopterygii) and the simultaneous appearance of novel ecomorphologies in Late Palaeozoic fishes. *Zoological Journal of the Linnean Society*, v. 2020, p. 1–28.
- Trümper, S., Gaitzsch, B., Schneider, J.W., Ehling, B.-C., Kleeberg, R., and Rößler, R., 2020a. Late Palaeozoic red beds elucidate fluvial architectures preserving large woody debris in the seasonal tropics of central Pangaea. *Sedimentology*, v. 67, pp. 1973–2012.
- Trümper, S., Schneider, J.W., Nemyrovska, T., Korn, D., Linnemann, U., Ren, D., and Béthoux, O., 2020b. Age and depositional environment of the Xiaheyan insect fauna, embedded in marine black shales (Early Pennsylvanian, China). *Palaeogeography, Palaeoclimatology, Palaeoecology*, v. 538, 109444.
- Viglietti, P. A., 2020. Biostratigraphy of the Daptocephalus Assemblage Zone (Beaufort Group, Karoo Supergroup), South Africa. *South African Journal of Geology* 2020, v. 123, p. 191–206.
- Viglietti, P. A., McPhee, B. W., Bordy, E. M., Sciscio, L., Barrett, P. M., Benson, R. B. J., ... and Choiniere, J. N., 2020a. Biostratigraphy of the Scalenodontoides Assemblage Zone (Stormberg Group, Karoo Supergroup), South Africa. *South African Journal of Geology* 2020, v. 123, p. 239–248.
- Viglietti, P. A., McPhee, B. W., Bordy, E. M., Sciscio, L., Barrett, P. M., Benson, R. B. J., ... and Choiniere, J. N., 2020b. Biostratigraphy of the Massospondylus Assemblage Zone (Stormberg Group, Karoo Supergroup), South Africa. *South African Journal of Geology* 2020, v. 123, p. 249–262.
- Voigt, S. and Fischer, J., 2020. GEOSKOP-Forschungsgrabung im südpfälzischen Zechstein. *Pollicchia Kurier*, v. 36, p. 53.
- Voigt, S., Schindler, T., Tichomirov, M., Käßner, A., Schneider, J.W., and Linnemann, U. (in review). First high-precision U-Pb age from the Pennsylvanian-Permian of the continental Saar-nahe basin, SW Germany.
- Werneburg; R., Spindler, F., Falconnet.J., Steyer, J.-S., Vianey-Liaud, M., and Schneider, J.W., 2021, in review. A new caseid synapsid from the Permian (Guadalupian) of the Lodève basin (Occitanie, France). *Palaeovertebrata*.
- Wu, Q., Ramezani, J., Zhang, H., Wang, J., Zeng, F. G., Zhang, Y. C., Liu, F., Chen, J., Cai, Y. F., Hou, Z. S., Liu, C., Yang, W., Henderson, C. M., and Shen, S. Z., 2021. High-precision U-Pb age constraints on the Permian floral turnovers, paleoclimate change, and tectonics of the North China block: *Geology*, v. 49, p. 677–681.
- Yang, W., Feng, Q., Liu, Y. Q., Tabor, N., Miggins, D., Crowley, J. L., Lin, J. Y., and Thomas, S., 2010. Depositional environments and cyclo- and chronostratigraphy of uppermost Carboniferous–Lower Triassic fluvial–lacustrine deposits, southern Bogda Mountains, NW China — A terrestrial paleoclimatic record of mid-latitude NE Pangea. *Global and Planetary Change*, v. 73, p. 15–113.
- Zouheir, T., Hminna, A., Klein, H., Lagnaoui, A., Saber, H., and Schneider, J.W., 2020. Unusual archosaur trackway and associated tetrapod ichnofauna from Irohalene member (Timezgadiouine formation, late Triassic, Carnian) of the Argana Basin, Western High Atlas, Morocco. *Historical Biology*, v. 32, p. 589–601.
- Zouicha, A., Voigt, S., Saber, H., Marchetti, L., Hminna, A., El Attari, A., Ronchi, A., and Schneider, J. W., 2021. First record of Permian continental trace fossils in the Jebilet massif, Morocco. *Journal of African Earth Sciences*, v. 173, 104015.

Q&A on the Guadalupian

Questions raised by a SPS corresponding member followed by the answers by Wu Qiong and Shen Shu-zhong

Question 1

There is a problem with the representation of the Guadalupian in *Permophiles* 68 compared with that in *Permophiles* 69 and 70.

The problem concerns the Roadian-Wordian boundary and the position of the end of the Kiaman Superchron, the 'Illawara Reversal'.

In the Permian stratigraphic framework in the Jan. 2020 issue of *Permophiles* (68, p.51) the Roadian-Wordian boundary, at the FAD of the conodont *Jinogondolella aserrata*, is placed at $268.8+/-0.5$ Ma, a date from Shen et al. 2019 (*Science China Earth Sciences* 62(1): 154-188), which is the same as that in Ramezani & Bowring 2018 (*Geol. Soc. Special Pub.* 450: 51-60), and the 'Illawara' is in the mid-Wordian, at c. 267.2 Ma.

In *Permophiles* 69 (Nov. 2020) and 70 (Jan. 2021) however, the R-W stage boundary, the FAD of *J. aserrata* and the 'Illawara' are all placed at 'c. 266.9 Ma'. These changes are attributed to Shen et al. 2020 (*Earth-Science Reviews* 211). I have looked through that paper but cannot find clear grounds for the changes, indeed, in the Abstract of that paper the 'Illawara' is said to be 'of early-middle Wordian age' which is not what appears in the timescale illustrated in those issues. Also, in that Abstract the age of the base of the Wordian is 'interpolated to be $266.9+/-0.4$ Ma', while in the Summary it is 'extrapolated' to that date. I am not sure what interpretation to put on the use of these differing terms; 'interpolated' is used in the same connection in the paper by Qiong Wu et al. (2020. *Palaeo* 3, 548) on U-Pb zircon age constraints on the Guadalupian in W. Texas.

Answer 1

The Guadalupian time scale was among the least internally constrained during the Permian. The previous R-W boundary age (268.8 ± 0.5 Ma) was interpolated based on the dates from the late Wordian (265.4 ± 0.2 Ma) and early Artinskian (288.21 ± 0.06 Ma), which have large uncertainties (Henderson et al., 2012). The new R-W boundary age (266.9 ± 0.4 Ma) is estimated based on the Guadalupian high-precision dates directly from the stratotype

area of the Guadalupian Series in Guadalupe Mountains National Park, West Texas (GMNP). The high-frequency sequences (HFSs) in the Delaware Basin, Texas and New Mexico have been studied in detail by the group of Prof. Charles Kerans (Playton and Kerans, 2018 and references therein). Wu et al. (2020) estimated average duration of 440 ± 12 kyr for each HFS based on dates from the top of the Rader Limestone Member and the basal part of the South Wells Member in the GMNP. It is unclear whether the HFSs in the GMNP represent eccentricity cycles (Shen et al., 2020), which will have a duration of 405 kyr for each HSF. As the current R-W boundary is placed on the top of the Getaway Member, one HFS below the high-precision date from the basal part of the South Wells Member (ca. 266.5 Ma) (Wu et al., 2020), the boundary age can be estimated at 266.9 ± 0.4 Ma, no matter the duration for each HSF is ca. 440 kyr or 405 kyr. And the error is constrained by the duration of the HSF as well, which is about 0.4 Ma as shown above.

As the R-W boundary is below the high-precision dates used to estimate it, 'extrapolated' might be more appropriate here. However, as the boundary horizon is quite close to those dates, 'extrapolated' or 'interpolated' will make no difference in this case.

Steiner (2006) positioned the Illawara Reversal (IR) in the backreef upper Grayburg Formation or the lowermost part of the overlying Queen Formation. This interval is correlated to the HFSs of G12-G13 (Playton and Kerans, 2018), and thus the IR can be constrained to the latest Roadian to earliest Wordian (267.4 ± 0.4 Ma to 266.5 ± 0.3 Ma) based on the present horizon of the Wordian GSSP at the Gateway Lodge Section in the GMNP. Thus, we put the IR close to the basal boundary of the Wordian in the figures to show the possible age constraints based on data in West Texas. Solid age constraints for the IR have not been obtained yet as reviewed in Section 6.4 in Shen et al. (2020). Recent fossil materials show that *Jinogondolella aserrata* may range downward into the Cherry Canyon Sandstone at the present GSSP section at the Gateway (Yuan et al., 2020), which may put the IR to the early to middle Wordian based on the new fossil data. Besides, Hounslow and Balabanov (2018) noted a possible short normal magnetic interval in the Roadian. If this normal interval is confirmed in future, the beginning of IR may become more complicated.

Question 2

There is a lot in these 2020 papers about uncertainties in conodont distribution in the Guadalupian stratotypes (in the USA). However, it seems that the differences in the representation of the chronology of part of the Guadalupian chronostratigraphy between *Permophiles* 68 and the two most recent issues need more than a passing reference to a publication in the captions for the SPS Permian stratigraphic frameworks in issues 69 and 70.

Answer 2

The Guadalupian conodont biostratigraphy in GMNP still needs more work. The detailed conodont biostratigraphic data at the Frijoles Section with a high-precision date (Shen et al., 2020) will be published later. And these uncertainties will have little impact on the basal Capitanian age, because the Capitanian GSSP

is constrained in the HSF of G20.

The recent fossil materials show that *Jinogondolella aserrata* may range downward into the Cherry Canyon Sandstone at the present GSSP section (Yuan et al., 2020). These uncertainties in conodont distribution in the Guadalupian stratotypes may indeed change the boundary ages if the Wordian GSSP position is revised officially in future. The boundary ages published in the recent papers are all based on the present GSSP positions.

Question 3

I hope SPS can give some guidance or clarification on this matter. The version of the Roadian-Wordian and 'Illawara' relationships in *Geologic Time Scale 2020* (vol.2: 875-902) by Henderson and Shen (who are both among the authors of the 2020 papers referred to above) corresponds with that in *Permophiles* 68, **not that in the two more recent issues**.

Answer 3

We are sorry that the GTS 2020 was actually ready to publish before those papers were published.

References

- Henderson, C. M., Davydov, V. I., Wardlaw, B. R., Gradstein, F. M., and Hammer, O., 2012. Chapter 24 - The Permian Period. In Gradstein, F. M., Ogg, J. G., Schmitz, M. D., and Ogg, G. M., (eds.), *The Geologic Time Scale*. Elsevier, Boston, p. 653–679.
- Hounslow, M. W., and Balabanov, Y. P., 2018. A geomagnetic polarity timescale for the Permian, calibrated to stage boundaries. Geological Society, London, Special Publications, v. 450, no. 1, p. 61–103.
- Playton, T. E., and Kerans, C., 2018. Architecture and genesis of prograding deep boundstone margins and debris-dominated carbonate slopes: examples from the Permian Capitan Formation, Southern Guadalupe Mountains, West Texas. *Sedimentary Geology*, v. 370, p. 15–41.
- Shen, S. Z., Yuan, D. X., Henderson, C. M., Wu, Q., Zhang, Y. C., Zhang, H., Mu, L., Ramezani, J., Wang, X. D., Lambert, L. L., Erwin, D. H., Hearst, J. M., Xiang, L., Chen, B., Fan, J. X., Wang, Y., Wang, W. Q., Qi, Y. P., Chen, J., Qie, W. K., and Wang, T., 2020. Progress, problems and prospects: An overview of the Guadalupian Series of South China and North America. *Earth-Science Reviews*, v. 211, p. 103412.
- Steiner, M. B., 2006. The magnetic polarity time scale across the Permian-Triassic boundary. Geological Society, London, Special Publications, v. 265, no. 1, p. 15–38.
- Wu, Q., Ramezani, J., Zhang, H., Yuan, D. X., Erwin, D. H., Henderson, C. M., Lambert, L. L., Zhang, Y. C. and Shen, S. Z., 2020. High-precision U-Pb zircon age constraints on the Guadalupian in West Texas, USA. *Palaeogeography, Palaeoclimatology, Palaeoecology*, v. 548, p. 109668.
- Yuan, D. X., Shen, S. Z., Henderson, C. M., Lambert, L. L., Hearst, J. M., Zhang, Y. C., Chen, J., Qie, W. K., Zhang, H., Wang, X. D., Qi, Y. P. and Wu, Q., 2020. Reinvestigation of the Wordian-base GSSP section, West Texas, USA. *Newsletters on Stratigraphy*, v. 54, no. 3, p. 301–315.

New age data for Permian strata on the Mogollon Rim, central Arizona, USA

Spencer G. Lucas

New Mexico Museum of Natural History, 1801 Mountain Road NW, Albuquerque, New Mexico 87104 USA

Email: spencer.lucas@state.nm.us

Charles M. Henderson

Department of Geoscience, University of Calgary, Calgary, Alberta, Canada T2N 1N4

Email: cmhender@ucalgary.ca

Darton (1910) introduced the term Supai Formation to refer to a relatively thick (at least 425 m) succession of upper Paleozoic siliciclastic red beds (with minor carbonate and gypsum interbeds) exposed across much of northern Arizona, especially in the Grand Canyon. Noble (1922) subsequently removed the upper 80-100 m of the Supai Formation and named it the Hermit Shale, a unit later well known to have an extensive paleoflora and tetrapod footprint assemblages of Early Permian age in the Grand Canyon (e.g., White, 1929; Marchetti et al., 2021). McKee (1975, 1982), working primarily in the Grand Canyon, regarded Supai as a group that includes Pennsylvanian and Permian strata, primarily of nonmarine origin, but with some age constraints provided by the biostratigraphy of intercalated marine strata. However, to the south of the Grand Canyon, along the Mogollon Rim (which is the southwestern edge of the Colorado Plateau: Fig. 1), strata assigned to the Supai Group (Formation) have only one marine intercalation and fewer age constraints.

Fieldwork by us in 2018-2019 has produced important new age constraints for Supai strata along the Mogollon Rim. The

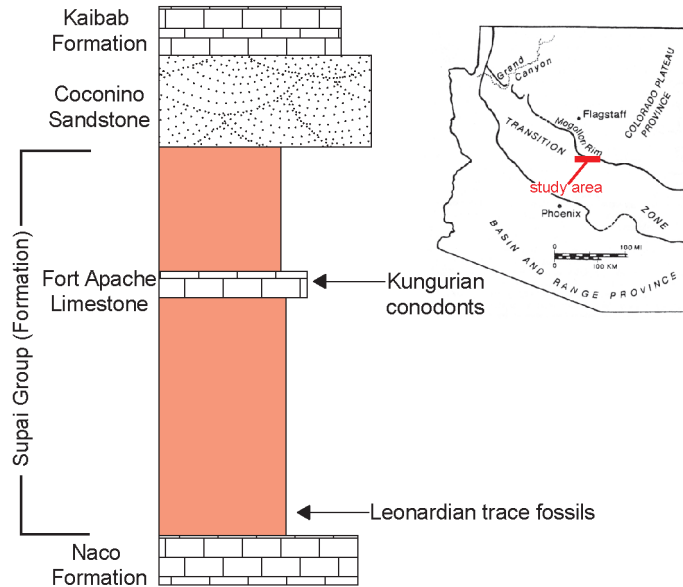


Fig. 1. Index map and generalized Permian stratigraphic section along the Mogollon Rim, Arizona, USA showing the two new biostratigraphic datums in the Supai Group established by recent field research.

upper Paleozoic strata exposed along the Mogollon Rim have a complex lithostratigraphic nomenclature not agreed on (e.g., Blakey, 1979, 1989; Peirce, 1977, 1989), and we present a generalized lithostratigraphy here that is well accepted (Fig. 1). Supai Group strata along the Mogollon Rim are 520-550 m thick. Marine strata of the Naco Formation below the Supai Group red beds yield fusulinids and macroinvertebrates (primarily brachiopods) that indicate an age range of Middle-Late Pennsylvanian (Atokan-Virgilian) (e.g., Huddle and Dobrovolny, 1945; Brew, 1965, 1979). Based on this, most workers have considered the Naco-Supai contact to be an approximation of the Pennsylvanian-Permian boundary (e.g., Eagar and Peirce, 1993), but Brew (1965, 1979) considered the contact highly diachronous, ranging in age from late Desmoinesian to latest Virgilian.

Our work establishes two important new age datums in the Supai Group section along the Mogollon Rim:

1. In the Tonto Creek area south of Payson, siliciclastic reds beds of the lower part of the Supai Formation yield tetrapod footprints and other trace fossils from strata 19-21 m above the stratigraphically highest marine limestone of the underlying Naco Formation (Lucas et al., 2019). The trace fossils are from a stratigraphic interval 2-3 m thick of laminated sandstone beds, and a low diversity walchian-conifer-dominated paleoflora with minor, diminutive *Supaia*, is associated with the trace fossils. The invertebrate trace fossils are mostly assignable to *Planolites*, *Sphaerapus* (Fig. 2), *Diplichnites* and *Taenidium*. The tetrapod footprints are mostly those of non-diapsid eureptiles (the “captorhinomorph” ichnogenera *Erpetopus* and *Varanopus*), small parareptiles or diapsids (*Dromopus*) and seymouriamorphs (*Amphisauropus*) (Fig. 2).

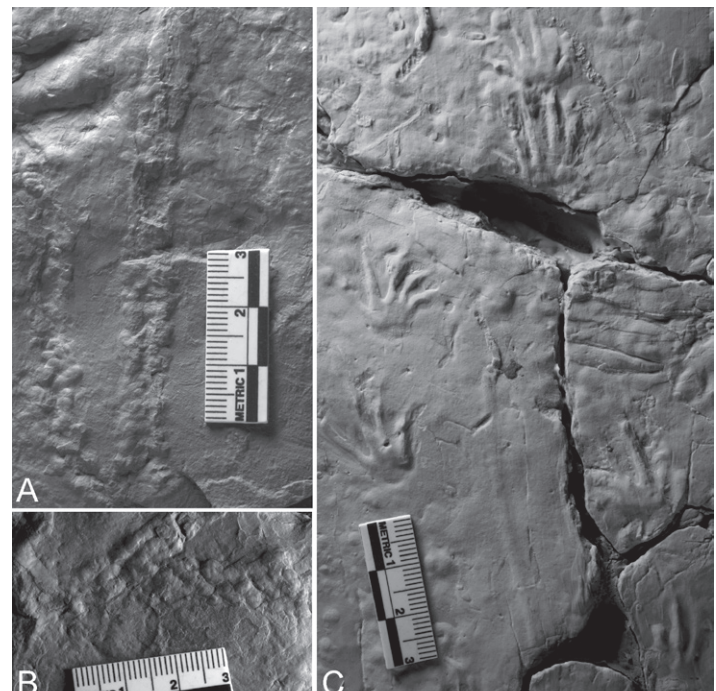


Fig. 2. Leonardian trace fossils from near the base of the Supai Group in the Tonto Creek area, Arizona. A-B, *Sphaerapus*, compaction burrows. C, *Varanopus*, part of trackway.

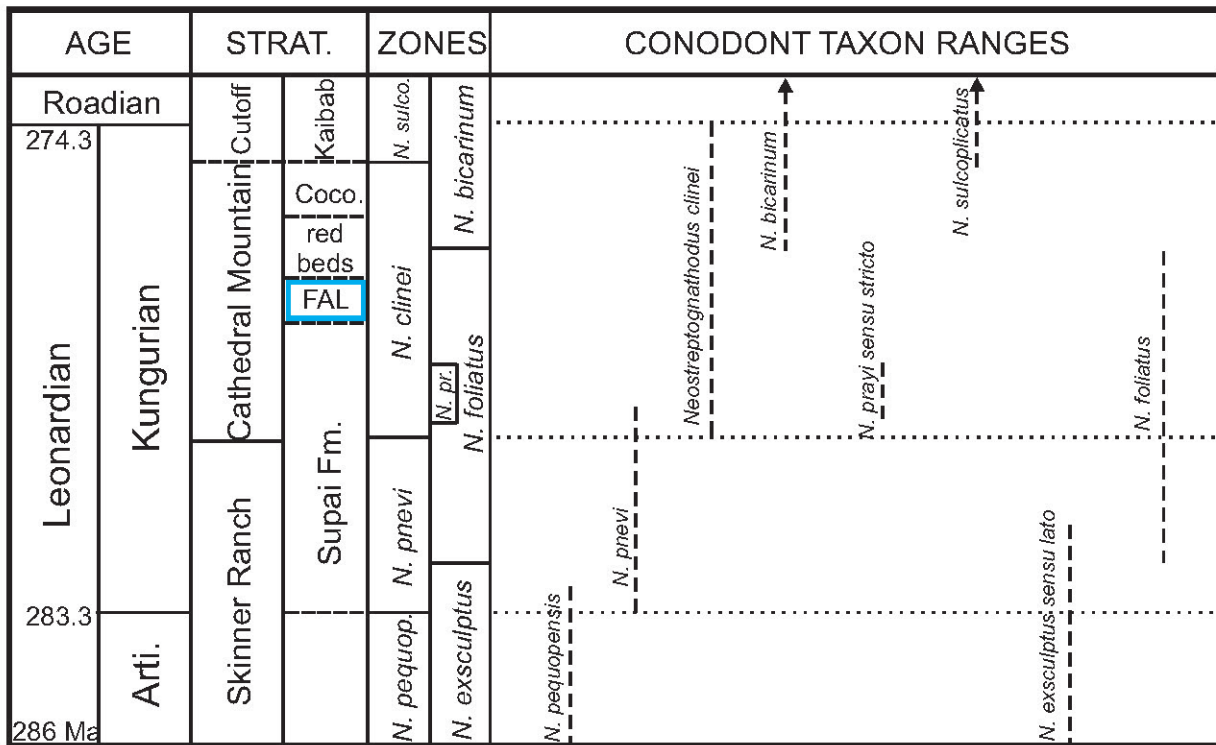


Fig. 3. Biostratigraphic ranges of Leonardian (upper Artinskian to Kungurian) conodont taxa. Ranges modified from Wardlaw and Nestell (2019). The blue box indicates the biostratigraphic correlation of the Fort Apache Limestone (FAL). Coco. = Coconino Fm.; Arti. = Artinskian.

These are footprints of the *Erpetopus* biochron, globally no older than Kungurian and no older than early Leonardian in New Mexico and Texas (e.g., Voigt and Lucas, 2018). The subsurface compaction burrow *Sphaerapus* is also not known from strata older than Leonardian (Lucas et al., 2013). This means that the tracksite is no older than early Leonardian, so that all or almost all of the Supai Group strata along the Mogollon Rim are of Leonardian age; thus, a Wolfcampian stratigraphic interval is very thin (if even present) in this area. Furthermore, assigning an early Leonardian age to strata near the base of the Supai Group on the Mogollon Rim indicates that some previous correlations of Pennsylvanian strata (e.g., Wescogame Formation) of the Supai Group in the Grand Canyon to the lower Supai Group along the Mogollon Rim are questionable.

2. The Fort Apache Limestone (FAL) is a carbonate interval less than 20 m thick in the upper part of the Supai Group section along the Mogollon Rim (Fig. 1). Nine samples were collected in the Payson area for conodonts. Six of these have been fully processed, and all were productive, but the species and number of specimens vary considerably. For this report, three samples (FAL1, 3, 5) were collected near the base of the FAL from two localities, and three samples (FAL 4, 8, 9) were collected near the top of the FAL sections. The lower samples include the following taxa: *Neostreptognathodus foliatus* (excellent growth series), *N. clinei* (excellent growth series), *Diplognathodus* sp., *Hindeodus* sp. (rare juveniles), *Ellisonia* sp. (rare), *Sweetognathus* aff. *huecoensis* (gerontic form), and *Gullodus?* sp. (rare). The upper samples had fewer specimens, and *Hindeodus* sp. and *Ellisonia* sp. were more common, which would be consistent with a

shallower depositional setting, suggesting a shoaling upward succession. The upper samples did contain a few specimens of *Neostreptognathodus foliatus* and *N. clinei* (transitional with *N. bicarinum*), indicating the same biozonal level for the lower and upper sample sets.

The ranges and taxonomic identification of these taxa are still debated (Henderson, 2018), but in general this assemblage indicates a mid-late Kungurian age (not latest) as shown in Figure 3. The specimens referred to *N. foliatus* have normally been referred to *N. prayi* based on specimens first illustrated by Behnken (1975), but the holotype of *N. prayi* (plate 2, fig. 19 in Behnken, 1975) is very different, with a moderately deep sulcus and a shape homeomorphic with the Pennsylvanian to early Sakmarian genus *Adetognathus*. This form has been recovered from the Yeso Group in SE New Mexico (manuscript in preparation). Paratypes of *N. prayi* illustrated by Behnken (1975; plate 2, figs. 14, 18) have no sulcus and bear transverse ridges that connect centrally on the platform; these specimens are identical to those illustrated from the Fort Apache Limestone (Fig. 4) and from the upper Skinner Ranch and lower Cathedral Mountain formations in West Texas (Wardlaw and Nestell, 2019, fig. 12.25 and 12.26 = their *N. prayi*). Specimens illustrated by Wardlaw and Nestell (2019) as *N. foliatus* and *N. exsculptus* (see also Lara-Pena et al., 2020) with flat transverse ridges separated by a narrow, but steep margined sulcus, are collectively referred to as *N. exsculptus* sensu lato. The first occurrence of *Neostreptognathodus pnevi* is proposed to define the base of the Kungurian (Henderson, 2018). It is interpreted as the descendent of *N. pequopenensis* by reduction of the anterior denticles to

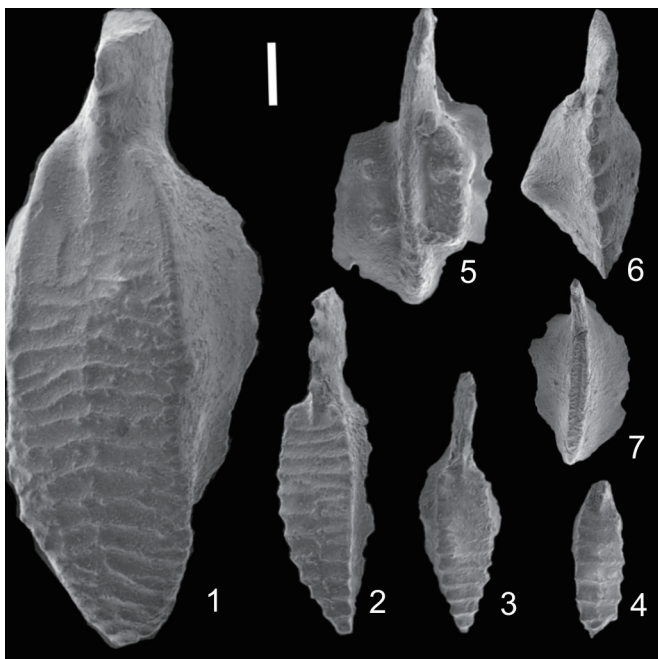


Fig. 4. Some key conodont taxa from the lower Fort Apache Limestone. Scale bar is 200 micrometres.

- 1-4. *Neostreptognathodus foliatus*, upper views of growth series, FAL1.
 5. *Sweetognathus* aff. *huecoensis*, upper view, FAL3.
 6. *Gullodus?* sp., upper view, FAL3.
 7. *Neostreptognathodus clinei*, upper view, FAL3.

smooth ridges on the platform margins or parapets. This trend continues with the full reduction of platform denticles (*N. clinei*) and shortening and narrowing of one parapet (*N. bicarinum*; this species was named by Wardlaw [2000] as *Sweetognathus bicarinum*, so this is a new combination).

Above the Fort Apache Limestone are ~ 150 m of red beds, overlain by the Coconino Sandstone (Fig. 1), which represents an erg that extended from northwestern Arizona to central New Mexico (in New Mexico, the Coconino-equivalent strata are termed the Glorieta Sandstone). The Coconino has an extensive trace fossil record that includes tetrapod footprints of the *Erpetopus* biochron (Marchetti et al., 2021). The overlying Kaibab Formation (Limestone) has yielded conodonts and brachiopods from its lower strata considered late Leonardian (late Kungurian) in age (e.g., Wardlaw and Collinson, 1978; Hopkins, 1990), and we are planning to further sample the Kaibab for conodonts to refine the age assignment.

Further work is planned on the Mogollon Rim and will aim to obtain more precise ages for the interval of upper Naco through Kaibab based on trace fossils, conodonts and any other biostratigraphically useful data that can be collected.

References

- Behnken, F. H., 1975. Leonardian and Guadalupian (Permian) conodont biostratigraphy in western and southwestern United States. *Journal of Paleontology*, v. 49, p. 284–315.
- Blakey, R. C., 1979. Stratigraphy of the Supai Group (Pennsylvanian-Permian), Mogollon Rim, Arizona. In Beus, S. S. and Rawson, R. R. (eds.) Carboniferous stratigraphy in the Grand Canyon country northern Arizona and southern Nevada. American Geological institute, Selected Guidebook Series No. 2, p. 89–104.
- Blakey, R. C., 1989. Pennsylvanian and Permian geology of Arizona. In Jenney, J. P. and Reynolds, S. J. (eds.) Geologic evolution of Arizona. Tucson, Arizona Geological Society Digest 17, p. 313–347.
- Blakey, R. C., 1990. Stratigraphy and geologic history of Pennsylvanian and Permian rocks, Mogollon Rim region, central Arizoan and vicinity. *Geological Society of America Bulletin*, v. 102, p. 1189–1217.
- Brew, D. C., 1965. Stratigraphy of the Naco Formation (Pennsylvanian) in central Arizona. Ph. D. thesis, Ithaca, Cornell University, 204 pp.
- Brew, D. C., 1979. Biostratigraphy of the Naco Formation (Pennsylvanian) in central Arizona. In Beus, S. S. and Rawson, R. R. (eds.). Carboniferous stratigraphy in the Grand Canyon country northern Arizona and southern Nevada. American Geological institute, Selected Guidebook Series No. 2, p. 119–125.
- Darton, N. H. 1910. A reconnaissance of parts of northwestern New Mexico and northern Artzona. U. S. Geological Survey Bulletin 435, 88 pp.
- Eagar, R. M. C. and Peirce, H. W., 1993. A nonmarine pelecypod assemblage in the Pennsylvanian of Arizona and its correlation with a horizon in Pennsylvania. *Journal of Paleontology*, v. 67, p. 61–70.
- Henderson, Charles M., 2018. Permian Conodont Biostratigraphy. In Lucas, S. G. & Shen, S. Z. (eds) The Permian Timescale. Geological Society, London, Special Publications, v. 450, p. 119–142.
- Hopkins, R. L., 1990. Kaibab Formation. In Beus, S. S. and Morales, M. (eds.). Grand Canyon geology. New York, Oxford University Press, p. 225–245.
- Huddle J. W. and Dobrovolny, E., 1945. Late Paleozoic stratigraphy of central and northeastern Arizona. U. S. Geological Survey Oil and Gas Investigations Preliminary Chart 10.
- Lara-Pena, R. A., Navas-Perejo, P., Amaya-Martinez, R., 2020. New conodont data related to the western Ouachita-Marathon-Sonora orogeny: age of the autochthonous Laurentian deformation. *Journal of South American Earth Sciences*, doi: <https://doi.org/10.1016/j.jsames.2020.102763>.
- Lucas, S. G., Voigt, S., Lerner, A. J and Rainforth, E. C., 2013. *Sphaerapus*, a poorly known invertebrate trace fossil from nonmarine Permian and Jurassic strata of North America. *Ichnos*, v. 20, p. 142–152.
- Lucas, S. G., Olson, T. J., Ludlow, B. and Rogers, J. B., 2019. Arizona's oldest extensive Permian tracksite and its stratigraphic significance. *Geological Society of America Abstracts with Programs*, v. 51, no. 5, doi: 10.1130/abs/2019AM-336596.
- Marchetti, L., Francischini, H., Lucas, S. G., Voigt, S., Hunt, A. P. and Santucci, V. L., 2021. Paleozoic vertebrate ichnology of Grand Canyon National Park. Utah Geological Association

- Special Publication 1, p. 171–204.
- McKee, E. D., 1975. The Supai Group—subdivision and nomenclature. U. S. Geological Survey Bulletin 1395-J, 11 pp.
- McKee, E. D., 1982. The Supai Group of Grand Canyon. U. S. Geological Survey, Professional Paper 1173, 504 pp.
- Noble, L. F., 1922. A section of the Paleozoic formations of the Grand Canyon at the Bass trail. U. S. Geological Survey Professional Paper 131, p. 23–73.
- Peirce, H. W., 1977. Survey of uranium favorability of Paleozoic rocks in the Mogollon Rim and slope region—east central Arizona. State of Arizona Bureau of Geology and Mineral Technology Circular 19, 60 pp.
- Peirce, H. W., 1989. Correlation problems of Pennsylvanian-Permian strata of the Colorado Plateau of Arizona. In Jenney, J. P. and Reynolds, S. J. (eds.) Geologic evolution of Arizona. Tucson, Arizona Geological Society Digest 17, p. 349–368.
- Voigt, S. and Lucas, S. G., 2018. Outline of a Permian tetrapod footprint ichnostratigraphy. In Lucas, S. G. and Shen, S. Z. (eds.), The Permian timescale: Geological Society, London, Special Publications v. 450, p. 387–404.
- Wardlaw, B. R., 2000. Guadalupian conodont biostratigraphy of the Glass and Del Norte Mountains. In Wardlaw, B.R., Grant, R.E., and Rohr, D.M. (eds.), The Guadalupian Symposium, Smithsonian Institution Press, p. 37–87.
- Wardlaw, B. R. and Collinson, J. S., 1978. Stratigraphic relations of Park City Group (Permian) in eastern Nevada and western Utah. American Association of Petroleum Geologists Bulletin, v. 62, p. 1171–1184.
- Wardlaw, B. R. and Nestell, M. K., 2019. Conodont biostratigraphy of Lower Permian (Wolfcampian-Leonardian) Stratotype sections of the Glass and Del Norte Mountains, West Texas, USA. In Ruppel, S.C. (ed.), Anatomy of a Paleozoic basin: the Permian Basin, USA (vol. 1, ch. 8), AAPG Memoir 118, p. 229–249.
- White, D., 1929. Flora of the Hermit Shale, Grand Canyon, Arizona. Carnegie Institution of Washington Publication 405, 221 pp.



Fig. 1. Location of the upper Pennsylvanian to ?Lower Triassic outcrops in SW Sardinia. Overlapping circles mean the formation units superpose on each other conformably.

known outcrops, and stratigraphic and thin section analysis of newly found outcrops have allowed the delineation of the history of the late to post-Variscan successions in SW Sardinia.

Geological Framework

In SW Sardinia over the Variscan basement, the succession starts unconformably with the upper Pennsylvanian limnic San Giorgio Fm. (Lower Rotliegend), formed mainly by alternations of coarse- to medium-grained siliciclastics. Fine siliciclastics are subordinated. Scattered intercalations of carbonates (mainly in the San Giorgio locality lower part) and volcanic rocks (in the Guardia Pisano locality upper part) are present (Barca and Costamagna, 2003a; Costamagna, 2019). The unit was deposited in a narrow warm-wet alluvial-to-lacustrine early collapse basin. The small 25 km-distant NW upper Pennsylvanian Tappa Niedda outcrop (Barca et al., 1994) records a succession about 14 m thick made up of conglomerates and sandstones (Costamagna and Barca, 2008), and is lithologically similar to the San Giorgio Fm. This outcrop testifies to the presence of contemporaneous limnic basins in SW Sardinia, possibly evolving later in the nearby Triassic Is Arenas basin (Costamagna and Barca, 2002).

The Lower – Middle (?) Permian red bed Guardia Pisano Fm. (Upper Rotliegend) follows: pelites, sandstones, and rare conglomerates are represented (Barca and Costamagna, 2006; Costamagna, 2019). Volcanic rocks occur in the coarser deposits as cm-sized pebbles of lavas and pyroclastic rocks. The unit was

Upper Pennsylvanian, Permian, and Lower? Triassic continental successions in SW Sardinia (Italy): a petro-sedimentological update of the molassoid Sulcis basin

Luca G. Costamagna

Dipartimento di Scienze Chimiche e Geologiche, Cittadella Universitaria, Blocco A, 09042 Monserrato (CA)

Introduction

In the SW Sardinia Sulcis-Iglesiente area, the continental late to post-Variscan upper Pennsylvanian, Permian, and Triassic successions are thin, fragmentary, restricted, and scattered (Fig.1). They are rarely superimposed on each other. So, the reconstruction of the sedimentary evolution of the basin as a whole depositional unit is difficult. More detailed stratigraphical-sedimentological analysis and investigations of historically

deposited in a warm-subarid alluvial, sinuous environment of mid-to low-energy.

The Guardia Pisano Fm. is followed by the Upper Permian - Lower Triassic red bed s.l. Rio Is Corras Fm. (Sardinian Buntsandstein Group?) (Costamagna and Barca, 2002; Barca and Costamagna, 2003b, Costamagna, 2019). This unit is formed by conglomerates and carbonates with rare sandstones, reddish pelites, and evaporites. The conglomerates contain dm-sized pebbles from the older upper Pennsylvanian-Permian deposits below. This unit was deposited in a warm(hot?)-arid fan-delta to lake environment of variable energy. The passage to the restricted marine Muschelkalk Campumari Fm. (Costamagna and Barca, 2002; Barca and Costamagna, 2003b) follows rapidly, marked by a possible weak unconformity (?). Stratigraphic type-sections have been described for all the mentioned units (Costamagna and Barca, 2002; Barca and Costamagna, 2003a, b, 2006).

In all SW Sardinia, scattered and isolated thin covers of pebbly to sandy red beds deposits referable to the Guardia Pisano Fm. or the Rio Is Corras Fm. are often unconformably deposited on the Lower Cambrian carbonates, these latter during Late Paleozoic times forming residual low reliefs all through the final peneplaning of the Variscan chain (Sinisi et al., 2014; Costamagna, 2019). Examples are known in all of SW Sardinia (e.g., from N to S: Planu Sartu mine, Baueddu, Sa Bagattu, Barega mine, Barbusi mine, Terraseo breccias: Pasci et al., 2016, and references therein). Their origin is variable, and sometimes even their age (Permian or Caenozoic?) is controversial (Moore McMahon, 1972). Some of them are red bed deposits filling partially through sinkholes and open fractures the upper karstic network developed underground in the Lower Cambrian carbonate rocks during late-to post-Variscan times (Bechstadt, 1983; de Waele et al., 2001). Others were simply part of a superficial alluvial cover that, due to the following tectonic events, are now squeezed and trapped between carbonate tectonic wedges of later age. A graphic history of those events in the collapsing Variscan chain frame is summarized in Costamagna, 2019 (Fig. 2).

Key sections: sedimentology

Along the SS130 motorway by-pass circling the outskirts of Iglesias, a peculiar San Giorgio basin stratigraphic section about 8 m thick is exposed on the roadcut (Fig. 3). This section shows in its lowest part significant differences if compared with the typical San Giorgio Fm. succession. It rests unconformably over the Variscan basement, and it starts through about 1 m of petromict clast-supported conglomerates made of well-rounded cm-sized quartz pebbles and rare lydites, and crushed fragments of metamorphic rocks forming a false matrix: the mutual percentage of those components is about 50%. This basal level peters out W-ward and is followed by 6 m of well-bedded, locally wavy- and cross-bedded, grey-yellowish medium- to coarse-grained quartz-rich marly sandstones -sandy dolostones with rare intercalations of cm-thick beds of graded dolostone microbreccias with erosive base. The section is terminated by about 1.5 m of grey carbonate sandstones and microconglomerates-microbreccias in coarsening-upward beds with an erosive base. These rudites are frequently matrix-supported and texturally immature.

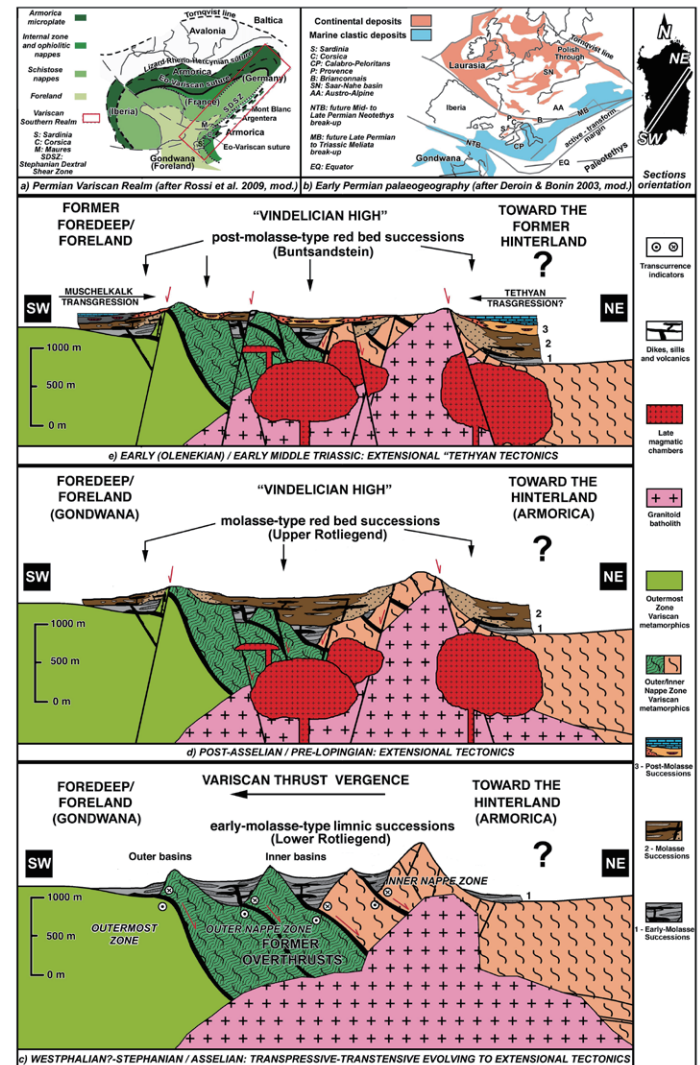


Fig. 2. Schematic comparison of the different evolutive stages of the Sardinian Pennsylvanian to lower Middle Triassic continental basin and their location in respect to the (a) general geodynamic and (b) palaeogeographic context. Scale and thicknesses are only indicative; the feeding of the late- extensional volcanic rocks is not fully represented in figures. (c) Pennsylvanian (?Westphalian–Stephanian) to Cisuralian (Asselian): limnic basins during transtensive/transpressive regime. Late-tectonic granitoids cut the former tectonic structures. (d) Guadalupian (post-Asselian) to Lopingian(?): red-bed basins. Basins open up, coalesce and their bottoms collapse: orographic barriers no longer exist and local climate changes from humid to dry. The Variscan peneplain develops. Post-tectonic intrusions take place. (e) Early Triassic (Olenekian?) – early Middle Triassic (late Anisian, Pelsonian–Illyrian boundary): Alpine red-bed basins, thin and rapidly submerged by the marine Muschelkalk transgression. From Costamagna, 2019, modified.

At Guardia Pisano the upper San Giorgio Fm. is finer than the lower one outcropping in the San Giorgio basin. The dark-grey limnic, thinly laminated, pelitic deposits with intercalated volcanic rocks, marl and carbonate bed of the upper San Giorgio Fm. are covered, through a weak but sharp unconformity, by

the sandstones of the Guardia Pisano Fm red beds (Fig. 3, 4A). Nonetheless, the Guardia Pisano Fm. contains here still rare thin beds of grey-reddish siliciclastics.

The new red bed outcrops found in the San Giorgio basin area (Iglesias) represent a missing stratigraphic link (Fig. 3, 4B). Here at Case Massidda - Case Lai the Rio Is Corras Fm. carbonate pebbles-rich conglomerates embedding rare thin calcrete beds are conformably posed through a gradual, alternated boundary over red bed tight metric alternations of massive, rarely laminated pelites, microbial carbonates with fenestral structures, evaporites, and subordinated cm-to dm-thick beds of sandstones and matrix-rich microbreccias with no carbonate pebbles; mud cracks and halokinetic folds are also visible. The well-exposed thickness of the whole succession is about 30 m, but there remains about 30 meters more of the Rio Is Corras Fm., poorly visible due to the vegetation cover. These deposits represent the lower-energy upper phase of the alluvial red bed Guardia Pisano Fm. Pedogenization evidence is here present too. The lowest part of this succession is hidden by the Campo Pisano mine waste cover.

This transition from the Guardia Pisano Fm. red beds to the

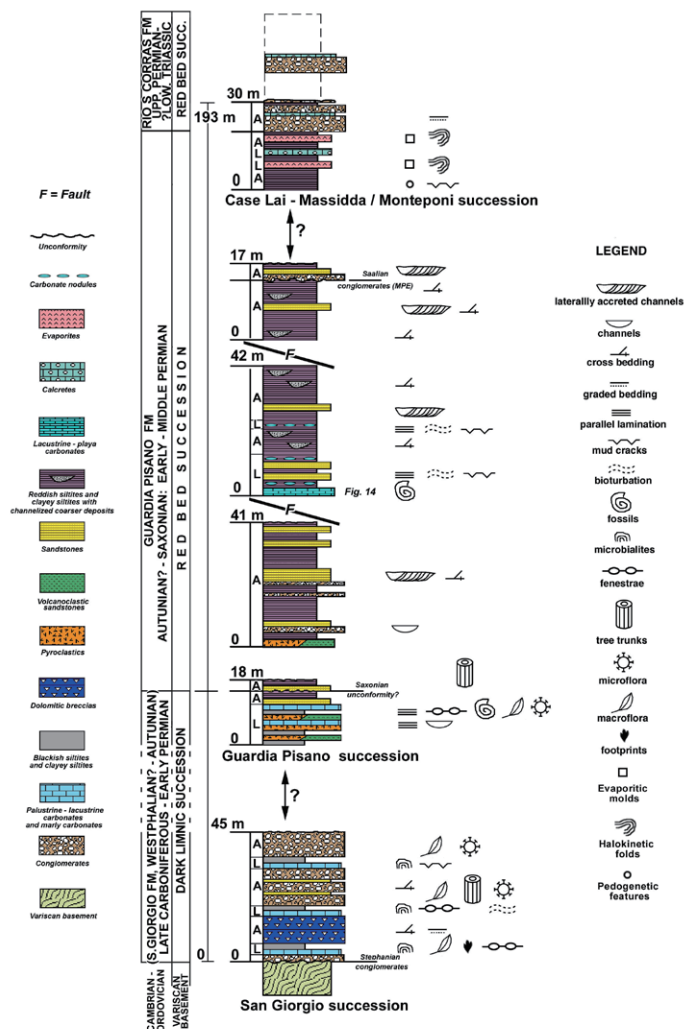


Fig. 3. Lithostratigraphic reconstruction of the late Pennsylvanian to ?Early Triassic Sulcis basin succession in SW Sardinia. A, alluvial deposits; L, lacustrine to playa deposits.

Rio Is Corras Fm. calcretes and oligomict conglomerates is also visible on a roadcut along the Iglesias-Gonnese motorway, close to the Monteponi mine waste cover and the Laveria Mameli mining building (Fig. 4C): here, about 20 m of well-bedded alternations of red pelites, calcretes, evaporites, and very rare matrix-supported breccias rest unconformably over the Variscan basement and are followed conformably by not more than 3 meters of coarse carbonate pebbles-rich conglomerates and calcretes.

2 km E to Iglesias are small sparse outcrops of oligomict conglomerates formed by Cambrian carbonate pebbles and referable to the Rio Is Corras Fm. resting over the Variscan basement.

In the Planu Sartu mine area, in the Lower Cambrian carbonates (Bechstadt and Boni, 1994, and reference therein) is evident an extensive karstic network, whose chaotic filling framework is made of Lower Cambrian carbonate boulders and cobbles: they are interpreted as collapse breccias. The breccia internal cavities are filled by red bed parallel- to cross-laminated sandstones forming internal sediments. Upwards, the breccia framework decreases in volume and element size and conversely, the sandy matrix percentage grows up. Next to the Planu Sartu gallery crop out well-bedded to laminated reddish sandy to silty-clayey deposits, organized in fining-upwards couplets, and showing in the sandstones parallel laminations, flute-casts, groove-casts, and parting lineations (Fig. 4D). These deposits rest over a coarse poorly-sorted calcite-cemented breccia made of Variscan basement highly-weathered schist pebbles and cobbles. This breccia lies over the coarse carbonate cave speleothem formed by Lower Cambrian carbonate boulders. This red bed matrix-rich breccia setup is not uncommon in SW Sardinia (Baueddu, Terraseo).

Southwards, the Sa Bagattu outcrop (Brusca et al., 1968), resting unconformably over the Lower Cambrian carbonates, is very small (about 100 m²) and about two meters thick: it is formed mainly by oligomict heterometric breccias built of cm- to dm-sized angular fragments of carbonates, quartz, lidite, chert, and rare barite. The pebbles are embedded in a yellowish-gray to reddish dolomitic-sandy matrix and show a mainly quartzose cement: dolomite as cement is very rare. The carbonate-rich matrix may contain small cavities lined by acicular crystals (dissolution of former evaporitic minerals?). According to Brusca et al. (1968) these deposits cover the barite clast-rich red beds filling the carbonate karstic network and a limited, superficial thickness of Lower Cambrian silicified carbonates. Above and laterally, the carbonate breccias pass to a coarse reddish-grey sandstone-petromict microconglomerate, thickly bedded and quartz-cemented. Pebbles of this lithofacies have been found in the Rio Is Corras Fm conglomerates.

One kilometer eastward, at Monte Barega, Bechstädt (1983) reports the finding of burrows (continental *Scyenia* icnofacies) and *Equisetales* prints, in red bed sandstone boulders from karstic filling and showing mud-cracks. These sediments were supposed to have fallen from subaerial environments through wide fractures and were deposited in karstic cavities during the Permian-Triassic? surfacing of the Variscan basement (Bechstadt and Boni, 1994).



Fig. 4. Stratigraphic transition locations: A) San Giorgio Fm. - Guardia Pisano Fm., Guardia Pisano area; B) Guardia Pisano Fm. - Rio Is Corras Fm., San Giorgio area; C) Guardia Pisano Fm. pelites, calcretes and evaporites resting directly over the Variscan basement, Laveria Mameli, San Giorgio area; D) Guardia Pisano Fm. red bed outcrop resting over a breccia karstic filling, Planu Sartu mine. F: Fault.

Unconformably resting over the Variscan basement, suspected outcrops of Upper Permian-Lower Triassic Rio Is Corras Fm. petromict conglomerates have been described in the Piolanas area (Pasci et al., 2016), but the report is controversial; based on the composition of the pebbles, these outcrops could be the result of debris mixing with younger Mesozoic deposits in the following Monte Margiani Sandstones, that is the terrigenous base of the Caenozoic Sulcis Coal basin (Barca and Costamagna, 2000). So, they would not be genuine Rio Is Corras Fm. outcrops, although they suggest their presence nearby and dismantling at Early Caenozoic times.

In the Nuraxi Figus coal mine (Caenozoic Sulcis Coal basin, Fadda et al., 1994), at 500 m below sea level, the underground works crossed terrigenous to carbonate rocks referred to the

Permian-Triassic succession (Murru and Salvadori, 1987), now attributable to the Guardia Pisano Fm. and Rio Is Corras Fm. red beds, and to the carbonate Campumari Fm. This at-times undifferentiated Permian-Triassic complex has been previously evidenced in the cores of the borehole 6/79 (Assorgia et al., 1992) by crossing 250 m of red bed terrigenous succession and 7 m of dolostones. The base of the red bed succession was never reached.

A new survey in the mine evidenced alternations of decimetric beds formed by red bed pelites, sandstones, and petromict conglomerates. The sandstones are parallel- to cross-bedded. The conglomerates are built of imbricated pebbles of cannibalistic sedimentary, igneous, and metamorphic nature and show a lower erosive boundary.

Key sections: petrographic notes

Preliminary modal analyses of the sandstone framework are informally represented in Fig. 5. The San Giorgio Fm. sandstones are litharenites, and specifically mainly phyllarenites. The metamorphic grains show a low-grade alteration. Carbonate-rich litharenites are frequent at the base of the San Giorgio Fm. stratigraphic section located along the SS130 motorway by-pass. Calchilithites whose feeding is related to the Lower Cambrian carbonate extraclasts are present in the lower part of the unit, forming a monomict interval with scattered quartz tiny grains; they suggest times of almost exclusive detrital contribution from the Lower Cambrian carbonates. No defined maturity evolutionary vertical trend has been evidenced; several fluctuations are visible. In the upper part of the San Giorgio Fm., volcanic rocks fragments appear.

The Tappa Niedda sandstones are phillarenites. The stratigraphic section is too short to allow any inference.

The Guardia Pisano sandstones are mainly litharenites with fragments of strongly weathered Variscan basement and volcanic rocks passing upwards locally to sublitharenites due to the growing contribution of K-feldspar from the erosion of coeval Permian volcanic rocks. A weak maturation trend upwards seems to be present, together with the replacement of the Variscan basement grains by the volcanic rocks and the feldspars grains.

The analysis of the Guardia Pisano Fm. sandstone samples collected underground in the Nuraxi Figus mine evidences a petrographic affinity with the lower part of the unit, given the abundance of Variscan basement grains.

The Rio Is Corras Fm. rare sandstones are all classifiable as calchilithites and rare phyllarenites almost devoid of quartz. The sandstone beds are still now too scarce in the bulk of the succession to evidence any trend whatsoever.

At Sa Bagattu, oligomict microbreccias made only by partially silicified angular carbonate pebbles with pervasive chalcedony cement are present.

At Planu Sartu, the red bed sandstones, both breccia void-filling and well-bedded sandstones alike are classifiable as litharenites.

Petro-sedimentological and stratigraphic results

The San Giorgio Fm., the Guardia Pisano Fm., and the Rio Is Corras Fm. rest conformably on each other, or directly and

unconformably on the Variscan basement. The younger the unit, the wider its extent apparently could have been, as implied by the distribution of the remains (Fig. 1). The stratigraphic and the environmental relationships among the units in the diverse sectors of the late to post-Variscan Sulcis basin, suggest the size of the depositional basin gradually enlarged at times. Some thin red bed outcrops, organized in lithological couplets and short fining-upward sequences, and showing structures evidencing upper-regime flows, represent the final subtle cover mantling cave speleothems of karstic origins; these latter were ultimately filled by (colluvial?) red beds falling through dissolution fractures in the Lower Cambrian carbonates and featured by ephemeral high-energy depositional regimes. Depositional and erosive areas were activated alternatively in the basin according to their location, perhaps in respect to the tectonic collapse evolution and the following modification of the accommodation space. So the different stratigraphic units rested either over the older ones or unconformably over the Variscan basement. Based on this evidence, a progressive widening of this depositional continental basin in times is suggested, starting as a narrow (pull-apart?) basin in late Pennsylvanian times (Elter et al., 2020) and merging in the end with the wider extensional basins related to the W-Tethys rifting. Borehole subsurface data suggest at least 250 m of total thickness; this is comparable with the thickness of the coeval basins of E and NW Sardinia (Costamagna, 2019, and references therein).

The SS 130 by-pass San Giorgio stratigraphic section is significant. Here the intermediate key – level of carbonate breccias is closer to the Variscan basement; it is separated from it only by thin marly sandstones-sandy dolostones and quartz-rich conglomerates and sandstones that are singular in the area. These breccias correspond to the carbonate breccias located in an upper position in the other San Giorgio main stratigraphic sections. So, if compared to the main San Giorgio basin area (Barca and Costamagna, 2003a), this zone could represent a side depositional area, where sedimentation started later with lower-energy deposits. This supports further a gradual enlargement of the basin.

The almost undisturbed passage from the San Giorgio Fm. to the Guardia Pisano Fm. indicates a smooth climatic and environmental transition towards drier alluvial, more open environments (Costamagna, 2019).

Also, the gradual passage from the upper Guardia Pisano Fm to the Rio Is Corras Fm. in the San Giorgio basin area (Fig. 3) marks a smooth passage from a low-energy playa environment with dominant fine pelitic deposits and evaporites (evolving from the previous alluvial sinuous environment of the lower Guardia Pisano Fm.) to a fan delta - lake environment. Pedogenization suggests interruptions in deposition. At Laveria Mameli, the Guardia Pisano Fm. lithological alternations rest directly over the Variscan basement; this again is evidence of the variable base of the Permian red bed succession and the gradual widening of the basin.

The progressive passage from the lower energy deposits of the Guardia Pisano Fm. to those of higher energy of the Rio Is Corras Fm. could be the response to a tectonic peak whose chronology is still undefined.

The red-bed well-bedded deposits locally covering the karstic network represent the final filling of the karstic network itself close to the topographic surface. As visible at the Sa Bagattu and Barega localities, the red bed facies karstic fillings can be sealed by a silicified breccia facies of younger age. This younger age is also suggested by the presence of the Sa Bagattu lithofacies reworked pebbles in the Upper Permian-?Lower Triassic Rio Is Corras Fm. conglomerates. These quartz-cemented, partially silicified deposits could be related to climatic (arid?) early silicretization processes (Summerfield, 1983) under stable tectonic conditions and might be of Early Triassic age, a renowned period with evidence of diffuse aridity (Bustillo, in Middleton et al., 2003; Boucot et al., 2013); they are associated with calcretes, dolocretes, and gypcretes under arid-semiarid and alkaline conditions.

In the limnic San Giorgio Fm., the debris source is essentially local. The sudden and ephemeral abundant feeding of extrabasinal carbonate grains giving place to the calcilithites could be related to the development of active fault scarps in the surrounding Lower Cambrian carbonates due to the progressive widening of the basin. For the same process, later those same faults were buried under the debris.

There is still no clear explanation of the mixing of the mature and immature debris of the basal San Giorgio Fm. The rounded quartz grains and pebbles provenance are enigmatic. The contemporaneous presence of carbonate angular boulders and quartzose rounded pebbles (textural inversion phenomena: Pettijohn et al., 1987) suggests a mix from different feeding sources, and, possibly, one of them being an older molassic depositional cycle. The rounded quartz provenance could be provided by the complete dismantling of an older Westphalian mature-fed collapse basin, now totally dismantled.

In the Permian Guardia Pisano Fm., the replacing of the Variscan basement grains by the volcanic rocks and the feldspar grains seems to be in good accord with the enlargement of the basin and a progressively increasing distance from its Variscan shoulders.

The restart of a dominant carbonate source in the Upper Triassic-?Lower Triassic Rio Is Corras Fm. sandstones suggest a new uplift of the Lower Cambrian carbonate rocks, leading to a subsequent dismantling cycle.

So, recurring compositional and textural maturity trends at times (Fig. 5) suggest repeated uplifting cycles under a wet to dry (warm to hot?) climate.

Conclusive remarks

The joint analysis of new and revised stratigraphic, sedimentological, and petrographic data for the Sulcis late- to post-Variscan collapse sedimentary continental basin suggest a more complex and more persistent history than previously hypothesized, the basin being active almost continuously, although in different, shifting areas, from late Pennsylvanian at least until Late Permian-Early Triassic times. A more complete stratigraphic column has been reconstructed, and the evolution of the several continental environments from each other has been better delineated. The cyclical increase of the depositional energy suggests several tectono-magmatic spikes remodeling

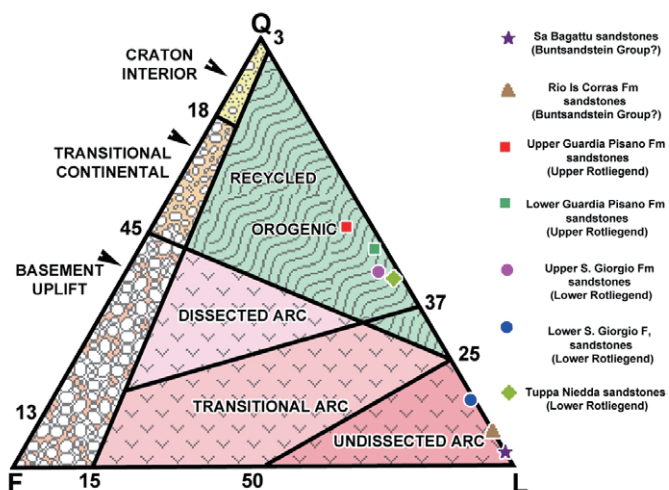


Fig. 5. Sketchy modal framework plot of the sandstones sampled in the upper Pennsylvanian to ?Lower Triassic succession in SW Sardinia. Discrimination fields after Dickinson et al. (1983).

the surrounding landscape. The feeding compositional and grain-size variation suggests too a gradual enlargement of the basin, repeated tectonic spikes, and consequent rejuvenations of the morphology. Based on the sedimentological evolution, a prevalently endoreic behavior of the fluvial network can be hypothesized. The late to post-Variscan Sulcis continental basin, of which the San Giorgio basin could have been the starting point and later the closer point to the depocenter, at its climax was much more extended than previously thought.

The thick Permian-Triassic succession resting under the Sulcis Caenozoic coal basin supports further the presence of a previous wider extension and thickness of the upper Pennsylvanian-Permian-Triassic? basin and its function as an ancestor of the Palaeogene Sulcis coal basin (Arthaud and Matte, 1977).

Acknowledgements

Thanks to Carbosulcis SpA for granting access to their underground works and Dr. F. Bordicchia for the assistance.

References

- Arthaud, F. and Matte, P., 1977. Late Paleozoic strike-slip faulting in southern Europe and northern Africa: result of a right lateral shear zone between the Appalachians and the Urals. *Geological Society of America Bulletin*, v. 88, p. 1305–1320.
- Assorgia, A., Brotzu, P., Callegari, E., Fadda, A., Lonis, R., Ottelli, L., Ruffini R., and Abbate, T., 1992. *Carta Geologica del distretto vulcanico cenozoico del Sulcis (Sardegna sud-occidentale)*. S.E.L.C.A., Firenze.
- Barca, S. and Costamagna, L. G., 2000. Il bacino paleogenico del Sulcis-Iglesiente (Sardegna SW): nuovi dati stratigrafico-strutturali per un modello geodinamico nell'ambito dell'orogenesi pirenaica. *Bollettino della Società geologica Italiana*, v. 119, p. 497–515.
- Barca, S. and Costamagna, L.G., 2003. The Upper Carboniferous S. Giorgio succession (Iglesiente, SW Sardinia): stratigraphy, depositional setting and evolution of a Post-Hercynian molassic basin. *Bollettino della Società geologica Italiana, Volume Speciale n°2, Special Proceeding of the Scientific Meeting “Late Palaeozoic to Early Mesozoic events of Mediterranean Europe, and additional regional reports” (Siena, April 30 – May 7 2001)*, 89–98.
- Barca, S. and Costamagna, L.G., 2003b. Analisi di facies e stratigrafia della successione permo?-triassica di Campumari-Coremò (Iglesiente, Sardegna SW). *Bollettino della Società geologica Italiana*, v. 122, p. 25–45.
- Barca, S. and Costamagna, L.G., 2006. Stratigrafia, analisi di facies ed architettura deposizionale della successione permiana di Guardia Pisano (Sulcis, Sardegna SW). *Bollettino della Società geologica Italiana*, v. 125, p. 3–19.
- Barca, S., Costamagna, L.G. and Del Rio, M., 1994. Affioramenti permo-carboniferi e mesotriassici fra Porto Piscinas e Punta Acqua Durci (Arburese, Sardegna SW). *Bollettino della Società Sarda di Scienze Naturali*, v. 30, p. 1–11.
- Bechstädt Th., 1983. Scyenia-ichnofacies within karstic internal red beds of a barite mine, SW Sardinia. *Neues Jahrbuch für Geologie und Paläontologie - Monatshefte*, v. 12, p. 705–712.
- Bechstädt Th. and Boni M., 1994. Sedimentological, stratigraphical and ore deposits field guide of the Autochthonous Cambro-Ordovician of Southwestern Sardinia. *Memorie Descrittive della Carta geologica d'Italia*, 436 p.
- Boucot A.J., Xu C. and Scotese C.R., 2013. Phanerozoic Paleoclimate: An Atlas of Lithologic Indicators of Climate. SEPM Concepts in Sedimentology and Paleontology, v. 11, 478 pp.
- Brusca, C., Pretti, S. and Tamburini, D., 1968. Le mineralizzazioni baritose delle coperture di Monte Sa Bagattu. *Res Assoc Mineraria Sarda*, v. 73, p. 89–106.
- Cocozza, T., 1967. Il Permo-Carbonifero del bacino di San Giorgio (Iglesiente, Sardegna sud-occidentale). *Memorie della Società Geologica Italiana*, v. 6, p. 607–642.
- Costamagna, L.G. and Barca, S., 2002. The “Germanic” Triassic of Sardinia (Italy): a stratigraphic, depositional and paleogeographic review. *Rivista Italiana di Paleontologia e Stratigrafia*, v. 108-1, 67–100.
- Costamagna, L.G. and Barca, S., 2008. Depositional architecture and Sedimentology of the Tuppa Niedda Conglomerates (Late Carboniferous, Arburese, SW Sardinia, Italy). *Bollettino della Società geologica Italiana*, v. 127, no. 3, p. 625–636.
- Costamagna, L.G., 2019. The carbonates of the post-Variscan basins of Sardinia: the evolution from Carboniferous–Permian humid-persistent to Permian arid-ephemeral lakes in a morphotectonic framework. *Geological Magazine*, v. 156, no. 11, p. 1892–1914.
- De Waele J., Forti P. and Perna G., 2001. Hyperkarstic phenomena in the Iglesiente Mining District., in Cidu, R. (ed.), *Water-Rock Interaction 2001: Villasimius, Lisse, The Netherlands*, Balkema, Proceedings, v. 1, p. 619–622.
- Deroïn, J.P. and Bonin, B., 2003. Late Variscan tectonomagmatic activity in Western Europe and surrounding areas: the Mid-Permian Episode. *Bollettino della Società geologica Italiana*, v. 2, p. 169–184.
- Dickinson W., Breard L., Brakenridge G., Erjavec J., Ferguson R., Inman K., Knepp R., Lindberg F. and Ryberg P., 1983.

- Provenance of North American Phanerozoic sandstones in relation to tectonic setting. Geological Society of America Bulletin, v. 94, p. 222–235.
- Elter, F.M., Gaggero, L., Mantovani, F., Pandeli, E. and Costamagna, L.G., 2020. The Atlas-East Variscan-Elbe shear system and its role in the formation of the pull-apart Late Palaeozoic basins. International Journal of Earth Sciences, v. 109, p. 739–760.
- Fadda, A., Ottelli, L. and Perna, G., 1994. Il Bacino lignitifero del Sulcis: Geologia, Idrogeologia, Miniere. Carbosulcis S.p.A., Cagliari.
- Middleton, G.V., 2003. Encyclopedia of Sediments and Sedimentary Rocks. Springer, 822 p.
- Moore J. McMahon, 1972. Supergene mineral deposits and physiographic development in South-West Sardinia. Applied Earth Sciences, v. 81, B59–B86.
- Murru, M. and Salvadori, A., 1987. Ricerche stratigrafiche sul bacino paleogenico del Sulcis (Sardegna sud-occidentale). Geologica Romana, v. 26, p. 149–165.
- Pasci S., Pertusati P.C., Salvadori I., Medda F., Murtas, A., Rizzo, R. and Uras V., 2016. Note illustrative del F°555 - Iglesias. Memorie Descrittive della Carta geologica d'Italia, APAT Servizio Geologico d'Italia, 416 p.
- Pettijohn, F.J., Potter P.E. and Siever, R., 1987. Sand and Sandstone. 2nd Ed, Springer-Verlag, 556 p.
- Rossi, Ph., Oggiano, G. and Cocherie, A., 2009. A restored section of the “southern Variscan realm” across the Corsica-Sardinia microcontinent. Comptes Rendus Geoscience, v. 341, p. 224–38.
- Sinisi, R., Mongelli, G., Mameli, P., and Oggiano, G., 2014. Did the Variscan relief influence the Permian climate of mesoeurope? Insights from geochemical and mineralogical proxies from Sardinia (Italy). Palaeogeography, Palaeoclimatology, Palaeoecology, v. 396, p. 132–154.
- Summerfield, M.A., 198Co3. Silcrete. In: Goudie, A.S., Pye, K., Guthrie, G.D. and Mossman, B.T. (Eds), Chemical Sediments and Geomorphology. Academic Press, London, p. 59–61.
- by Upper Carboniferous–Lower Permian sediment fillings of the Gehren Subgroup and the Rotliegend Group, which are subdivided lithostratigraphically in multiple formations (for details see Lützner et al., 2012). In places, rhyolite and doleritic rocks intercalate with the sedimentary succession, allowing for high-precision (CA-ID-TIMS) U-Pb isotope geochronology for some of the rhyolitic volcanics (Lützner et al., 2021). Within the Rotliegend Group, distinctive changes in sediment rock colour from grey at its base to red at its top reflect a general trend from a semi-humid towards a semi-arid palaeoclimate (Roscher and Schneider, 2006). Semi-arid palaeoclimate conditions are indicated by characteristic red-bed deposits from the upper part

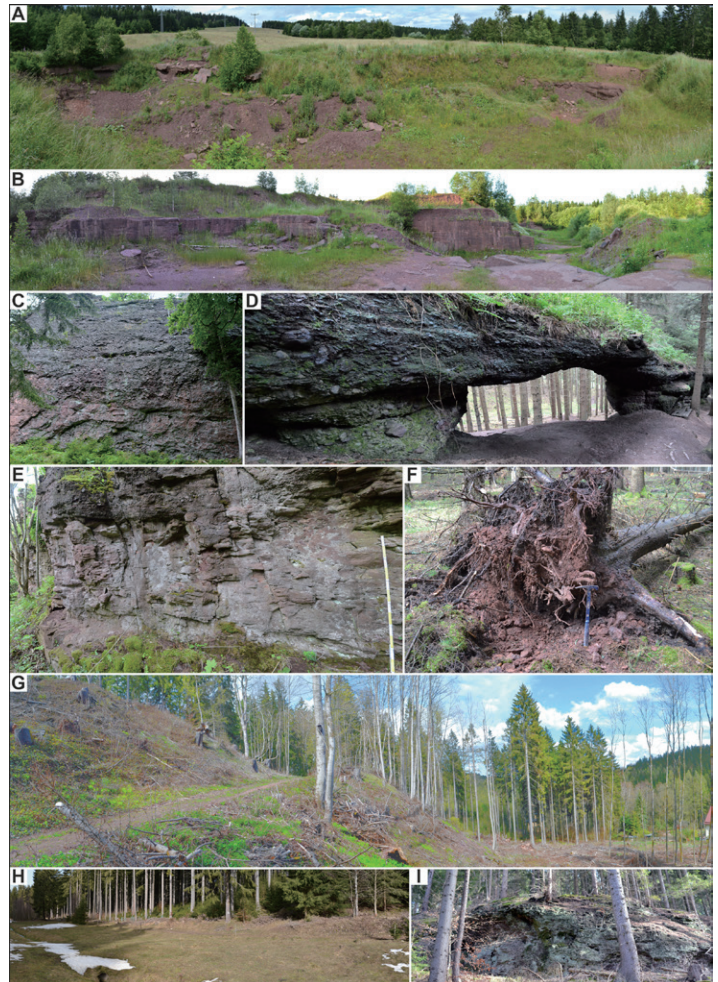


Fig. 1. Exemplified outcrop conditions of the Tambach Formation in the Tambach-Dietharz basin. A–B: The Tambach Sandstone Member exposed in the paleontological excavation site (A) and the present-day quarry section (B) at the Bromacker. C–D: The Bielstein Conglomerate Member at the Bielstein cliff section (C) and the Steinernes Tor section (D). E–F: The Finsterbergen Conglomerate Member at the Hainfelsen cliff section (E) and an uprooted exposure on the forested top of the Hainfelsen plateau (F). G: Abandoned quarry at the Hüllrod section, a formerly important outcrop in the northern part of the basin that is nowadays overgrown by vegetation. H–I: Kesseltal valley poorly exposing the lateral contact between the Tambach Sandstone Member (H) and the Finsterbergen Conglomerate Member (I).

Digital geological modelling of the Tambach Formation around the Bromacker fossil-lagerstätte (Early Permian, Germany)

Frank Scholze

Friedrich Schiller University Jena, Institute for Geoscience, Burgweg 11, 07749 Jena, Germany
Email: Frank.Scholze@uni-jena.de

Introduction

The Tambach-Dietharz sedimentary basin of Early Permian (Artinskian [Schneider et al., 2020]) age is part of the superordinate Thuringian Forest Basin, which is exposed by numerous surface and subsurface outcrops in the Thuringian Forest mountain region (southern Thuringia, central Germany). Its tectonically uplifted Variscan basement is composed of metamorphic and plutonic rocks that became deeply incised

of the Rotliegend Group in the Thuringian Forest Basin, such as in the Tambach Formation (Upper Rotliegend 1 Subgroup) that is of solely interest in the present study.

The present study is a contribution to an interdisciplinary research project ('Bromacker Project', 2020–2025) on the fossiliferous Tambach Formation deposits at the Bromacker locality (Fig. 1A, B). North of the town Tambach-Dietharz, the Bromacker is an outcrop area that is well-known for its Lower Permian occurrence of both fully terrestrial-adapted four-limbed vertebrates (Tetrapoda: Diadectidae) and their trace fossils (e.g., *Ichniotherium*). The spectacular fossil record includes, e.g., specimens of *Diadectes* and *Orobates* (e.g., Berman et al., 1998, 2004) allowing for a diadectid trackmaker-track correlation (e.g., Voigt et al., 2007; Nyakatura et al., 2019). Other tetrapod taxa (e.g., the bipedal reptile *Eudibamus*; e.g., Berman et al., 2000), remains of invertebrates and plants, and invertebrate trace fossils occur at the Bromacker as well. Consequently, the local red-bed deposit of the Tambach Formation had been designated as a fossil lagerstätte (e.g., Martens, 2018) and became an attractive excursion site for a wide scientific community (e.g., Schneider et al., 2014: p. 95–99; Buchwitz et al., 2019: p. 117–123).

The Tambach Formation has been selected herein for digital geological modelling, which involves both collecting and digitizing multiple kinds of its geologic setting information. The newly generated model is based on a Geographic Information System (GIS). Most of the relevant GIS data were obtained from German literature, which can be difficult to find for a non-local readership. Gathering all data in a single GIS-file, and georeferencing its respective components (i.e., raster images, polygons, lines, points) to a single geographic coordinate system, are the main advantages of the present work.

Materials and Methods

The study area is defined by the present-day geographic distribution of the Tambach Formation around Tambach-Dietharz (Fig. 2). The area is dispersed across four official geologic maps published by the geologic survey of the state of Thuringia in the scale 1:25.000 (“GK25”), which particularly includes the GK25-sheets no. 5229 (Tambach-Dietharz), no. 5129 (Waltershausen), no. 5230 (Oberhof), and no. 5130 (Ohrdruf). They were all obtained from the official website of the Thuringian geologic survey (<https://antares.thueringen.de/cadenzia/q/5NL>). Additionally, a geologic map showing parts of the Tambach Formation and its basement along the western and southwestern margins of the Tambach-Dietharz basin had been published by Andreas and Lützner (2009: appendix 1a). In order to collect general information on the stratigraphy of the study area, localities of wells in the Tambach-Dietharz basin were gathered in a shape-file, which had been kindly provided by the geologic survey of Thuringia; similar locality information were also kindly provided by the regional Geopark consulting engineer’s office. Data on shallow drill cores (i.e., coordinates and lithostratigraphic determination) from previous research projects were obtained either from literature (Krause et al., 2006; Martens et al., 2009) or personal communications (e.g., field trips in 2020/2021 guided by Dr. Th. Martens). An unpublished basemap from the present Bromacker quarry indicates the position of a former

exploration drill site, which is nowadays covered by a rock dump on the quarry ground. Additionally, a ~150 m deep well from the year 1846 located north of Tambach-Dietharz (probably near the exit of the Seeberger Fahrt field road) had been reported previously (e.g., Ernst, 2000), but its distinct geographic position is nowadays unclear. Further well sites (i.e., Tambach-Dietharz 2/1947–1948; Tambach-Dietharz 3/1949) had been described in a diploma thesis by Eyrich (1964); however, geographic notes

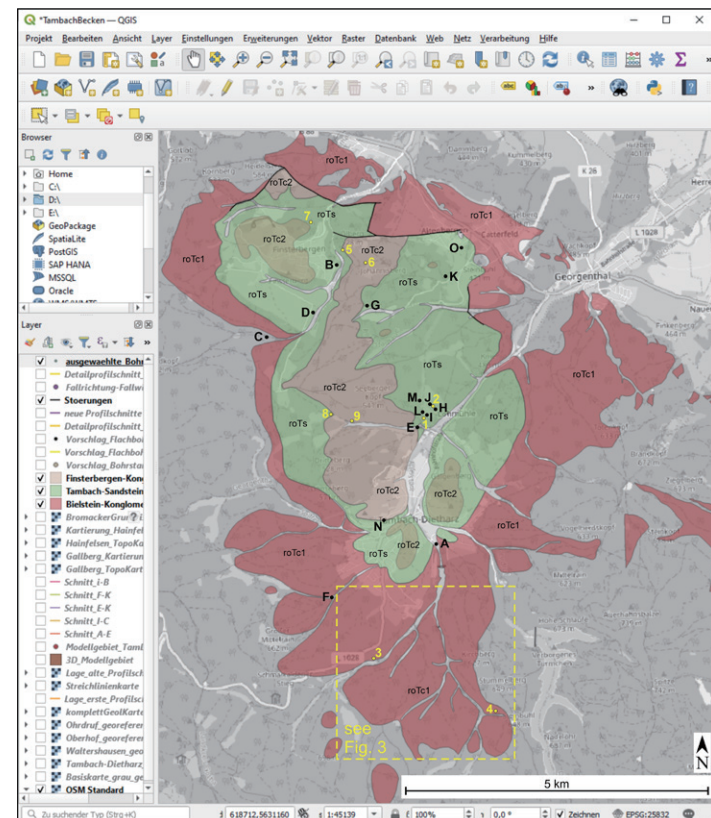


Fig. 2. QGIS-screenshot from the digital geological model, showing a close-up view of the main part of the Tambach-Dietharz basin. The Tambach Formation is subdivided lithostratigraphically into three members: the Bielstein Conglomerate (roTc1), the Tambach Sandstone (roTs), and the Finsterbergen Conglomerate (roTc2); their respective contour-lines were obtained from the official 1:25.000 maps ("GK25"-sheets no. 5229, 5129, 5230, 5130). Designations of drill core sites (A–O): TB Hy Tambach-Dietharz 1/46 (A), TB Hy Leinagrund 1/57 (B), Finsterbergen 1/62 (C), Finsterbergen 2/73 (D), Tambach-Dietharz 9/74 (E), Tambach-Dietharz 1978 (F), Hy Paulfeld 1/90 (G), Bromacker 1/99 (H), FB Bromacker 1/2004 (I), FB Bromacker 2/2004 (J), FB Altenbergen 1/2005 (K), FB Bromacker BK1/2008 (L), FB Bromacker BK2/2008 (M), EWS Tambach-Dietharz 1–3/2008 (N), and EWS Altenbergen 1–4/2010 (O). Selected surface outcrops (1–9) mentioned in the text (cf. Fig. 1): excavation site (1) and quarry (2) at the Bromacker section, Bielstein cliff section (3), Steinernes Tor section (4), Hainfelsen cliff section (5), uprooted tree exposures on the Hainfelsen forested plateau (6), abandoned Hüllrod quarry section (7), meadow of the Kesselbach stream in the Kesseltal valley (8), and Kesseltal valley slope section (9).

therein on the respective well localities apparently need further examination.

Aerial view images indicating the landscape morphology, distribution of vegetated areas (i.e., forests, grassland), positions of relevant outcrops (including abandoned quarries), and roads in the study area were obtained from the software Google Earth Pro. Stratigraphic dipping values of the Tambach Formation in the study area had been insufficiently included in the official GK25-sheets. Instead, generalized stratigraphic dipping data can be obtained from a map figured by Andreas and Lützner (2009: appendix 1c), which also contains contour-lines of the Tambach Sandstone Member resembling a previous map that had been published by Chrobok (1967: fig. 2). Further, primary data were also newly collected during recent fieldworks (e.g., local mapping and profile documentation), utilizing a Garmin eTrex handheld GPS-device for coordinate measurements and a geologic compass (360°, with a hinge inclinometer) for orientation measurements of the lithostratigraphic dipping (values measured in 0°–360° direction/0°–90° angle).

Finally, the software QGIS, version 3.18.3, was used for digital geological modelling. Its georeferenced basemap is linked to the geographic OpenStreetMap database, and became altered herein to a greyscale background layer. The model includes contour-lines of lithostratigraphic units, localities of representative outcrops, drill sites with confirmed localities, faults, and dipping measurement values. Seismic cross sections do not exist in the study area. Crop-out contours of the Tambach Formation became digitized as polygon-shapefile layers using QGIS, based on the above mentioned four official GK25-sheets for the study area. Faults were included into the digital geological model as a line-shapefile from the same official GK25-sheets.

Results and Discussion

Most of the present-day Tambach Formation distribution concentrates on the GK25-sheets of Tambach-Dietharz (no. 5229) and Waltershausen (no. 5129). Explanation of these sheets can be read in official descriptions written by Kühn (1920) and Zimmermann (1924); further descriptions were based on revisional mappings (unpublished diploma theses) by Eyrich (1964) and Thalheimer (1965). The plausibility of the contour-lines published in the official GK25-sheets has been initially checked during recent fieldworks, which will be continued during ongoing field campaigns. Preliminary results showed that faults sparsely indicated in these official GK25-sheets can be basically confirmed in this study. However, the author had been unable to measure their distinct orientations during recent fieldwork due to the problematic nature of outcrop conditions (i.e., zones of assumed faults in the study area were covered either by natural soil/vegetation or water streams).

Lithostratigraphically, the Tambach Formation is subdivided into three units (see Figure 2), which agrees to both official GK25-sheets and results of other working groups (for a state-of-the-art summary see Lützner et al., 2012: p. 462–466). In practice, these three stratigraphic units can be distinguished according to their respective lithologic properties (i.e., colour, grain size, clast composition). Each of these three units correspond to the lithostratigraphic rank of members, which were designated as

follows (in stratigraphically ascending order): the Bielstein Conglomerate (also designated as ‘Lower Conglomerate’, abbreviated as roTc1 in Fig. 2), the Tambach Sandstone (roTs), and the Finsterbergen Conglomerate (‘Upper Conglomerate’, roTc2). The Bielstein Conglomerate Member (e.g., exposure at the Bielstein cliff section [see Fig. 1C]; Steinernes Tor section [Fig. 1D]) consists of poorly sorted conglomerates that are composed predominantly of rhyolite clasts. In its proximal setting, the conglomerates had been deposited by debris flows; its rhyolite clasts were erosive products of the underlying/flanking Oberhof volcano complex (Oberhof Formation, Lower Rotliegend Subgroup, Rotliegend Group). Towards the basin centre, the Bielstein Conglomerate Member gradually shifts into the overlying Tambach Sandstone Member, which is mainly composed of high-energy fluvial deposits of internal massive to cross-bedded, fine- to medium-grained, red coloured sandstones (e.g., in the Bromacker quarry section; Fig. 1B), as well as laminated mudstones (e.g., Bromacker excavation site; Fig. 1A). The sandstones are variably sorted and, occasionally, also gravel clasts occur in the Tambach Sandstone Member; locally, clayey to silty breccias and immature palaeosoils with carbonate nodules occur as well. The overlying, reddish coloured Finsterbergen Conglomerate Member contains predominantly clasts of rhyolite, granite, and metamorphic rocks (although some of these clasts already occur in the upper part of the underlying Tambach Sandstone Member), as well as, more rarely, also clasts of dolerite. In particular, the granite and metamorphic clasts indicate a shift in the sediment delivery direction coming from the Ruhla Crystalline basement located northwest to the Tambach-Dietharz basin. The Finsterbergen Conglomerate Member is composed of partially fanglomeratic, horizontally more or less stratified, alluvial braidplain conglomerates; however, layers of medium- to coarse-grained sandstones occur as well.

Outcrops of the Finsterbergen Conglomerate Member occur in the Tambach-Dietharz basin almost without exception in forest or meadow landscapes. The Finsterbergen Conglomerate Member is only locally well-exposed along the Leinagrund valley that is located east-southeast of the town Finsterbergen, such as at the Hainfelsen cliff section (Fig. 1E). However, in most areas of the Finsterbergen Conglomerate Member, their natural outcrop conditions are generally poor, due to intense vegetation cover. The latter does also account for a forested plateau on top of the Hainfelsen cliff section, where most lithostratigraphic surface information is restricted to loose blocks that are often only exposed by overturned tree roots (Fig. 1F). In this area, some discrepancies observed between the GK25-sheet no. 5129 (Waltershausen) and the map published by Andreas and Lützner (2009: appendix 1c) are ascribed herein as consequence of difficult outcrop situations. For example, the latter map shows an irregular distribution of the Tambach Sandstone Member in the east of the Hainfelsen cliffs. Superimposing georeferenced raster-shapefiles in the QGIS model of both this map (Andreas and Lützner, 2009: appendix 1c) and an aerial view (from Google Earth Pro) indicates a local matching between the contour-lines of the Tambach Sandstone Member and meadow outlines within that particular area. Similarly, intense vegetation and soil nowadays also cover abandoned quarries that had been important

outcrops for previous workers (e.g., Thalheimer, 1965), such as the former section of the abandoned Hüllrod quarry (Fig. 1G) in the northern part of the Tambach-Dietharz basin.

More detailed lithostratigraphic data from the deeper underground of the study area are generally rare, because of a low number of drill cores that had been formerly obtained from deep well sites in the Tambach-Dietharz basin (Fig. 2). Problematically, lithologic descriptions of former drill core sections are also difficult to convert into the present lithostratigraphic subdivision schemas of both the Rotliegend Group and the Tambach Formation. More recently described drill core sections of Martens et al. (2009) had been originally derived from shallow drillings and, therefore, cannot be used for a total thickness calculation of the Tambach Sandstone Member or the underlying Bielstein Conglomerate Member. Nevertheless, these shallow core sections (Krause et al., 2006) provided valuable insights in both the depositional setting and fossil habitats of the Tambach Sandstone Member (Martens et al., 2009).

Based on preliminary results, the nature of lithostratigraphic contacts between respective members of the Tambach Formation in the study area seems to be challenging for present mapping and digital modelling activities, because of both the local outcrop conditions and the present state of knowledge. For example, a direct contact between the Bielstein Conglomerate Member and the overlying Tambach Sandstone Member is not well-exposed in the study area. Although a boundary between these two lithostratigraphic units had been clearly indicated in previously published maps, the present study does not provide any kind of new data that can either confirm nor contradict such a demarcation practice in the field. The traditional differentiation between the Bielstein Conglomerate and Tambach Sandstone members is maintained preliminarily herein (see contacts between ‘roTc1’ and ‘roTs’ in Figure 2) until more data will become available that could contribute to the question whether or not this problem is controlled by tectonic (e.g., faults, discordances) or lithofacies (i.e., gradual transitions). Similarly, this does also account preliminarily for the contacts between the Tambach Sandstone Member and the overlying Finsterbergen Conglomerate Member (see contacts between ‘roTs’ and ‘roTc2’ in Figure 2). A sharp boundary between these two members could not be observed during recent field mapping, whereas it is not clear whether or not this is only a consequence of insufficient outcrop conditions (i.e., soil and vegetation cover). Locally, a mixed sandy/conglomeratic transition (as discussed in detail by Eyrich [1964] and Thalheimer [1965]) can be observed between the Tambach Sandstone and the Finsterbergen Conglomerate members (such as at the Hainfelsen cliff section); however, a stronger lateral replacement between these two members is also inferred locally (such as in the Kesseltal valley; Fig. 1H, I). In the latter case, it seems possible that a lateral adjoining between the Tambach Sandstone Member and Finsterbergen Conglomerate Member is a direct consequence of fault tectonics (e.g., an assumed subsurface fault in the Kesseltal valley to which the recent path of the Kesselbach stream has aligned to).

Conclusions and Outlook

Although the sedimentology of the Tambach Formation had

already been described in multiple aspects (see, e.g., Lützner, 1981; Martens et al., 1981, 2009; Eberth et al., 2000; Martens, 2007), more distinct information either on the total thicknesses of the Bielstein Conglomerate, the Tambach Sandstone, and the Finsterbergen Conglomerate members as well as the presence of faults had been published only sparsely in previous studies. This does also account for, so far, sparsely published stratigraphic dipping values. Additionally, a deviation in lithostratigraphic contour-lines between the official GK25-sheets and a more recent map (Andreas and Lützner, 2009: appendix 1c) of the Tambach Formation was ascertained herein, which indicates the necessity of conducting new fine-scale field mapping as part of further research. Revised mapping for some parts of the study area were carried out through former fieldwork of Eyrich (1964) and Thalheimer (1965); unfortunately, their unpublished original maps were not available for the present study (cf. summarized map published by Chrobok, 1967: fig. 2). The respective position and orientation of tectonic faults indicated previously in revised maps (Chrobok, 1967: fig. 2; Andreas and Lützner, 2009: appendix 1c) also deviate from the official GK25-sheets (no. 5129); therefore, a detailed tectonic mapping (i.e., faults) is required in order to better understand the real outline of the Tambach-Dietharz basin along its northern basin margin. The latter does also account for the question whether or not the Tambach-Dietharz basin continues towards the northern margin of the superordinate Thuringian Forest Basin.

At a wider scale, the lateral and vertical variations observed between volcanic and sedimentary units as basement adjacent to the western–southwestern margin of the Tambach-Dietharz basin (see the map in Andreas and Lützner, 2009: appendix 1a) should be similarly expected for the basement that is underlying the Tambach Formation inside this basin. Interestingly, Chrobok (1964) already described a pre-Tambach Formation palaeorelief that includes both valleys and hilltops of rhyolite (Oberhof Formation) varying in their palaeo-elevations. This supports the herein assumed heterogenic nature of the lithostratigraphic units directly underlying the Tambach Formation.

Future deep core drilling projects in the Tambach Formation would have great scientific potential in order to better understand both vertical and lateral lithological–stratigraphic variations (e.g., thickness) in the Tambach-Dietharz basin as well as the kind of contacts between the respective lithostratigraphic members of the Tambach Formation. Despite often unfavorable outcrop conditions, primary data on local stratigraphic dipping values had been newly measured (e.g., see Fig. 3), whereas further fieldwork and refinements of the new digital geological model are in progress. For example, the 2D-model presented herein could be successively expanded to a 3D/4D-model as part of further research. Nevertheless, this study shows the great potential of using GIS for digital geological modelling in difficult basin settings, contributing to a better understanding of Lower Permian red-bed palaeo-landscapes.

Acknowledgements

The current interdisciplinary research project involves four institutions (Museum für Naturkunde Berlin, Stiftung Schloss Friedenstein Gotha, Geopark Thüringen Inselsberg–

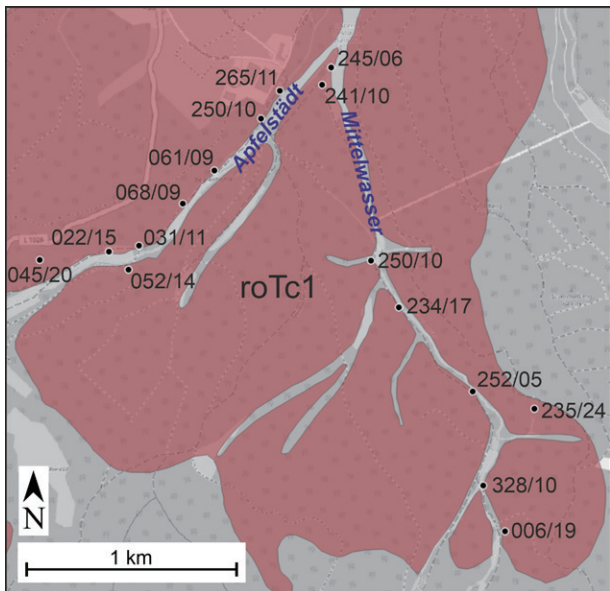


Fig. 3. Close-up view of the southern Tambach-Dietharz basin showing the Bielstein Conglomerate Member (roTc1) along the Apfelstädt and Mittewasser valleys; roTc1 contour-lines follow the official GK25-sheet no. 5229. Orientation measurement values (direction°/angle°) of the stratigraphic dipping result from current fieldworks for the present study.

Drei Gleichen, Friedrich-Schiller-Universität Jena) and further cooperating persons. Respective project partners, colleagues and student assistants at the University of Jena, and all external cooperation partners, as well as all colleagues at the geological survey of Thuringia and from the consulting engineer office of the regional Geopark are highly acknowledged for their various supports. Particular thanks to Dr. Thomas Martens for literature, drill core information, and joint field trips. The Bromacker Project receives funding from the German federal ministry of education and research (BMBF).

The study contributes to the Non-marine–Marine Correlation Working Group (under the leadership of Prof. Jörg W. Schneider) of the international Subcommission on Permian Stratigraphy. The Permophiles chief-editor (Prof. Yichun Zhang) is thanked for handling of the manuscript.

References

- Andreas, D. and Lützner, H., 2009. Schichtenfolge und Paläotektonik des Rotliegenden im mittleren Thüringer Wald zwischen Friedrichroda und Steinbach-Hallenberg. Geowissenschaftliche Mitteilungen von Thüringen, v. 13, p. 141–161.
- Berman, D. S., Sumida, S. S. and Martens, T., 1998. Diadectes (Diadectomorpha: Diadectidae) from the Early Permian of central Germany, with description of a new species. Annals of the Carnegie Museum, v. 67, p. 53–93.
- Berman, D. S., Reisz, R. R., Scott, D., Henrici, A. C., Sumida, S. S. and Martens, T., 2000. Early Permian Bipedal Reptile. Science, v. 290, p. 969–972.
- Berman, D. S., Henrici, A. C., Kissel, R. A., Sumida, S. S. and Martens, T., 2004. A new diadectid (Diadectomorpha), Orobates pabsti, from the Early Permian of Central Germany. Bulletin of Carnegie Museum of Natural History, v. 35, p. 1–36.
- Buchwitz, M., Falk, D., Klein, H. and Wings, O., 2019. 3rd International Conference of Continental Ichnology 2019 Field Trip Guide. Hallesches Jahrbuch für Geowissenschaften, Beiheft, v. 46, p. 97–150.
- Chrobok, S. M., 1964. Über ein prätambacher Relief im Bereich der nördlichen Tambacher Mulde (Thüringer Wald). Geologie, v. 13, p. 1013–1016.
- Chrobok, S. M., 1967. Verschüttung und Exhumierung eines Reliefs in einer varistischen Innensenke. Geologische Rundschau, v. 56, p. 520–528.
- Eberth, D. A., Berman, D., Sumida, S. S. and Hopf, H., 2000. Lower Permian terrestrial paleoenvironments and vertebrate paleoecology of the Tambach basin (Thuringia, Central Germany): The upland holy grail. Palaios, v. 15, p. 293–313.
- Ernst, W., 2000. Steinkohle bei Tambach-Dietharz? Abhandlungen und Berichte des Museums der Natur Gotha, v. 21, p. 99–102.
- Eyrich, A., 1964. Der Tambacher Sandstein (Beitrag zur Revisionskartierung des Blattes Waltershausen–Friedrichroda). Diploma thesis, Humboldt University of Berlin, Berlin, 78 p. (unpublished).
- Krause, T., Martens, T. and Gores, G., 2006. Die Forschungsbohrungen Bromacker 1/2004, Bromacker 2/2004 und Altenbergen 1/2005 im Gebiet zwischen Bromacker und Kandelaber bei Tambach-Dietharz - Zielstellung, technische Arbeiten und erste Ergebnisse. Abhandlungen und Berichte des Museums der Natur Gotha, v. 24, p. 199–202.
- Kühn, B., 1920. Erläuterungen zur geologischen Karte von Preußen und benachbarten Bundesstaaten, Lieferung 183, Blatt Tambach. Preußische Geologische Landesanstalt, Berlin, 62 pp.
- Lützner, H., 1981. Sedimentation der variszischen Molasse im Thüringer Wald. Schriftenreihe für geologische Wissenschaften, v. 17, p. 1–217.
- Lützner, H., Andreas, D., Schneider, J. W., Voigt, S. and Werneburg, R., 2012. Stefan und Rotliegend im Thüringer Wald und seiner Umgebung. Schriftenreihe der Deutschen Gesellschaft für Geowissenschaften, v. 61, p. 418–487.
- Lützner, H., Tichomirowa, M., Käßner, A. and Gaupp, R., 2021. Latest Carboniferous to early Permian volcano-stratigraphic evolution in Central Europe: U–Pb CA-ID–TIMS ages of volcanic rocks in the Thuringian Forest Basin (Germany). International Journal of Earth Sciences, v. 110, p. 377–398.
- Martens, T., 2007. Die Bedeutung der Sedimentmarken für die Analyse der Klimaelemente im kontinentalen Unterperm. Zeitschrift für geologische Wissenschaften, v. 35, p. 177–211.
- Martens, T., 2018. Scientific importance of the Fossillagerstätte Bromacker (Germany, Tambach Formation, Lower Permian) – vertebrate fossils. Cuvillier Verlag, Göttingen, 47 pp.
- Martens, T., Schneider, J. and Walter, H., 1981. Zur Paläontologie und Genese fossilführender Rotsedimente - Der Tambacher Sandstein, Oberrotliegendes, Thüringer Wald. Freiberger Forschungshefte, C, v. 363, p. 75–100.
- Martens, T., Hahne, K. and Naumann, R., 2009.

- Lithostratigraphie, Taphofazies und Geochemie des Tambach-Sandsteins im Typusgebiet der Tambach-Formation (Thüringer Wald, Oberrotliegend, Unteres Perm). Zeitschrift für geologische Wissenschaften, v. 37, p. 81–119.
- Nykatura, J. A., Melo, K., Horvat, T., Karakasiliotis, K., Allen, V. R., Andikfar, A., Andrada, E., Arnold, P., Laströer, J., Hutchinson, J. R., Fischer, M. S. and Ijspeert, A. J., 2019. Reverse-engineering the locomotion of a stem amniote. *Nature*, v. 565, p. 351–355.
- Roscher, M. and Schneider, J. W., 2006. Permo-Carboniferous climate: Early Pennsylvanian to Late Permian climate development of central Europe in a regional and global context. Geological Society, London, Special Publications, v. 265, p. 95–136.
- Schneider, J. W., Rößler, R., Werneburg, R., Scholze, F. and Voigt, S., 2014. The Carboniferous–Permian basins in Saxony, Thuringia, and Saxony-Anhalt of East Germany. *Wissenschaftliche Mitteilungen des Instituts für Geologie der TU Bergakademie Freiberg*, v. 46, p. 55–121.
- Schneider, J. W., Lucas, S. G., Scholze, F., Voigt, S., Marchetti, L., Klein, H., Opluštil, S., Werneburg, R., Golubev, V. K., Barrick, J. E., Nemyrovska, T., Ronchi, A., Day, M. O., Silantiev, V. V., Rößler, R., Saber, H., Linnemann, U., Zharinova, V. and Shen, S. Z., 2020. Late Paleozoic-early Mesozoic continental biostratigraphy – links to the Standard Global Chronostratigraphic Scale. *Palaeoworld*, v. 29, 186–238.
- Thalheimer, H., 1965. Die Tambacher Schichten, Beitrag zur Revisionskartierung des Blattes Waltershausen–Friedrichroda. Diploma thesis, Humboldt University of Berlin, Berlin, 48 p. (unpublished).
- Voigt, S., Berman, D. S. and Henrici, A. C., 2007. First well-established track-trackmaker association of Paleozoic tetrapods based on *Ichniotherium* trackways and diadectid skeletons from the Lower Permian of Germany. *Journal of Vertebrate Paleontology*, v. 27, p. 553–570.
- Zimmermann, E., 1924. Erläuterungen zur geologischen Karte von Preußen und benachbarten Bundesstaaten, Lieferung 183, Blatt Waltershausen-Friedrichroda. *Geologische Landesanstalt*, Berlin, 82 pp.

Recent progress and prospect of high-precision U-Pb age constraints on the Permian marine-terrestrial system of the North China block

Qiong Wu

State Key Laboratory for Mineral Deposits Research and School of Earth Sciences and Engineering, Nanjing University, Nanjing 210023, China

Jahandar Ramezani

Department of Earth, Atmospheric and Planetary Sciences, Massachusetts Institute of Technology, Cambridge, MA 02139, USA

Hua Zhang

Jun Wang

State Key Laboratory of Palaeobiology and Stratigraphy, Nanjing Institute of Geology and Palaeontology, Chinese Academy of Sciences, Nanjing 210008, China
Center for Excellence in Life and Paleoenvironment, Chinese Academy of Sciences, Nanjing 210008, China
Email: hzhang@nigpas.ac.cn (H.Zhang)

Fan-gui Zeng

Department of Earth Science & Engineering, Taiyuan University of Technology, Taiyuan 030024, China

Yi-chun Zhang

Feng Liu

State Key Laboratory of Palaeobiology and Stratigraphy, Nanjing Institute of Geology and Palaeontology, Chinese Academy of Sciences, Nanjing 210008, China
Center for Excellence in Life and Paleoenvironment, Chinese Academy of Sciences, Nanjing 210008, China

Jun Chen

State Key Laboratory of Isotope Geochemistry, Guangzhou Institute of Geochemistry, Chinese Academy of Sciences, Guangzhou 510640, China

Yao-feng Cai

State Key Laboratory of Palaeobiology and Stratigraphy, Nanjing Institute of Geology and Palaeontology, Chinese Academy of Sciences, Nanjing 210008, China
Center for Excellence in Life and Paleoenvironment, Chinese Academy of Sciences, Nanjing 210008, China

Zhang-shuai Hou

State Key Laboratory for Mineral Deposits Research and School of Earth Sciences and Engineering, Nanjing University, Nanjing 210023, China

Chao Liu

Department of Earth Science & Engineering, Taiyuan University of Technology, Taiyuan 030024, China

Wan Yang

Geology and Geophysics Program, Missouri University of Science and Technology, Rolla, MO 65409, USA

Charles M. Henderson

Department of Geoscience, University of Calgary, Calgary, AB T2N 1N4, Canada

Shu-zhong Shen

State Key Laboratory for Mineral Deposits Research and School of Earth Sciences and Engineering, Nanjing University, Nanjing 210023, China
Center for Excellence in Life and Paleoenvironment, Chinese Academy of Sciences, Nanjing 210023, China
Key Laboratory of Continental Collision and Plateau Uplift, Institute of Tibetan Plateau Research and Center for Excellence in Tibetan Plateau Earth Sciences, Chinese Academy of Sciences,

Beijing 100101, China
Email: szshen@nju.edu.cn

Introduction

The late Paleozoic ice age (LPIA) was the last major pre-Cenozoic ice age which has long been regarded as the unique analogue of the Quaternary ice age (Gastaldo et al., 1996). The deglaciation of LPIA is the only record for the vegetated earth transforming from an icehouse to a greenhouse period (Montañez et al., 2007). The North China block is one of the most important regions where preserves highly diverse and abundant plant fossils (Wang, 2010; Stevens et al., 2011; Wang et al., 2012; Liu et al., 2015) and records the paleoclimate change during this transition in the Upper Carboniferous and Permian deposits. It provides a superb window to study the interactions between the terrestrial biotic turnovers in middle paleolatitudes and the global climate changes during the aftermath of the LPIA.

However, the thorough understanding of the biological events, climate changes and their relationships in the North China block has long been hampered by the uncertain temporal framework. The Penchi and Taiyuan Formations have been well correlated and constrained by fusuline and conodont fossils from the interbedded limestone beds, as well as new U-Pb geochronology by the CA-ID-TIMS method (Schmitz et al., 2020; Yang et al., 2020). Some tuff zircon geochronology by *in-situ* techniques (SIMS and LA-ICPMS) were reported from this horizon as well: 296.7 ± 2.1 Ma for the upper part of the Taiyuan Formation (Wang et al., 2020), 293.0 ± 2.5 Ma for the upper part of the Shansi Formation (Yang et al., 2014), 290.1 ± 5.8 Ma for the Lower Permian coals which were correlative with the Taiyuan and/or Shansi Formations (Cope et al., 2005), and 296 ± 4 Ma for the Hongmiaoling Formation which was correlative with the Lower and Upper Shihhotse Formations (Zhang et al., 2007).

Nevertheless, the temporal framework of the Permian stratigraphic correlation after the seawater completely withdrew from the North China block has long been a subject of debate. The Shansi Formation and Lower Shihhotse Formation were roughly assigned to the Cisuralian, the Upper Shihhotse Formation to the Guadalupian and the Sunjiagou Formation to the Lopingian in the classic area of Shanxi Province in China. The assignments were mainly based on palynostratigraphy and phytostratigraphy which are fairly coarse (Wang, 2010; Liu et al., 2015) and have not been constrained by the reliable radioisotopic ages or diagnostic marine fossils. Repeated detrital zircon geochronology from the Permian volcaniclastic sandstones in the North China block (Zhu et al., 2014; Yang et al., 2017; Liang et al., 2020; and references therein) was not precise enough to resolve the issues, because these dates were obtained by LA-ICPMS method with uncertainties up to ca. 4% (Klötzli et al., 2009). Furthermore, some of the youngest dates might be spurious and not reproducible due to Pb-loss in zircons (Crowley et al., 2014; Coutts et al., 2019). Magnetostratigraphy was carried out in the North China block (Embleton et al., 1996), but strong controversies remained (Menning and Jin, 1998).

New geochronology and temporal framework

Intensive search of potential ash beds qualified for high-

precision CA-ID-TIMS dating from North China has been carried out during the last decade to solve the above issues. A set of seven new weighted mean $206\text{Pb}/238\text{U}$ dates by the CA-ID-TIMS method from bentonites of the Palougou and Qiaotou sections in northern Shanxi Province in North China have been obtained. The Bayesian age-stratigraphic model was established based on these dates and for the first time provided a near-complete reliable temporal calibration for the Permian system of the North China block (Fig. 1). Detailed data were published in Wu et al. (in press) recently.

The new temporal framework assigns the upper Taiyuan Formation to the Lower Shihhotse Formation to Asselian. The Upper Shihhotse Formation is constrained to the latest Asselian to early Kungurian in the northern North China block rather than Guadalupian as previously documented. The Sunjiagou Formation can be assigned to Lopingian based on the reported detrital zircon ages and integrated biostratigraphic data (Zhu et al., 2020).

Implications and prospects

The new dates in Wu et al. (2021) reveal a considerable unconformity for ca. 20 m.y. during the late Cisuralian to Guadalupian on the top of the Upper Shihhotse Formation in the northern North China block (Fig. 1). An analogous unconformity was reported from correlative Permian successions in eastern Xinjiang (Yang et al., 2010). The unconformity along the margins of the Paleo-Asian Ocean (PAO) may have been related to strong subduction of PAO generating arc-continent and retroarc fold-thrust deformation or its final closure leading to continental collision during the late Cisuralian to Guadalupian (ca. 280–265 Ma) (Xiao et al., 2018; Zhao et al., 2018; Liu et al., 2019). The reported *in situ* detrital zircon geochronology reveals a similar age gap as well, despite that the duration may vary across the North China block as the function of proximity to the collisional zone in the north. The closure or partly closure of PAO provided a pathway for the widespread invasion of Angaran flora to North China.

The climate aridification trends were well underway during the Cisuralian in North China based on the new framework in Wu et al. (2021), coincident with that in the middle to low paleolatitude Euramerica (Montañez et al., 2007; Tabor and Poulsen, 2008; Boucot et al., 2013; Schneider et al., 2019) (Fig. 1). It indicates that aside from the regional tectonic controls and/or northward continental movement (Rees et al., 1999; Cope et al., 2005; Tabor and Poulsen, 2008) the Cisuralian climate aridification was controlled by factors that can have global impacts. Here, large igneous province (LIP) volcanism during the Cisuralian was considered as the major contributor to the aridification due to the coincidence between the LIPs, $p\text{CO}_2$ excursions and significant retreat of the LPIA (Zhang et al., 1999; Torsvik et al., 2008; Xu et al., 2014; Shellnutt, 2018; Soreghan et al., 2019; Richey et al., 2020).

The great loss of highly diverse and abundant Cathaysian flora in the topmost Upper Shihhotse Formation are coincident with the strong uplift and the Tarim LIP rather than the Emeishan LIP (Bond et al., 2010; Stevens et al., 2011). Further work is needed as it is possible that the floral disappearance in the top

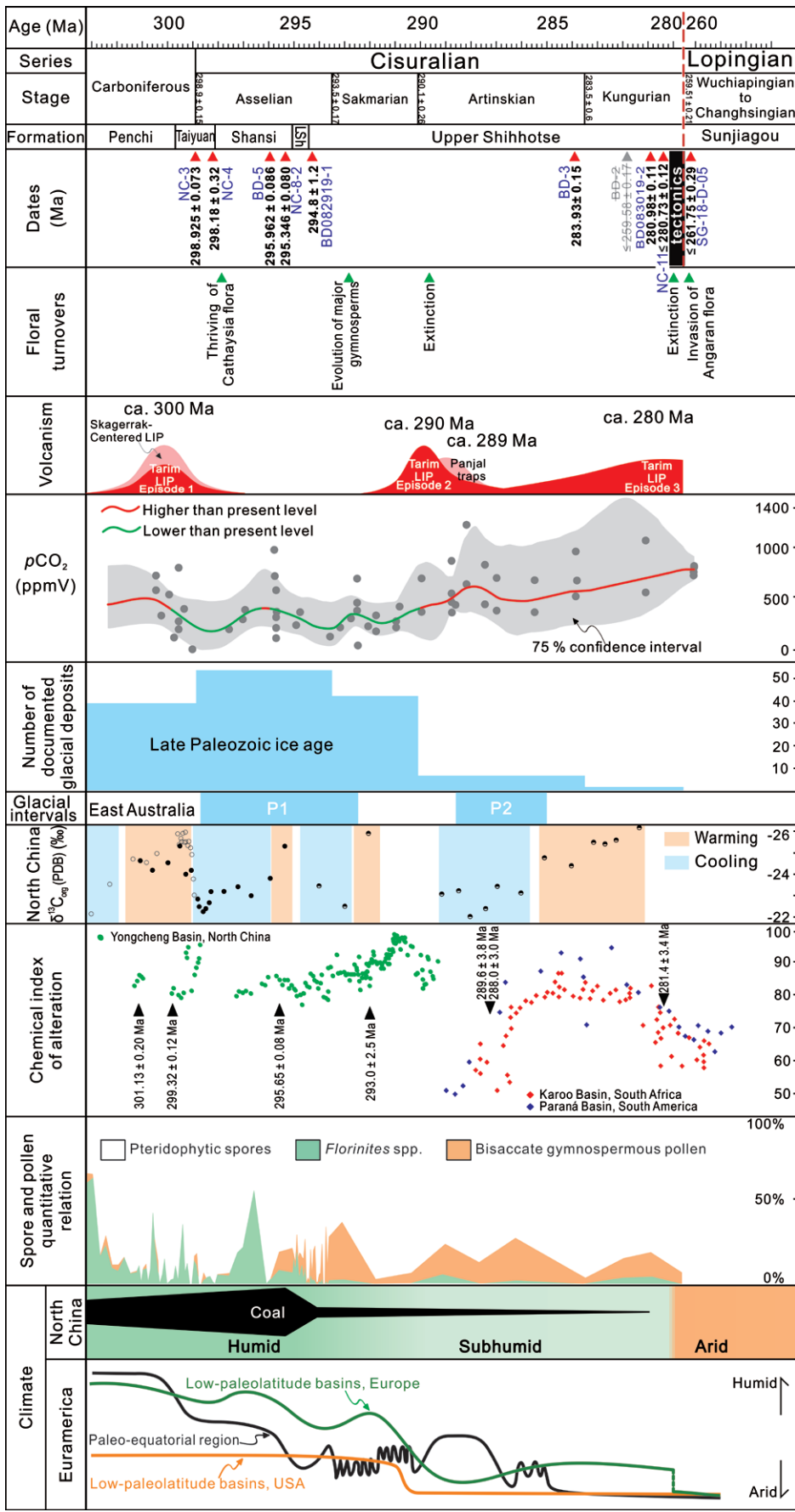


Fig. 1. Compilation of the Permian global events in parallel to Earth system changes in the North China block (Wu et al., 2021). Red dashed line represents the unconformity from the late Cisuralian to Guadalupian (ca. 280–260 Ma) between the Upper Shihhotse and Sunjiagou formations. LSh—Lower Shihhotse. Red triangles indicate dated samples. Floral turnover patterns in the North China block are modified from Wang (2010) and Stevens et al. (2011). Main episodes of Panjal Traps, Skagerrak-Centered large igneous province (LIP) and Tarim LIP volcanism are after Shellnutt (2018), Torsvik et al. (2008), and Xu et al. (2014), respectively. Global atmospheric pCO₂ curve is after Richey et al. (2020). Documented glacial deposits are after Soreghan et al. (2019). Glacial intervals in Australia are after Garbelli et al. (2019). δ13Corg (PDB—Pee Dee belemnite) of coals in North China is after Zhang et al. (1999). Chemical index of alteration and ages marked as black triangles are after Yang et al. (2014, 2020) and references therein. Quantitative relation of Permian spore and pollen in the North China block is after Liu et al. (2015). Cisuralian Euramerican climate transitions are after Tabor and Poulsen (2008).

Upper Shihhotse Formation is not an evolutionary event but the truncation caused by loss of fossil records due to the long hiatus. Besides, it is also possible that the disappearance of Cathaysian flora and invasion of Angaran flora in the North China block happened gradually during the late Cisuralian to Guadalupian, concomitant with the progressive aridification and closure of PAO, but its exact story and timing is uncertain due to the long hiatus.

The new terrestrial Permian framework in the North China block demonstrates the possible first order relationships between the extensive volcanisms, atmospheric $p\text{CO}_2$ variations and climate changes, but other controls with a more detailed view, e.g., CO_2 sinks and consumers, plant evolutions and extinctions, carbonate factories, wildfires, still need further study. The progress in terrestrial Permian framework demonstrates the North China block a superb area for further study on relationships between floral evolution and atmospheric $p\text{CO}_2$ variations and/or thresholds in the future. And further studies about more detailed Cisuralian floral evolution and climate variations in the North China block is necessary for a thorough understanding of their mechanisms during this crucial interval.

References

- Bond, D.P.G., Hilton, J., Wignall, P.B., Ali, J.R., Stevens, L.G., Sun, Y.D., and Lai, X.L., 2010, The Middle Permian (Capitanian) mass extinction on land and in the oceans: *Earth-Science Reviews*, v. 102, p. 100–116.
- Boucot, A.J., Chen, X., Scotese, C.R., and Morley, R.J., 2013, Phanerozoic paleoclimate: an atlas of lithologic indicators of climate, SEPM Concepts in Sedimentology and Paleontology, Printed Map Folio, No. 11, Society for Sedimentary Geology, Society of Economic Paleontologists and Mineralogists.
- Cope, T., Ritts, B.D., Darby, B.J., Fildani, A., and Graham, S., 2005, Late Paleozoic sedimentation on the northern margin of the North China block: implications for regional tectonics and climate change: *International Geology Review*, v. 47, p. 270–296.
- Coutts, D.S., Matthews, W.A., and Hubbard, S.M., 2019, Assessment of widely used methods to derive depositional ages from detrital zircon populations: *Geoscience Frontiers*, v. 10, p. 1421–1435.
- Crowley, Q.G., Heron, K., Riggs, N., Kamber, B., Chew, D., McConnell, B., and Benn, K., 2014, Chemical abrasion applied to LA-ICP-MS U-Pb zircon geochronology: *Minerals*, v. 4, p. 503–518.
- Embleton, B.J.J., McElhinny, M.W., Ma, X., Zhang, Z., and Xiang Li, Z., 1996, Permo-Triassic magnetostratigraphy in China: the type section near Taiyuan, Shanxi Province, North China: *Geophysical Journal International*, v. 126, p. 382–388.
- Garbelli, C., Shen, S.Z., Immenhauser, A., Brand, U., Buhl, D., Wang, W.Q., Zhang, H., and Shi, G.R., 2019, Timing of Early and Middle Permian deglaciation of the southern hemisphere: Brachiopod-based $87\text{Sr}/86\text{Sr}$ calibration: *Earth and Planetary Science Letters*, v. 516, p. 122–135.
- Gastaldo, R., DiMichele, W., and Pfefferkorn, H., 1996, Out of the icehouse into the greenhouse—a Late Paleozoic analog for modern global vegetational change: *GSA Today*, v. 6, p. 1–33.
- Klötzli, U., Klötzli, E., Günes, Z., and Kosler, J., 2009, Accuracy of laser ablation U-Pb zircon dating: Results from a test using five different reference zircons: *Geostandards and Geoanalytical Research*, v. 33, p. 5–15.
- Liang, J.W., Xiao, J., and Tao, W.X., 2020, Detrital zircon U-Pb ages of Middle–Late Permian sedimentary rocks from the southwestern margin of the North China Craton: Implications for provenance and tectonic evolution: *Gondwana Research*, v. 88, p. 250–267.
- Liu, F., Zhu, H.C., and Ouyang, S., 2015, Late Pennsylvanian to Wuchiapingian palynostratigraphy of the Baode section in the Ordos Basin, North China: *Journal of Asian Earth Sciences*, v. 111, p. 528–552.
- Liu, Q., Zhao, G.C., Han, Y.G., Zhu, Y.L., Wang, B., Eizenhöfer, P.R., Zhang, X.R., and Tsui, R.W., 2019, Timing of the final closure of the middle segment of the Paleo-Asian Ocean: Insights from geochronology and geochemistry of Carboniferous–Triassic volcanosedimentary successions in western Inner Mongolia, China: *Geological Society of America Bulletin*, v. 131, p. 941–965.
- Menning, M., and Jin, Y.G., 1998, Comment on 'Permo-Triassic magnetostratigraphy in China: the type section near Taiyuan, Shanxi Province, North China' by B.J.J. Embleton, M.W. McElhinny, X. Ma, Z. Zhang and Z.X. Li: *Geophysical Journal International*, v. 133, p. 213–216.
- Montañez, I.P., Tabor, N.J., Niemeier, D., DiMichele, W.A., Frank, T.D., Fielding, C.R., Isbell, J.L., Birgenheier, L.P., and Rygel, M.C., 2007, CO₂-forced climate and vegetation instability during Late Paleozoic deglaciation: *Science*, v. 315, p. 87–91.
- Rees, P.M., Gibbs, M.T., Ziegler, A.M., Kutzbach, J.E., and Behling, P.J., 1999, Permian climates: Evaluating model predictions using global paleobotanical data: *Geology*, v. 27, p. 891–894.
- Richey, J.D., Montañez, I.P., Goddérus, Y., Looy, C.V., Griffis, N.P., and DiMichele, W.A., 2020, Influence of temporally varying weatherability on CO₂-climate coupling and ecosystem change in the late Paleozoic: *Clim. Past*, v. 16, p. 1759–1775.
- Schmitz, M.D., Pfefferkorn, H.W., Shen, S.Z., and Wang, J., 2020, A volcanic tuff near the Carboniferous–Permian boundary, Taiyuan Formation, North China: Radioisotopic dating and global correlation: *Review of Palaeobotany and Palynology*, doi: 10.1016/j.revpalbo.2020.104244.
- Schneider, J.W., Lucas, S.G., Scholze, F., Voigt, S., Marchetti, L., Klein, H., Opluštil, S., Werneburg, R., Golubev, V.K., Barrick, J.E., Nemyrovska, T., Ronchi, A., Day, M.O., Silantiev, V.V., Rößler, R., Saber, H., Linnemann, U., Zharinova, V., and Shen, S.Z., 2019, Late Paleozoic–early Mesozoic continental biostratigraphy—Links to the Standard Global Chronostratigraphic Scale: *Palaeoworld*, v. 29, p. 186–238.
- Shellnutt, J.G., 2018, The Panjal Traps: *Geological Society, London, Special Publications*, v. 463, p. 59–86.
- Soreghan, G.S., Soreghan, M.J., and Heavens, N.G., 2019, Explosive volcanism as a key driver of the late Paleozoic ice age: *Geology*, v. 47, p. 600–604.
- Stevens, L.G., Hilton, J., Bond, D.P., Glasspool, I.J., and Jardine,

- P.E., 2011, Radiation and extinction patterns in Permian floras from North China as indicators for environmental and climate change: *Journal of the Geological Society*, v. 168, p. 607–619.
- Tabor, N.J., and Poulsen, C.J., 2008, Palaeoclimate across the Late Pennsylvanian–Early Permian tropical palaeolatitudes: A review of climate indicators, their distribution, and relation to palaeophysiological climate factors: *Palaeogeography, Palaeoclimatology, Palaeoecology*, v. 268, p. 293–310.
- Torsvik, T.H., Smethurst, M.A., Burke, K., and Steinberger, B., 2008, Long term stability in deep mantle structure: Evidence from the ~300 Ma Skagerrak-Centred Large Igneous Province (the SCLIP): *Earth and Planetary Science Letters*, v. 267, p. 444–452.
- Wang, J., 2010, Late Paleozoic macrofloral assemblages from Weibei Coalfield, with reference to vegetational change through the Late Paleozoic Ice-age in the North China Block: *International Journal of Coal Geology*, v. 83, p. 292–317.
- Wang, J., Pfefferkorn, H.W., Zhang, Y., and Feng, Z., 2012, Permian vegetational Pompeii from Inner Mongolia and its implications for landscape paleoecology and paleobiogeography of Cathaysia: *Proceedings of the National Academy of Sciences*, v. 109, p. 4927–4932.
- Wang, M., Zhong, Y.T., He, B., Denyszyn, S.W., Wang, J., and Xu, Y.G., 2020, Geochronology and geochemistry of the fossil-flora-bearing Wuda Tuff in North China Craton and its tectonic implications: *Lithos*, v. 364–365, p. 105485.
- Wu, Q., Ramezani, J., Zhang, H., Wang, J., Zeng, F.G., Zhang, Y.C., Liu, F., Chen, J., Cai, Y.F., Hou, Z.S., Liu, C., Yang, W., Henderson, C.M., and Shen, S.Z., in press, High-precision U-Pb age constraints on the Permian floral turnovers, paleoclimate change and tectonics of the North China block: *Geology*, v. 49, no. 6, p. 677–681.
- Xiao, W.J., Windley, B.F., Han, C.M., Liu, W., Wan, B., Zhang, J.E., Ao, S.J., Zhang, Z.Y., and Song, D.F., 2018, Late Paleozoic to early Triassic multiple roll-back and orocinal bending of the Mongolia collage in Central Asia: *Earth-Science Reviews*, v. 186, p. 94–128.
- Xu, Y.G., Wei, X., Luo, Z.Y., Liu, H.Q., and Cao, J., 2014, The Early Permian Tarim Large Igneous Province: Main characteristics and a plume incubation model: *Lithos*, v. 204, p. 20–35.
- Yang, D.B., Yang, H.T., Shi, J.P., Xu, W.L., and Wang, F., 2017, Sedimentary response to the paleogeographic and tectonic evolution of the southern North China Craton during the late Paleozoic and Mesozoic: *Gondwana Research*, v. 49, p. 278–295.
- Yang, J.H., Cawood, P.A., Du, Y.S., Feng, B., and Yan, J.X., 2014, Global continental weathering trends across the Early Permian glacial to postglacial transition: Correlating high- and low-paleolatitude sedimentary records: *Geology*, v. 42, p. 835–838.
- Yang, J.H., Cawood, P.A., Montañez, I.P., Condon, D.J., Du, Y.S., Yan, J.X., Yan, S.Q., and Yuan, D.X., 2020, Enhanced continental weathering and large igneous province induced climate warming at the Permo-Carboniferous transition: *Earth and Planetary Science Letters*, v. 534, p. 116074.
- Yang, W., Feng, Q., Liu, Y.Q., Tabor, N., Miggins, D., Crowley, J.L., Lin, J.Y., and Thomas, S., 2010, Depositional environments and cyclo- and chronostratigraphy of uppermost Carboniferous–Lower Triassic fluvial–lacustrine deposits, southern Bogda Mountains, NW China — A terrestrial paleoclimatic record of mid-latitude NE Pangea: *Global and Planetary Change*, v. 73, p. 15–113.
- Zhang, H., Shen, G.L., and He, Z.L., 1999, A carbon isotopic stratigraphic pattern of the Late Palaeozoic Coals in the North China Platform and its palaeoclimatic implications: *Acta Geologica Sinica (English Edition)*, v. 73, p. 111–119.
- Zhang, S.H., Zhao, Y., Song, B., and Yang, Y.H., 2007, Zircon SHRIMP U-Pb and in-situ Lu-Hf isotope analyses of a tuff from Western Beijing: evidence for missing Late Paleozoic arc volcano eruptions at the northern margin of the North China block: *Gondwana Research*, v. 12, p. 157–165.
- Zhao, G.C., Wang, Y.J., Huang, B.C., Dong, Y.P., Li, S.Z., Zhang, G.W., and Yu, S., 2018, Geological reconstructions of the East Asian blocks: From the breakup of Rodinia to the assembly of Pangea: *Earth-Science Reviews*, v. 186, p. 262–286.
- Zhu, X.Q., Zhu, W.B., Ge, R.F., and Wang, X., 2014, Late Paleozoic provenance shift in the south-central North China Craton: Implications for tectonic evolution and crustal growth: *Gondwana Research*, v. 25, p. 383–400.
- Zhu, Z.C., Kuang, H.W., Liu, Y.Q., Benton, M.J., Newell, A.J., Xu, H., An, W., Ji, S.A., Xu, S.C., Peng, N., and zhai, Q.G., 2020, Intensifying aeolian activity following the end Permian mass extinction: Evidence from the Late Permian–Early Triassic terrestrial sedimentary record of the Ordos Basin, North China: *Sedimentology*, v. 67, p. 2691–2720.
-
- ## Upper Permian brachiopods from the Abadeh section, Central Iran
- Marco Viaretti**
Dipartimento di Scienze della Terra “A. Desio”, Via Mangiagalli 34, 20133 Milano
Email: marco.viaretti@studenti.unimi.it
- Gaia Crippa**
Dipartimento di Scienze della Terra “A. Desio”, Via Mangiagalli 34, 20133 Milano
Email: gaia.crippa@unimi.it
- Shuzhong Shen**
School of Earth Sciences and Engineering, Nanjing University, 163 Xianlin Avenue, Nanjing, Jiangsu 210023, P.R. China
Email: szshen@nju.edu.cn
- Lucia Angiolini**
Dipartimento di Scienze della Terra “A. Desio”, Via Mangiagalli 34, 20133 Milano
Email: lucia.angiolini@unimi.it
- A countless number of studies have been devoted to describe the Permian-Triassic succession of Abadeh since its discovery in 1967, focusing in particular on the Permian-Triassic boundary

(e.g. Taraz et al., 1981; Gallet et al., 2000; Korte et al., 2004; Kozur, 2007; Richoz et al., 2010; Shen and Mei, 2010; Liu et al., 2013; Shen et al., 2013; Chen et al., 2020; Baud et al. 2021), whose position still remains strongly debated (see discussion in Horacek et al., 2021 and Chen et al. this Permophiles issue).

The Abadeh section, located in Central Iran (Fig. 1), records a complete marine succession spanning from the Early Permian to the Early Triassic. It comprises three Permian formations, Surmaq Formation, Abadeh Formation and Hambast Formation, and the Triassic Elikah Formation (Taraz et al., 1981). The Permian-Triassic boundary interval is represented by the Boundary Clay, or boundary shale, which is a 10-30 cm bed of claystones, followed by microbialites and then bioturbated marly limestones. As said above, the position of the Permian-Triassic boundary in the section is a highly debated topic (Horacek et al., 2021). Here, we follow the conodont-based interpretation of Shen and Mei (2010) - well studied by one of the co-authors (S.Z. Shen) - in placing the PTB at 80 cm above the top of the *Paratirolites* Limestone, in the microbialites based on conodonts and the carbon isotope excursion (Shen et al., 2013). A very recent study of the Abadeh section by Chen et al. (2020) provides a high-resolution isotopic record of the Late Permian-Early Triassic time interval based on conodont apatite.

Notwithstanding their abundance in the Permian part of the Abadeh succession, brachiopods have not been described in detail up to now. A field campaign in 2017 by an Italian-Chinese-Iranian

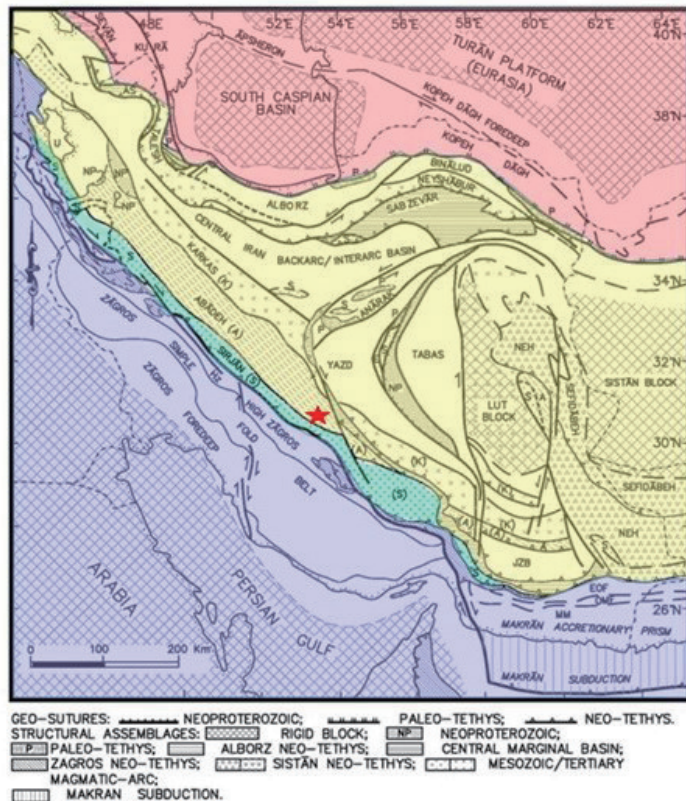


Fig.1. Tectonic domains of the Iranian region. Modified from Berberian, 2014. Red: Eurasia; yellow: Cimmerian terranes; green: Sanandaj-Sirjan; blue: Gondwana. Red star: Abadeh section.

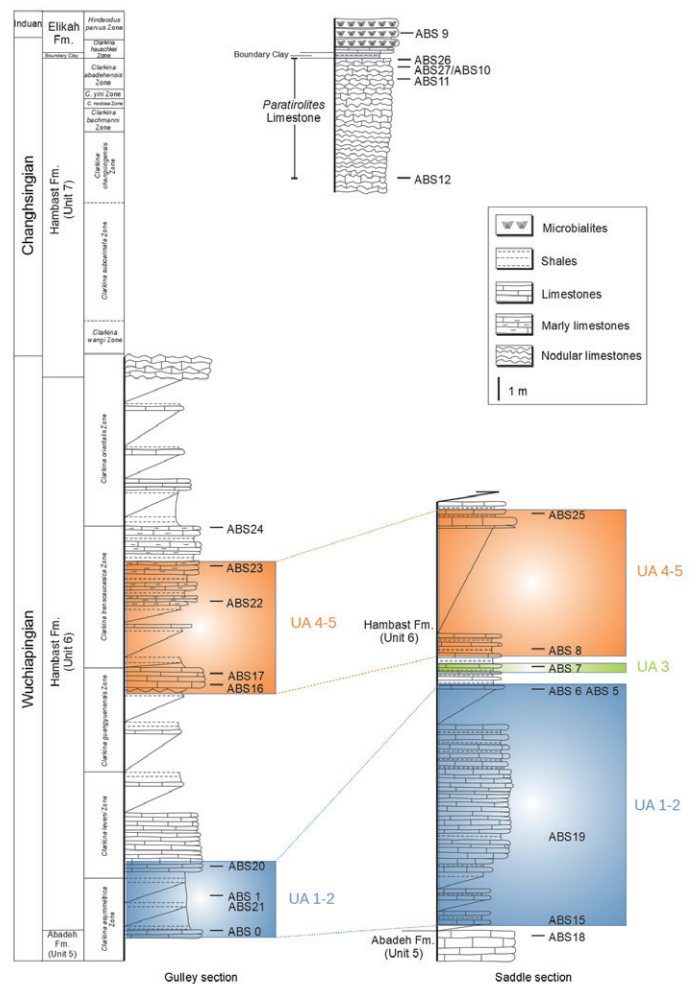


Fig. 2. Stratigraphic logs of the Abadeh section.

research team (Angiolini et al., 2017) allowed to sample bed-by-bed about 430 brachiopod specimens from 30 fossiliferous beds from the base of Unit 6 of the Hambast Formation to the top of the *Paratirolites* Limestone (Hambast Formation, Unit 7), along two sections, the Gulley section and Saddle section (Fig. 2). An in-depth systematic study was then performed to test their potential as biostratigraphic tools at a regional scale and other implications.

The study of the brachiopod fauna allowed to identify 29 species belonging to 13 genera: *Spinomarginifera* sp., *S. helica*, *S. iranica*, *S. pygmaea*, *S. spinosocostata*, *Araxilevis intermedius*, *Tschernyschewia typica*, *Leptodus* sp., *L. cf. L. richtofeni*, *L. nobilis*, *Permianella* sp., *Orthotetina* sp., *O. persica*, *Perigeyerella* spp., *Perigeyerella* aff. *P. costellata*, *P. aff. P. tricosa*, *Araxathyris* spp., *A. abichi*, *A. bruntoni*, *A. felina*, *A. quadrilobata*, *?Rectambitus* sp., *Gruntallina* sp., *?Spirigerella* sp., *Transcaucasathyris* spp., *T. araxensis*, *T. kandevani*, *T. lata*, *Paracurothyris pygmaea* and *?Permophricodothyris* sp. A few poorly preserved specimens have been identified as belonging to the Tylolectini and to the Athyrididae. This represents a step forward compared to the first survey by who identified only 14 brachiopod species (Taraz et al., 1981). The systematic descriptions of this fauna will be submitted for publication soon (Viaretti et al., in progress).

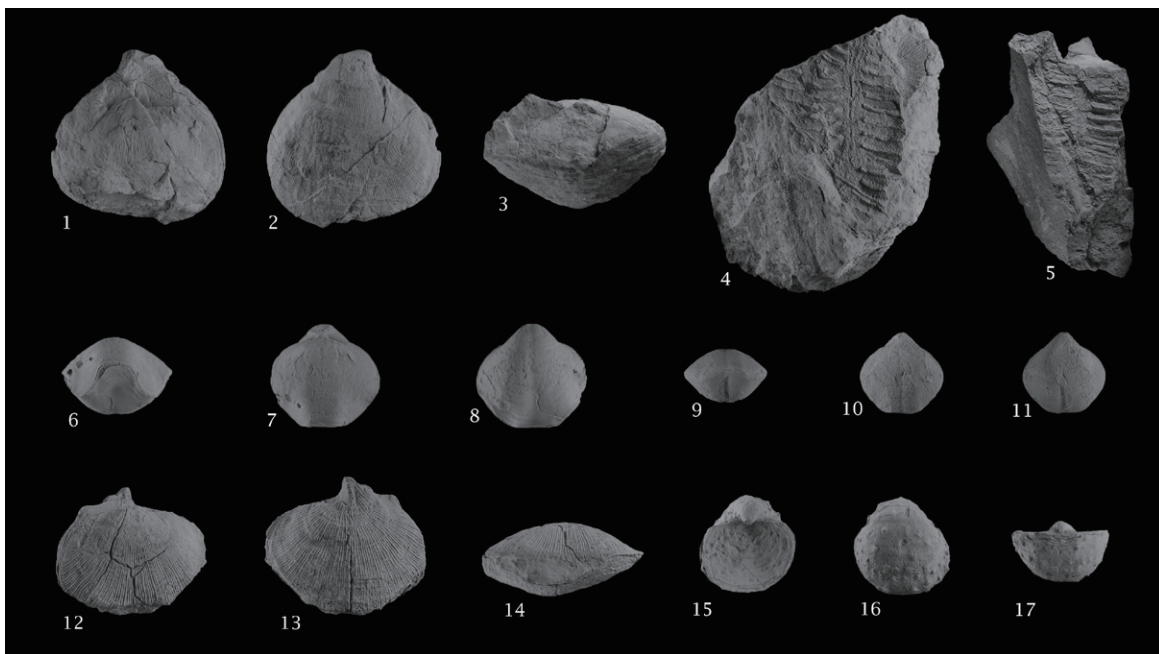


Fig. 3. Brachiopod specimens from the Abadeh section. 1-3: *Perigeyerella* aff. *costellata* (ABS21-10), dorsal, ventral and anterior view, 1x. 4-5: *Leptodus nobilis* (ABS6-6, ABS20-8), 1x. 6-8: *Araxathyris bruntoni* (ABS17-9), anterior, dorsal and ventral view, 2x. 9-11: *Transcaucasathyris araxensis* (ABS16-6), anterior, dorsal and ventral view, 2x. 12-14: *Perigeyerella* aff. *tricosa* (ABS7-2), dorsal, ventral and anterior view, 1x. 15-17: *Spinomarginifera pygmaea* (ABS8-29), dorsal, ventral and anterior view, 2x.

The stratigraphic distribution of the brachiopods in the Abadeh section has been analyzed with the PAST software (Hammer et al., 2001) using the Unitary Association (UA) method (Guex, 1991) to correlate the two sections at Abadeh. The resulting UAs which allow to correlate the two sections are: UA1-2, taxonomically identified by the taxa *Perigeyerella* aff. *costellata* and *Leptodus nobilis* in the lower part of the sections and UA4-5, taxonomically identified by the taxa *Araxathyris bruntoni* and *Transcaucasathyris araxensis*, in the upper part of the sections. Another UA was found only in the Saddle section (UA3), taxonomically identified by the taxa *Perigeyerella* aff. *tricosa* and *Spinomarginifera pygmaea*; this UA has no reproducibility and cannot be used for correlation (Fig. 3). The single occurrence of *Paracrurithyris pygmaea* in the *Paratirolites* Limestone was not treated in the analysis, but it represents an important element of correlation with other sections in Iran. In fact, a further analysis involving also the brachiopods of the Julfa section in NW Iran (Ghaderi et al., 2014; Garbelli et al. 2014) lead to identify three brachiopod biozones: the *Araxilevis intermedius* – *Leptodus nobilis* zone, the *Permophricodothyris ovata* – *Araxathyris quadrilobata* zone and lastly the *Paracrurithyris pygmaea* zone which allow a good correlation between the composite sections of NW Iran and Central Iran (Viaretti et al. in progress). These brachiopod biozones have thus proved to be good tools for the regional correlation of the Upper Permian successions of Iran.

Not only brachiopods from Abadeh have a good potential in regional correlation, but future studies will be devoted to analyze the shell microstructure of the identified brachiopod taxa to better constrain the biotic change during the dramatic end-Permian events (volcanism, global warming and ocean acidification). Of

the five brachiopod orders identified, Productida and Athyridida show a marked dominance and alternate in the succession up to the middle part of Unit 6. The upper part of Unit 6 and Unit 7 are instead dominated by taxa of the order Athyridida. The two orders are characterized by different shell microstructures: Productida have an organic-rich laminar shell, while Athyridida have a less organic-rich fibrous shell; therefore, based on the stratigraphic distribution depicted above, the fibrous taxa are more common than the laminar ones in the upper part of the section, as already underscored for other end-Permian sections in Iran and South China (Garbelli et al., 2017). Yet another proof that acidification (pH drop) played an important role in the causational trigger of the mass extinction in the latest Permian (Jurikova et al., 2020).

References

- Berberian, M., 2014. Earthquakes and coseismic surface faulting on the Iranian Plateau. In Series of Developments in Earth Surface Processes. 1st ed., Amsterdam, Elsevier, 776 p.
- Baud, A., Richoz, S., Brandner, R., Krystyn, L., Heindel, K., Mohtat, T., Mohtat-Aghai, P. and Horacek, M., 2021. Sponge Takeover from End-Permian Mass Extinction to Early Induan Time: Records in Central Iran Microbial Buildups. Frontiers in Earth Science, v. 9, p. 1–23.
- Chen, J., Shen, S. Z., Zhang, Y. C., Angiolini, L., Gorgij, M. N., Crippa, G., Wang W., Zhang H., Yuan D. X., Li X. H. and Xu, Y. G., 2020. Abrupt warming in the latest Permian detected using high-resolution in situ oxygen isotopes of conodont apatite from Abadeh, central Iran. Palaeogeography, Palaeoclimatology, Palaeoecology, v. 560, p. 1–11.
- Gallet, Y., Krystyn, L., Besse, J. and Ricou, L.E., 2000. New

- constraints on the Upper Permian and Lower Triassic geomagnetic polarity timescale from the Abadeh section (central Iran). *Journal of Geophysical Research*, v. 105, no. B2, p. 2805–2815.
- Garbelli, C., Angiolini, L., Shen, S., Crippa, G., Yuan, D., Bahrammanesh, M., Abbasi, S. and Birjandi, M., 2014. Additional brachiopod findings from the Lopingian succession of the Ali Bashi Mountains, NW Iran. *Rivista Italiana Di Paleontologia e Stratigrafia*, v. 120, p. 119–126.
- Garbelli, C., Angiolini, L., and Shen, S. Z., 2017. Biomineralization and global change: a new perspective for understanding the end-Permian extinction. *Geology*, v. 45, no. 1, p. 19–22.
- Guex, J., 1991. Biochronological correlations. Springer, Berlin. 252 p.
- Hammer, Ø., Harper, D.A.T. and Ryan, P.D., 2001. PAST: paleontological statistics software package for education and data analysis. *Palaeontology Electronica*, v. 4, p. 1–9.
- Horacek, M., Krystyn, L. and Baud, A., 2021. Comment to Chen et al., 2020: Abrupt warming in the latest Permian detected using high-resolution in situ oxygen isotopes of conodont apatite from Abadeh, central Iran. Importance of correct stratigraphic correlation, reporting of existing data and their scientific interpretation. *Permophiles*, v. 70, p. 33–36.
- Jurikova, H., Gutjahr, M., Wallmann, K., Flögel, S., Liebetrau, V., Posenato, R., Angiolini, L., Garbelli, C., Brand, U., Wiedenbeck, M. and Eisenhauer, A., 2020. Permian–Triassic mass extinction pulses driven by major marine carbon cycle perturbations. *Nature Geoscience*, v. 13(11), p. 745–750.
- Korte, C., Kozur, H.W., Joachimski, M.M., Strauss, H., Veizer, J. and Schwark, L., 2004. Carbon, sulfur, oxygen and strontium isotope records, organic geochemistry and biostratigraphy across the Permian/Triassic boundary in Abadeh, Iran. *International Journal of Earth Sciences*, v. 93, p. 565–581.
- Kozur, H. W., 2007. Biostratigraphy and event stratigraphy in Iran around the Permian-Triassic Boundary (PTB): Implications for the causes of the PTB biotic crisis. *Global and Planetary Change*, v. 55, p. 155–176.
- Liu, X.C., Wang, W., Shen, S.Z., Gorgij, M.N., Ye, F.C., Zhang, Y.C., Furuyama, S., Kano, A. and Chen, X.Z., 2013. Late Guadalupian to Lopingian (Permian) carbon and strontium isotopic chemostratigraphy in the Abadeh section, central Iran. *Gondwana Research*, v. 24, p. 222–232.
- Richoz, S., Krystyn, L., Baud, A., Brandner, R., Horacek, M. and Mohtat-Aghai, P., 2010. Permian–Triassic boundary interval in the Middle East (Iran and N. Oman): Progressive environmental change from detailed carbonate carbon isotope marine curve and sedimentary evolution. *Journal of Asian Earth Sciences*, v. 39, no. 4, p. 236–253.
- Shen, S. Z., and Mei, S. L. (2010). Lopingian (Late Permian) high-resolution conodont biostratigraphy in Iran with comparison to South China zonation. *Geological Journal*, v. 45, no. 2–3, p. 135–161.
- Shen, S. Z., Cao, C. Q., Zhang, H., Bowring, S. A., Henderson, C. M., Payne, J. L., Davydov V. I., Chen B., Yuan D. X., Zhang Y. C., Wang W. and Zheng, Q. F., 2013. High-resolution $\delta^{13}\text{C}_{\text{carb}}$ chemostratigraphy from latest Guadalupian through earliest Triassic in South China and Iran. *Earth and Planetary Science Letters*, v. 375, p. 156–165.
- Taraz, H., Golshani, F., Nakazawa, K., Shimura, D., Bando, Y., Ishii, K.I., Maurata, M., Okimura, Y., Sakamura, S., Nakamura, K. and Tokuoka, T., 1981. The Permian and the Lower Triassic Systems in Abadeh Region, Central Iran. *Memoirs of the Faculty of Science, Kyoto University, Series of Geology and Mineralogy*, v. 47, p. 62–133.
-
- Reply to the Comment of Horacek et al. (2021) on the Permian-Triassic boundary at the Abadeh section, central Iran**
- Jun Chen**
State Key Laboratory of Isotope Geochemistry, Guangzhou Institute of Geochemistry, Chinese Academy of Sciences, and CAS Center for Excellence in Deep Earth Science, Guangzhou 510640, China
- Dong-xun Yuan**
School of Resources and Geosciences, China University of Mining and Technology, Xuzhou 221116, China
- Shu-zhong Shen**
State Key Laboratory for Mineral Deposits Research, School of Earth Sciences and Engineering and Frontiers Science Center for Critical Earth Material Cycling, Nanjing University, Nanjing 210023, China
- We thank Horacek et al. for their Comment (Horacek et al., 2021a) on a paper we recently published in PALAEO-3 (Chen et al., 2020) regarding the Abadeh section, central Iran, particularly about the position of the Permian-Triassic boundary (PTB). Indeed, the Abadeh section, located in the Hambast Valley, central Iran is widely regarded as one of the most important PTB sections in the world, therefore, robust biostratigraphic framework, especially around the PTB, is critical for any type of investigation. However, such importance does not exclude disagreements.
- Horacek et al. (2021a) claimed that our study (Chen et al., 2020) has disregarded major published work. We disagree. Our paper (Chen et al., 2020) is essentially a geochemical study based on conodont elements. Therefore, we did not present a lengthy section to review the history of conodont taxonomy and biostratigraphy of the Abadeh section. Instead, we summarized the overall geological setting, introduced the key boundaries, and presented our biostratigraphic framework in the forms of figure and table (Fig.2, Fig.3, and Table 1 in Chen et al., 2020). We appreciate the effort of Horacek et al. (2021a) to present a more or less complete review on various studies about the Abadeh section. However, most, if not all of the works mentioned in Horacek et al. (2021a) were cited in our paper.
- It is also important to note that the way Horacek et al. (2021a) forced some published work into GROUP 1 (Taraz et al., 1981; Gallet et al., 2000; Horacek et al., 2007; Richoz et al., 2010; Kershaw et al., 2012; Liu et al., 2013; Shen et al., 2013; Dudas et

al., 2017) and GROUP 2 (Korte et al., 2004; Kozur, 2004, 2005, 2007; Korte et al., 2010; Shen and Mei, 2010; Chen et al., 2020), on the basis of the position of PTB relative to the “Microbialite Bed”. In our opinion, this way of grouping may be misleading. For instance, Kershaw et al. (2012) only cited the conodont biostratigraphy of the Abadeh section (named as the “Hambast, Iran” section) from Richoz et al. (2010), and independent conodont investigation was not conducted. Liu et al. (2013), Shen et al. (2013), and Dudas et al. (2017) shared the same set of samples (bulk rock and conodonts) collected in 2009 (Shen et al., 2009), and defined the PTB in the middle of the “Microbialite Bed”. This is different from the definition of other studies in the so-called “GROUP 1” (Taraz et al., 1981; Gallet et al., 2000; Horacek et al., 2007; Richoz et al., 2010), which placed the PTB at the base of the “Microbialite Bed”. Therefore, it is obvious that those studies (Taraz et al., 1981; Gallet et al., 2000; Horacek et al., 2007; Richoz et al., 2010; Kershaw et al., 2012; Liu et al., 2013; Shen et al., 2013; Dudas et al., 2017) cannot be put into the same group, regarding the position of the PTB.

Among four publications (Taraz et al., 1981; Gallet et al., 2000; Horacek et al., 2007; Richoz et al., 2010) that defined the PTB at the base of the “Microbialite Bed” in Abadeh, only Richoz et al. (2010) illustrated conodont specimens, therefore we use their results as an example to discuss whether such definition is correct. In the critical interval from the base of “boundary clay” to the top of “Microbialite Bed”, three samples (94/263, 94/264, and 94/265) were productive in the study of Richoz et al. (2010). Richoz et al. (2010) claimed that they found *H. parvus* 25 cm above the lithological boundary (sample 94/264) between the Hambast and Elikah formations, which is located at the base of “boundary clay”. According to their data, eight specimens were recovered from sample 94/264, with six of them (75%) being *Hindeodus* elements. However, they only illustrated one fragmentary specimen with broken tips of denticles, as well as a broken and strongly recurved cusp (Richoz et al., 2010, plate 2, fig. 6). According to our evaluation, because (1) insufficient specimens have been illustrated, and (2) the illustrated single specimen is poorly preserved, it is arbitrary to claim that the illustrated specimen is *H. parvus*, thus defining the PTB at 25 cm above the base of “boundary clay”. Using the “sample-population” method, and with abundant specimens illustrated, Chen et al. (2009) demonstrated the lineage of *Hindeodus praeparvus* – *H. parvus* – *H. postparvus* around the “Microbialite Bed” at the Dawen section in southern Guizhou, China, showing possible morphological variations of each species. We think that the illustrated fragmentary specimens from Richoz et al. (2010) (plate 2, fig. 6) is identifiable between *H. praeparvus* and *H. parvus*. More conodont elements from that key sample 94/264 are required to make a proper assessment.

Horacek et al. (2021a) were highly critical of our biochronology and lithostratigraphy at the Abadeh section (Chen et al., 2020) and listed four so-called “problems”. Our response are as follows:

(1) Horacek et al. (2021a) argues that we ignored the existence of one (*C. meishanensis* – *H. praeparvus*) or two (*C. meishanensis* – *H. praeparvus* and *M. ultima* – *S. ?mostleri*) uppermost Permian conodont zones above the *C. hauschkei* Zone.

As anybody working in the field of biostratigraphy would do, we primarily rely on our own fossil materials to identify species and/or subspecies in each sample, draw range charts of each species and/or subspecies, and establish range zones. Therefore, we cannot ignore some species that are not present in our samples. For instance, in the five samples covering the critical interval from -1.5 m to 0 m (Chen et al., 2020), we did not find *M. ultima* and *S. ?mostleri*. Moreover, using the “sample-population” method, Shen and Mei (2010) compared high-resolution conodont biostratigraphy in Iran and South China and presented a framework for correlation. We agree with this framework, in which the *C. hauschkei* Zone in Iran correlates with the upper part of the *C. meishanensis* Zone in South China, containing abundant *Hindeodus praeparvus*, rare specimens morphologically close to *H. parvus* and some *H. changxingensis*. In other words, the *Hindeodus praeparvus*, *H. changxingensis*, the upper part of the *Clarkina meishanensis* and the *C. hauschkei* zones all overlap in stratigraphic ranges and are largely equivalent in time (Shen and Mei, 2010, p.149, fig. 13). All of them are succeeded by the index *H. parvus* Zone of the earliest Triassic. Since we regard *C. hauschkei* as a junior synonym, or more likely a geographic cline of *C. meishanensis*, and the fact *H. praeparvus* in our samples is in a very short range and partially overlapping with *C. hauschkei*, there is no need to show *C. meishanensis* Zone, *H. praeparvus* Zone, or *C. meishanensis* – *H. praeparvus* Zone at the Abadeh section, although we admit that we could have explained this more clearly in our paper.

(2) Horacek et al. (2021a) claimed that our way of placing the PTB in Abadeh is “unsound and non-scientific”. One of their arguments is that we did not present enough evaluation on previous publications about the Abadeh section (i.e., published work divided into their so-called “GROUP 1” and “GROUP 2”). As explained above, our publication (Chen et al., 2020) is essentially a geochemical study focusing on the seawater temperature evolution during the Late Permian – earliest Triassic. We presented our biostratigraphic framework with appropriate explanation. Whether such kind of presentation is proper is subjective. Horacek et al. (2021a) also argued that we “did not document our own conodont material”. We presume that Horacek et al. expected that we should present a lengthy section of our paper in the form of a detailed biostratigraphic work. Again, this was out of the scope of our paper. First, the conodont biostratigraphic framework of our samples collected in 2009 has been presented previously (Liu et al., 2013; Shen et al., 2013; Dudas et al., 2017). Second, we were planning to present a comprehensive work solely on conodont biostratigraphy, combining our collections from Abadeh in central Iran and Kuh-e-Ali Bashi in NW Iran. Therefore, we feel that it is not a necessity for us to “document our own conodont material” from the Abadeh section in detail at the moment.

Horacek et al. (2021a) also suggested that we have wrongly quoted Kershaw et al. (2012). This is not true. As mentioned above, Kershaw et al. (2012) only cited the conodont biostratigraphy of the Abadeh section (Hambast, Iran) from Richoz et al. (2010), in which the PTB is located at 25 cm above the base of “boundary clay”. In our paper, we clearly stated that “a worldwide survey on the stratigraphic distribution

of PTB microbialites (Kershaw et al., 2012) indicated that the biostratigraphic boundary is most likely close to the top of “Microbialite Bed”. It is obvious that our quotation of Kershaw et al. (2012) is not solely about their take on the PTB at the Abadeh section, but more about their “worldwide survey”, which was partly displayed in Fig. 1 of Kershaw et al. (2012).

(3) The third so-called “problem” listed by Horacek et al. (2021a) is difficult for us to fathom. We presume they were arguing about the thickness of the interval from the top of “Paratirolites Bed” to the top of “Microbialite Bed”, whether it is 1.50 m as indicated in our paper, or 1.90 m as they suggested. Since the thickness of stratigraphic units around the PTB slightly vary in the Hambast Valley, especially for the “Microbialite Bed”, and we are not sure whether the measured sections for various research groups are at the same spot. For instance, in Kozur (2005), the total thickness of the interval from the base of “boundary clay” to the top of “Microbialite Bed” is 1.38 m, which is different from our measurement, as well as the thickness of Baud et al. (2007), Richoz et al. (2010), and Kershaw et al. (2012), which is about 2 m.

(4) The fourth so-called “problem” listed by Horacek et al. (2021a) is that we produced “confusion and uncertainty in the stratigraphy of the Abadeh section”, mainly about citation of published studies. As explained above, the way we presented our work, especially regarding to previous studies on the Abadeh section, is subjective. There is not a single way to do so, as Horacek et al. (2021a) expected.

Additionally, since those four “problems” listed by Horacek et al. (2021a) can be reasonably explained, the so-called “consequences” argued by Horacek et al. (2021a) are not significant in our opinion. Moreover, we strongly oppose the suggestion by Horacek et al. (2021a) that we modified our results regarding the position of PTB at the Abadeh section to “find an agreement with the recently published seawater-temperature curve of Joachimski et al. (2020)”. Such a suggestion is not fair. Our paper was based on conodont samples collected during the 2009 field trip in Iran (Shen et al., 2009), and analyses of oxygen isotopes were conducted in the summer of 2014. All the results, including conodont biostratigraphic framework, were finalized in 2016, before the second field trip in Abadeh, central Iran (Angiolini et al., 2017). We were not aware of the study of Joachimski et al. (2020) in Armenia until their results were released in June, 2019. Their original results (Joachimski et al., 2020), and recent arguments (Horacek et al., 2021b; Joachimski et al., 2021), have no bearing on our study of the Abadeh section.

Finally, we should emphasize that, there are many reasons that could result in different views from researchers to place the PTB at different levels. Taxonomic approach is clearly a key issue. In our opinion, single specimen is not reliable to identify species. After examining many *Hindeodus* populations around the PTB in various regions, we found that the *Hindeodus praeparvus* population is transitional to *Hindeodus parvus* population. *Hindeodus praeparvus* can range into the *Hindeodus parvus* Zone, and rare specimens morphologically similar to *Hindeodus parvus* can also occur in the underlying *Hindeodus praeparvus* Zone (Jiang et al., 2007; Zhang et al., 2014; Yuan et al., 2015). Another major reason is the sampling intensity, yield of conodont

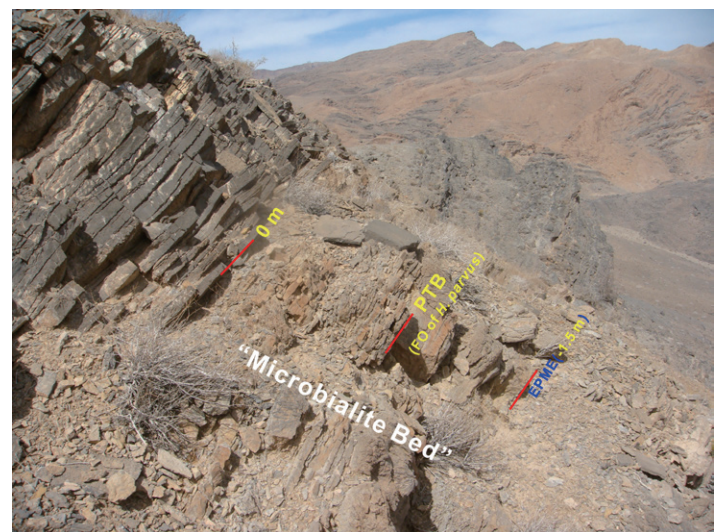


Fig. 1: Field photo showing the overall view of the Permian-Triassic boundary (PTB) interval at the Abadeh section, central Iran. Our re-evaluation suggests that the position of PTB is located in the middle of the “Microbialite Bed”, to be precise, 0.8 m above the end-Permian mass extinction (EPME) horizon (i.e., base of the “boundary clay”), or 0.7 m below the top of the “Microbialite Bed” (i.e., base of the thin-bedded, dark-colored limestone unit).

elements, and conodont preservation. It's a common sense that all fossil records are incomplete depending upon the sampling intensity carried out by different researchers. Since the PTB interval is the most intensively studied interval, sampling effect may cause significant differences too.

Nonetheless, after re-evaluating all of our conodont materials obtained from the samples collected in 2009 and 2017 (Shen et al., 2009; Angiolini et al., 2017), we now have slightly modified results about conodont biostratigraphy at the Abadeh section. Among a series of samples collected in the interval from the top of “Paratirolites Bed” to the top of “Microbialite Bed”, the first occurrence of *Hindeodus parvus* is in the sample of TEH-(-0.65 m ~ 0.7 m); the PTB is in the middle of the “Microbialite Bed”, to be precise, 0.8 m above the base of “boundary clay” and 0.7 m below the top of “Microbialite Bed” (Fig. 1). In other words, the modified position of PTB at the Abadeh section is 0.7 m lower than our previous placement in Chen et al. (2020). We should also emphasize that this modification (Fig. 2) does not change the core finding of an abrupt warming around the PTB at the Abadeh section, central Iran. The only difference is the duration of this warming event. New results suggest that, an abrupt warming with a magnitude of ~10 °C (i.e., a decrease of ~2‰ in $\delta^{18}\text{O}$ apatite) occurs in the lowest part of Unit a (Elikah Formation), or to be precise, in the Clarkina hauschkei Zone of the uppermost Changhsingian and the lower part of *Hindeodus parvus* Zone of the lowest Triassic, above the mass extinction horizon and continued across the Permian-Triassic boundary. Based on correlation with the Meishan GSSP section, we now estimate that the abrupt warming of ~10 °C at Abadeh occurred between ~251.941 and ~251.871 Ma, and took only a maximum duration of ~70 kyr.

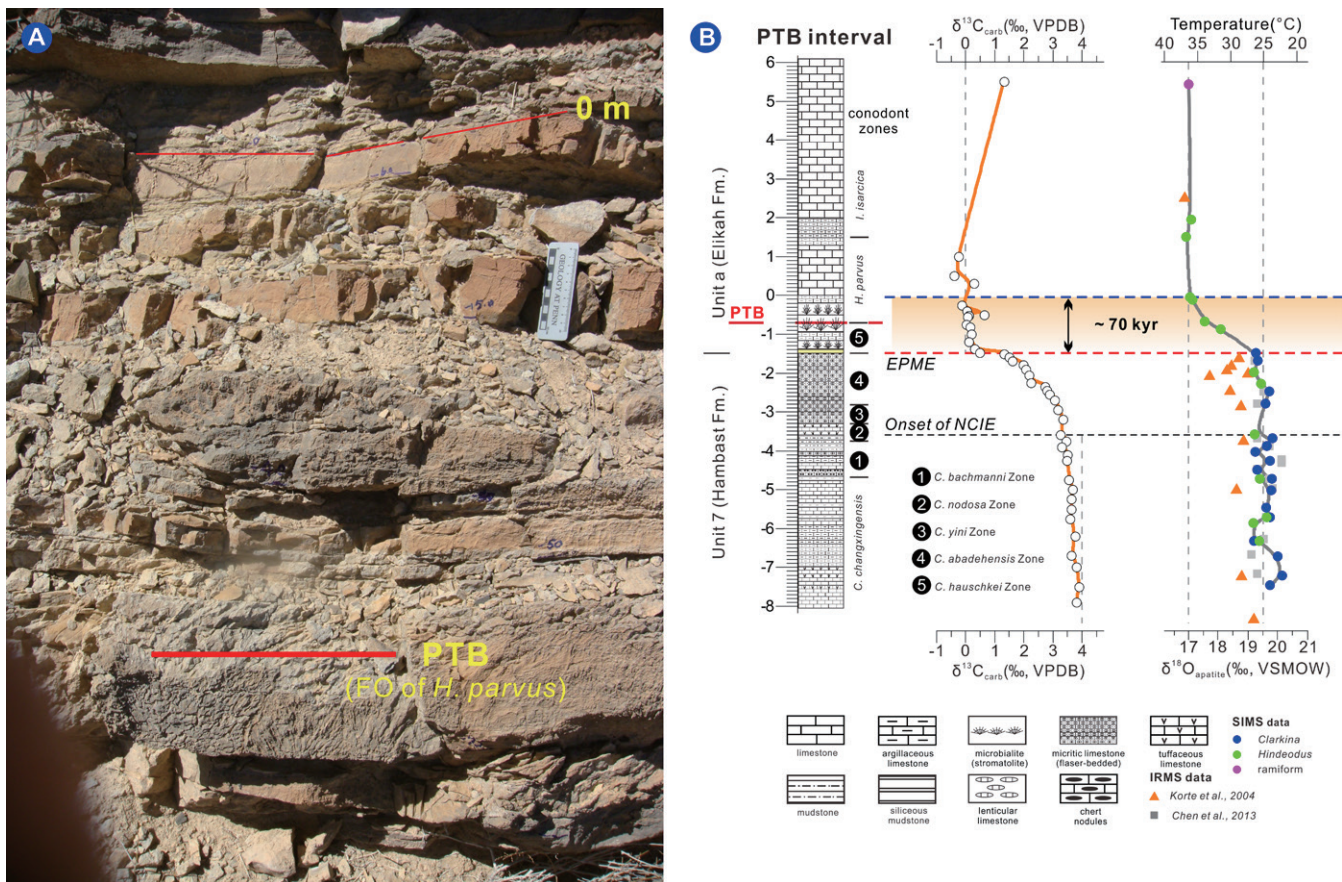


Fig. 2: (A) Close-up view of the PTB interval at the Abadeh section, central Iran; the position of PTB, marked by the first occurrence (FO) of conodont *Hindeodus parvus*, is located at -0.7 m, 0.7 m lower than our previous placement in Chen et al. (2020). (B) Revised column section of the PTB interval at Abadeh, comparing to Fig. 3B in Chen et al. (2020). Note that the ranges of three conodont zones are slightly modified, including: *Clarkina hauschkei* Zone, -1.50 m to -0.70 m; *Hindeodus parvus* Zone, -0.70 m to 1.50 m; *Isarcicella isarcica* Zone, 1.50 m to top of our investigated section (precise location uncertain in our study). An abrupt warming of ~10 °C at the Abadeh section, indicated by the highlighted interval, occurred above the mass extinction horizon and continued across the PTB, with a total duration of ~70 kyr.

References

- Angiolini, L., Crippa, G., Shen, S.Z., Zhang, H., Zhang, Y.C., Ghorbani, M., Ghorbani, M. and Ovissi, M., 2017. Report of the Chinese, Italian, Iranian working group: The Permian-Triassic boundary sections of Abadeh revisited. *Permophiles*, v. 65, p. 24–27.
- Baud, A., Richoz, S. and Pruss, S., 2007. The lower Triassic anachronistic carbonate facies in space and time. *Global and Planetary Change*, v. 55, p. 81–89.
- Chen, J., Beatty, T.W., Henderson, C.M. and Rowe, H., 2009. Conodont biostratigraphy across the Permian-Triassic boundary at the Dawen section, Great Bank of Guizhou, Guizhou Province, South China: Implications for the Late Permian extinction and correlation with Meishan. *Journal of Asian Earth Sciences*, v. 36, p. 442–458.
- Chen, J., Shen, S.Z., Zhang, Y.C., Angiolini, L., Gorgij, M.N., Crippa, G., Wang, W., Zhang, H., Yuan, D.X., Li, X.H. and Xu, Y.G., 2020. Abrupt warming in the latest Permian detected using high-resolution in situ oxygen isotopes of conodont apatite from Abadeh, central Iran. *Palaeogeography, Palaeoclimatology, Palaeoecology*, v. 560, p. 109973.
- Dudas, F.O., Yuan, D.X., Shen, S.Z. and Bowring, S.A., 2017. A conodont-based revision of the 87Sr/86Sr seawater curve across the Permian-Triassic boundary. *Palaeogeography, Palaeoclimatology, Palaeoecology*, v. 470, p. 40–53.
- Gallet, Y., Krystyn, L., Besse, J., Saidi, A. and Ricou, L.E., 2000. New constraints on the Upper Permian and Lower Triassic geomagnetic polarity timescale from the Abadeh section (central Iran). *Journal of Geophysical Research-Solid Earth*, v. 105, p. 2805–2815.
- Horacek, M., Krystyn, L. and Baud, A., 2021a. Comment to Chen et al., 2020: abrupt warming in the latest Permian detected using high-resolution in situ oxygen isotopes of conodont apatite from Abadeh, central Iran. Importance of correct stratigraphic correlation, reporting of existing data and their scientific interpretation. *Permophiles*, v. 70, p. 33–36.
- Horacek, M., Krystyn, L. and Baud, A., 2021b. Siberian Trap volcanism, global warming and the Permian-Triassic mass extinction: New insights from Armenian Permian-Triassic sections: Comment. *GSA Bulletin*.
- Horacek, M., Richoz, S., Brandner, R., Krystyn, L. and Spötl, C., 2007. Evidence for recurrent changes in Lower Triassic

- oceanic circulation of the Tethys: The $\delta^{13}\text{C}$ record from marine sections in Iran. *Palaeogeography, Palaeoclimatology, Palaeoecology*, v. 252, p. 355–369.
- Jiang, H.S., Lai, X.L., Luo, G.M., Aldridge, R.A., Zhang, K.X. and Wignall, P.B., 2007. Restudy of conodont zonation and evolution across the P/T boundary at Meishan section, Changxing, Zhejiang, China. *Global and Planetary Change*, v. 55, p. 39–55.
- Joachimski, M.M., Alekseev, A.S., Grigoryan, A. and Gatovsky, Y.A., 2020. Siberian Trap volcanism, global warming and the Permian-Triassic mass extinction: New insights from Armenian Permian-Triassic sections. *Geological Society of America Bulletin*, v. 132, p. 427–443.
- Joachimski, M.M., Alekseev, A.S., Grigoryan, A. and Gatovsky, Y.A., 2021. Siberian Trap volcanism, global warming and the Permian Triassic mass extinction: New insights from Armenian Permian-Triassic sections: Reply. *GSA Bulletin*.
- Kershaw, S., Crasquin, S., Li, Y., Collin, P.Y., Forel, M.B., Mu, X., Baud, A., Wang, Y., Xie, S., Maurer, F. and Guo, L., 2012. Microbialites and global environmental change across the Permian-Triassic boundary: a synthesis. *Geobiology*, v. 10, p. 25–47.
- Korte, C., Kozur, H.W., Joachimski, M.M., Strauss, H., Veizer, J. and Schwark, L., 2004. Carbon, sulfur, oxygen and strontium isotope records, organic geochemistry and biostratigraphy across the Permian/Triassic boundary in Abadeh, Iran. *International Journal of Earth Sciences*, v. 93, p. 565–581.
- Korte, C., Pande, P., Kalia, P., Kozur, H.W., Joachimski, M.M. and Oberhänsli, H., 2010. Massive volcanism at the Permian-Triassic boundary and its impact on the isotopic composition of the ocean and atmosphere. *Journal of Asian Earth Sciences*, v. 37, p. 293–311.
- Kozur, H.W., 2004. Pelagic uppermost Permian and the Permian-Triassic boundary conodonts of Iran. Part I: Taxonomy. *Hallesches Jahrbuch für Geowissenschaften B Beiheft*, v. 18, p. 39–68.
- Kozur, H.W., 2005. Pelagic uppermost Permian and the Permian-Triassic boundary conodonts of Iran. Part II: investigated sections and evaluation of the conodont faunas. *Hallesches Jahrbuch für Geowissenschaften B Beiheft*, v. 19, p. 49–86.
- Kozur, H.W., 2007. Biostratigraphy and event stratigraphy in Iran around the Permian-Triassic Boundary (PTB): Implications for the causes of the PTB biotic crisis. *Global and Planetary Change*, v. 55, p. 155–176.
- Liu, X.C., Wang, W., Shen, S.Z., Gorgij, M.N., Ye, F.C., Zhang, Y.C., Furuyama, S., Kano, A. and Chen, X.Z., 2013. Late Guadalupian to Lopingian (Permian) carbon and strontium isotopic chemostratigraphy in the Abadeh section, central Iran. *Gondwana Research*, v. 24, p. 222–232.
- Richoz, S., Krystyn, L., Baud, A., Brandner, R., Horacek, M. and Mohtat-Aghai, P., 2010. Permian-Triassic boundary interval in the Middle East (Iran and N. Oman): Progressive environmental change from detailed carbonate carbon isotope marine curve and sedimentary evolution. *Journal of Asian Earth Sciences*, v. 39, 236–253.
- Shen, S.Z., Cao, C.Q., Zhang, H., Bowring, S.A., Henderson, C.M., Payne, J.L., Davydov, V.I., Chen, B., Yuan, D.X., Zhang, Y.C., Wang, W. and Zheng, Q.F., 2013. High-resolution $\delta^{13}\text{C}_{\text{carb}}$ chemostratigraphy from latest Guadalupian through earliest Triassic in South China and Iran. *Earth and Planetary Science Letters*, v. 375, p. 156–165.
- Shen, S.Z., Gorgij, M.N., Wang, W., Zhang, Y.C., Khamar, H.R. and Tanatabaei, S.H., 2009. Report of field trip of the Permian stratigraphy in Central and Eastern Iran. *Permophiles*, v. 53, p. 2–5.
- Shen, S.Z. and Mei, S.L., 2010. Lopingian (Late Permian) high-resolution conodont biostratigraphy in Iran with comparison to South China zonation. *Geological Journal*, v. 45, p. 135–161.
- Taraz, H., Golshani, F., Nakazawa, K., Shimizu, D., Bando, Y., Ishii, K. I., Murata, M., Okimura, Y., Sakagami, S., Nakamura, K. and Tokuoka, T., 1981. The Permian and the Lower Triassic systems in Abadeh region, central Iran. *Memoirs of the Faculty of Science, Kyoto University, Series of Geology and Mineralogy*, v. 47, p. 61–133.
- Yuan, D.X., Chen, J., Zhang, Y.C., Zheng, Q.F. and Shen, S.Z., 2015. Changhsingian conodont succession and the end-Permian mass extinction event at the Daijiagou section in Chongqing, Southwest China. *Journal of Asian Earth Sciences*, v. 105, p. 234–251.
- Zhang, Y., Zhang, K.X., Shi, G.R., He, W.H., Yuan, D.X., Yue, M.L. and Yang, T.L., 2014. Restudy of conodont biostratigraphy of the Permian-Triassic boundary section in Zhongzhai, southwestern Guizhou Province, South China. *Journal of Asian Earth Sciences*, v. 80, p. 75–83.

Short Note about ethical publishing - and about the temperature change around the Permian-Triassic Boundary (PTB)

Micha Horacek

Department of Lithospheric Research, University of Vienna, Althanstrasse 14, 1090 Vienna, Austria

Leopold Krystyn

Department for Palaeontology, University of Vienna, Althanstrasse 14, 1090 Vienna, Austria

Aymon Baud

Institute of Earth Sciences, Lausanne University, Lausanne, Switzerland

Our recent comment (Horacek et al., 2021a) was submitted at the latest possible date for acceptance in *Permophiles* without sufficient time to adjust the Acknowledgement in the article. We would like to address this issue now. Our article was a comment about the paper by Chen et al., 2020: "Abrupt warming in the latest Permian detected using high-resolution in situ oxygen isotopes of conodont apatite from Abadeh, central Iran.", but at the time of submission we did not note that the editors of *Permophiles* were among the authors of the article we commented on, and thus potentially created an awkward position for them. Even more we appreciate their competent, scientific and ethical behaviour in

handling our manuscript and its quick publication. In our opinion, the editors of *Permophiles* demonstrated an outstanding level of professionalism as well as scientific integrity, something we deem worthy to and we thus want to underline.

We have now produced a correlation figure (Fig. 1) of the Abadeh and Meishan sections to demonstrate the better fit with the biochronology proposed by us in Horacek et al., 2021a. For a detailed explanation see the figure caption. Furthermore, we

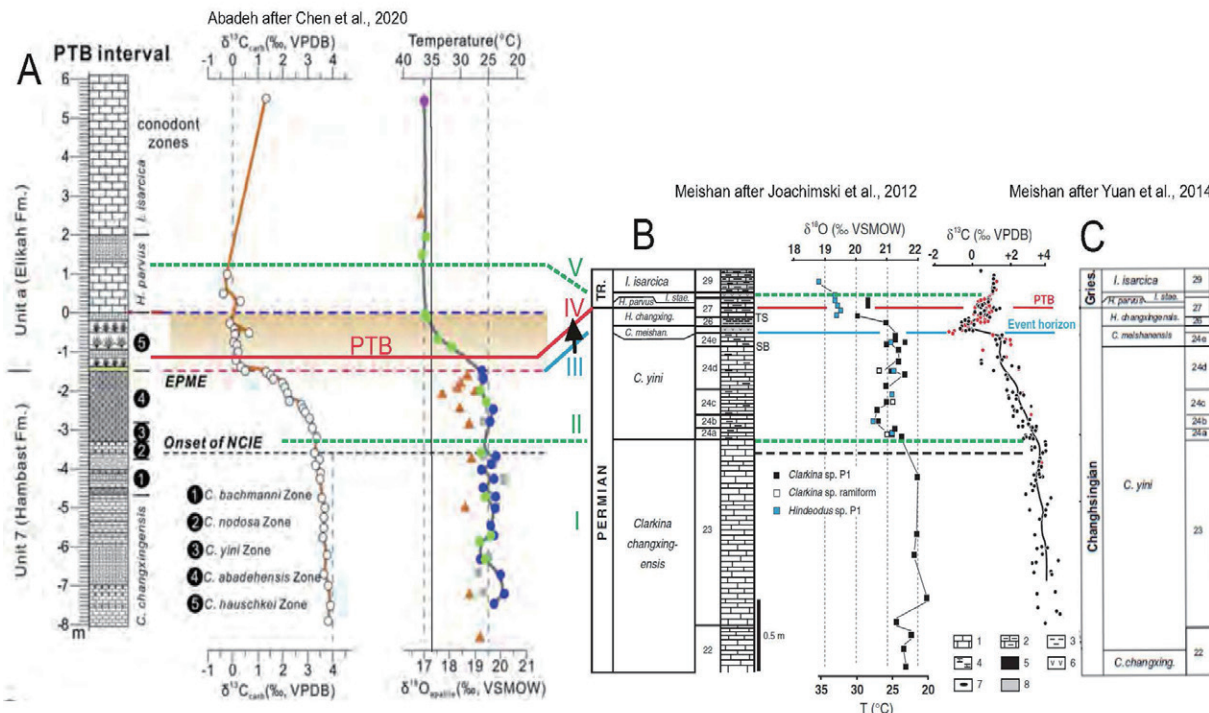


Fig. 1. Correlation of the PTB-interval of Abadeh (modified after Chen et al., 2020: A) and Meishan (modified after Joachimski et al., 2012: B, and the conodont stratigraphy after the revision by Yuan et al., 2014: C) sections. By applying the (in our opinion) correct biochronology there is an excellent agreement of the temperature curves showing values mainly below 30°C beneath the extinction event, and a strong and steady increase in temperature from the extinction event with maximum temperatures in the upper *parvus* or the *isarcica* Zones. Note that Chen et al., 2020, show additional conodont zones that have not been identified in South China. The horizontal black dashed line shows the start of the negative carbon isotope excursion (NCIE), as described in Chen et al., 2020. Green "I" denotes *Clarkina (C.) changxingensis* Zone sensu Zhang et al., 2009. First green dashed line (II) identifies the correlation of base of *C. yini* Zone sensu Zhang et al., 2009. The uppermost part of the *C. abadehensis* Zone in the Abadeh section, immediately below the red dashed/blue line (III) identifying the End-Permian Mass Extinction Event (EPME, Event Horizon) contains the *C. hauschkei* Zone, which has been incorrectly assigned to the interval above the mass extinction event by Chen et al., 2020 (shown as Nr. 5). The *C. hauschkei* Zone can now also be identified in the Meishan section spanning bed 24e, see below. Above this line (III) indicating the mass extinction event follows the latest Permian immediate post-extinction interval, marked in the Abadeh section by a boundary shale, and in Meishan section by beds 25, 26 and 27ab (a volcanic tuff layer, followed by a thin shale layer, succeeded by two thin carbonate layers, respectively). In the uppermost shale in the Abadeh section and at the base of bed 27c in Meishan section the Permian-Triassic Boundary (PTB) has been identified by *Hindeodus* (*H.*) *parvus* (Abadeh: Richoz et al., 2010, Horacek et al., 2021a; also see discussion therein; Meishan: Zhang et al., 2009, Yuan et al., 2014) marked by the red line (IV). The blue dashed line marks the PTB position of Chen et al., 2020. The green dashed line (V) marks the base of the *Isarcicella* (*I.*) *isarcica* Zone in Abadeh (after Taraz et al., 1981, Richoz et al., 2010, Baud et al., 2021) and Meishan section (Joachimski et al., 2012). Chen et al., 2020, identified *I. isarcica* in Abadeh section slightly further upwards. Note that the conodont stratigraphy in Meishan has been revised by Yuan et al., 2014, (C). In the latter work *C. yini* was revised and its range downwards enlarged and now includes a substantial part of the former *C. changxingensis* Zone. While we see the reasoning for this revision, we think it beneficial to also keep the definition of *C. yini* sensu Zhang et al., 2009. The latter is regarded by Yuan et al., 2014, as transition form to *C. meishanensis*, but represents the *C. yini* and *zhangi* forms found in Abadeh and generally the western (Neo-) Tethys, enabling a direct correlation. Yuan et al., 2014, also enlarge the range of *C. meishanensis* downwards below the extinction horizon to the base of Meishan bed 24e. As *C. meishanensis* also has (rarely) been found in Iranian sections below the extinction horizon in the *C. hauschkei* Zone, this zone can now be identified also in the Meishan section and in analogy encompasses Meishan bed 24e. There is a discrepancy concerning conversion of $\delta^{18}\text{O}$ -values into temperature data due to different calculations, but both studies use the same seawater $\delta^{18}\text{O}$ -value. TR, Triassic; SB, sequence boundary; TS, transgressive surface; 1, limestone; 2, marly limestone; 3, claystone; 4, siliceous marl; 5, black shale; 6, volcanic ash; 7, chert; 8, dysaerobic to anaerobic facies.

noted in our mentioned comment that also in a second recent work on the temperature change around the Permian-Triassic Boundary (PTB) (Joachimski et al., 2020, investigating the Chanakhchi section, Armenia), the exact position of the PTB is debated. We have further delved into this matter and the outcome is a second comment (Horacek et al., 2021b). By amending the biochronology we now obtain an improved agreement between the two PTB sections (Abadeh, and also Chanakhchi) and the GSSP section Meishan with respect to the seawater temperature evolution. In short: According to our interpretation, the temperature change/increase started at the end-Permian Mass Extinction and ended slightly above the PTB in all investigated sections – instead of quickly after the extinction event and before the PTB in the Iranian and Armenian sections.

The problem of precise identification of the PTB in Iran and Armenia may exist in other regions, too, and should encourage us to further continue our efforts to obtain detailed descriptions of PTB boundary sections, including easily identifiable definitions of marker and index fossils, extensive collaboration and open-minded discussion on the interpretation of the results.

Acknowledgments

We thank the editors for very skilful handling. This is a contribution to International Geoscience Programme (IGCP) projects 630 and 710.

References

- Baud, A., Richoz, S., Brandner, R., Krystyn, L., Heindel, K., Mohtat, T., Mohtat-Aghai, P., and Horacek, M., 2021, Sponge takeover from End-Permian mass extinction to early Induan time: Records in Central Iran microbial buildups, *Front. Earth Sci.*, 8, <https://doi.org/10.3389/feart.2021.586210>.
- Chen, J., Shen, S.Z., Zhang, Y.C., Angiolini, L., Gorgij, M.N., Crippa, G., Wang, W., Zhang, H., Yuan, D.X., Li, X.H., and Xu, Y.G., 2020, Abrupt warming in the latest Permian detected using high-resolution *in situ* oxygen isotopes of conodont apatite from Abadeh, central Iran: *Palaeogeography, Palaeoclimatology, Palaeoecology*, v. 560, <https://doi.org/10.1016/j.palaeo.2020.109973>.
- Horacek, M., Krystyn, L., Baud, A., 2021a, Comment to Chen et al., 2020: "Abrupt warming in the latest Permian detected using high-resolution *in situ* oxygen isotopes of conodont apatite from Abadeh, central Iran." Importance of correct stratigraphic correlation, reporting of existing data and their scientific interpretation. *Permophiles*, vol. 70, p. 33–36.
- Horacek, M., Krystyn, L., Baud, A., 2021b, Siberian Trap volcanism, global warming and the Permian-Triassic mass extinction: New insights from Armenian Permian-Triassic sections: Comment. *Geological Society of America Bulletin*. <https://doi.org/10.1130/B36099.1>.
- Joachimski, M.M., Lai, X.L., Shen, S.Z., Jiang, H.S., Luo, G.M., Chen, B., Chen, J., Sun, Y.D., 2012. Climate warming in the latest Permian and the Permian-Triassic mass extinction. *Geology* 40, 195–198.
- Joachimski, M.M., Alekseev, A.S., Grigoryan, A., and Gatovsky, Y.A., 2020, Siberian Trap volcanism, global warming and the Permian-Triassic mass extinction: New insights from Armenian Permian-Triassic sections: Geological Society of America Bulletin, v. 132, p. 427–443. <https://doi.org/10.1130/B36214.1>.
- Richoz, S., Krystyn, L., Baud, A., Brandner, R., Horacek M., Mohtat-Aghai, P., 2010, Permian-Triassic boundary interval in Middle East (Iran and N. Oman): progressive environmental change from detailed carbonate carbon isotope marine curve and sedimentary evolution. *Journal of Asian Earth Sciences*, vol. 39/4, p. 236–253. doi: 10.1016/j.jseaes.2009.12.014
- Taraz, H., Golshani, F., Nakazawa, K., Shimizu, D., Bando, Y., Ishii, K.I., Murata, M., Okimura, Y., Sakagami, S., Nakamura, K., Tokuoka, T., 1981. The Permian and the Lower Triassic systems in Abadeh region, central Iran. *Memoirs of the Faculty of Science, Kyoto University, Series of Geology and Mineralogy* 47, 61–133.
- Yuan, D.X., Shen, S.Z., Henderson, C.M., Chen, J., Zhang, H., and Feng, H.Z., 2014, Revised conodont-based integrated high-resolution timescale for the Changhsingian Stage and end-Permian extinction interval at the Meishan sections, South China: *Lithos*, v. 204, p. 220–245, <https://doi.org/10.1016/j.lithos.2014.03.026>.
- Zhang, K.X., Lai, X.L., Tong, J.N., Jiang, H.S., 2009. Progresses on study of conodont sequence for the GSSP section at Meishan, Changxing, Zhejiang province, South China. *Acta Palaeontologica Sinica* 48, 474–486.

Proposal for the Global Stratotype Section and Point (GSSP) for the base-Artinskian Stage (Lower Permian)

Valery V. Chernykh

Zavaritskii Institute of Geology and Geochemistry, Ural Branch, Russian Academy of Sciences, Pochtovy per. 7, Yekaterinburg, 620219 Russia;
Email: chernykh@igg.uran.ru

Charles M. Henderson

Department of Geoscience, University of Calgary, Calgary, Alberta, Canada T2N 1N4
Email: cmhender@ucalgary.ca

Ruslan V. Kutygin

Diamond and Precious Metal Geology Institute, Siberian Branch of the Russian Academy of Sciences (DPMGI SB RAS), Lenina ave., 39, Yakutsk, 677007, Russia
Email: rkutygin@mail.ru

Tatiana V. Filimonova

Geological Institute of the Russian Academy of Sciences (GIN RAS), Pyzhevsky lane, 7, Moscow, 119017, Russia
Email: filimonova@ginas.ru

Guzal M. Sungatullina

Kazan Federal University (KFU), Kremlyovskaya str, 18, Kazan

420008, Russia

Email: Guzel.Sungatullina@kpfu.ru

Marina S. Afanasieva

Paleontological Institute of Russian Academy of Sciences (PIN PAS), Profsoyuznaya, str. 123, Moscow, 117647, Russia
Email: afanasieva-marina@mail.ru

Tatiana N. Isakova

Geological Institute of the Russian Academy of Sciences (GIN RAS), Pyzhevsky lane, 7, Moscow, 119017, Russia
Email: isakova@ginras.ru

Rafael Kh. Sungatullin

Kazan Federal University (KFU), Kremlyovskaya str, 18, Kazan 420008, Russia
Email: Rafael.Sungatullin@kpfu.ru

Michael H. Stephenson

British Geological Survey, Keyworth, Nottingham NG12 5GG, UK

Lucia Angiolini

Dipartimento di Scienze della Terra “A. Desio”, Università degli Studi di Milano, 20133 Milano, Italy

Boris I. Chuvashov

Zavaritskii Institute of Geology and Geochemistry, Ural Branch, Russian Academy of Sciences, Pochtovy per. 7, Yekaterinburg, 620219 Russia

Introduction

Considerable new data have been generated and understanding has considerably improved regarding a potential GSSP level for the base-Artinskian since the reports provided in *Permophiles* 41 (Chuvashov et al., 2002) and *Permophiles* 58 (Chuvashov et al., 2013). Work has focused on the Dal’ny Tulkas Section in Russia and the FAD position of *Sweetognathus* aff. *whitei*, but the uncertain taxonomy delayed final completion. Kotlyar et al. (2016) showed additional progress at Dal’ny Tulkas as did Chernykh (2020). Henderson (2020) indicated that the base-Artinskian GSSP should be ready to go. Finally, it was reported in *Permophiles* 70 that there is now an agreement (Henderson and Chernykh, 2021) that this species is *Sweetognathus asymmetricus* Sun and Lai. The Dal’ny Tulkas section is data-rich making it an excellent GSSP site. It also includes, ammonoids, fusulines, small foraminifers, palynology, radiolaria, geochronologic ages, carbon isotopic trends, and Sr isotopic data that provide additional constraints on how to correlate the GSSP into other regions and realms. A proposal for the GSSP definition is provided to conclude this paper.

Acknowledgements

Charles Henderson acknowledges research support from NSERC Discovery Grant program. Mike Stephenson publishes

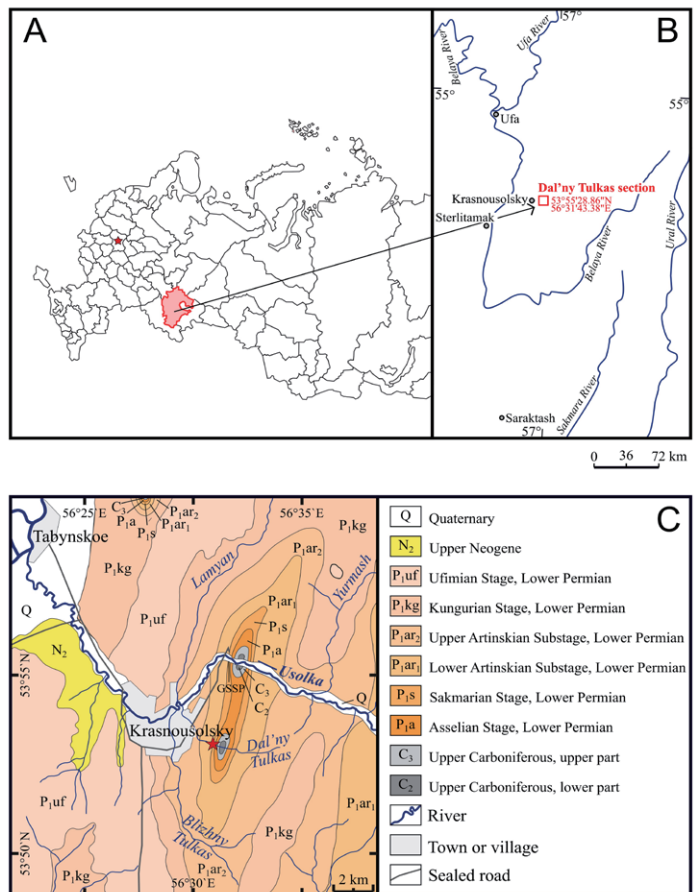


Fig. 1. Geology location map of the Dal’ny Tulkas section. Base of section is 53.88847N and 056.51615E.

with the permission of the Director of the British Geological Survey (NERC). The foraminiferal study was made as a part of the research on the State Program of Geological Institute of RAS No. 0135-2019-0062. Valery Chernykh and Boris Chuvashov acknowledge support from the Russian Academy of Sciences. Lucia Angiolini thanks the International Commission on Stratigraphy for financial support to complete this GSSP proposal.

Historical Considerations and Lithologic Succession

The boundary deposits of Sakmarian and Artinskian are represented most fully in the section on the stream Dal’ny Tulkas, located on the southern end of the Usolka anticline near the eastern outskirts of the settlement Krasnousol’sky, Bashkortostan (Fig. 1). The Kurort suite includes predominantly the Sterlitamakian horizon of Sakmarian Stage and the Tulkas suite includes the Artinskian Stage (Chuvashov et al., 1990) within the Dal’ny Tulkas section boundary interval. The Kurort suite comprises beds of dark-coloured carbonate mudstone, argillite, sandstone, and occasional bioclastic limestone with fusulines, rare ammonoids, radiolaria, palynology, and a few bivalves. The Sterlitamakian horizon is transitional to the Artinskian Stage and is typically poorly exposed. In 2003 a bulldozer cleared this

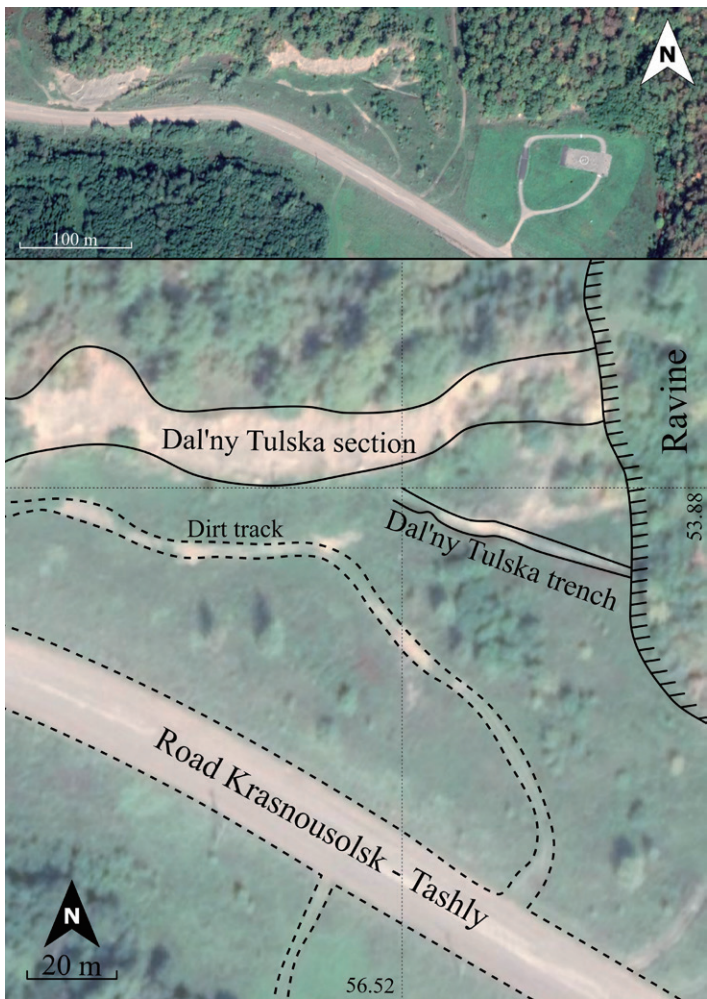


Fig. 2. Air photo of the Dal'ny Tulkas section and trench.

part of the section and exposed all beds (Figs. 2), which include resistant beds of sandy-argillaceous limestone with rare interbeds of detrital limestone and carbonate-clay concretions; all beds have been sampled for fusulines, ammonoids and conodonts. Most of the conodont samples proved to be productive. In the Artinskian part of the section there are four ash tuff layers.

The lower boundary of the Artinskian Stage is determined by the level of the appearance in the middle of bed 4 of the cosmopolitan conodont *Sweetognathus asymmetricus* in the phylogenetic lineage – *Sw. expansus* to *Sw. aff. merrilli* to *Sw. binodosus* to *Sw. anceps* to *Sw. asymmetricus* to *Sw. clarki*. The first Artinskian complex of fusulines is noted in the section 2.5 m higher, at the base of bed 5, which also includes Artinskian ammonoids and conodonts.

The schematic lithologic column of the Dal'ny Tulkas section with indications of the paleontologic samples is given below (Figs. 3, 4), including detailed description and lists of identified ammonoids, fusulines conodonts, small foraminifers and radiolarians (Table 1).

Section Description

Sakmarian Stage

Sterlitamakian horizon

Kurort suite

Bed 1. Monotonous silty mudstone, grey on fresh fracture, brownish-grey on altered surface, microlayered (2 to 5 cm-thick). Fossil content: rare ammonoids, fish-scales, non-calcareous algae. Thickness: 3 m.

Bed 2. Calcareous clayey siltstone and fine-grained sandstone in 15-20 cm-thick beds. Fossil content: noncalcareous algae and plant remains. Thickness: 1.7 m.

Bed 3. Brownish-grey limestone in 10-15 cm-thick beds with mudstone in the middle part of the bed. Carbonate concretions in the upper part of the bed. Fossil content: radiolarians, fusulines, conodonts (*Sweetognathus cf. obliquidentatus* (Chern.). Thickness: 0.7 m.

Bed 4a. Monotonous brownish-dark grey platy mudstone, with some interbeds of siltstone. In the lower part of the layer, there are 5-7 cm-thick beds of recessive bioclastic limestone with fusulines (*Pseudofusulina callosa* Rauser, *P. callosa proconcavatas* Rauser, *P. jaroslavkensis fraudulenta* Kireeva, *P. cf. parajaroslavkensis* Kireeva, *P. blochini* Korzhenevski), bryozoans, crinoids, conodonts (*Mesogondolella bisselli* (Clark et Behnken), *Sweetognathus anceps* Chern., *Sw. obliquidentatus* (Chern.), transitional forms between *Sw. anceps* Chern. to *Sw. asymmetricus* Sun and Lai). Thickness: 1.8 m.

Artinskian Stage

Burtsevian horizon

Kurort suite

Bed 4b. Mudstone with carbonate concretions at 0.6 m with conodonts (*Mesogondolella bisselli* (Clark et Behnken), *Sweetognathus anceps* Chern., transitional forms between *Sw. anceps* Chern. to *Sw. asymmetricus* Sun and Lai, *Sw. asymmetricus* Sun and Lai). 1.2 m above along the section, a level with small carbonate concretions yields conodonts (*Mesogondolella bisselli* (Clark and Behnken), *Sw. obliquidentatus* (Chern.), *Sw. asymmetricus* Sun and Lai). The upper part of the unit consists of a 42 cm-thick coarse-grained graded bed of bioclastic limestone with fusulines (*Pseudofusulina aff. longa* Kireeva, *P. fortissima* Kireeva, *P. anostriata* Kireeva, *P. plicatissima* Rauser, *P. urdalensis abnormis* Rauser), bryozoans, crinoids, conodonts (*Mesogondolella bisselli* (Clark and Behnken), *Sw. obliquidentatus* (Chern.). Thickness: 2.6 m

Tulkas suite

Bed 5. Brownish-grey silty mudstone in the lower part of the layer (60 cm) with numerous mudstone concretions. The upper part of the bed consists of laminar mudstone with lenses of detrital bioclastic limestone. Fossil content: fusulines in the lower part of the bed (*Pseudofusulina callosa* Rauser, *P. plicatissima* Rauser, *P. plicatissima irregularis* Rauser, *P. urdalensis* Rauser, *P. fortissima* Kireeva, *P. concavatas* Vissarionova, *P. juresanensis* Rauser, *P. consobrina* Rauser, *P. paraconcessa* Rauser), ammonoids in the lower and upper parts of the bed (*Popanoceras annae* Ruzhencev, *P. tschernowi* Maximova, *P. congregale* Ruzhencev, *Kargalites* sp., *Neopronorites skvorzovi* Tscherenow, rare *Artinskia* sp.), conodonts in the lower and upper parts of the bed (*Mesogondolella bisselli* (Clark et Behnken), *Sweetognathus asymmetricus* Sun and Lai, *Sw. obliquidentatus* (Chern.), *Sw. gravis* Chern.). Thickness: 1.5 m

Bed 6. Dark-greenish-grey claystone with carbonate

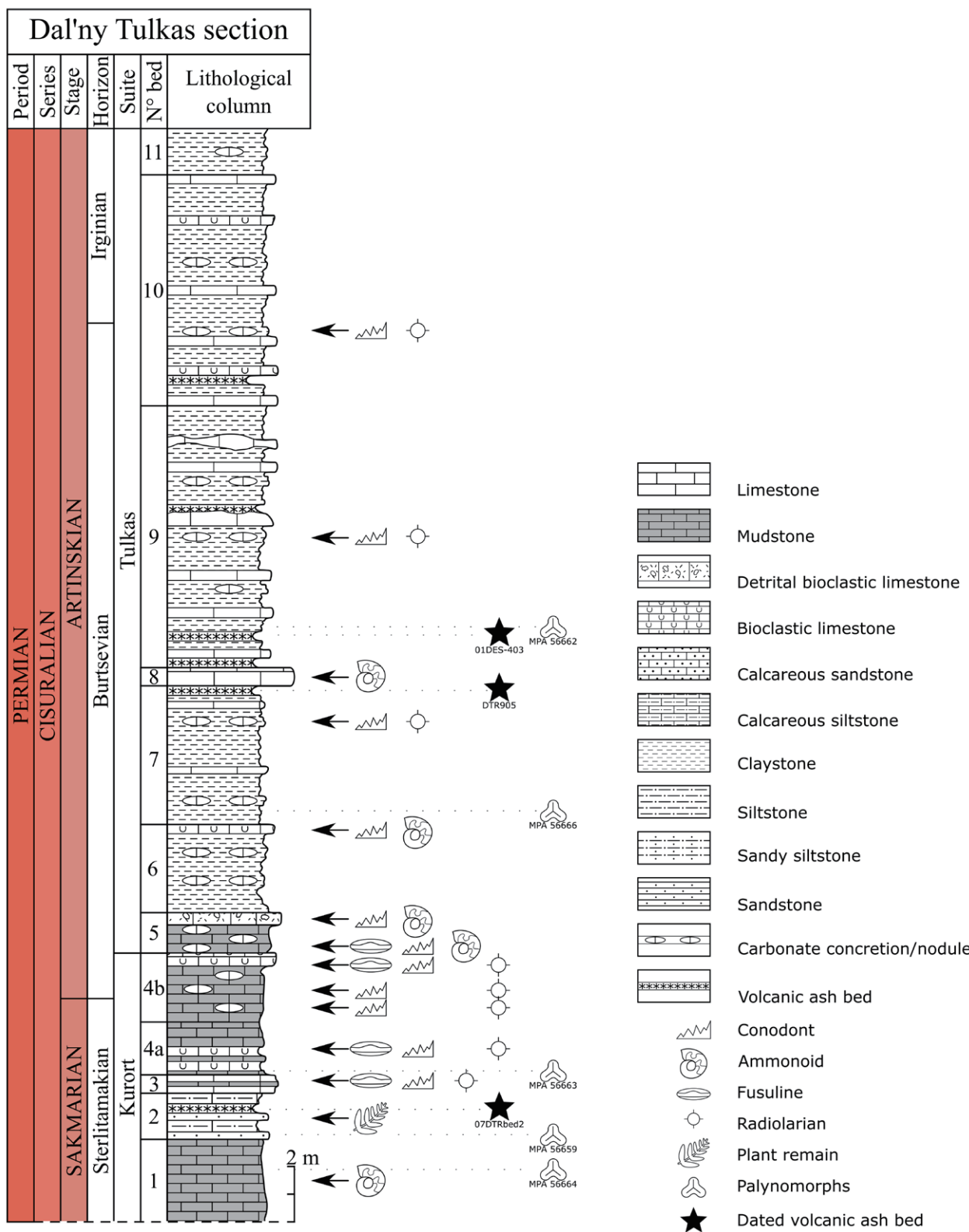


Fig. 3. Stratigraphic column with distribution of samples collected for conodonts, ammonoids, fusulines, and radiolarians in the Dal'ny Tulkas section.



Fig. 4. Photos of the Dal'ny Tulkas section. A: general view of the section, the arrow indicates bed 8; B: beds at the transition Sakmarian-Artinskian; C: lower Artinskian part of the succession, arrow points to bed 5.

concretions and with 20 cm-thick interbeds of bluish-grey mudstone, locally bioclastic at the top. Fossil content: ammonoids (as in bed 5), conodonts (*Mesogondolella bisselli* (Clark and Behnken), *M. bisselli* n. sub sp.). Thickness: 3.2 m.

Bed 7. Claystone, dark-brownish-grey on fresh fracture, greenish-grey on altered surface, with thin interbeds of marly limestone in the upper part. At 1.1 m from the top of the unit a large (0.5 x 20 cm) concretion of mudstone yields numerous radiolarians and conodonts (*Mesogondolella bisselli* (Clark and Behnken)). Thickness: 5 m.

Bed 8. Limestone, bluish-grey on fresh fracture, whitish on altered surface, locally bioclastic. In the lower 20 cm, 4 cm-thick clayey interbeds occur. At the base and top of the bed, yellowish silicified tuffs up to 10 cm-thick.

Fossil content: ammonoids (*Sakmarites postcarbonarius* (Karpinsky), *Agathiceras uralicum* (Karpinsky), *Kargalites typicus* (Ruzhencev), *Paragastrioceras* sp., and *Crimites subkrotowi* Ruzhencev). Thickness (decreasing westwards): 0.7-0.5 m.

Bed 9. Claystone with periodically repeated (about every 1-2.5 m) 5-10 cm-thick interbeds of steel-grey marly limestone and frequent yellowish-light grey 1-5 cm-thick silicified tuffs. Lenticular concretions of steel-grey marly limestone. In the middle part of the bed, one of the concretions yields numerous

radiolarians and conodonts (*Mesogondolella bisselli* (Clark et Behnken)). Thickness: 9.4 m

Artinskian Stage

Irginian horizon

Bed 10. Claystone as below, but with more frequent and thicker (15-20 cm) limestone interbeds and concretions and bioclastic limestone accompanied by 3-10 cm-thick yellowish-light grey silicified tuffs. Fossil content: radiolarians, conodonts (*Sweetognathus asymmetricus* Sun and Lai, *Sw. clarki* (Kozur), *Sw. aff. binodosus* Chern., *Mesogondolella bisselli* (Clark et Behnken), and *M. laevigata* Chern.). Thickness: 8.3 m.

Bed 11. Claystone with rare small carbonate concretions. Thickness: 1.7 m

Trench section description (Fig. 5, 6)

Sakmarian Stage

Sterlitamakian horizon

Bed 1. Sandy siltstone, grey, unevenly thin-bedded, with interbeds of clayey mudstone, with a large amount of scattered bioclasts. Fossil content: conodonts (*Mesogondolella* sp.). Thickness: 0.6 m.

Bed 2. Sandy siltstone, microlayered, separated by interbeds of claystone; in the lower part the bedding is poorly expressed, at the top the bedding is very thin. Fossil content: abundant radiolarians and algae. Thickness: 2.1 m.

Bed 3. Sandy siltstone, grey, microlayered with interbeds of clayey sandstone. Fossil content: calamite trunks, algae, fish scales. Thickness: 1.2 m.

Bed 4. Dark grey, thin-bedded siltstone with an interbed of red tuff at the base. Fossil content: algae, radiolarians, and fish scales. Thickness: 0.45 m.

Bed 5. Calcareous clayey siltstone with interbeds of fine-grained sandstone and reddish tuffs. Fossil content: fish scales, numerous radiolarians, and algae. Thickness: 1.5 m.

Bed 6. Calcareous sandstone, silty. Thickness: 0.2 m.

Bed 7-1. Grey mudstone, microlayered, platy. Concretions of brownish-grey limestone at the base and the top. Fossil content: radiolarians. Thickness: 2.6 m.

Bed 7-2, 7-3. Mudstone with silty interbeds, brownish-dark grey, platy. In the lower part of the bed, there is a 5-7 cm-thick bed of bioclastic limestone with fusulines, bryozoans, crinoids. Thickness: 1.8 m.

Bed 7-4, 7-5. Silty mudstone, grey, with carbonate nodules. Thickness: 2.6 m.

Artinskian Stage

Burtsevian horizon

Bed 8. Bioclastic limestone, coarse-grained. Fossil content: abundant fusulines. Thickness: 0.15 m.

Bed 9. Dark grey mudstone with thin beds of siltstone and numerous limestone nodules. Fossil content: ammonoids (9-4), radiolarians. Thickness: 2.2 m.

Bed 10. Bioclastic limestone, grey, fine-grained, with interbeds of mudstone. Fossil content: large plant remains, fusulines, radiolarians, brachiopods, cephalopods. Thickness: 0.5 m.

Bed 11. Silty mudstone with nodules and interbeds of grey limestone. Fossil content: radiolarians, plant remains, and brachiopods. Thickness: 2.2 m.

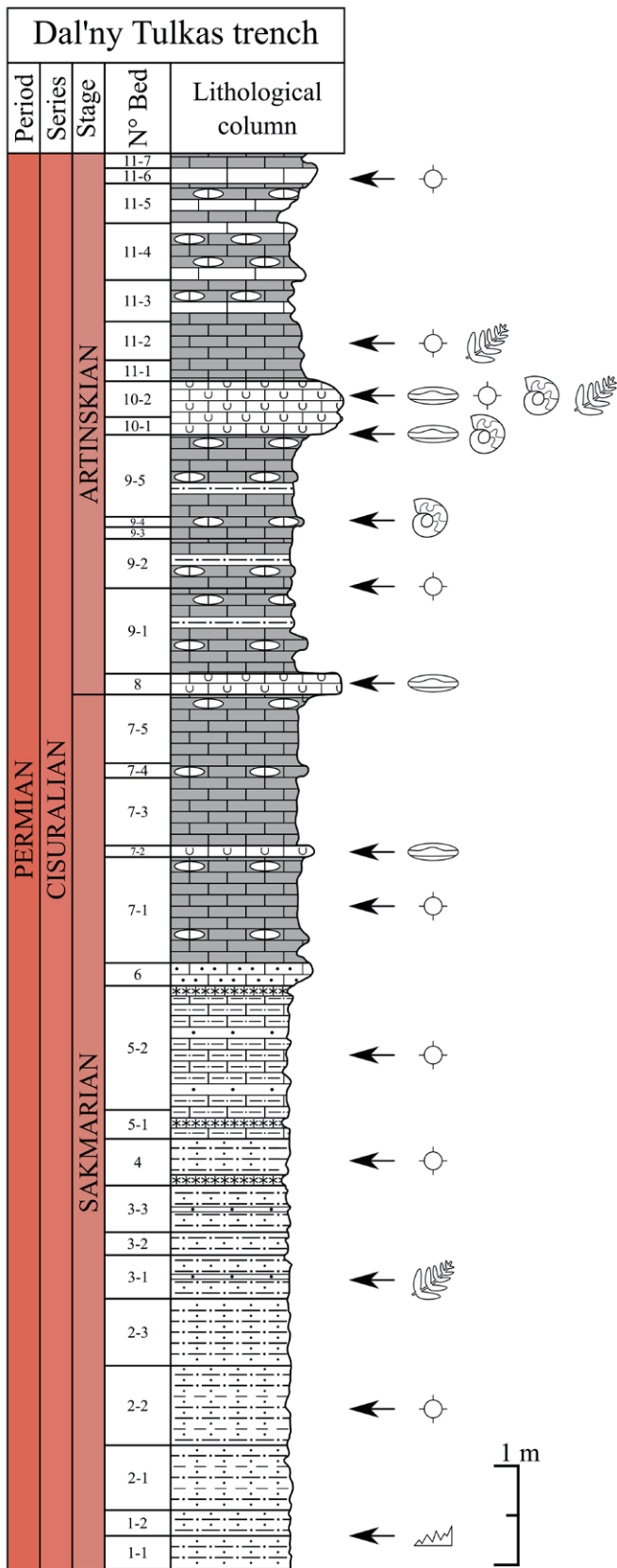


Fig. 5. Stratigraphic column with distribution of samples collected for conodonts, ammonoids, fusulines, and radiolarians in the Dal'ny Tulkas trench. For the legend see Fig. 3.



Fig. 6. Photos of the Dal'ny Tulkas trench. A: general view of the trench and the section; B: Sakmarian part of the succession; C: Sakmarian-Artinskian boundary, bed 8.

Interpreted Sequence Stratigraphy

In several sections in the world the Artinskian succession is associated with a transgressive systems tract and a maximum flooding surface. This is best illustrated in the Raanes and Great Bear Cape formations in the Canadian Arctic (Beauchamp et al., 2021; Chernykh et al., 2020). The section at Dal'ny Tulkas has not been investigated in detail for the sequence stratigraphy, but it does exhibit features that can be interpreted as a sequence boundary and transgressive systems tract. For example, non-calcareous algae, plant remains, and *Calamites* have been recovered from Beds 3 and 4 in the trench and bed 2 in the main section. Units above these levels (above lowest dashed line in Fig. 7) include carbonate mudstone, with increasingly diverse and abundant marine fossils. A little higher the base-Artinskian boundary is correlated between the trench and main section (solid red line in Fig. 7). This provides a strong sequence biostratigraphic signature for correlation.

Biostratigraphy

The Dal'ny Tulkas section and trench have been studied extensively for biostratigraphic content. The following sections provide details regarding the occurrence and biostratigraphic utility of conodonts, ammonoids, fusulines, small foraminifers, palynomorphs, and radiolarians.

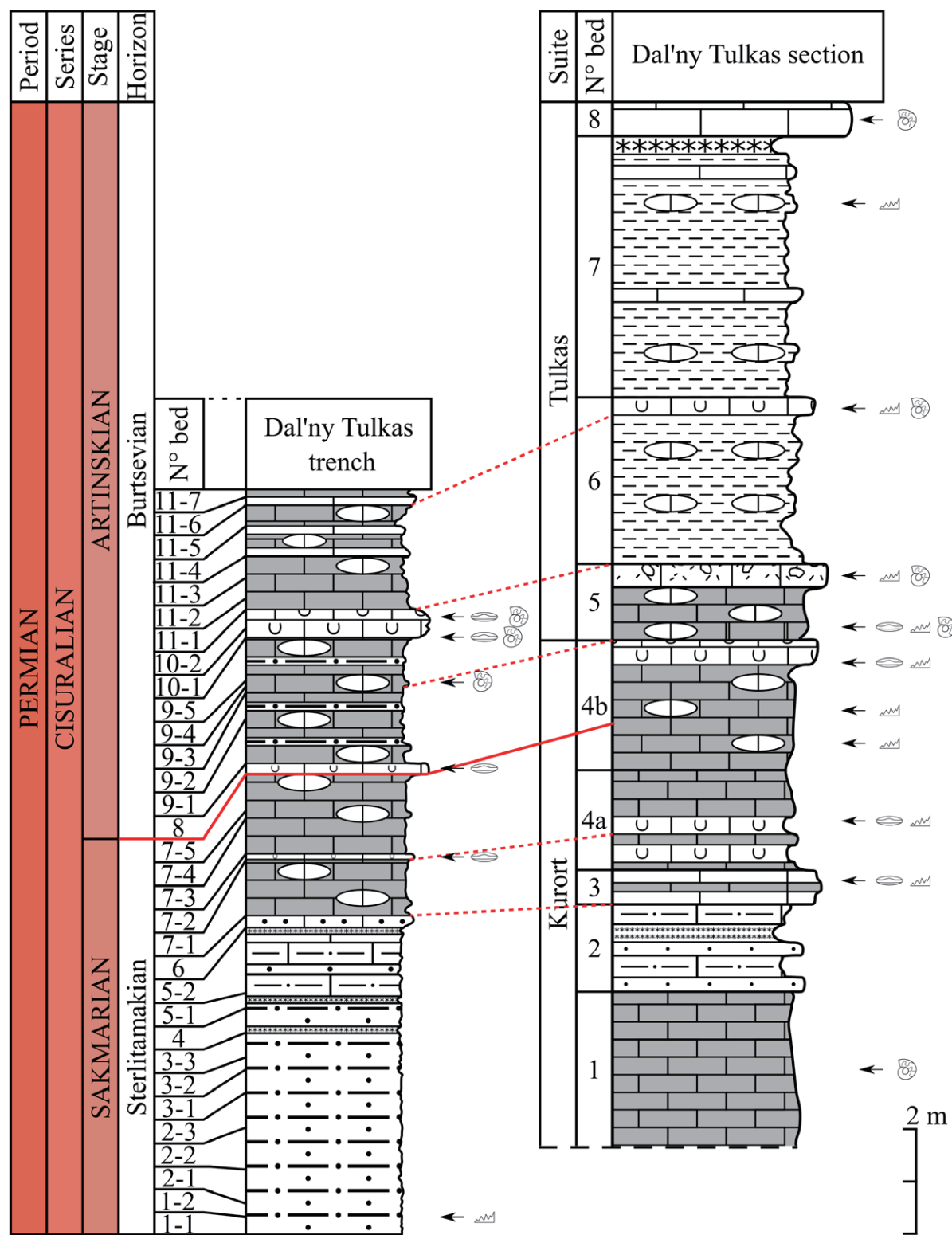


Fig. 7. Correlation of the Dal'ny Tulkas beds at the section and trench.

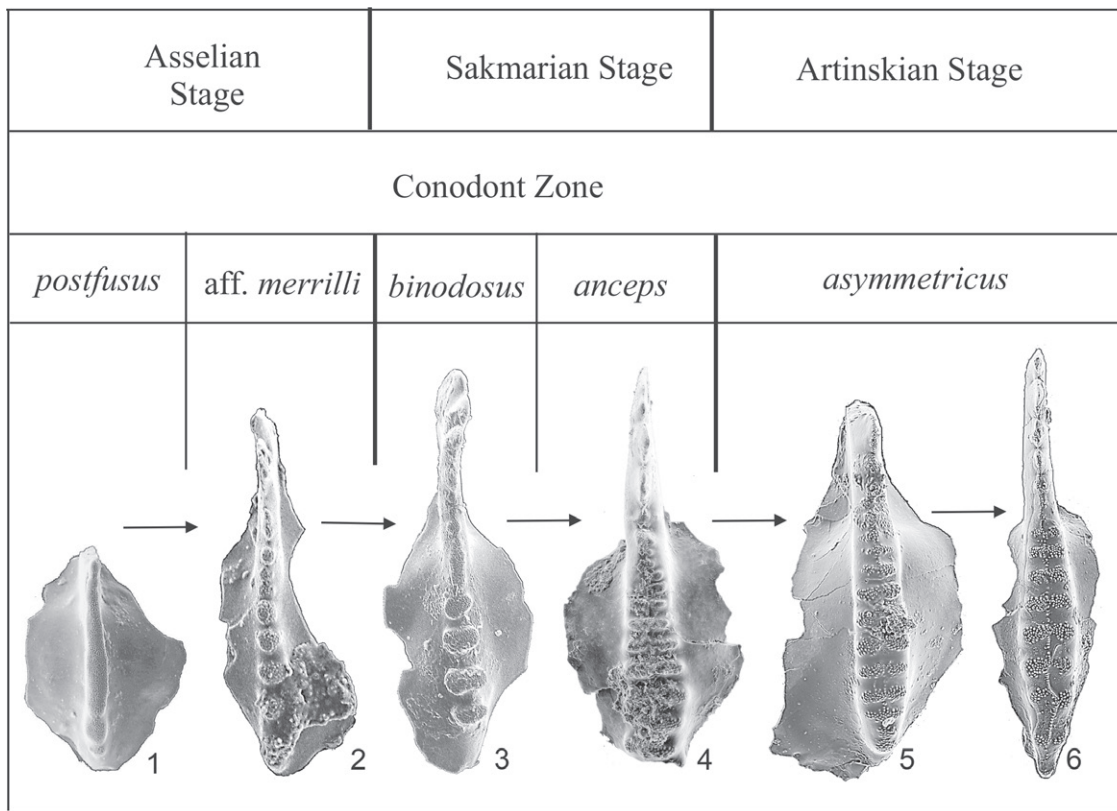


Fig. 8. The evolutionary lineage: 1. *Sweetognathus expansus* (Perlmutter), (Usolka section, bed 21); 2. *Sw. aff. merrilli* Kozur (Usolka section, bed 26/2); 3. *Sw. binodosus* Chern. (Usolka section, bed 26/3); 4. *Sw. anceps* Chern. (D. Tulkas section, bed 4a); 5 - transitional from *Sw. anceps* to *Sw. asymmetricus* Sun and Lai (D. Tulkas section, bed 4b); 6. *Sw. asymmetricus* Sun and Lai (D. Tulkas, bed 4b).

Conodonts

Conodonts are considered the primary biostratigraphic tool for this interval (Henderson, 2018), which makes it possible to clearly fix the desired boundary and carry out its global correlation with the appearance of the cosmopolitan form – *Sweetognathus asymmetricus* Sun and Lai, whose position in the chronomorphocline (Fig. 8) *Sw. binodosus* - *Sw. anceps* - *Sw. asymmetricus* is confirmed by the study of the Dal'ny Tulkas section (Henderson and Chernykh, 2021). The Dal'ny Tulkas section provides the best information with respect to conodonts of the genus *Sweetognathus* in the region (Chernykh, 2005; 2006).

In order to explain the value of these new data, it is useful to consider the previously published information about the development of this group of conodonts in the Usolka section (Chernykh and Chuvashov, 2004). The primitive form, *Sweetognathus expansus* (Perlmutter), in which the beginning of the carinal differentiation (Fig. 8) occurs, appears in middle to late Asselian. In latest Asselian to early Tastubian it evolves into *Sweetognathus aff. merrilli* (this form is significantly different from the type *Sw. merrilli* Kozur of mid-Asselian age; see Boardman et al., 2009; Petryshen et al., 2020) with carinal development forming rounded nodes in upper view (Fig. 8). Further evolution of this group leads to the appearance in the Tastubian horizon of such forms, which have few carinal nodes, but those nodes are laterally elongated with a tendency toward

the bilobate dumbbell-like structure. These forms are referred to as the species *Sweetognathus binodosus* Chernykh (Fig. 8).

The special features of further evolution of this group during Sterlitamakian and Artinskian time are revealed in the trenched part of the Dal'ny Tulkas section. The development of the carina of Sterlitamakian representatives of the line *Sweetognathus expansus*- *Sw. aff. merrilli* - *Sw. binodosus* continues in the direction of the differentiation of carinal nodes, that led to the appearance of *Sw. anceps* Chernykh (Fig. 9) that possess dumbbell-like nodes. In addition to these forms, there appear forms that include fragmentary development of the pustulose, mid-carinal connecting ridge, which are considered as transitional to *Sw. asymmetricus*. Forms of *Sw. anceps* with the rudiments of mid-carinal pustulose ridge continue to be encountered above in the section until finally there appear specimens of *Sweetognathus* with fully developed dumbbell-like nodes and a complete middle pustulose connecting ridge. We identify such forms to the species *Sweetognathus asymmetricus* (Figs. 9, 10) whose representatives are widely known in many regions where deposits of Artinskian age are present. Proposals to use the appearance of *Sw. asymmetricus* (then identified as *Sw. whitei*, a form now known as a late Asselian homeomorph; see Rhodes, 1963, Riglos Suarez et al., 1987 and Holterhoff et al., 2013 for examples of the homeomorph; problems discussed in Henderson, 2018; lineages discussed in Petryshen et al., 2020) for determining the lower boundary of Artinskian Stage were noted previously by different

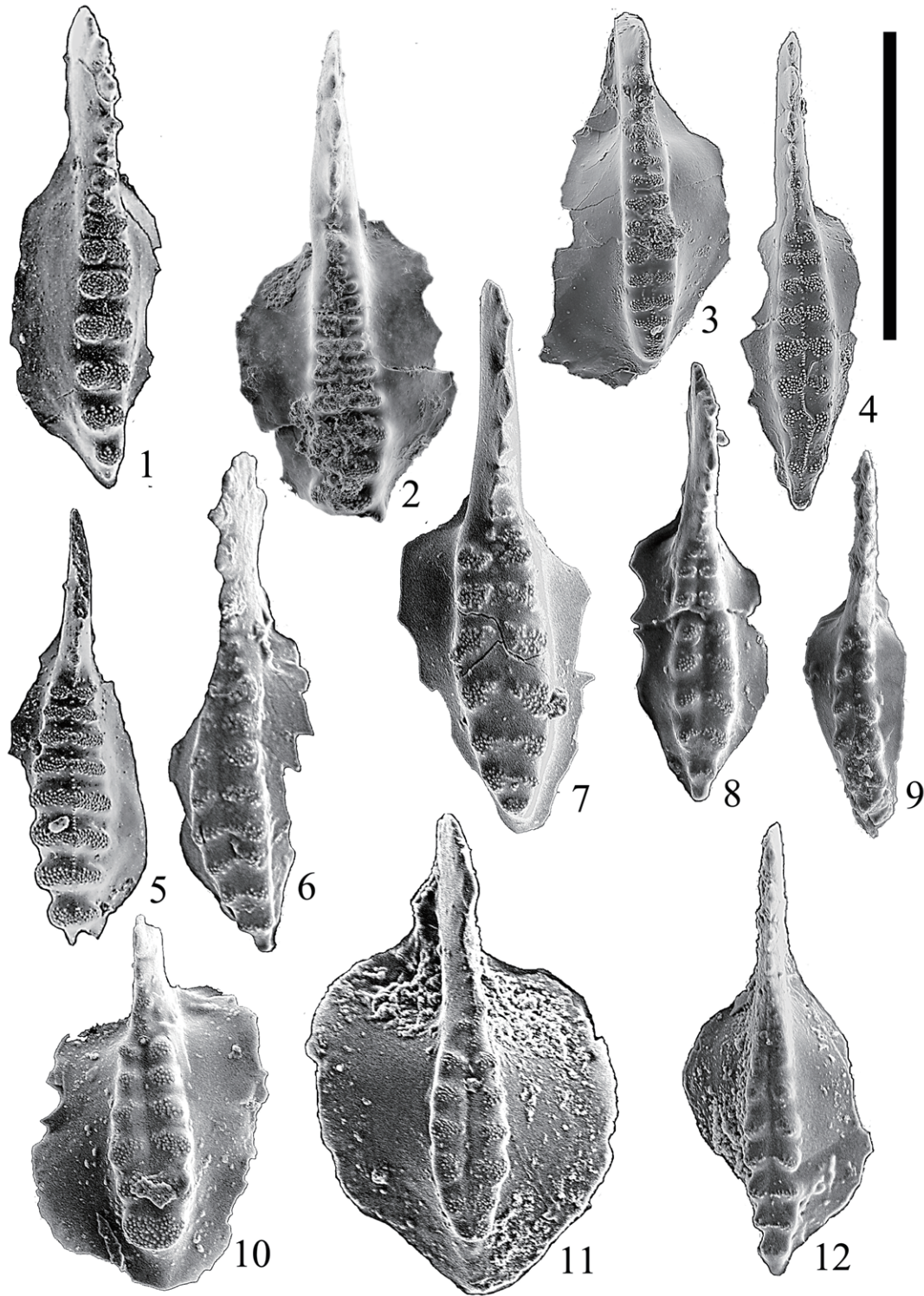


Fig. 9. Upper Sakmarian-Lower Artinskian conodonts in Dal'ny Tulkas section (x90). Scale bar = 500 μ m
1, 2. *Sweetognathus anceps* Chernykh, 2005. 1, holotype DT19-1, **bed 5**; lower part of Artinskian, asymmetricus Zone; 2, DT24, **bed 4a**; upper Sakmarian, Sterlitamakian horizon, *anceps* Zone. **3-5.** *Sweetognathus asymmetricus* Sun and Lai, 2017. 3, DT-18a, transitional form from *Sweetognathus anceps* Chernykh to *Sw. asymmetricus* Sun and Lai; 4, DT-18b, typical specimen with a fully developed median ridge; **bed 4b**; 5, T-19-3, specimen with symmetrically built carina; **bed 5**, lower part of Artinskian, Burtsevian horizon, asymmetricus Zone. **6-8.** *Sweetognathus obliquidentatus* (Chernykh), 1990. 6, holotype ZSP-1070/19v; 7, DT40-3; 8, T/19-1-5; **bed 5**; lower part of Artinskian, Burtsevian horizon, asymmetricus Zone. **9, 12.** *Sweetognathus aff. ruzhencevi* (Kozur), 1976: 9, DT40-6; 12, DT40-13; **bed 5**; lower part of Artinskian, Burtsevian horizon, asymmetricus Zona. **10, 11.** *Sweetognathus gravis* Chernykh, 2006: 10, DT40-10k; 11, holotype U40-9b; **bed 5**; lower part of Artinskian, Burtsevian horizon, asymmetricus Zone.

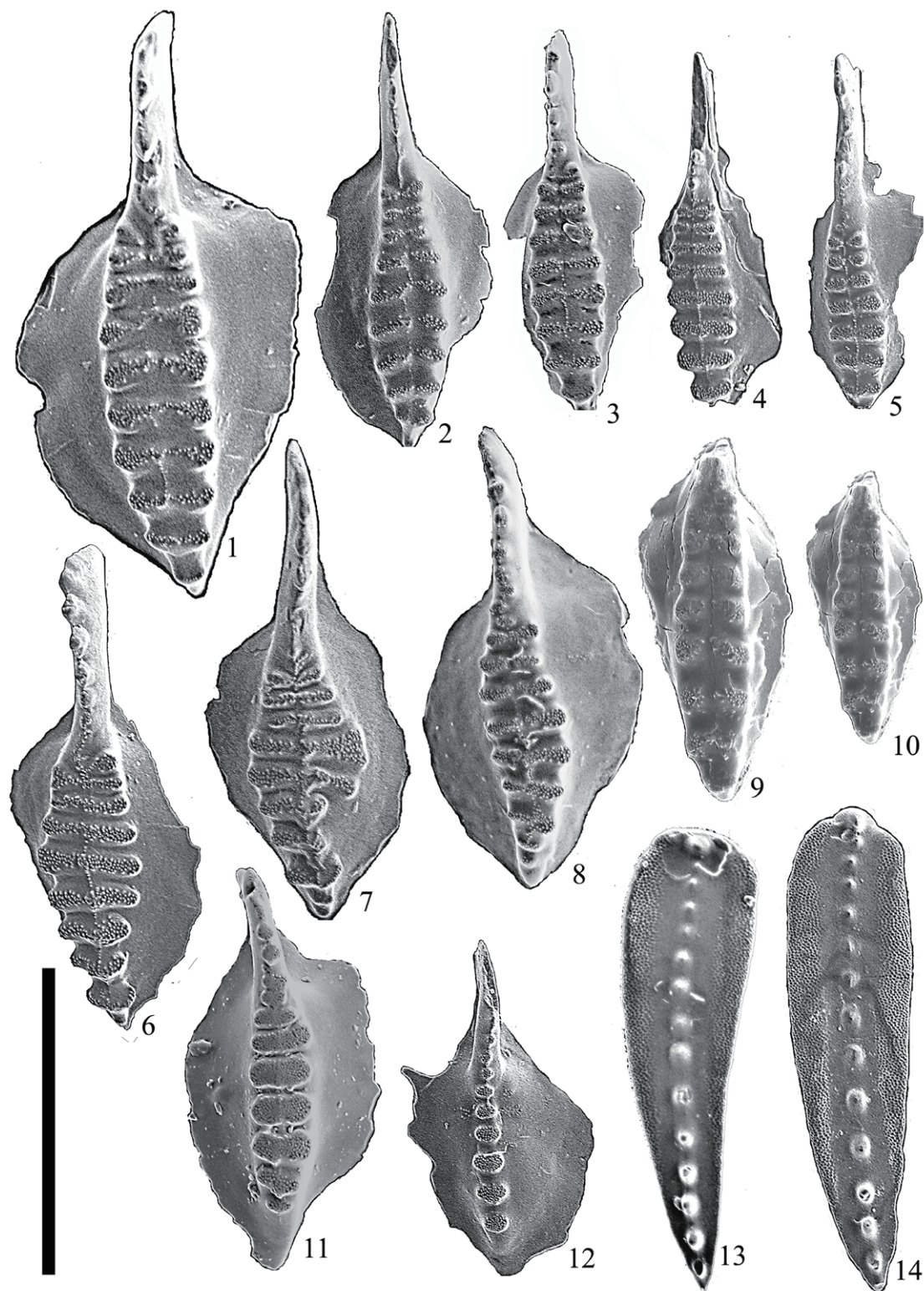


Fig. 10. Lower Artinskian conodonts in bed 10 (Artinskian, lower part of Irginian horizon, clarki Zone in Dal'ny Tulkas section (x90). Scale bar = 500 μ m

1, 4-8. *Sweetognathus asymmetricus* Sun and Lai, 2017: 1, DT40-27, the relicts of the longitudinal middle ridge are visible; 4, DT40-29, the middle ridge is located above upper surface of carinal nodes; 5, DT40-17, the middle ridge is located lower upper surface of carinal nodes; 6, DT40-24; 7, DT40-19; 8, DT40-21. **2, 3.** *Sweetognathus* aff. *clarki* (Kozur), 1976: 2, DT40-18; 3, DT40-22, the relicts of the longitudinal middle ridge are visible. **9, 10.** *Sweetognathus clarki* (Kozur), 1976: 9, DT40-33; 10, DT40-32. **11, 12.** *Sweetognathus* aff. *binodosus* Chernykh, 2005: 11, DT40-23; 12, DT40-20. **13, 14.** *Mesogondolella laevigata* Chernykh, 2005. 13, U40-26; 14, holotype DT40-25.

researchers (Kozur, 1977; Mei et al., 2002; Ritter, 1986; Wang et al., 1987); however, at the time there was insufficient knowledge about the early members of the evolutionary lineage of this group of conodonts. Forms referred to the independent species *Sweetognathus anceps*, also occur widely, but until now they were encountered together with the typical *Sw. asymmetricus*, and the majority of researchers identified those specimens, without the fully developed middle connecting ridge, as *Sweetognathus cf. whitei*. The gradual passage from *Sw. anceps* to *Sw. asymmetricus* is traced for the first time giving the complete picture of the development of these conodonts in the evolutionary lineage *Sweetognathus expansus* - *Sw. aff. merrilli* - *Sw. binodosus* - *Sw. anceps* - *Sw. asymmetricus* (Fig. 8).

The chronomorphoclone *Sw. binodosus* - *Sw. anceps* - *Sw. asymmetricus* can also be recognized in transgressive facies of uppermost Raanes and lower Great Bear Cape formations (Beauchamp et al., 2021; Chernykh et al., 2020), southwest Ellesmere Island, Canadian Arctic (Henderson, 1988; Henderson, 1999; Beauchamp and Henderson, 1994; Mei et al., 2002), Riepetown Formation, Moorman Ranch, Nevada (Ritter, 1986), upper Riepe Springs Limestone, Elko County, Nevada (Read and Nestell, 2018), Buckskin Mountain Formation in Carlin Canyon, Nevada (Dehari, 2016), Ross Creek Formation in southeastern British Columbia (Henderson and McGugan, 1986), and many other regions. In South China, in the Loudian section (Guizhou), there is a sequence *Sw. binodosus*-*Sw. asymmetricus* at 316 m above the base of the section (Wang Zhi-hao, 1994). In beds 18-23 at the Tieqiao section of south China, *Sweetognathus asymmetricus* appears, but this occurrence seems to be high in the range of the species (Wang et al., 1987; Shen et al., 2007; Sun et al., 2017).

Ammonoids

Little has been known about the ammonoids of the Dal'ny Tulkas. Previously, Boris Chuvashov and colleagues made invertebrate collections at two levels of the lower part of the Artinskian stage (bed 5), in which M.F. Bogoslovskaya identified *Popanoceras annae* Ruzhencev, *P. tschernowi* Maximova, *P. congregale* Ruzhencev, *Kargalites* sp. and *Neopronorites skvorzovi* (Tchernow) (Chuvashov et al., 2002). This assemblage dates the host beds as early Artinskian. Rare specimens of *Artinskia* sp. are found here. In 2016, R.V. Kutygin searched for fossil cephalopods in the natural outcrop of the Dal'ny Tulkas, as well as in a trench dug by an excavator along this outcrop.

In the Sakmarian interval, ammonoids were not found. At 1.6 m above the Sakmarian-Artinskian Stage boundary, a small accumulation of *Popanoceras annae* Ruzhencev shells were found in clay-carbonate concretions in interbed 9-4 of bed 9 of the trench. This is the most common Artinskian ammonoid of the Southern Urals. The vertical interval of distribution of *Popanoceras annae* Ruzhencev covers both substages of the Artinskian Stage; however most of the known specimens come from the lower substage (Aktastinian).

In the bioclastic limestone of the trench section, many more young juvenile ammonoids are scattered 2.5 m above the Sakmarian-Artinskian boundary (bed 10-1 of the trench; Fig. 11; Table 1). Rare medium-sized and large ammonoid

specimens are usually represented only by fragments. The collection of cephalopods is dominated by *Eothinites kargalensis* Ruzhencev, which is often found in the Aktastinian of the southern Urals. Among the Eothinites, several specimens have prominent transverse ornamentation (Figs. 11.4, 11.5), previously identified as *Eothinites* aff. *usvensis* Bogoslovskaya. Possessing ornamentation very similar to representatives of *E. usvensis* from the Urmanskaya Formation (upper of part Artinskian) of the Middle Urals (Bogoslovskaya, 1962), the Tulkas specimens differ in the less evolute shell. In addition to Eothinites, the assemblage contains *Popanoceras annae* Ruzhencev, *P. congregale* Ruzhencev, and *Daraelites elegans* Tchernow, which characterize the Artinskian Stage of the Urals. Paragastrioceratids are rare; they are represented by small specimens of *Uraloceras involutum* (Voinova) and *U. gracilentum* Ruzhencev.

The species *Uraloceras involutum* (Voinova) is the most common of the Artinskian paragastrioceratids of the southern Urals, with the best finds occurring in the lower substage (Aktastinian). In addition to the Southern Urals, the species *Uraloceras involutum* (Voinova) is also known from the Urmanskaya Formation of the Middle Urals (Bogoslovskaya, 1962), in the Kosva Formation of the Pechora Basin (Bogoslovskaya and Shkolin, 1998), in the upper Raanes ("Assistance") Formation of Ellesmere Island of the Canadian Arctic Archipelago (Nassichuk et al., 1966; Nassichuk, 1975), in the Jungle Creek Formation of the northern Yukon Territory (Nassichuk, 1971), in the Eagle Creek Formation of Alaska (Schiappa et al., 2005), as well as possibly in British Columbia and in Nevada (Schiappa et al., 2005).

A rare Aktastinian species of *Uraloceras gracilentum* Ruzhencev has features of the oldest paragastrioceratids, expressed by unusually slow coiling for the genus *Uraloceras*. According to V. E. Ruzhencev (1956), the possible ancestor of *Uraloceras gracilentum* Ruzhencev is the late Sakmarian species *Uraloceras limatum* Ruzhencev, which probably belongs to a separate genus from *Uraloceras*. Also here were found the shells of the genera *Crimites* and *Aktubinskia*, but poorly preserved.

In the natural outcrop of Dal'ny Tulkas section, ammonoids were collected from Bed 8. The ammonoids found in this locality belong to the families Daraelitidae, Pronoritidae, Medlicottiidae, Agathiceratidae, Eothinitidae, Metalegoceratidae, Paragastrioceratidae, Marathonitidae, and Popanoceratidae. Earlier from the same location (Bed 8) Tamra Schiappa identified *Sakmarites postcarbonarius* (Karpinsky), *Agathiceras uralicum* (Karpinsky), *Kargalites typicus* (Ruzhencev), *Paragastrioceras* sp., and *Crimites subkrotowi* Ruzhencev (Chuvashov et al., 2013) (Table 1).

The ammonoid assemblage of the Dal'ny Tulkas section is typical of the lower Artinskian (Aktastinian). Among ammonoids, a number of stratigraphically important genera, of which *Daraelites*, *Aktubinskia*, *Eothinites*, and *Popanoceras* have been recognized at Dal'ny Tulkas and appear in the Aktastinian. The entry of *Neopronorites skvorzovi* (Tchernow), *Uraloceras involutum* (Voinova), *U. gracilentum* Ruzhencev, *Popanoceras tschernowi* Maximova and *P. annae* Ruzhencev are important indicators of the Sakmarian-Artinskian boundary. Considering the abundance of *Uraloceras involutum* (Voinova)

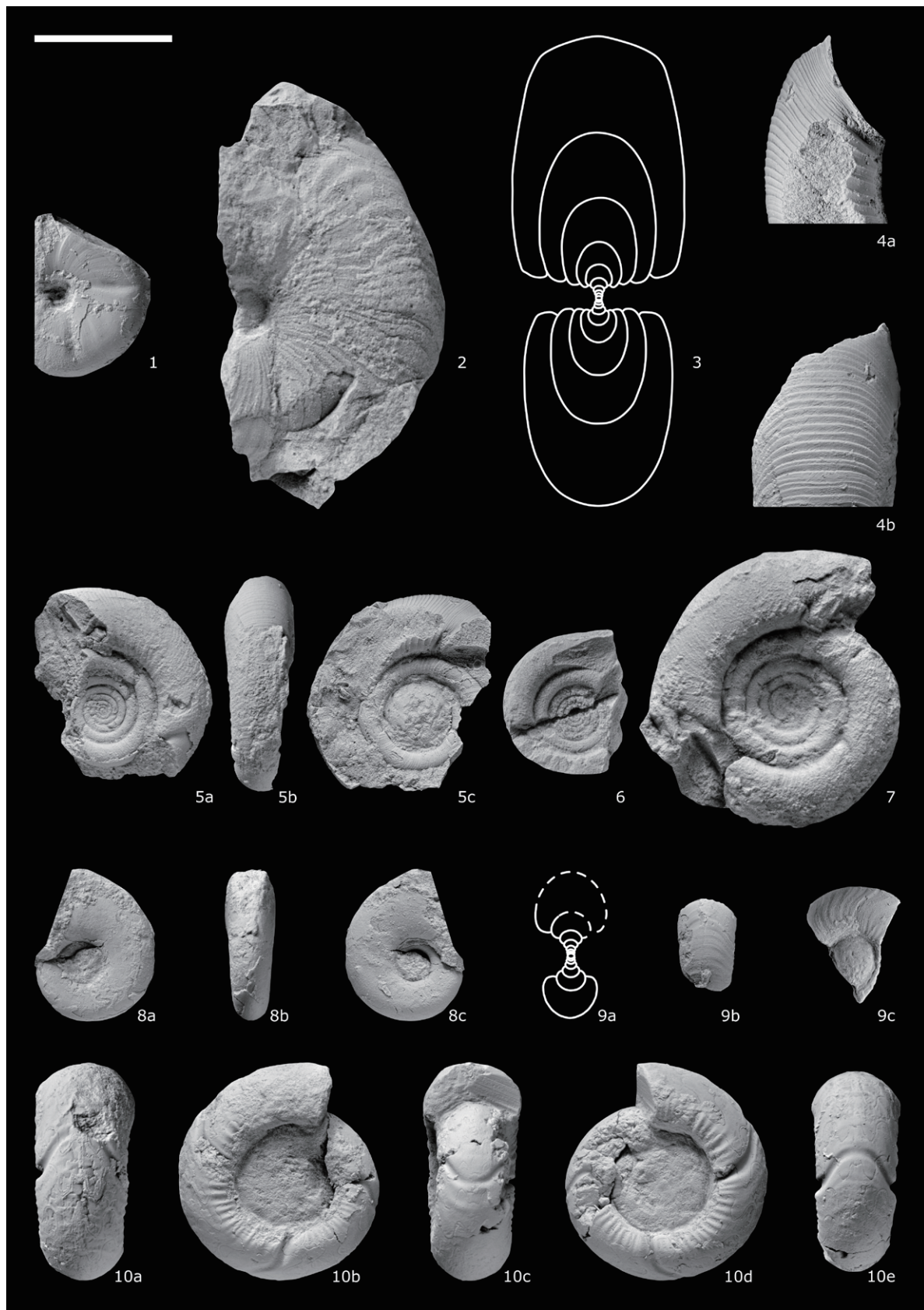


Fig. 11. Ammonoids from the Dal'ny Tulkas trench, **bed 10-1**. Scale bar: 10 mm for figs 1-3, 5-10; 5 mm for figs 4a-b.
1. *Popanoceras congregale* Ruzhencev. **2, 3.** *Popanoceras annae* Ruzhencev. **4, 5.** *Eothinites* aff. *usvensis* Bogoslovskaya. **6, 7.** *Eothinites kargalensis* Ruzhencev. **8.** *Daraelites elegans* Tchernow. **9.** *Uraloceras involutum* (Voinova). **10.** *Uraloceras gracilemum* Ruzhencev.

in the lower part of the Artinskian stage in the southern Urals, and its wide geographical range, the interval of the Dal'ny Tulkas section containing lower Artinskian ammonoids is proposed to be designated as "Beds with *Uraloceras involutum*". The biostratigraphic value of Permian ammonoids is summarized in Leonova (2018).

Foraminifers

Dal'ny Tulkas section

Fusulines with Sakmarian conodonts are represented by Sakmarian species: *Pseudofusulina callosa* Rauser, *P. callosa proconavatas* Rauser, *P. jaroslavensis fraudulenta* Kireeva, *P. cf. parajaroslavensis* Kireeva, *P. blochini* Korzh. A redeposited complex of Sterlitamakian fusulines was found in the limestones with Artinskian conodonts: *P. aff. longa* Kireeva, *P. fortissima* Kireeva, *P. anostriata* Kireeva, *P. plicatissima* Rauser., *P. urdalensis abnormis* Rauser. Burtsevian fusulines are found in carbonate mud matrix: *P. callosa* Rauser., *P. plicatissima* Rauser, *P. plicatissima irregularis* Rauser., *P. urdalensis* Rauser., *P. fortissima* Kireeva, *P. concavatas* Vissarionova, *P. juresanensis* Rauser., *P. consobrina* Rauser, *P. paraconcessa* Rauser (Chernykh et al., 2015) (Table 1).

Dal'ny Tulkas trench

New excavation needed for ratification and re-testing of the section was carried out in 2016. The thickness of the trench section is 12.5 m. The lower part of the section consists of interbedded sandstone, mudstone with carbonate nodules, as well as layers of ash tuffs. The upper part is composed mainly of shale with interlayers of siltstone and bioclastic limestone (grainstone and rudstone). Limestones are often boudinaged within the siltstone matrix. Fusulines and small foraminifers were found in limestones at four levels. Fusulines are illustrated in figure 12 and small foraminifers are illustrated in figures 13 and 14; both are listed in Table 1.

Three complexes are distinguished in the trench. The first assemblage (bed 8-1) consists of 4 species of fusulines and 11 species of small foraminifers (SF). Species of *Boultonia*, *Schubertella*, and *Pseudofusulina* are characteristic for the Sakmarian and the Artinskian. *Fusiella schubertellinoides* Suleimanov is typical for the upper Asselian-Sakmarian. Most SF species are Burtsevian (lower substage of Artinskian): *Dentalina particulata* Baryshnikov, *Geinitzina lysvaensis* Baryshnikov, *Nodosinelloides kislovi* (Koscheleva), *N. dualis* (Baryshnikov), *Howchinella aff. turae* (Baryshnikov), ?*Rectoglandulina* sp., *Postmonotaxinoides costiferus* (Lipina), *Endothyra lipinae lata* Zolotova. Nodosariida is predominant among them. There are *Rectoglandulina* and *Howchinella*, which appear at the base of the Burtsevian H. (Baryshnikov et al., 1982).

The second assemblage (bed 8-2) consists of species of 5 genera of fusulines: *Boultonia*, *Schubertella*, *Pseudofusulina*, *Fusiella* and *Mesoschubertella*. Fusulines include the frequent and varied *Schubertella*, *Pseudofusulina paraconcessa* Rauser, which are characteristic for the Sakmarian and Artinskian, and *Ps. ex gr. pedissequa* Vissarionova, *Ps. abortiva* Tchuvashov of the Irginian and Sarginian regional substages. *Ps. seleukensis* Rauser, *Ps. urasbajevi* Rauser of the Sarginian are characteristic of Artinskian Stage. Generally the age of this assemblage is

Artinskian. Among the 32 small foraminifer species of the second assemblage, in addition to the species from the first assemblage, there are *Langella*, Artinskian species - *Nodosinelloides bella kamaenis* (Baryshnikov), *N. jaborovensis* (Koscheleva), *N. incelebrata novosjolovi* (Baryshnikov), *Nodosinelloides netchaewi rasik* (Baryshnikov), *Endothyra soshkinae* Morozova, numerous *Postmonotaxinoides costiferus* (Lipina), *Bradyina ex gr. lucida* Morozova, *Br. lucida* Morozova, *Br. compressa* Morozova, *Deckerella elegans multicamerata* Zolotova, *Pseudoglomospira elegans* (Lipina), and the first *Hemigordius* sp. The Artinskian SF assemblages in the Urals are distinguished by the appearance of *Hemigordius*. The second assemblage also contains *Deckerella media bashkirica* Morozova, *D. elegans* Morozova, *Bradyina compressa minima* Morozova, *Tetrataxis ex gr. conica* Ehrenberg, *T. plana* Morozova, *T. hemisphaerica* Morozova, *T. hemisphaerica elongata* Morozova, *T. lata* Spandel, characteristic of Sakmarian assemblages, and *Lateenoglobivalvulina spiralis* (Morozova), *Trepeilopsis* sp., and others of Cisuralian assemblages.

The third assemblage (bed 10) consists of fusulines: *Schubertella aff. usimica* Baryshnikov, *Mesoschubertella* sp. 2. Twenty-two small foraminifer species from the first and the second assemblages are found in the third assemblage, and 15 species of small foraminifers appeared for the first time in the trench. These are Burtsevian-Irginian species - *Bradyina subtrigonalis* Baryshnikov, *Endothyranella protracta maxima* Baryshnikov, *Tetrataxis lata novosjolovi* Baryshnikov, ?*Uralogordius* sp., ?*Pachyhloia* sp., *Geinitzina richteri kasib* Koscheleva, *Nodosinelloides ex gr. netchaewi* (Tcherdynzev), *N. jazvae* Koscheleva and Cisuralian species - *Endothyra rotundata* Morozova, *E. symmetrica* Morozova, *E. lipinae* Morozova, *Pseudoagathammina regularis* (Lipina), *Pseudoglomospira vulgaris* (Lipina), and the upper Artinskian-lower Kungurian *Midiella aff. ovatus minima* (Grozdilova).

All three small foraminifer assemblages are of early Artinskian age. They are similar in composition to early Yakhtashian assemblages from Turkey and northern Pamir (Filimonova, 2010). The first fusuline assemblage is of Sakmarian age, the second and third are Artinskian. The schubertellid-fusuline foraminiferal assemblages of late Asselian-Sakmarian age are replaced by typical Artinskian assemblages. Artinskian forms of foraminiferal communities are present throughout the entire boundary interval. Their diversity and abundance increase up section.

Palynology

The palynological succession of the beds above and below the proposed Artinskian GSSP at Dal'ny Tulkas was established in two sections: one a natural exposure running E-W, the other a narrow specially-excavated trench running WNW to ESE (Fig. 2). Palynological data has been gathered from both sections; the first by Michael Stephenson and the second by M.V. Oshurkova (Chernykh pers. comm. 2021).

Dal'ny Tulkas section

Materials for study comprise samples collected by Michael Stephenson between June 25 and July 4, 2007 (Stephenson, 2007). Samples (mass <200g) were collected and processed

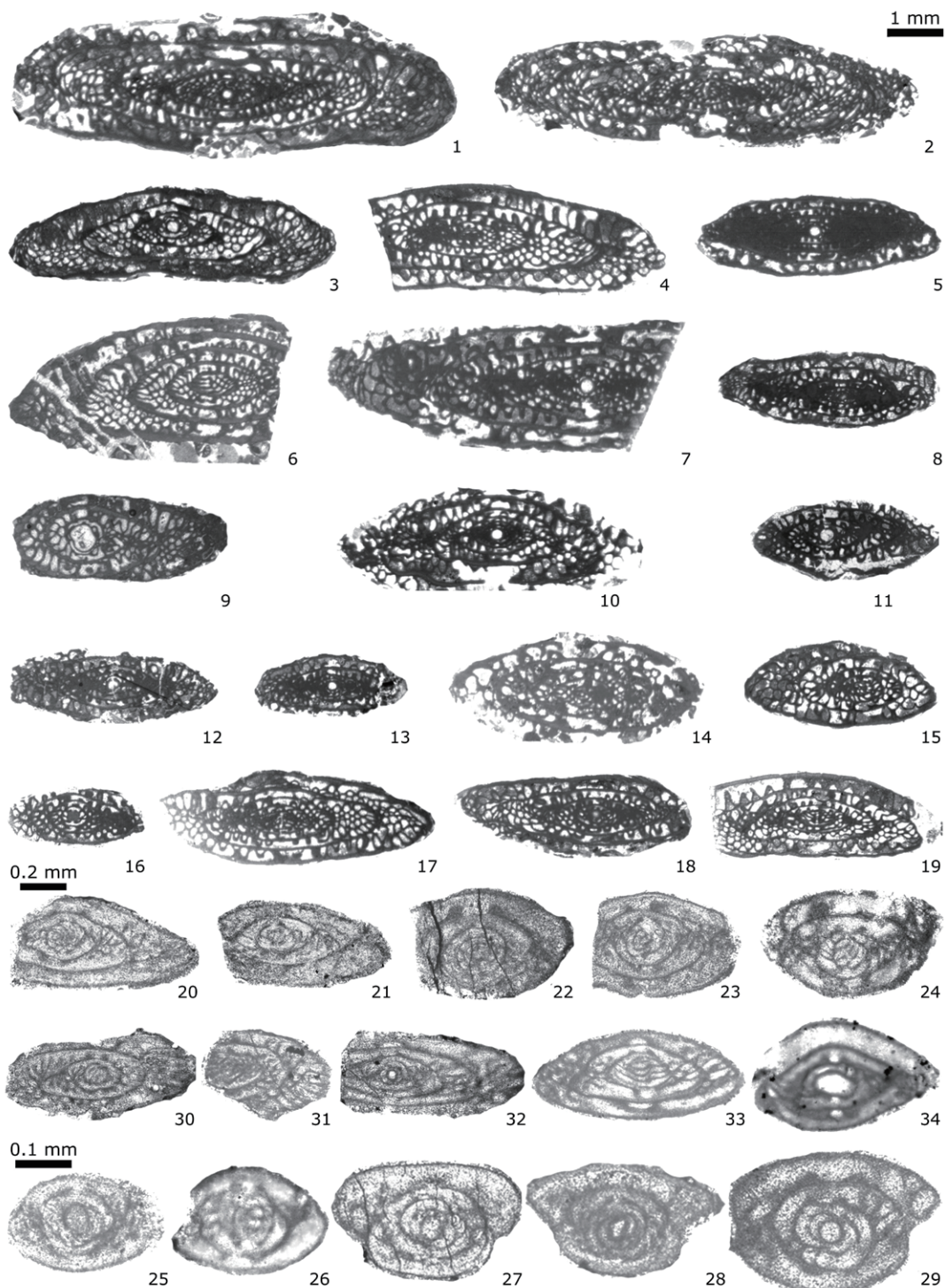


Fig. 12. Fusulines from Dal'ny Tulkas trench, beds 8-1, 8-2, 10. Scale bar: 1 mm for figs 1-19; 0.2 mm for figs 20-29; 0.1 mm for figs 30-34.

1-2. *Pseudofusulina paraconcessa* Rauser, bed 8-2. **3-4.** *Pseudofusulina ex gr. pedissequa* Vissarionova, bed 8-2. **5.** *Pseudofusulina abortiva* Tchuvashov, bed 8-2. **6.** *Pseudofusulina cf. utilis* Tchuvashov, bed 8-2. **7.** *Pseudofusulina cf. salva* Vissarionova, bed 8-2. **8, 12-13.** *Pseudofusulina seleukensis* Rauser, bed 8-2. **9.** *Pseudofusulina* sp. 1, bed 8-2. **10-11.** *Pseudofusulina ex gr. seleukensis* Rauser, bed 8-2. **14-15.** *Pseudofusulina* sp. 2, bed 8-2. **16-19.** *Pseudofusulina urasbajevi* Rauser, bed 8-2. **20-21.** *Schubertella ex gr. kingi* Dunbar & Skinner, bed 8-2. **22-23.** *Schubertella ex gr. paramelonica* Suleimanov, bed 8-2. **24.** *Schubertella* sp. A, bed 8-2. **25-26.** *Boultonia* sp.; 25, bed 8-1; 26, bed 8-2. **27.** *Fusiella schubertellinoides* Suleimanov, bed 8-1. **28.** *Mesoschubertella* sp. 1, bed 8-2. **29.** *Mesoschubertella* sp. 2, bed 10. **30-31.** *Schubertella aff. uffimica* Baryshnikov, bed 10. **32-34.** *Schubertella* sp. B; 32-33: bed 10; 34: bed 8-2.

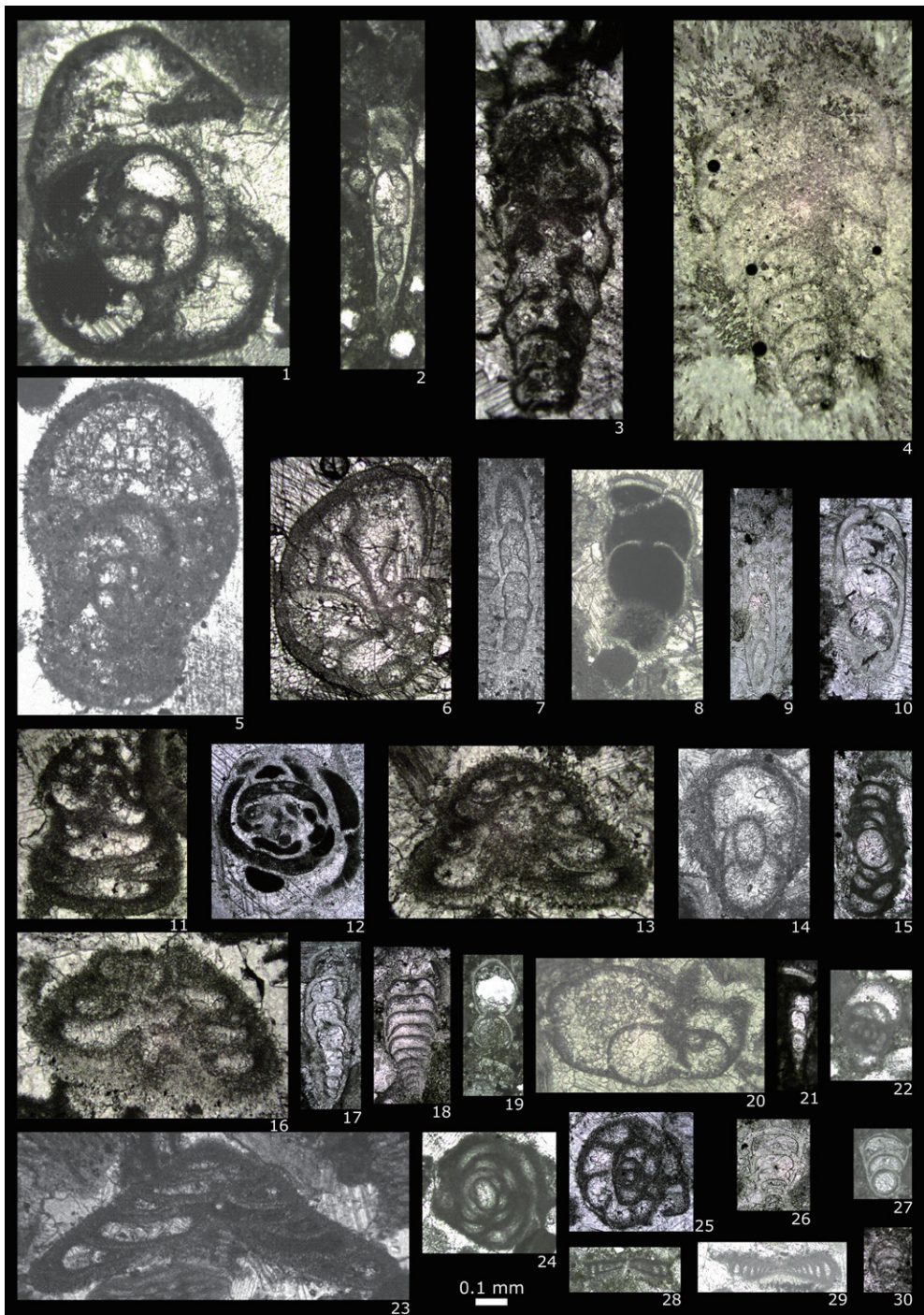


Fig. 13. Small foraminifers from the Dal'ny Tulkas trench, beds 8-1, 8-2. Scale bar: 0.1 mm.

- 1.** *Bradyina lucida* Morozova, bed 8-2. **2.** *Dentalina particulata* Baryshnikov, bed 8-1. **3.** *Deckerella media bashkirica* Morozova, bed 8-2. **4.** *Deckerella elegans multicamerata* Zolotova, bed 8-2. **5.** *Bradyina compressa* Morozova, bed 8-2. **6.** *Globivalvulina* sp., bed 8-2. **7.** *Dentalina particulata* Baryshnikov, bed 8-2. **8.** *Nodosinelloides bella kamaensis* (Baryshnikov), bed 8-2. **9.** *Nodosinelloides incelebrata novosjolovi* Baryshnikov, bed 8-2. **10.** *Nodosinelloides netchaewi rasik* (Baryshnikov), bed 8-2. **11.** *Tetrataxis hemisphaerica elongata* Morozova, bed 8-2. **12.** *Pseudoagathammina dublicita* (Lipina), bed 8-2. **13.** *Tetrataxis lata* Spandel, bed 8-2. **14.** *Bradyina compressa minima* Morozova, bed 8-2. **15.** *Hemigordius harltoni* Cushman & Waters, bed 8-2. **16.** *Tetrataxis hemisphaerica* Morozova, bed 8-2. **17.** *Nodosinelloides jaborvensis* Koscheleva, bed 8-2. **18.** *Geinitzina spandeli* Tscherdynzew, bed 8-1. **19.** *Nodosinelloides kislovi* (Koscheleva), bed 8-1. **20.** *Lateenoglobivalvulina spiralis* (Morozova), bed 8-2. **21.** *Nodosinelloides dualis* (Baryshnikov), bed 8-1. **22.** *Endothyra lipinae lata* Zolotova, bed 8-1. **23.** *Tetrataxis plana* Morozova, bed 8-2. **24.** *Pseudogloboospira elegans* (Lipina), bed 8-2. **25.** *Endothyra soshkinae* Morozova, bed 8-2. **26.** *Geinitzina lysvaensis* Baryshnikov, bed 8-1. **27.** ?*Rectoglandulina* sp., bed 8-1. **28.** *Postmonotaxinoides costiferus* (Lipina), bed 8-1. **29.** *Postmonotaxinoides costiferus* (Lipina), bed 8-2. **30.** *Howchinella turae* (Baryshnikov), bed 8-1.

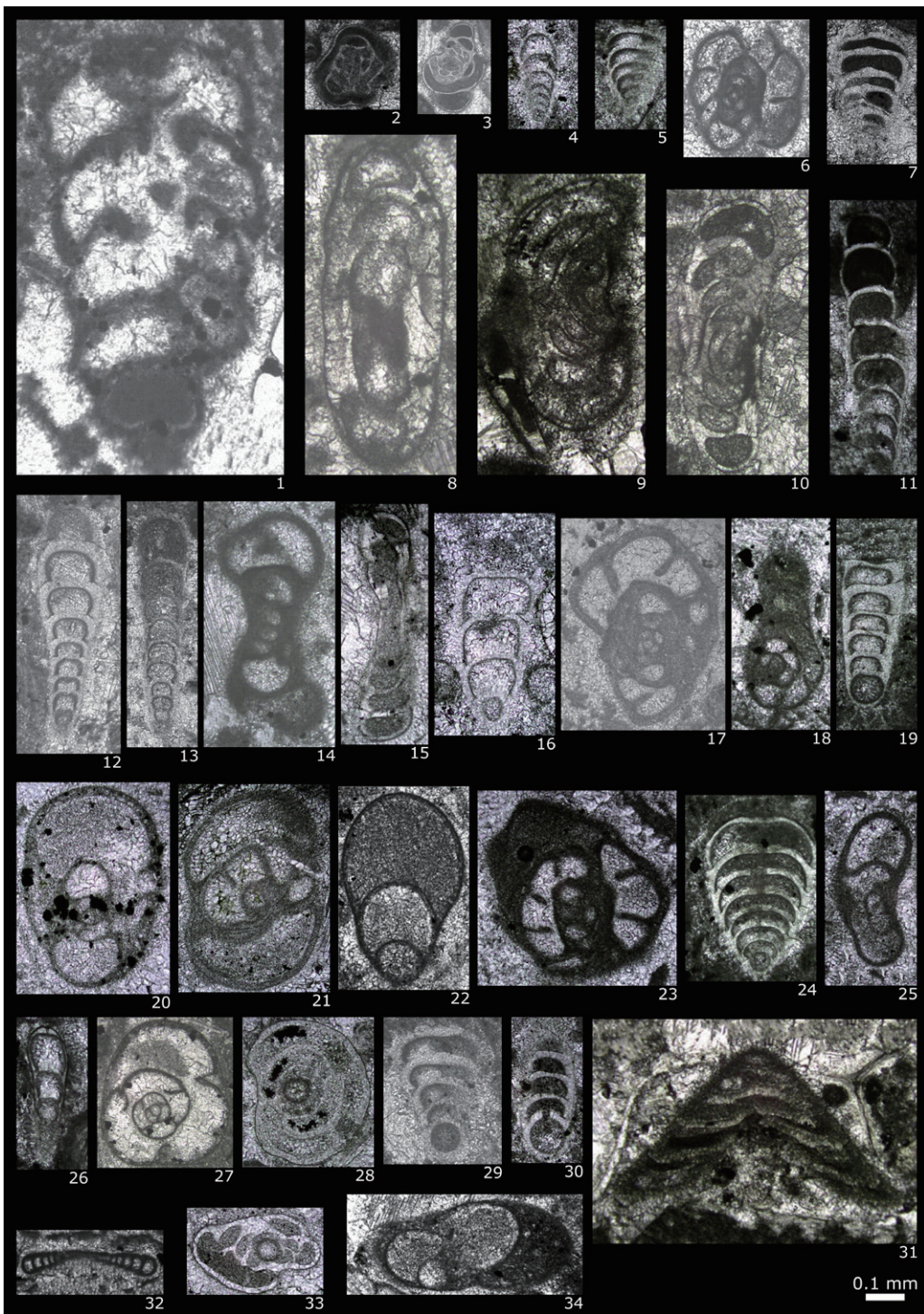


Fig.14. Small foraminifers from the Dal'ny Tulkas trench, bed 10. Scale bar: 0.1 mm.

1. *Deckerella media bashkirica* Morozova.
2. *Pseudogloboospira elegans* (Lipina).
3. *Pseudoagathammina dublicita* (Lipina).
4. *Howchinella turae* (Baryshnikov).
5. *Geinitzina postcarbonica* Spandel.
6. *Endothyra rotundata* Morozova.
7. *Geinitzina richteri kasib* Koscheleva.
- 8-10. *Uralogordius?* sp.,
11. *Nodosinelloides bella kamaensis* (Baryshnikov).
12. *Nodosinelloides netchaewi* (Tcherdynzev).
13. *Nodosinelloides jaborovensis* Koscheleva.
14. *Endothyra symmetrica* Morozova.
15. *Hemigordius harltoni* Cushman & Waters.
16. *Nodosinelloides netchaewi rasik* (Baryshnikov).
17. *Endothyra soshkinae* Morozova.
18. *Endothyranella protracta maxima* Baryshnikov.
19. *Geinitzina lysvaensis* Baryshnikov.
20. *Bradyina compressa* Morozova.
21. *Endothyra lipinae lata* Zolotova.
22. *Lateenoglobivalvulina spiralis* (Morozova).
23. *Endothyra rotundata* Morozova.
24. *Pachyphloia* sp.
25. *Bradyina compressa minima* Morozova.
26. *Nodosinelloides dualis* (Baryshnikov).
27. *Bradyina subtrigonialis* Baryshnikov.
28. *Hemigordius ovatus minimus* Grozdilova.
29. *Geinitzina richteri kasib* Koscheleva.
30. *?Langella* sp.
31. *Tetrataxis lata novosjolovi* Baryshnikov.
32. *Postmonotaxinoides costiferus* (Lipina).
33. *Pseudogloboospira vulgaris* (Lipina).
34. *Lateenoglobivalvulina spiralis* (Morozova).

using standard techniques (Wood et al. 1996) at the palynological laboratories of the British Geological Survey. The section sampled is shown in (Fig. 3) and consists of carbonate mudstone, siltstone and thin limestone.

The eleven samples yielded large amounts of organic residue including palynomorphs, sheet cellular material, woody material and amorphous organic matter. Palynomorphs were common in several samples, but were universally poorly preserved, showing signs of contemporaneous oxidation such that spore and pollen exine was near colourless and transparent in some cases. Saccate pollen was particularly poorly preserved with sacci commonly separated from corpi. The poor preservation necessitated staining with Safranin O to improve possibility of determination.

The most diverse and best preserved of the samples are MPA 56664, 56659, 56663, 56666 and 56662. This sample range spans the proposed GSSP, which is within Bed 4 (Fig. 3).

Overall the samples are dominated by indeterminate non-taeniate and taeniate bisaccate pollen (often detached corpi or sacci), *Cycadopites* (mainly *C. ?glaber* (Luber & Valts) Hart) and *Vittatina* spp. (mainly *V. minima* Jansonius, *V. vittifera* (Luber & Valts) Samoilovich and *V. subsaccata* Samoilovich). ?Algal forms such as *Azonaletes* cf. *compactus* Luber and 'Algal palynomorph sp. A' (see Stephenson, 2007) are also locally common. Other taxa recorded include ?*Complexisporites* sp., *Alisporites indarraensis* Segroves, *Cordaitina* spp. (including *C. uralensis* (Luber & Valts) Samoilovich), *Crucisaccites ornatus* (Samoilovich) Dibner, *Florinites luberae* Samoilovich, *Hamiapollenites bullaeformis* (Samoilovich) Jansonius, indeterminate monosaccate pollen, *Knoxisporites* sp., *Limitsporites elongatus* Lele & Karim, *L. monstruosus* Luber & Valts, *Maculatasporites* sp., *Potonieisporites grandis* Tshudy & Kosanke, *Protohaploxylinus* spp., *Punctatisporites* sp. and *Sulcatisporites* spp. (Fig. 15).

'Algal palynomorph sp. A' is non-haptotypic and has a distinctive ornament of ring-like elements (Fig. 15). In the three lower samples, large ?algal palynomorphs (mean diameter approx. 100 µm) with an indistinct reticulate surface are very common, and are particularly conspicuous in slides because they do not absorb the Safranin O stain, remaining a translucent lemon yellow colour. For the present they are assigned to *Azonaletes* cf. *compactus*.

The lower parts of the succession from beds 1, 2 and 3 appear to be dominated by probable algal palynomorphs such as *Azonaletes* cf. *compactus*, though indeterminate bisaccate pollen are common, including taeniate indeterminate bisaccate pollen, as well as species of *Vittatina* are present.

Beds 7 to 9 contain very few algal palynomorphs such as *Azonaletes* cf. *compactus*, and *Cycadopites* [mainly *C. ?glaber* (Luber and Valts) Hart] become more common above the proposed boundary level as do species of *Vittatina*.

Dal'ny Tulkas Trench

From beds 1 to 3 in the trench section (Fig 5), M.V. Oshurkova reported common pollen such as *Vestigisporites* sp., *Hamiapollenites* sp., *Protohaploxylinus* sp., *Striatopodocarpites* spp. and *Vittatina vittifer*. Spores such as *Crassispora* sp., *Apiculatisporites* sp. and *Anaplanisporites* sp. are also present.

In beds 5 and 6, *Hamiapollenites* sp., *Protohaploxylinus* sp., and *Vittatina* spp. are again common in the trench section.

Beds 7 to 9 contain *Crassispora* sp., *Cordaitina* spp. (including *C. rotata*), *Florinites luberae*, *Hamiapollenites* spp. (including *H. bullaeformis*), *Protohaploxylinus* sp., *Striatopodocarpites* spp., and *Vittatina* spp. (including *V. vittifer* and *V. striata*). A small number of *Weylandites* specimens were also recorded.

As a general comment on palynology for correlation of the base of the Artinskian, there are no markers among the spores and pollen that would provide a correlation point for the GSSP. However the probable algal taxon *Azonaletes* cf. *compactus* appears to be very common below the proposed boundary and absent above (Fig. 16). Data on the wider stratigraphic occurrence of *Azonaletes* cf. *compactus* and its biological affinity would help to decide whether it has any value as a palynological marker for the base of the Artinskian. The abundance of this taxon, in this case, coincides with proximity to the sequence boundary. The role of Permian palynological biostratigraphy is summarized by Stephenson (2018).

Radiolarians

Numerous radiolarian have been recovered from several samples from the Sakmarian and Artinskian within the trench section (Figs. 17, 18; Table 1). These will become valuable for future correlations. Zhang et al. (2018) summarize the biostratigraphy potential of radiolarians. One taxon, *Pseudoalbaillella scalprata* (Fig. 18.13), is among the index taxa noted in Zhang et al. (2018) for the Sakmarian to Kungurian. Most of the specimens illustrated from the trench include spumellarian taxa.

U-Pb geochronology

M. Schmitz and V. Davydov (2012) carried out radiometric studies, based upon high-precision, isotope dilution-thermal ionization mass spectrometry (ID-TIMS) U- Pb zircon ages for interstratified volcanic ash beds in the parastratotype sections of the southern Urals, including in the Dal'ny Tulkas section. Here they selected ash tuffs at three levels (see black stars for levels in Figure 3) - in the upper part of bed 2 (4 m lower than base of Artinskian, in the upper part of bed 7 and in the base of bed 9 (2 m higher than the previous sample).

In bed 2, of eight analyzed grains of zircon, six grains yielded a weighted mean $206\text{Pb}/238\text{U}$ date of 290.81 ± 0.09 Ma. Seven of eight analyzed grains from bed 7 produced a weighted mean $206\text{Pb}/238\text{U}$ date of 288.36 ± 0.10 Ma. And from the third interlayer of ash tuff (bed 9) all eight investigated grains gave a $206\text{Pb}/238\text{U}$ date of 288.21 ± 0.06 Ma. "The three dated samples allow the calculation of a relatively constant accumulation rate through the lower portion of the section" (Schmitz and Davydov, 2012, p. 561). These zircons provided an interpolated geochronologic age of $290.1 \text{ Ma} \pm 0.2 \text{ Ma}$ (Schmitz and Davydov, 2012; Henderson et al., 2012) and $290.5 \text{ Ma} \pm 0.4 \text{ Ma}$ (Henderson and Shen, 2020) for the base-Artinskian.

Strontium isotopes

Schmitz et al. (2009) in a presentation at the International Conodont Symposium indicated a consistent secular trend of $87\text{Sr}/86\text{Sr}$ isotopic values from conodont elements through the Early Permian. The $87\text{Sr}/86\text{Sr}$ isotopic value for the base-

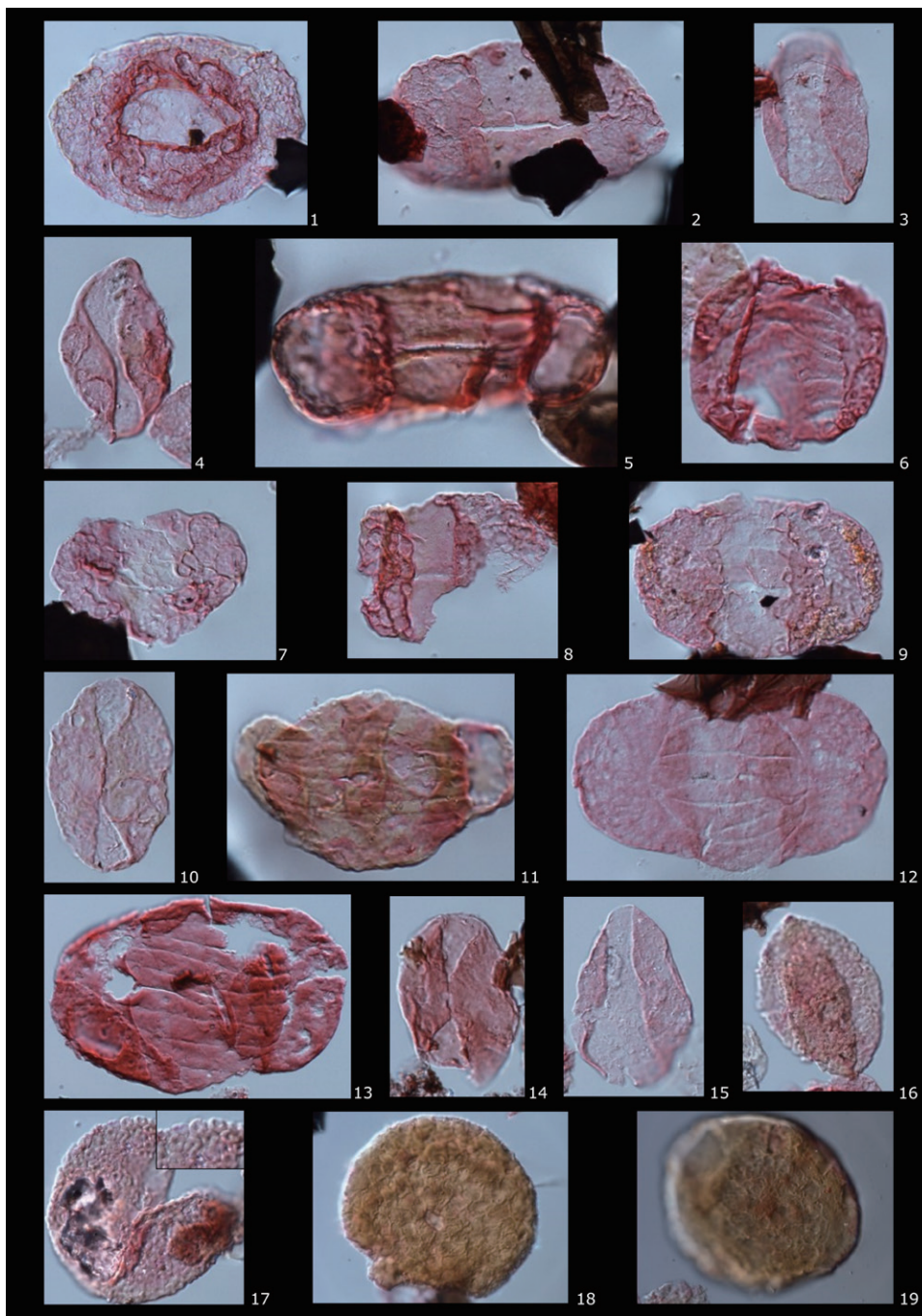


Fig. 15. Palynomorphs from the Dal'ny Tulkas natural exposure section. Slides are held in the collection of the BGS, Keyworth, Nottingham, NG12 5GG, UK. Locations of specimens are given first by England Finder code, then by BGS collections numbers. (MPA, MPK). The maximum dimension of each specimen is given in microns. **1.** *Potonieisporites grandis* Tshudy & Kosanke 1966, E44, MPA 56666, MPK 13629, 110 µm; **2.** *Limitsporites monstruosus* Luber & Valts, F68/4, MPA 56666, MPK 13630, 95 µm; **3.** *Cycadopites ?glaber* (Luber & Valts) Hart, E47, MPA 56666, MPK 13631 50 µm; **4.** *Cycadopites ?glaber*, M57, MPA 56666, MPK 13632, 30 µm; **5.** *Limitsporites monstruosus*, D52/2, MPA 56666, MPK 13633, 55 µm; **6.** *Vittatina subsaccata* Samoilovich, D52/1, MPA 56666, MPK 13634, 45 µm. **7.** *Alisporites indarraensis* Segroves, D56/4, MPA 56666, MPK 13635, 50 µm; **8.** *Limitsporites monstruosus*, D52, MPA 56666, MPK 13636, 60 µm; **9.** *Protohaploxylinus* sp., S67, MPA 56666, MPK 13637, 65 µm; **10.** *Cycadopites ?glaber*, O60/1, MPA 56666, MPK 13638, 40 µm; **11.** *Hamiapollenites bullaeformis* (Samoilovich) Jansonius, N63/3, MPA 56666, MPK 13639, 65 µm; **12.** *?Complexisporites* sp. O61/4, MPA 56666, MPK 13640, 80 µm; **13.** *Protohaploxylinus* sp., L59/3, MPA 56659, MPK 13641, 90 µm; **14.** *Cycadopites ?glaber*, O60/1, MPA 56659, MPK 13642, 40 µm; **15.** *Cycadopites ?glaber*, O52/2, MPA 56659, MPK 13643, 40 µm; **16.** Algal palynomorph sp. A, M46/2, MPA 56659, MPK 13644, 60 µm; **17.** Algal palynomorph sp. A, O61/3, MPA 56659, MPK 13645, 60 µm (inset detail of ornament); **18.** *Azonaletes cf. compactus* Luber, F51, MPA 56659, MPK 13646, 95 µm; **19.** *Azonaletes cf. compactus*, G57, MPA 56664, MPK 13647, 95 µm.

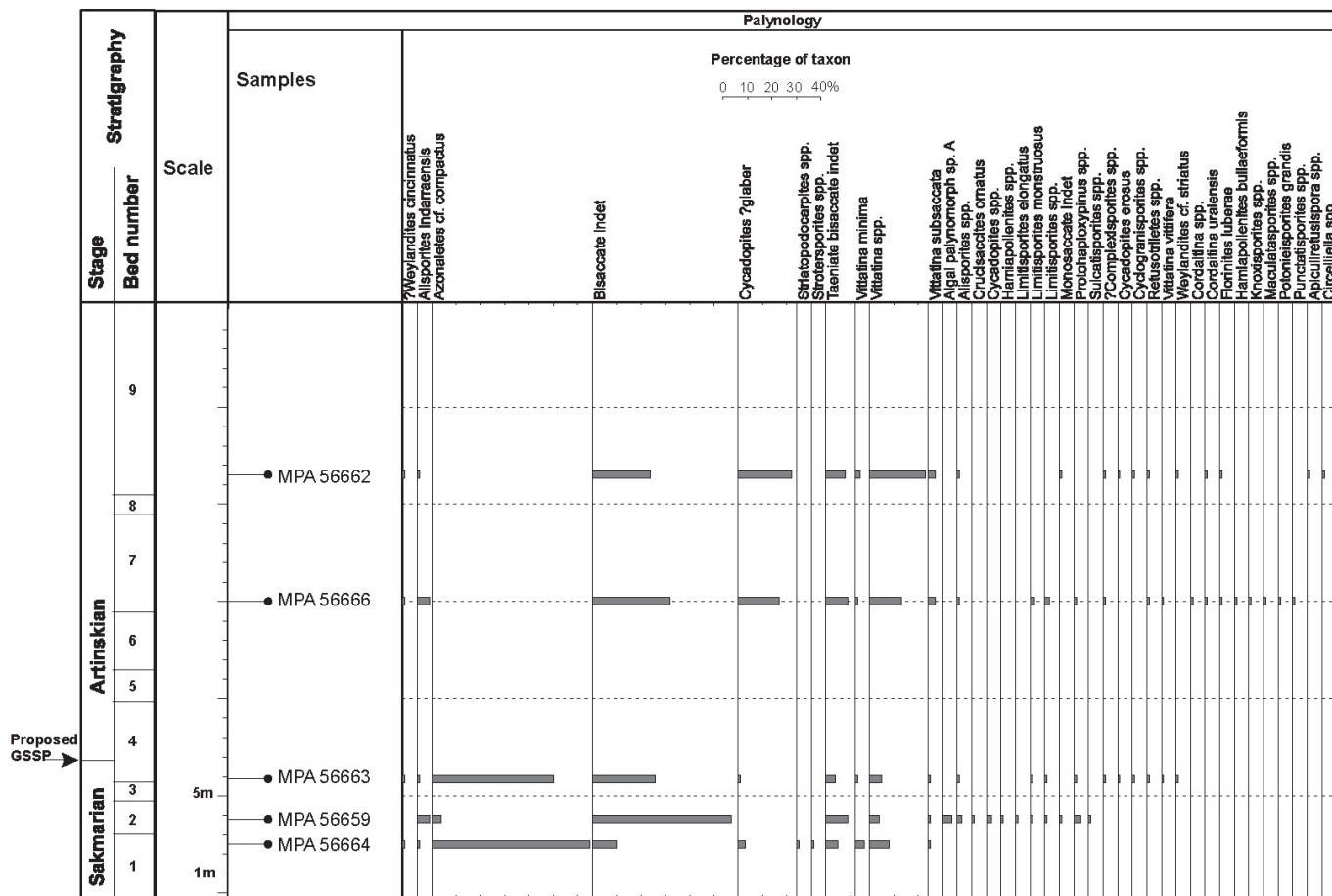


Fig. 16. Simplified sedimentological log of the Dal'ny Tulkas section showing characteristics of the palynological samples.

Artinskian was approximately 0.70765 (Schmitz et al., 2009). Strontium isotopes from individual conodont elements can be integrated with geochronologic ages to produce a time model. The strontium isotopic composition of seawater at the base of the Artinskian Stage is now calculated at $87\text{Sr}/86\text{Sr} = 0.70767$ (Chernykh et al., 2012).

Carbon isotope chemostratigraphy

A group of Chinese researchers with the participation of V.I. Davydov (USA, Boise State University) conducted a study of carbon and oxygen stable isotopes in the GSSP candidate sections of the South Urals – Usolka, Dal'ny Tulkas and Kondurovsky (Zeng et al., 2012). Basic results, obtained from the section Dal'ny Tulkas are given below.

In the Dal'ny Tulkas section the curves of $\delta^{13}\text{C}$ and $\delta^{18}\text{O}$ display a general concurrent tendency of change and are characterized by a rapid and sharp drop near the Sakmarian-Artinskian boundary and a long-term depletion in the subsequent interval of the Artinskian Stage (Fig. 19). The values of $\delta^{13}\text{C}$ present a dramatic depletion from $-4.7\text{\textperthousand}$ to $-11.7\text{\textperthousand}$ near the Sakmarian-Artinskian boundary in the Dal'ny Tulkas section, and for a long time remains a deeply negative level higher in the Artinskian Stage, with exception of one point with a value of $-2.2\text{\textperthousand}$ in the early Artinskian (Fig. 7). A somewhat similar trend,

but with very different values (4\textperthousand to 2\textperthousand) is shown by Buggisch et al. (2011) near the Sakmarian-Artinskian boundary at Luodian, China.

These very low values would normally be attributed to diagenesis, and Zeng et al. (2012) noted that the sharp drop in $\delta^{13}\text{C}$ and its retention for a long time and its associated normal $\delta^{18}\text{O}$ values between $1.1\text{\textperthousand}$ to $-2.2\text{\textperthousand}$ is difficult to explain. One potential explanation for those anomalous negative values is that the incorporation of ^{12}C derived from oxidized organic matter from organic-rich sediments with low CaCO_3 around the Sakmarian/Artinskian boundary at the Dal'ny Tulkas section. A similar excursion is also present around the Wuchiapingian-Changhsingian boundary GSSP at the Meishan section in South China (Shen et al., 2013). Another possible interpretation of such sharp variation in the $\delta^{13}\text{C}$ value is due to isotopic refractionation of the microbial chemosynthetic processes on the buried organic matter. However, significant $\delta^{13}\text{C}$ excursions from Sakmarian to Artinskian at the Luodian section in South China were also revealed (Buggisch et al., 2011) although precise correlation between South China and southern Urals still needs further study. If a similar sharp excursion is confirmed during further study in other regions, it could be very useful for the correlation of the distant sections.

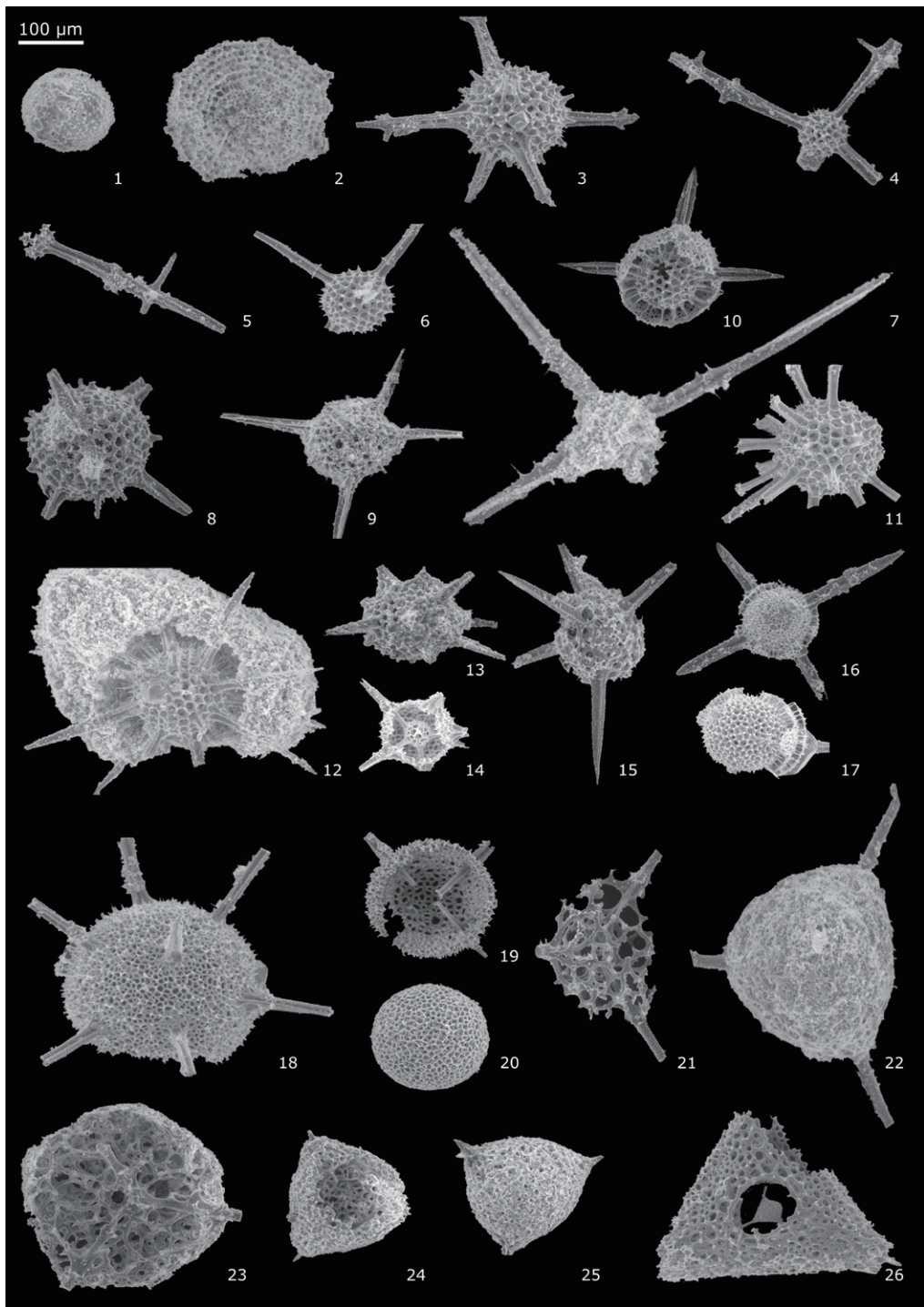


Fig. 17. Radiolarians from Dal'ny Tulkas trench, beds 5-2, 7-2. Scale bar: 100 μm

1-2. *Copicynta fragilispinosa* Kozur & Mostler, bed 5-2. **3.** *Apophysiacus sakmaraensis* (Kozur & Mostler), bed 7-2. **4.** *Apophysiacus* sp. D, bed 7-2. **5.** *Apophysiacus praepycnoclada* (Nazarov & Ormiston), bed 7-2. **6.** *Entactinia dolichoacus* Nazarov in Isakova & Nazarov, bed 7-2. **7.** *Entactinia densissima* Nazarov & Ormiston, bed 7-2. **8.** *Entactinia mariannae* Afanasieva & Amon, bed 7-2. **9.** *Entactinia chernykhii* Afanasieva & Amon, bed 7-2. **10.** *Microporosa permica* (Kozur & Mostler), bed 7-2. **11.** *Astroentactinia* sp. G, bed 7-2. **12.** *Astroentactinia helioforma* (Kozur & Mostler), bed 7-2. **13.** *Astroentactinia inscita* Nazarov in Isakova & Nazarov, bed 7-2. **14.** *Bientactinosphaera morozovi* Afanasieva, bed 7-2. **15.** *Bientactinosphaera* sp. H, bed 7-2. **16-17.** *Pluristratoentactinia lusikae* Afanasieva, bed 7-2. **18.** *Somphoentactinia?* sp. A, bed 7-2. **19.** *Spongentactinia crassitunicata* Afanasieva, bed 7-2. **20.** *Somphoentactinia?* saecularis Afanasieva & Amon, bed 7-2. **21.** *Tetragregnon vimineum* Amon, Braun & Chuvashov, bed 7-2. **22.** *Tetragregnon tunicatus* Nazarov in Isakova & Nazarov, bed 7-2. **23.** *Tetragregnon sphaericus* Nazarov in Isakova & Nazarov, bed 7-2. **24.** *Nazarovisponges pavlovi* Kozur, bed 7-2. **25.** *Nazarovisponges aequilateralis* (Nazarov in Isakova & Nazarov), bed 7-2. **26.** *Kozurisponges circumfusum* (Nazarov and Ormiston), bed 7-2.

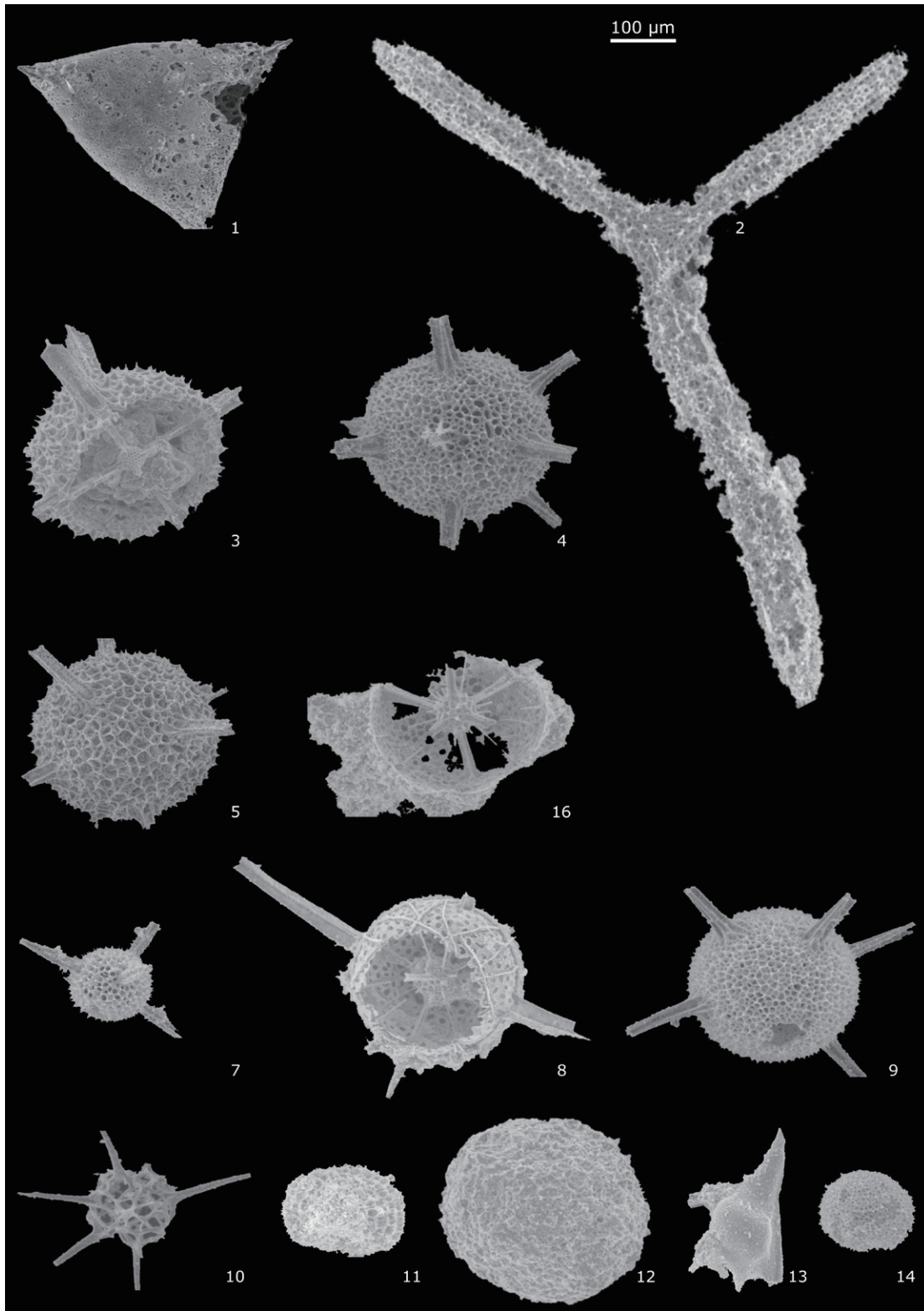


Fig. 18. Radiolarians from Dal'ny Tulkas trench, beds 7-2, 10-1, 11-2, 11-3. Scale bar: 100 μm .

1. *Latentidiota promiscuus* (Nazarov and Ormiston), bed 7-2. **2.** *Latentifistula heteroextrema* Nazarov in Isakova & Nazarov, bed 7-2. **3.** *Bientactinosphaera* sp. I, bed 10-1. **4.** *Somphoentactinia?* sp. C, bed 10-1. **5.** *Somphoentactinia?* sp. B, bed 10-1. **6.** *Bientactinosphaera* sp. F, bed 11-2. **7.** *Bientactinosphaera* sp. E, bed 11-2. **8.** *Paratriposphaera strangulata* (Nazarov & Ormiston), bed 11-2. **9.** *Somphoentactinia* sp. B, bed 11-2. **10.** *Secuicollacta amoenitas* Nazarov & Ormiston, bed 11-2. **11.** *Rectotomentum fornicatum* Nazarov & Ormiston, bed 11-2. **12.** *Palaeodiscaleksus* cf. *punctus* (Hinde), bed 11-2. **13.** *Pseudoalbaillella scalprata* Holdsworth & Jones, bed 11-2. **14.** *Spongentactinia fungosa* Nazarov, bed 11-3.

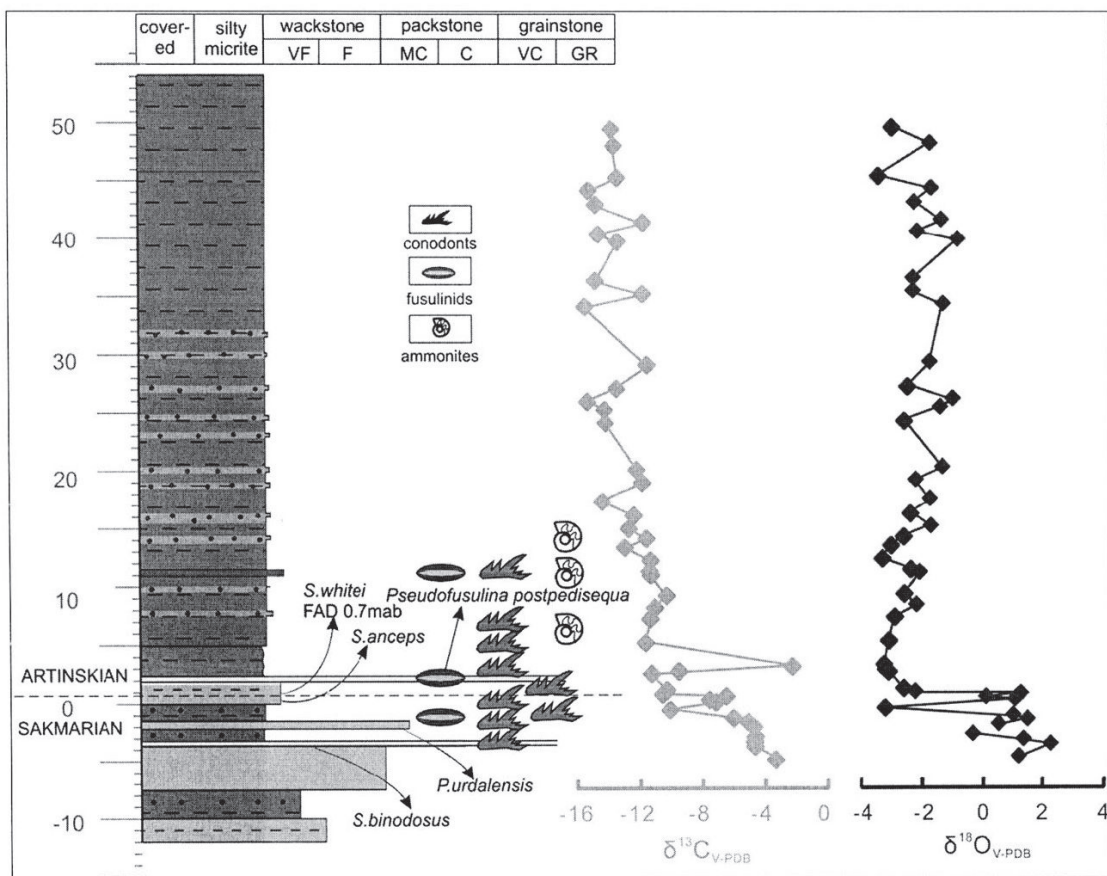


Fig. 19. Carbon and oxygen isotopic trends of the Dal'ny Tulkas section (from Zeng et al., 2012). Explanation in the text.

Conclusion

The Dal'ny Tulkas section, as a candidate for the reference section (GSSP) of the Artinskian Stage, has the following characteristics necessary to substantiate its status.

1. The section is easily accessible and currently has a complete paleontological record for three key Permian biostratigraphic groups of micro- and macrobiota — conodonts, ammonoids, and foraminifers.

2. In the section, the lower boundary of the Artinskian Stage was recorded according to the first appearance of the marker species *Sweetognathus asymmetricus* Sun and Lai in the continuous phylogenetic lineage of development of *Sweetognathus expansus* - *Sw. aff. merrilli* - *Sw. binodosus* - *Sw. anceps* - *Sw. asymmetricus*.

3. The ammonoids *Neopronorites skvorzovi* (Tchernow), *Uraloceras involutum* (Voinova), *U. gracilementum* Ruzhencev, and *Popanoceras annae* Ruzhencev represent markers of the Sakmarian-Artinskian boundary. The interval of the Dal'ny Tulkas section containing early Artinskian ammonoids is proposed to be designated as "Uraloceras involutum Beds".

4. The foraminiferal assemblages indicate that in the Sakmarian-Artinskian boundary interval of the Dal'ny Tulkas section, the schubertellid-fusuline foraminiferal assemblages of late Asselian-Sakmarian age are replaced by typical Artinskian forms. In small foraminifer communities throughout the entire

boundary interval, there are Artinskian forms present with wide stratigraphic distribution.

5. Volcanic ash beds are present and geochronologic ages of zircons have been interpolated between 290.1 and 290.5 Ma.

6. Sr isotopic value (.70767) and carbon isotopic trends provide additional means for correlation.

7. Numerous additional fossil groups have also been recorded from Dal'ny Tulkas including radiolarians, acritarchs, palynomorphs, brachiopods, fishes, and plant remains (algae and calamite trunks). The large diversity of fossils makes this section very attractive for paleontologists and for geotourism.

8. The base-Artinskian occurs within a transgressive systems tract and close to a major maximum flooding surface. This succession occurs above cyclic deposits and coupled with detailed biostratigraphy, it forms a recognizable sequence biostratigraphic signature.

9. Davydov et al. (2007) reported in *Permophiles* 50 that government agreement has been reached to protect all of the defined and proposed Cisuralian GSSP sites. The Dal'ny Tulkas site is now included in the Toratau Geopark and in the future may become one of the educational and tourist centres in the Republic of Bashkortostan, Russia. Currently, work is underway to prepare the section for a visit by members of the ICS Subcommission on Permian Stratigraphy.

Table 1. Distribution list of conodonts, ammonoids, fusulinids, and radiolarians from the Dal'ny Tulkas section and trench

SECTION	Conodonts	Ammonoids	Fusulines
Bed 13	<i>Sweetognathus clarki</i> (Kozur), <i>Sw. asymmetricus</i> Sun & Lai, <i>Sweetognathus</i> aff. <i>rughenchevi</i> , <i>Mesogondolella bisselli</i> (Clark & Behnken)		
Bed 10	<i>Sweetognathus clarki</i> (Kozur), <i>Sw. asymmetricus</i> Sun & Lai, <i>Sweetognathus</i> aff. <i>binodosus</i> , <i>Sweetognathus</i> aff. <i>whitei</i> , <i>Sw. aff. clarki</i> , <i>Mesogondolella laevigata</i> Chernykh; base Irginian		
Bed 9	<i>Mesogondolella bisselli</i> (Clark & Behnken); top Bursevian		
Bed 8		<i>Sakmarites postcarbonarius</i> (Karpinsky), <i>Agathiceras uralicum</i> (Karpinsky), <i>Kargalites typicus</i> (Ruzhencev), <i>Paragastrioceras</i> sp., <i>Crimites subkrotowi</i> Ruzhencev	
Bed 7	<i>Mesogondolella bisselli</i> (Clark & Behnken)		
Bed 6	<i>Mesogondolella bisselli</i> (Clark & Behnken)		
Bed 5	<i>Sweetognathus gravis</i> Chernykh, <i>Sweetognathus obliquidentatus</i> Chernykh, <i>Sweetognathus asymmetricus</i> Sun & Lai, <i>Mesogondolella bisselli</i> (Clark & Behnken)	<i>Popanoceras annae</i> Ruzhencev, <i>P. tschernovi</i> Maximova, <i>P. congregale</i> Ruzhencev, <i>Kargalites</i> sp. and <i>Neopronorites skvorzovi</i> (Tchernow), rare <i>Artinskia</i> sp.	<i>Pseudofusulina callosa</i> Rauser, <i>P. plicatissima</i> Rauser, <i>P. plicatissima irregularis</i> Rauser, <i>P. urdalensis</i> Rauser, <i>P. fortissima</i> Kireeva, <i>P. concavatas</i> Vissarionova, <i>P. juresanensis</i> Rauser, <i>P. consobrina</i> Rauser, <i>P. paraconcessa</i> Rauser
Bed 4b	Upper part - <i>Sweetognathus obliquidentatus</i> Chernykh, <i>Mesogondolella bisselli</i> (Clark & Behnken) 1.2 m - <i>Sweetognathus obliquidentatus</i> Chernykh, <i>Sweetognathus asymmetricus</i> Sun & Lai, <i>Mesogondolella bisselli</i> (Clark & Behnken) 0.6 m - <i>Sweetognathus anceps</i> Chernykh, transitional form between <i>Sweetognathus anceps</i> and <i>Sweetognathus asymmetricus</i> Sun & Lai, <i>Sweetognathus asymmetricus</i> Sun & Lai, <i>Mesogondolella bisselli</i> (Clark & Behnken); base Bursevian		<i>Pseudofusulina</i> aff. <i>longa</i> Kireeva, <i>P. fortissima</i> Kireeva, <i>P. anostata</i> Kireeva, <i>P. plicatissima</i> Rauser, <i>P. urdalensis abnormis</i> Rauser
Bed 4a	<i>Sweetognathus obliquidentatus</i> Chernykh, <i>Sweetognathus anceps</i> Chernykh, transitional form between <i>Sweetognathus anceps</i> and <i>Sweetognathus asymmetricus</i> Sun & Lai, <i>Mesogondolella bisselli</i> (Clark & Behnken); top Steriltamakian		<i>Pseudofusulina callosa</i> Rauser, <i>P. callosa proconcavatas</i> Rauser, <i>P. jaroslavensis fraudulenta</i> Kireeva, <i>P. cf. parajaroslavensis</i> Kireeva, <i>P. blochini</i> Korzhenevskii
Bed 3	<i>Sweetognathus obliquidentatus</i> Chernykh		

TRENCH	Ammonoids	Fusulines	Small Foraminifers	Radiolarians
Bed 11-6				<i>Copicynta fragilispinosa</i> Kozur & Mostler, <i>Somphoentactinia?</i> saecularis Afanasieva & Amon.
Bed 11-3				<i>Copicynta fragilispinosa</i> Kozur & Mostler, <i>Spongentactinia fungosa</i> Nazarov.
Bed 11-2				<i>Apophysiacus sakmaraensis</i> (Kozur et Mostler), <i>Apophysiacus</i> sp. D, <i>Astroentactinia inscita</i> Nazarov in Isakova & Nazarov, <i>Astroentactinia</i> sp. G, <i>Bientactinosphaera</i> sp. E, <i>Bientactinosphaera</i> sp. F, <i>Entactinia densissima</i> Nazarov & Ormiston, <i>Latentifistula heteroextrema</i> Nazarov in Isakova & Nazarov, <i>Palaeodiscaleksus cf. punctus</i> (Hinde), <i>Paratrisposphaera strangulata</i> (Nazarov & Ormiston), <i>Pluristratoentactinia lusikae</i> Afanasieva, <i>Pseudoaibaillella scalprata</i> Holdsworth & Jones, <i>Rectotormentum fornicateum</i> Nazarov & Ormiston, <i>Secuicollacta amoena</i> Nazarov & Ormiston, <i>Somphoentactinia?</i> sp. C, <i>Spongentactinia crassitunicata</i> Afanasieva, <i>Tetraregnon vimineum</i> Amon, Braun & Chuvashov.
Bed 11-1				<i>Copicynta fragilispinosa</i> Kozur & Mostler
Bed 10	(Bed 10-1) <i>Eothinites kargalensis</i> Ruzhencev, <i>Eothinites</i> aff. <i>usvensis</i> Bogoslovskaya, <i>Popanoceras annae</i> Ruzhencev, <i>P. congregale</i> Ruzhencev, <i>Daraelites elegans</i> Tchernow, <i>Uraloceras gracilellum</i> Ruzhencev, <i>U. involutum</i> (Voinova), <i>Crimites</i> sp., <i>Aktubinskia</i> sp.	<i>Schubertella</i> aff. <i>ufimica</i> Baryshnikov, <i>Mesoschubertella</i> sp. 2	<i>Bradyina subtrigonalis</i> Baryshnikov, <i>Endothyranella protracta maxima</i> Baryshnikov, <i>Tetrataxis lata novosjolovi</i> Baryshnikov, <i>Pachyphloia</i> sp., <i>Geinitzina richteri</i> Kasib Koscheleva, <i>Nodosinelloides</i> ex gr. <i>netchaevi</i> (Tcherdynev), <i>?Uralogordius</i> sp., <i>N. jazvae</i> Kosheleva, <i>Endothyra rotundata</i> Morozova, <i>E. symmetrica</i> Morozova, <i>E. lipinae</i> Morozova, <i>Pseudogaathamina regularis</i> (Lipina), <i>Pseudoglomospira vulgaris</i> (Lipina), <i>Midiella</i> aff. <i>ovatus minima</i> (Grozdilova)	(Bed 10-1) <i>Apophysiacus sakmaraensis</i> (Kozur & Mostler), <i>Apophysiacus</i> sp. D, <i>Astroentactinia inscita</i> Nazarov in Isakova & Nazarov, <i>Astroentactinia</i> sp. G, <i>Bientactinosphaera</i> sp. I, <i>Entactinia densissima</i> Nazarov & Ormiston, <i>Entactinia dolichocacus</i> Nazarov in Isakova & Nazarov, <i>Latentifistula heteroextrema</i> Nazarov in Isakova & Nazarov, <i>Pluristratoentactinia lusikae</i> Afanasieva, <i>Somphoentactinia?</i> sp. B, <i>Somphoentactinia?</i> sp. C, <i>Spongentactinia crassitunicata</i> Afanasieva, <i>Tetraregnon vimineum</i> Amon, Braun & Chuvashov.
Bed 9-4	<i>Popanoceras annae</i> Ruzhencev			

Bed 8-2		<i>Boultonia</i> sp., <i>Schubertella</i> sp. A, <i>Schubertella</i> sp. B, <i>S. sphaerica chomatifera</i> Zolotova, <i>S. turaevkensis</i> Baryshnikov, <i>S. turaevkensis elliptica</i> Baryshnikov, <i>S. ex gr. kingi</i> Dunbar & Skinner, <i>S. ex gr. paramelonica</i> Suleimanov, <i>Mesoschubertella</i> sp. 1, <i>Mesoschubertella</i> sp. 2, <i>Pseudofusulina</i> sp. 1, <i>Pseudofusulina</i> sp. 2, <i>P. paraconcessa</i> Rauser, <i>P. ex gr. pedissequa</i> Vissarionova, <i>P. insignita</i> Vissarionova, <i>P. abortiva</i> Tchuvashov, <i>P. seleukensis</i> Rauser, <i>P. urashajevi</i> Rauser, <i>P. cf. utilis</i> Tchuvashov, <i>P. cf. salva</i> Vissarionova	<i>Langella</i> sp., <i>Dentalina particulata</i> Baryshnikov, <i>Hemigordius</i> sp., <i>H. harltoni</i> Cushman & Waters, <i>Nodosinelloides incelebrata novosjolovi</i> (Baryshnikov), <i>N. netchaevi rasilis</i> (Baryshnikov), <i>N. bella kamaensis</i> (Baryshnikov), <i>N. jaborovensis</i> (Koscheleva), <i>Endothyra soshkinae</i> Morozova, <i>Bradyina lucida</i> Morozova, <i>B. compressa</i> Morozova, <i>B. compressa minima</i> Morozova, <i>Pseudoagathammina dublicita</i> (Lipina), <i>Deckerella elegans</i> Morozova, <i>D. elegans multicamerata</i> Zolotova, <i>D. media bashkirica</i> Morozova, <i>Pseudoglomonospira elegans</i> (Lipina), <i>?Mesolasioidiscus costiferus</i> (Lipina), <i>Postmonotaxinooides costiferus</i> (Lipina), <i>Tetrataxis ex gr. conica</i> Ehrenberg, <i>T. plana</i> Morozova, <i>T. hemisphaerica</i> Morozova, <i>T. hemisphaerica elongata</i> Morozova, <i>T. tata</i> Spandel, <i>Lateenoglobivalvulina spiralis</i> (Morozova), <i>Trepeilopsis</i> sp., <i>Globivalvulina</i> sp.	
Bed 8-1		<i>Boultonia</i> sp., <i>Schubertella</i> sp., <i>Fusielia schubertellinoides</i> Suleimanov, <i>Pseudofusulina</i> sp.	<i>Dentalina particulata</i> Baryshnikov, <i>Geinitzina lysvaensis</i> Baryshnikov, <i>G. spandeli</i> Tscherdyntsev, <i>Nodosinelloides kislovi</i> (Koscheleva), <i>N. dualis</i> (Baryshnikov), <i>Howchinella turae</i> (Baryshnikov), <i>Postmonotaxinooides costiferus</i> (Lipina), <i>Endothyra lipiniae</i> Zolotova, <i>?Rectoglandulina</i> sp.	
Bed 7-2				<i>Apophysiacus praepycnoclada</i> (Nazarov & Ormiston), <i>Apophysiacus sakmaraensis</i> (Kozur & Mostler), <i>Apophysiacus</i> sp. D, <i>Astroentactinia helioforma</i> (Kozur & Mostler), <i>Astroentactinia inscita</i> Nazarov in Isakova & Nazarov, <i>Astroentactinia</i> sp. G, <i>Bientactinosphaera morozovi</i> Afanasyeva, <i>Bientactinosphaera</i> sp. H, <i>Entactinia chernykhii</i> Afanasyeva & Amon, <i>Entactinia densissima</i> Nazarov & Ormiston, <i>Entactinia dolichoacus</i> Nazarov in Isakova & Nazarov, <i>Entactinia mariannae</i> Afanasyeva & Amon, <i>Kozurispongus circumfusum</i> (Nazarov & Ormiston), <i>Latentidiota promiscuus</i> (Nazarov & Ormiston), <i>Latentifistula heteroextrema</i> Nazarov in Isakova & Nazarov, <i>Microporosa permica</i> (Kozur & Mostler), <i>Nazarovispongus aequilateralis</i> (Nazarov in Isakova & Nazarov), <i>Nazarovispongus pavlovi</i> Kozur, <i>Pluristratoentactinia lusikae</i> Afanasyeva, <i>Somphoentactinia?</i> <i>saeularis</i> Afanasyeva & Amon, <i>Somphoentactinia?</i> sp. A, <i>Spongientactinia crassitunicata</i> Afanasyeva, <i>Tetragregnon sphaericus</i> Nazarov in Isakova & Nazarov, <i>Tetragregnon tunicatus</i> Nazarov in Isakova & Nazarov, <i>Tetragregnon vimineum</i> Amon, Braun & Chuvashov.
Bed 5-2				<i>Copicynta fragilispinosa</i> Kozur & Mostler, <i>Palaeodiscaleksus</i> cf. <i>punctus</i> (Hinde)

Proposal

It is requested that SPS corresponding members comment on this Global Stratotype Section and Point proposal prior to voting this Fall by SPS Voting Members. SPS proposes that the base-Artinskian GSSP be defined at 1.2 m above the base of bed 4b at the Dal'ny Tulkas section in the southern Urals of Russia (53.88847N and 056.51615E). This point corresponds to the First Appearance Datum of the conodont *Sweetognathus asymmetricus*, which is part of a well defined and widely distributed lineage. Additional markers for correlation include a geochronologic age interpolated between 290.1 and 290.5 Ma, a strontium isotopic ratio of .70767, and many additional fossils groups, particularly ammonoids and fusulines, but also including small foraminifers, radiolarians, and palytomorphs. Finally, the boundary occurs within a transgressive succession, near or at a maximum flooding surface, thereby forming a distinctive sequence biostratigraphic signature in the field.

References

- Baryshnikov, V. V., Zolotova, V. P., Kosheleva, V. F., 1982. Novye vidy foraminifer artinskogo yarusa Permskogo Priuralia [New Species of Artinskian Foraminifers from the Permian Cis-Urals] Preprint No., UNTs AN SSSR, Sverdlovsk, 54p. [in Russian].
- Beauchamp, B. and Henderson, C.M., 1994. The Lower Permian Raanes, Great Bear Cape and Trappers Cove formations, Sverdrup Basin, Canadian Arctic: stratigraphy and conodont zonation. Bull. of Canadian Petroleum Geology, v. 42 (4), p. 562–597.
- Beauchamp, B., Calvo Gonzalez, D., Henderson, C.M., Baranova, D.V., Wang, H.Y., and Pelletier, E. in press for 2021. Late Pennsylvanian–early Permian tectonically-driven stratigraphic sequences and carbonate sedimentation along northern margin of Sverdrup Basin (Otto Fiord Depression), Arctic Canada. In Henderson, C.M., Ritter, S., and Snyder, W.S. (eds.), Late Paleozoic Tectonostratigraphy and Biostratigraphy of western Pangea. SEPM Special Publication No. 113. doi: 10.2110/sempsp.113.
- Boardman, D.R., Wardlaw, B.R. and Nestell, M.K. 2009. Stratigraphy and conodont biostratigraphy of uppermost Carboniferous and Lower Permian from North American Midcontinent. Kansas Geological Survey Bulletin, v. 255, 253p.
- Bogoslovskaya, M.F., 1962. Artinskian Ammonoids of the Central Urals. Proceedings of the Paleontological Institute of the Academy of Sciences of the USSR, v. 87, p. 3–117 [in Russian].
- Bogoslovskaya, A. F., and Shkolin, A. A., 1998. Ammonoidea. In Grunt, T. A., Esaulova, N. K., and Kanev, G. P.(eds.), Biota of the East European Russia at the Early/Late Permian boundary. Geos, Moscow, p. 137–155 (in Russian).
- Buggisch, W., Wang, X. D., Alekseev, A. S., Joachimski, M. M., 2011. Carboniferous–Permian carbon isotope stratigraphy of successions from China (Yangtze platform), USA (Kansas) and Russia (Moscow Basin and Urals). Palaeogeography, Palaeoclimatology, Palaeoecology, v. 301, p. 18–38.
- Chernykh V.V., 2005. Zonal method in biostratigraphy, zonal conodont scale of the Lower Permian in the Urals. Institute of Geology and Geochemistry of RAN, Ekaterinburg, 217 p. (in Russian)
- Chernykh, V.V., 2006. Lower Permian conodonts of the Urals. Institute of Geology and Geochemistry of RAN, Ekaterinburg, 130 p. (in Russian)
- Chernykh, V.V., 2020. A brief review of the Dal'ny Tulkas Section (southern Urals, Russia) – potential candidate for a GSSP to define the base of the Artinskian stage in the global chronostratigraphic scale. Permophiles, v. 69, p. 9–14.
- Chernykh, V. V. and Chuvashov, B. I., 2004. Conodont biochronotype of Lower boundary of Sakmarian Stage. Annual-2003 of Institute of Geology and Geochemistry, Urals Branch of RAS. Ekaterinburg, UB RAS, p. 28–33. (In Russian).
- Chernykh, V. V., Chuvashov, B. I., Davydov, V. I. and Schmitz, M. D., 2012, Mechetlino Section: A candidate for the Global Stratotype and Point (GSSP) of the Kungurian Stage (Cisuralian, Lower Permian). Permophiles, v. 56, p. 21–34.
- Chernykh, V.V., Chuvashov, B.I., Davydov, V.I., Henderson, C.M., Shen, S., Schmitz, M.D., Sungatullina, G.M., Barrick, J.E., Shilovsky, O.P., 2015. Southern Urals. Deep water successions of the Carboniferous and Permian. A Field Guidebook of XVIII International Congress on Carboniferous and Permian. Pre-Congress A3 Trip, August, 6-10, 2015. Academy of Sciences of the Republic of Tatarstan Press, Kazan, 88 p.
- Chernykh, V.V., Chuvashov, B.I., Shen, S., Henderson, C.M., Yuan, D.X., and Stephenson, M.H., 2020. The Global Stratotype Section and Point (GSSP) for the base-Sakmarian Stage (Cisuralian, Lower Permian). Episodes, v. 43, no. 4, p. 961–979. <https://doi.org/10.18814/epiiugs/2020/020059>.
- Chuvashov, B.I., Chernykh, V.V., Bogoslovskaya, M.F., 2002. Biostratigraphic Characteristic of Stage Stratotypes of the Permian System. Stratigraphy and Geological Correlation, v. 10, no. 4, p. 317–333.
- Chuvashov, B. I., Chernykh, V. V., Leven, E. Y., Davydov, V.I., Bowring, S., Ramezani, J., Glenister, B. F., Henderson, C., Schiappa, T. A., Northrup, C. J., Snyder, W. S., Spinosa, C. and Wardlaw, B. R., 2002. Progress report on the base of the Artinskian and base of the Kungurian by the Cisuralian Working Group. Permophiles, v. 41, 13–16.
- Chuvashov, B.I., Chernykh, V.V., Shen, S., and Henderson, C.M., 2013. Proposal for the Global Stratotype Section and Point (GSSP) for the base-Artinskian Stage (Lower Permian). Permophiles, v. 58, p. 26–34.
- Chuvashov, B. I., Dyupina, G. V., Mizens, G. A. and Chernykh, V. V., 1990, Reference sections of the Upper Carboniferous and Lower Permian of western flank Urals and Preurals. Academy of Sciences, USSR, 369 p. [in Russian]
- Davydov, V. I., Chuvashov, B. and Gareev, E., 2007. Report: Established and Proposed GSSPs of the Cisuralian Stages are Protected. Permophiles, v. 50, p. 18–22.
- Davydov, V. I. and Henderson, C. M., 2007. The Cisuralian GSSP Field Workshop. Permophiles, v. 49, p. 4–6.
- Dehari, E., 2016. Upper Pennsylvanian–Lower Permian Carbonate Sedimentology and Conodont Biostratigraphy of

- the Strathearn and Buckskin Mountain formations, Carlin Canyon, Nevada [unpublished MSc thesis]. University of Calgary, Calgary, Alberta. 237 p.
- Filimonova, T. V., 2010. Smaller Foraminifers of the Lower Permian from Western Tethys. *Stratigraphy and Geological Correlation*, v. 18, no. 7, p. 687–811.
- Henderson, C. M., 1988. Conodont paleontology and biostratigraphy of the Upper Carboniferous to Lower Permian Canyon Fiord, Belcher Channel, Nansen, unnamed, and Van Hauen formations, Canadian Arctic Archipelago. Unpublished Ph.D. thesis, University of Calgary, Alberta, Canada, 287 pp.
- Henderson, C. M., 1999. Correlation of Cisuralian and Guadalupian stages in the Sverdrup Basin, Canadian Arctic Archipelago. XIV ICCP. Pander Society. *Can. Paleontol. Conf. Abstrs.* Calgary, p. 57–58.
- Henderson, C.M., 2018. Permian conodont biostratigraphy. In Lucas, S.G. and Shen S.Z. (eds), *The Permian Timescale*. Geological Society, London, Special Publication, v. 450, p. 119–142.
- Henderson, C.M., 2020. Are we ready yet to propose a GSSP for base-Artinskian and base-Kungurian? *Permophiles*, v. 69, p. 23–26.
- Henderson, C.M. and Chernykh, V.V., 2021. TO BE OR NOT TO BE Sweetognathus asymmetricus? *Permophiles*, v. 70, p. 10–13.
- Henderson, C. M., Davydov, V. I. and Wardlaw, B. R., 2012. The Permian Period. In Gradstein, F.M., Ogg, J.G., Schmitz, M.D. and Ogg, G.M. (eds), *The Geological Timescale 2012*, vol. 2. Elsevier, Amsterdam, p. 653–680.
- Henderson, C. M. and McGugan, A., 1986. Permian conodont biostratigraphy of the Ishbel Group, southwestern Alberta and southeastern British Columbia. Contribution to Geology, University of Wyoming, v. 24. p. 219–235.
- Henderson, C.M. and Shen, S.Z., 2020. Chapter 24-The Permian Period, in F.M. Gradstein, J.G. Ogg, M.D. Schmitz, and G.M. Ogg (eds.), *The Geologic Time Scale 2020*. v. 2. Elsevier, p. 875–902.
- Holterhoff, P.F., Walsh, T.R. and Barrick, J.E., 2013. Artinskian (Early Permian) conodonts from the Elm Creek Limestone, a heterozoan carbonate sequence on the eastern shelf of the Midland Basin, West Texas, USA. In Lucas, S.G., Nelson, W.J. et al. (eds), *The Carboniferous–Permian Transition*. New Mexico Museum of Natural History and Science Bulletin, v. 60, p. 109–119.
- Kotlyar, G., Sungatullina, G., and Sungatullin, R., 2016. GSSPs for the Permian Cisuralian Series stages. *Permophiles*, v. 63. p. 32–37.
- Kozur H., 1977. Beiträge zur Stratigraphie des Perms. Teil I. Probleme der Abgrenzung und Gliederung des Perms. Freiberg. Forschungsheft, C334. Leipzig, p. 85–161.
- Leonova, T.B., 2018. Permian ammonoid biostratigraphy. In Lucas, S.G. and Shen S.Z. (eds), *The Permian Timescale*. Geological Society, London, Special Publication v. 450, p. 185–203.
- Mei, S. L., Henderson C. M. and Wardlaw B. R, 2002. Evolution and distribution of the conodonts Sweetognathus and Iranognathus and related genera during the Permian, and their implications for climate change. *Palaeogeography, Palaeoclimatology, Palaeoecology*, v. 180, p. 57–91.
- Nassichuk, W.W., 1971. Permian ammonoids and nautiloids, south eastern Eagle Plain, Yukon Territory. *Journal of Paleontology*, v. 45, p. 6, p. 1001–1021.
- Nassichuk, W.W., 1975. The stratigraphic significance of Permian ammonoids on Ellesmere Island. In *Current Research, Part B, Geological Survey of Canada, Paper 75-1b*, p. 277–283.
- Nassichuk, W.W., Furnish, W.M., and Glenister, B.F., 1966. The Permian ammonoids of Arctic Canada. *Geological Survey of Canada, Bulletin 131*.
- Park, Su-In, 1989. Microfossils of the Permo-Carboniferous Strata of Nongam Area in Mungyeong Coalfield. *Journ. Korean Earth Science Society*, v. 10, no.1, p. 102–110
- Petryshen, W., Henderson, C.M., de Baets, K., and Jarochowska, E., 2020. Evidence of parallel evolution in the dental elements of Sweetognathus conodonts. *Proceedings of the Royal Society B*, v. 287, 202001922.
- Read, M.T. and Nestell, M.K., 2018. Cisuralian (Early Permian) Sweetognathid conodonts from the upper part of the Riepe Springs Limestone, north Spruce Mountain ridge, Elko County, Nevada. In D. Jeffrey Over and Charles M. Henderson (eds.), *Conodont studies dedicated to the careers and contributions of Anita Harris, Glenn Merrill, Carl Rexroad, Walter Sweet, and Bruce Wardlaw*. *Bulletins of American Paleontology*, no. 395–396, p. 89–113.
- Rhodes, F. H. T., 1963. Conodonts from the topmost Tensleep sandstone of the Eastern Big Horn Mountains, Wyoming. *Journal of Paleontology*, v. 37, no. 2, p. 401–408.
- Riglos Suárez, M., Hünicken, M. A. and Merino, D., 1987. Conodont biostratigraphy of the Upper Carboniferous–Lower Permian rocks of Bolivia. In Austin, R.L. (ed.), *Conodonts: investigative techniques and applications*, British Micropalaeontological Society, Ellis Horwood Publishers, London, p. 317–325.
- Ritter, S. M., 1986. Taxonomic revision and Phylogeny of post-early crisis bisselli-whitei Zone conodonts with comments on Late Paleozoic diversity. *Geologica et Palaeontologica*, v. 20. p. 139–165.
- Ruzhencev, V.E., 1956. Lower Permian ammonites of the Urals – Ammonites of the Artinskian Stage. Trudy Paleontologicheskogo Instituta Akademii Nauk SSSR, v. 60, p. 1–271.
- Schiappa, T.A., Hemmesch, N.T., Spinosa, C., and Nassichuk, W.W., 2005. Cisuralian ammonoid genus Uraloceras in North America. *Journal of Paleontology*, v. 79, no. 2, p. 366–377.
- Schmitz M. D. and Davydov V. I., 2012. Quantitative radiometric and biostratigraphic calibration of the Pennsylvanian–Early Permian (Cisuralian) time scale and pan-Euramerican chronostratigraphic correlation. *GSA Bulletin*, v. 124, no. 3–4, p. 549–577.
- Schmitz, M. D., Davydov, V. I., and Snyder, W. S., 2009. Permo-Carboniferous Conodonts and Tuffs: High precision marine Sr isotope geochronology. *Permophiles*, v. 53, Supplement 1 (ICOS 2009 Abstracts edited by C.M. Henderson and C. MacLean), p. 48.
- Shen, S.Z., Wang, Y., Henderson, C.M., Cao, C.Q., and Wang,

- W., 2007. Biostratigraphy and lithofacies of the Permian System in the Laibin-Heshan area of Guangxi, South China. *Palaeoworld*, v. 16, p. 120–139.
- Shen, S.Z., Cao, C.Q., Zhang, H., Bowring, S.A., Henderson, C.M., Payne, J.L., Davydov, V.I., Zheng, Q.F., 2013. High resolution $\Delta^{13}\text{C}_{\text{carb}}$ chemostratigraphy from latest Guadalupian through earliest Triassic in South China and Iran. *Earth and Planetary Science Letters*, v. 375, p. 156–165.
- Stephenson, M.H., 2007. Preliminary results of palynological study of the Dal'ny Tulkas section, location of the proposed basal Artinskian GSSP. *Permophiles*, v. 50, p. 22–25.
- Stephenson, M.H., 2018. Permian palynostratigraphy: a global review. In Lucas, S.G. and Shen S.Z. (eds.), *The Permian Timescale*. Geological Society, London, Special Publication, v. 450, p. 321–347.
- Sun, Y.D., Liu, X.T., Yan, J.X., Li, B., Chen, B., Bond, D.P.G., Joachimski, M.M., Wignall, P.B., Wang, X. and Lai, X.L., 2017. Permian (Artinskian to Wuchiapingian) conodont biostratigraphy in the Tieqiao section, Laibin area, South China. *Palaeogeography, Palaeoclimatology, Palaeoecology*, v. 465, p. 42–63.
- Wang C.Y., Ritter S.M., and Clark D.L., 1987. The Sweetognathus complex in the Permian of China: implications for evolution and homeomorphy. *Journal of Paleontology*. v. 61, no. 5, p. 1047–1057.
- Wang, Z.H., 1994. Early Permian conodonts from the Nashui section, Luodian of Guizhou. *Palaeoworld*, v. 4, p. 203–224.
- Wood, G. D., Gabriel, A. M. and Lawson, J. C. 1996. Palynological techniques – processing and microscopy. In Jansonius, J. and McGregor, D. C. (eds.) *Palynology: Principles and Applications*. American Association of Stratigraphical Palynologists Foundation vol. 1, p. 29–50.
- Zeng, J., Cao, C. Q., Davydov, V. I. and Shen, S. Z., 2012. Carbon isotope chemostratigraphy and implications of paleoclimatic changes during the Cisuralian (Early Permian) in the southern Urals, Russia. *Gondwana Research*, v. 21, p. 601–610.
- Zhang, L., Feng, Q.L., He, W.H., 2018. Permian radiolarian biostratigraphy. In Lucas, S.G. and Shen S.Z. (eds.), *The Permian Timescale*. Geological Society, London, Special Publication, v. 450, p. 143–163.



Prof. He Xilin was looking at some rocks in his lab in China University of Mining and Technology in Xuzhou, Jiangsu Province, China

areas of Jiangxi Province in August of 1924. Growing up, Prof. He was ever the bright and diligent student filled with curiosity. He gained admittance to the Medical School of National Central University as a graduate student in 1948, but having read a report on the 18th International Geological Congress held in London that year, He promptly decided to pursue his passion in Geology. So, in August of 1948, as a young man filled with passion and enthusiasm, Prof. He was admitted to the Geology Department of Peking University to kickoff what was a promising career. As an energetic young student, Prof. He always felt inspired by the full English lectures presented by his professors on Geology and Paleontology. This helped Prof. He realized the importance of having an international mindset throughout his career.

After graduation from Peking University in 1952 with a bachelor degree, Prof. He was assigned a teaching position at Peking Mining College where he began his distinguished career. As much as Prof. He excelled at teaching and research he was faced with a unique problem – there were no specimens or textbooks on Geology at the college. In fact, there wasn't even a Geology department. This proved no obstacle to Prof. He's passion as he personally traversed the wilderness of southern China and collected dozens of boxes of specimens. Armed with the treasures of his excursions and his in-depth knowledge of regional geology, Prof. He and his colleagues formally founded a new Department of Geology at the college in 1953. This department born on Prof. He and his colleagues' labor would later evolve into the present School of Resources and Geosciences of the China University of Mining and Technology. Prof. He leveraged his newfound department to participate in more than 10 major projects including coal exploration and geological surveying in southern China as well as Xizang (Tibet). Through working with his colleagues on geological mapping and biostratigraphic correlations, Prof. He collected thousands of brachiopod and plant fossils in southern China in the 1970s, which paved the way for future generations on the study of these fossils. Among the specimens they collected, Prof. He and his wife, Prof. Zhu Meili, found some bizarre brachiopods from the Upper Permian coal-bearing Lungtan Formation in Jiangxi and Sichuan provinces of South China. Profs. He and Zhu found

Obituary

Professor He Xilin (1924-2021)

Prof. He Xilin, a world-renowned scientist of Permian stratigraphy, Brachiopoda and paleobotany at the China University of Mining and Technology, passed away peacefully at 9:33 pm on January 10, 2021 in the Central Hospital of Xuzhou, China, aged 98. Prof. He is survived by his wife Prof. Zhu Meili, son, daughter and two grandchildren. Prof. He was a distinguished Late Paleozoic stratigrapher, brachiopodologist and paleobotanist and the author of more than 100 papers and monographs.

Prof. He was born into a working-class family in the rural



Profs. He Xilin and Zhu Meili and his three students attended the 22nd Annual Meeting of the Paleontological Society of China held in 2003, in Chengdu, Sichuan Province, China. From right to left, Shen Shuzhong, He Xilin, Zhu Meili, Zeng Yong and Sun Bainian.

those brachiopods were previously assigned to different phyla, classes and orders by different authors. Following extensive research Profs. He and Zhu were convinced these fossils had been misidentified and should belong to a new order within the Phylum Brachiopoda. Thus, a new genus, *Permianella* He and Zhu, 1979, accompanied by a new supra-genus classification system up to the new Order *Permianellida* He and Zhu, 1979, was established (He and Zhu, 1979). This was the first order and superfamily in the Phylum Brachiopoda proposed by Chinese paleontologists. The Superfamily *Permianelloidea* He and Zhu, 1979 has since been widely accepted by international authorities and brachiopod colleagues (Brunton et al. 2000; Rong et al., 2017). Permianellid brachiopods have been widely reported from southern China (He and Zhu, 1979; Liang, 1990; Mou and Liu, 1989; Shen et al., 1994; Shen and Shi, 1998; Yang, 1984), Inner Mongolia of North China (Wang and Jin, 1991), Transcaucasia (Kotlyar et al., 2004; Shen and Shi, 1997), Japan (Shen and Tazawa, 1997; Tazawa, 2008; Yanagida, 1963) and Malaysia (Campi et al., 2002, 2005). Profs. He and Zhu (1985) also established a few new genera under the Superfamily *Orthotetidea* Waagen, 1884 including *Paraorthotetina*, *Parameekella*; *Alatorthotetina* and *Parageyerella* He and Zhu, 1985. Two monographs, one on the Permian brachiopods from southern China (Zeng et al., 1995), the other on the brachiopods from the Penchi and Taiyuan formations in Shanxi, northern China (Fan and He, 1999) were published. Prof. He and his students also contributed various enlightening papers on the Permian brachiopod assemblages from South China for global correlations (He and Shi, 1995; Shen and He, 1994; Shen et al., 1995).

Prof. He was an outstanding mentor to those of us who have been fortunate enough to study under his direction. During his career, Prof. He supervised 26 postgraduate students and seven of them would later be inspired to follow in his footsteps and pursue careers studying Permian Brachiopoda and stratigraphy. I was one of the seven. My career began under Prof. He's supervision on September of 1983. My somewhat complicated Master's thesis "On the Changhsingian brachiopods and the biotic turnover

across the Permian-Triassic boundary at Zhongliang Hill, Chongqing, South China" led me to continue studying with Prof. He as I pursued my PhD. Amongst my peers was Prof. Guang Shi who was enrolled into China University of Mining and Technology in 1984 as a postgraduate student of Prof. He. Prof. He recognized Shi's research potential and recommended him to study Brachiopoda abroad under the world-renowned brachiopod expert Prof. Bruce Waterhouse at the Queensland University in Australia. During my own postgraduate studies, Prof. He iterated the importance of researching and understanding the end-Permian mass extinction (the largest mass extinction event during the last 541 millions of years which wiped out more than 81% of marine life of Earth). Prof. He guided me on identifying the nuances of biotic change which occurred during this critical stage of Earth's history. Both Prof. Shi and I have pursued Brachiopoda, Permian stratigraphy and mass extinctions as our major fields of study until this day. In addition, we are proud to be joined by Profs. Zeng Yong, Zhang Zhipei, Fan Bingheng who have studied brachiopods for their scientific career and have published numerous important monographs and papers on Carboniferous and Permian Brachiopoda (Fan and He, 1999; Zeng et al., 1995; Zhang et al., 1993).

Carboniferous and Permian plant fossils were another spot of interest for Prof. He. Having collected large amounts of specimens from the Permian coal-bearing strata in southern China, Prof. He found that some conifers from China previously described by Chinese and Japanese colleagues were arbitrarily assigned to some similar species from the Permian of Europe based on their form characters. However, after careful examination, Prof. He was convinced that the specimens from southern China greatly differed from those of western Europe in both shape and epidermal structure. Subsequently, Prof. He created several new families, genera and species. Prof. He and his students published a monograph on the Permian floras from Jiangxi Province which described 157 species of 61 genera including 5 new genera (He et al., 1996). Prof. Sun Bainian of Lanzhou University, who received his PhD in 1995 while studying under Prof. He, has astoundingly published nearly 200 papers on plant fossils.



Prof. He Xilin visited Deakin University of Australia in 1994. From right to left: L. McKay, Neil Archbold, He Xilin, Zhan Lipei, G. Beeson, Shi G.R.

Prof. He devoted his career to Carboniferous and Permian stratigraphy of China. During the 11th International Congress on Carboniferous held in 1987 in Beijing, China. Prof. He was not afraid of publicly criticizing some Chinese authorities for the subdivision scheme of the Carboniferous and Permian systems at that time. He urged the Chinese authorities to take an international scheme rather than adopting a local Chinese scale, an unpopular view at the time but one that was ultimately adopted by the National Stratigraphic Committee of China. Prior to this, the Carboniferous-Permian boundary in China was placed at a sequence boundary between the Chihsia and Maping/Chuanshan formations, which is largely equivalent to the base of Artinskian Stage of the present international timescale. Prof. He led the paleontological and stratigraphic team of China University of Mining and Technology to conduct extensive investigations on the Carboniferous and Permian in northern China which eventually led to the publication of two monographs (He et al., 1990, 1995) and many papers. Prof. He proposed a local stage-level timescale for the Permian of northern China, which is still used today by many Chinese colleagues for regional correlations.

Prof. He was a man with a deep passion for science. Every time I visited Prof. He, I would be treated with an exciting flow of information and latest updates on Permian stratigraphy, mass extinctions and Brachiopoda. Prof. He was a passionate mentor who cared for his students. Those of us who were fortunate enough to partake of his wisdom continue to be guided by them until this day. Prof. He was a scholar and a gentleman of immense intellect and humanity who has left an enduring legacy for the Permian stratigraphy, Brachiopoda and paleobotany both in China and globally. Prof. He was a cherished husband, father, grandfather, colleague, mentor, and, to me most importantly, a teacher and friend. May the memory of Prof. He be as eternal as the fossils he dedicated his life to. Prof. He will be sorely missed.

References

- Campi, M. J., Shi, G. R. and Leman, A. S., 2005. Guadalupian (Middle Permian) brachiopods from Sungal Toh, a Leptodus Shale locality in the Central Belt of Peninsular Malaysia - Part I: Lower Horizons. *Palaeontogr Abt. A*, v. 273, p. 97–160.
- Campi, M. J., Shi, G. R. and Leman, M. S., 2002. The Leptodus Shales of central Peninsular Malaysia: distribution, age and palaeobiogeographical affinities. *Journal of Asian Earth Sciences*, v. 20, p. 703–717.
- Fan, B. H. and He, X. L., 1999. Research on brachiopod fauna and stratigraphy of the Late Paleozoic in North China Platform. China University of Mining and Technology Press, Xuzhou, 179 p.
- He, X. L., Liang, D. S. and Shen, S. Z., 1996. Research on the Permian flora from Jiangxi Province, China. China University of Mining & Technology Press, Xuzhou, 300 p.
- He, X. L. and Shi, G. R. 1995. The sequence of Permian brachiopod assemblages in South China. 3rd International Brachiopod Congress, Abstracts, Sudbury, Canada, p. 32.
- He, X. L., Zhang, Y. J., Zhu, M. L., Zhang, G. Y., Zhuang, S. Q., Zeng, Y. and Song, P., 1990. Research on the Late Paleozoic coal-bearing stratigraphy and biota in Jungar, Nei Mongol (Inner Mongolia). China University of Mining and Technology Press, Xuzhou, 407 p.
- He, X. L. and Zhu, M. L., 1979. A new form of brachiopods and its systematical classification. *Journal of China Institute of Mining Technology*, p. 131–140.
- He, X. L. and Zhu, M. L., 1985. Some Upper Permian new genera and species of Orthotetacea in Southwest China. *Acta Palaeontologica Sinica*, v. 24, p. 198–204.
- He, X. L., Zhu, M. L., Fan, B. H., Zhuang, S. Q., Ding, H. and Xue, Q. Y., 1995. The Late Paleozoic stratigraphic classification, correlation and biota from Eastern hill of Taiyuan City, Shanxi Province. Jilin University Press, Changchun, 149 p.
- Kotlyar, G. V., Zakharov, Y. D. and Polubotko, I. V., 2004. Late Changhsingian fauna of the northwestern Caucasus Mountains, Russia. *Journal of Paleontology*, v. 78, p. 513–527.
- Liang, W. P., 1990. Lengwu Formation of Permian and its brachiopod fauna in Zhejiang Province. Geological Publishing House, Beijing, 522 p.
- Mou, C. J. and Liu, C. L., 1989. A new type of brachiopods—Guangdongina and its ecological environment. *Acta Palaeontologica Sinica*, v. 28, p. 455–462.
- Shen, S. Z., Fan, B. H., Zhang, C. and Zhang, X. P., 1994. A new species of permianellids (Brachiopoda): Taxonomic and palaeoecologic significance. *Geobios*, v. 27, p. 477–485.
- Shen, S. Z. and He, X. L., 1994. Brachiopod assemblages from the Changxingian to lowermost Triassic of southwest China and correlations over the Tethys. *Newsletters on Stratigraphy*, v. 31, p. 151–165.
- Shen, S. Z., He, X. L. and Shi, G. R., 1995. Biostratigraphy and correlation of several Permian-Triassic boundary sections in southwestern China. *Journal of Southeast Asian Earth Sciences*, v. 12, p. 19–30.
- Shen, S. Z. and Shi, G. R., 1997. Permianella (Brachiopoda) from the Upper Permian of Transcaucasia. *Science Reports of Niigata University, Series E, Geology and Mineralogy*, p. 19–27.
- Shen, S. Z. and Shi, G. R., 1998. Taxonomy, stratigraphy and palaeobiogeography of permianellids (Brachiopoda). *Proceedings of the Royal Society of Victoria*, v. 110, p. 267–279.
- Shen, S. Z. and Tazawa, J., 1997. Two permianellids (Brachiopoda) from the Middle Permian of the Southern Kitakami Mountains, Northeast Japan. *Paleontological Research*, v. 1, p. 285–290.
- Tazawa, J. I., 2008. Permian brachiopods from the Mizukoshi Formation, central Kyushu, SW Japan: Systematics, palaeobiogeography and tectonic implications. *Paleontological Research*, v. 12, p. 37–61.
- Wang, H. Y. and Jin, Y. G., 1991. On permianellids (Brachiopoda). *Acta Palaeontologica Sinica*, v. 30, p. 481–501, 482 Pls.
- Yanagida, J., 1963. Brachiopods from the Upper Permian Mizukoshi Formation, Central Kyushu. Kyushu University, Faculty of Science, Memoirs (Geology), Ser.D, v. 14, p. 69–78.
- Yang, D. L., 1984. Brachiopoda. In: Feng, S. N., Xu, S. Y., Lin, J. X. and Yang, D. L. (Eds.), *Biostratigraphy of the Yangtze Gorge Area, 3- Late Paleozoic Era*. Geological Publishing House, Beijing, p. 203–239.
- Zeng, Y., He, X. L. and Zhu, M. L. 1995. Brachiopod communities and their succession and replacement in the Permian of Huayingshan area. China University of Mining and Technology Press, Xuzhou, 187 p.
- Zhang, Z. P., He, X. L., Zhu, M. L. and Zhu, W. K., 1993. The assemblage characters of the Upper Permian brachiopod in Chen County-Jiahe area, southern Hunan Province. *Journal of China University of Mining and Technology*, v. 22, p. 36–47.

Shu-zhong Shen, Professor

School of Earth Sciences and Engineering
Nanjing University, Nanjing 210023, China
Email: szshen@nju.edu.cn



Call for funded projects

- SPS would like to fund a limited number of small one-year projects in stratigraphy and correlation, each to a maximum value of Euros 1000
- The call is open to all PhD students and Postdocs studying the Permian and focussing on Permian correlation
- For details contact SPS Chair Prof Lucia Angiolini and see application form

Subcommission on Permian Stratigraphy

SUBMISSION GUIDELINES FOR ISSUE 72

It is best to submit manuscripts as attachments to E-mail messages. Please send messages and manuscripts to Yichun Zhang's E-mail address. Hard copies by regular mail do not need to be sent unless requested. To format the manuscript, please follow the TEMPLATE that you can find on the SPS webpage at <http://permian.stratigraphy.org/>.

Please submit figures files at high resolution (600dpi) separately from text one. Please provide your E-mail addresses in your affiliation. All manuscripts will be edited for consistent use of English only.

Prof. Yichun Zhang (SPS secretary)

Nanjing Institute of Geology and Palaeontology, Chinese Academy of Sciences, Nanjing, Jiangsu, 210008, P.R.China, Email: yczhang@nigpas.ac.cn

The deadline for submission to Issue 72 is December, 31th, 2021

Age (Ma)	Series/stage	Magnetic polarity units	Conodonts	Fusulines	Radiolarians
250	Triassic		<i>Isarcicella isarcica</i> <i>Hindeodus parvus</i>		
252	Changhsingian	LP3	<i>L.11-L13</i> <i>Clarkina changxingensis</i>	<i>Palaeofusulina sinensis</i>	Unzoned <i>Albaillella yaoi</i> <i>Albaillella optima</i> <i>Albaillella triangularis</i> <i>Neoalbaillella ornithoformis</i>
254		LP2	<i>Clarkina subcarinata</i> <i>Clarkina wangi</i>	<i>Palaeofusulina minima</i>	
256	Lopingian	LP1	<i>Clarkina orientalis</i> <i>Clarkina transcaucasica</i> <i>Clarkina guangyuanensis</i>	<i>Gallowayinella meitiensis</i>	<i>Albaillella excelsa</i> <i>Albaillella levis</i>
258	Wuchiapingian	LP1r	<i>Clarkina leveni</i> <i>Clarkina asymmetrica</i>	<i>Nanlingella simplex</i> - <i>Codonofusiliella kwangsiana</i>	<i>Albaillella cavitata</i>
260		LP0r	<i>Clarkina dukouensis</i> <i>Clarkina postbitteri postbitteri</i>		
262	Capitanian	GU3n	<i>Clarkina postbitteri hongshuiensis</i> <i>Jinogondolella granti</i> <i>Jinogondolella xuanhanensis</i> <i>Jinogondolella prexuanhanensis</i> <i>Jinogondolella altudaensis</i> <i>Jinogondolella shannoni</i>	<i>Lantschichites minima</i> <i>Metadololima multivoluta</i>	<i>Follicucullus charveti</i> <i>Follicucullus scholasticus</i>
264	Guadalupian	Gu1n	<i>Jinogondolella postserratia</i>	<i>Yabeina gubleri</i>	<i>Follicucullus porrectus</i> <i>Follicucullus monacanthus</i>
266	Wordian	Gu2n.1n			
268		GU1r	<i>Jinogondolella aserrata</i>	<i>Afghanella schencki</i> / <i>Neoschwagerina margaritae</i>	
270	Kuhfengian	Gu1n.3n	Illawarra Reversal	<i>Neoschwagerina craticulifera</i>	
272	Roadian	Cl3r.1n	<i>Jinogondolella nankingensis</i>		<i>Pseudoalbaillella globosa</i>
274	Xiangbaian	C15	<i>Mesogondolella lamberti</i>	<i>Neoschwagerina simplex</i>	<i>Pseudoalbaillella ishigai</i>
276		Cl3n	<i>Sweetognathus subsymmetricus</i> / <i>Mesogondolella siciliensis</i>	<i>Cancellina liuzhiensis</i>	<i>Albaillella sinuata</i>
278	Kungurian	C14	<i>Sweetognathus guizhouensis</i>	<i>Maklaya elliptica</i>	
280		C13		<i>Shengella simplex</i> <i>Misellina claudiae</i>	
282	Luodianian	C12	<i>Neostreptognathodus pnevi</i>	<i>Misellina termieri</i>	<i>Albaillella xiaodongensis</i>
284	Zisongian	Cl2n	<i>Neostreptognathodus exsculptus</i> / <i>N. pequopensis</i>	<i>Misellina (Brevaxina) dyhrenfurthi</i>	
286	Longlidian	C10	<i>Sweetognathus asymmetricus</i>	<i>Pamirina darvasica</i> / <i>Laxifusulina-Chalaroschwagerina inflata</i>	<i>Pseudoalbaillella rhombothoracata</i>
288		C9	<i>Mesogondolella bisselli</i> / <i>Sweetognathus anceps</i>		
290	Artinskian	C8	<i>Mesogondolella manifesta</i>	<i>Robustoschwagerina ziyunensis</i>	<i>Pseudoalbaillella lomentaria</i> - <i>Ps. sakmarensis</i>
292	Sakmarian	C7	<i>Mesogondolella monstrosa</i> / <i>Sweetognathus binodosus</i>		
294		C6	<i>Sweetognathus aff. merrilli</i> / <i>Mesogondolella uralensis</i>	<i>Sphaeroschwagerina moelleri</i>	<i>Pseudoalbaillella u-forma</i> - <i>Ps. elegans</i>
296	Asselian	C5	<i>Streptognathodus barskovi</i>	<i>Robustoschwagerina kahleri</i>	
298		C4	<i>Streptognathodus fusus</i>		
300	Carboniferous	C3	<i>Streptognathodus constrictus</i>	<i>Pseudoschwagerina uddeni</i>	<i>Pseudoalbaillella bulbosa</i>
		C2	<i>Streptognathodus sigmoidalis</i>		
		C1	<i>Streptognathodus isolatus</i>	<i>Triticites</i> spp.	
		Cl1n	<i>Streptognathodus wabaunsensis</i>		

High-resolution integrative Permian stratigraphic framework (after Shen et al., 2019. Permian integrative stratigraphy and timescale of China. Science China Earth Sciences 62(1): 154-188. Guadalupian ages modified after (1) Shen et al., 2020. Progress, problems and prospects: An overview of the Guadalupian Series of South China and North America. Earth-Science Reviews, 211: 103412 and (2) Wu et al., 2020, High-precision U-Pb zircon age constraints on the Guadalupian in West Texas, USA. Palaeogeography, Palaeoclimatology, Palaeoecology, 548: 109668. Lopingian ages modified after Yang et al., 2018, Early Wuchiapingian cooling linked to Emeishan basaltic weathering? Earth and Planetary Science Letters, 492: 102-111.